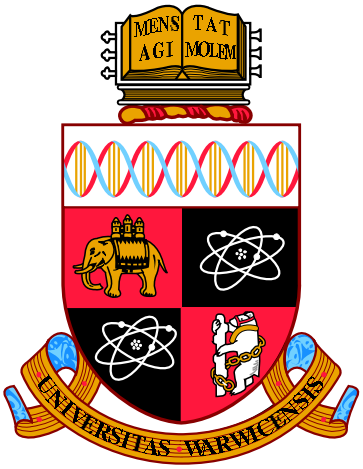

The Role of the Kidney in Diabetic Thiamine Deficiency

by

James Robert Larkin

Thesis

Submitted to the University of Warwick

for the degree of

Doctor of Philosophy in Medical Sciences

Warwick Medical School

November 2010

THE UNIVERSITY OF WARWICK

Contents

List of Figures vii

List of Tables x

Acknowledgments xi

Dedication xii

Declarations xiii

Copyright Permissions xiv

Abstract xv

Abbreviations and Symbols xvi

Chapter 1 Introduction to diabetes 1

1.1 Definition and classification . . . 1
1.2 Aetiology and prevalence . . . 1
1.3 Historical perspective . . . 3
1.4 Diagnosis and symptoms . . . 4
1.5 Therapy . . . 5
1.6 Chronic complications of diabetes mellitus . . . 6
1.6.1 Micro and macro-vascular complications . . . 6
1.6.2 Diabetic nephropathy . . . 8
1.6.2.1 Progression . . . 8
1.6.2.2 Diagnosis . . . 11
1.6.2.3 Risk factors . . . 11
1.6.2.4 The glomerulus . . . 11
1.6.2.5 Molecular pathology . . . 12
1.6.2.6 The role of TGF-β . . . 13
1.6.3 Diabetic retinopathy . . . 15
1.6.4 Diabetic neuropathy . . . 17
1.7 Biochemical theories on mechanisms of hyperglycaemia-induced damage . . . 18
1.7.1 Polyol pathway flux . . . 18
1.7.2 Advanced glycation endproducts . . . 20
1.7.3 Activation of protein kinase C . . . 21
1.7.4 Activation of the hexosamine pathway . . . 22
1.7.5 Oxidative stress . . . 22
1.8 Therapeutic approaches to prevent diabetic complications . . . 24

1.8.1 Antioxidants . . . 25
1.8.2 Aldose reductase inhibitors . . . 27
1.8.3 Aminoguanidine . . . 27
1.8.4 Thiamine and Benfotiamine . . . 28

Chapter 2 Introduction to thiamine **29**
2.1 Discovery and historical significance . . . 29
2.2 Structure and structural analogues . . . 31
2.3 Metabolism of thiamine . . . 33
2.4 Thiamine in the diet . . . 37
2.5 Physiological role of thiamine . . . 39
2.6 The pentose phosphate pathway . . . 41
2.6.1 Control of the pentose phosphate pathway . . . 43
2.6.2 Transketolase . . . 44
2.7 Assay of thiamine . . . 45
2.8 Thiamine transporters . . . 46
2.8.1 THTR-1 . . . 47
2.8.2 THTR-2 . . . 48
2.8.3 Mitochondrial thiamine pyrophosphate transporter . . . 49
2.8.4 Promoter elements of *SLC19A2* and *SLC19A3* . . . 50
2.8.5 Characteristics of thiamine transport . . . 51
2.8.6 Cellular trafficking of THTR-1 and THTR-2 . . . 53

Chapter 3 Introduction to glycosylation and Sp1 **56**
3.1 The *O*-GlcNAc modification . . . 57
3.2 Control of *O*-GlcNAc cycling . . . 58
3.2.1 *O*-GlcNAc transferase . . . 59
3.2.2 *O*-GlcNAcase . . . 60
3.3 Functions of *O*-GlcNAc . . . 61
3.4 *O*-GlcNAc in diabetes . . . 62
3.5 The Sp family of transcription factors . . . 64
3.5.1 Sp1 transcription factor . . . 64
3.5.2 Sp1 post-translational modifications . . . 65
3.5.3 Translocation of Sp1 to the nucleus . . . 66
3.5.4 Insulin and Sp1 . . . 67
3.5.5 Other effects of Sp1 glycosylation . . . 68
3.5.6 Sp1 phosphorylation . . . 68
3.5.7 Sp1 and the thiamine transporter genes . . . 69

Chapter 4 Project-specific background **70**
4.1 Thiamine deficiency in diabetes . . . 70
4.2 Thiamine and biochemical dysfunction *in vitro* . . . 73
4.3 Thiamine intervention therapy *in vivo* . . . 74
4.4 Mode of action for thiamine therapy . . . 75
4.5 The HK-2 cell line . . . 75

Chapter 5 Aims and hypotheses **77**

Chapter 6 Materials and methods **80**
6.1 Materials . . . 80
6.1.1 Cells and tissues . . . 80
6.1.2 Cell culture reagents . . . 80
6.1.3 Enzymes, substrates, cofactors and inhibitors . . . 81
6.1.4 Antibodies . . . 81
6.1.5 Analytical and preparative kits . . . 82
6.1.6 Chromatographic materials . . . 82
6.1.7 Immunohistochemistry materials . . . 82
6.1.8 Analytical standards . . . 83
6.1.9 Other reagents and consumables . . . 83
6.1.10 Instrumentation . . . 84
6.1.11 Software . . . 85
6.2 Cell culture methods . . . 86
6.3 Proximal tubule epithelial cell extraction . . . 86
6.4 Thiamine assay . . . 89
6.4.1 Principle of assay . . . 89
6.4.2 Chromatographic conditions . . . 89
6.4.3 Assay standardization . . . 90
6.4.3.1 Chloroethylthiamine synthesis . . . 90
6.4.4 Calibration of stock solutions . . . 90
6.4.5 Preparation of standard curves . . . 91
6.4.6 Preparation of samples . . . 92
6.4.7 Chromatography of samples . . . 95
6.4.8 Assay validation . . . 95
6.5 Hexosamine pathway intermediate assay . . . 100
6.5.1 Aim and principle . . . 100
6.5.2 Standard preparation . . . 100
6.5.3 Sample preparation . . . 100
6.5.4 Solid phase extraction . . . 101
6.5.5 HPLC conditions . . . 102
6.6 Real-time quantitative PCR . . . 105
6.6.1 Principle of assay . . . 105
6.6.2 Primer design . . . 105
6.6.3 RNA extraction . . . 106
6.6.3.1 RNA quality control . . . 107
6.6.4 Reverse transcription . . . 107
6.6.5 Testing of primers . . . 107
6.6.6 Assay controls . . . 109
6.6.7 Primer efficiency . . . 110
6.6.8 Design of experiments . . . 112
6.6.9 Sample analysis . . . 112
6.6.10 Interpretation and analysis of amplification data . . . 113
6.7 Immunohistochemistry . . . 115
6.8 Immunoblotting . . . 116
6.8.1 Enrichment of membrane proteins . . . 119
6.9 Enzyme-linked immunosorbent assay . . . 119
6.10 Transketolase activity assay . . . 120
6.10.1 Calibration standard curve . . . 120
6.10.2 Preparation of assay cocktail . . . 120
6.10.3 Analysis of samples . . . 122

6.11 Thiamine transport studies . . . 123
6.11.1 Tritiated thiamine uptake study . . . 123
6.11.2 Tritiated thiamine release study . . . 124
6.11.3 Transwell inserts . . . 125
6.11.4 Lucifer yellow permeability . . . 125
6.11.5 Epithelial transport studies . . . 127
6.12 Protein assays . . . 127
6.12.1 Bradford assay . . . 128
6.12.2 DC protein assay . . . 128
6.13 Glucose assay . . . 128
6.14 Thiamine supplementation trial . . . 129
6.15 Statistical analysis . . . 130

Results and Discussion

Chapter 7 Immunohistochemistry characterisation of human kidney cells 132

Chapter 8 Immunohistochemistry thiamine transporter staining 141
8.1 Immunostaining of kidney thiamine transporters . . . 141
8.2 Immunostaining of thiamine transporters in primary PTECs . . . 150

Chapter 9 mRNA and thiamine transporter protein abundance in PTECs *in vitro* 157
9.1 mRNA quantitation . . . 157
9.1.1 Primary PTEC mRNA quantitation *in vitro* . . . 157
9.1.2 HK-2 cell mRNA quantitation *in vitro* . . . 159
9.1.3 Comparison of gene expression in HK-2 cells and human kidney cortex 163
9.2 Thiamine transporter protein abundance . . . 164
9.2.1 Primary PTEC THTR-1 protein abundance *in vitro* . . . 164
9.2.2 HK-2 cell THTR-1 protein abundance *in vitro* . . . 165
9.2.3 Discussion . . . 165

Chapter 10 The hexosamine pathway, glycosylation and Sp1 in PTECs *in vitro* 170
10.1 Hexosamine pathway metabolite concentration . . . 170
10.1.1 Primary PTEC hexosamine pathway metabolite concentration *in vitro* 170
10.1.2 HK-2 cell hexosamine pathway metabolite concentration *in vitro* . . . 171
10.1.3 Hexosamine pathway metabolite assay controls . . . 171
10.1.4 Discussion . . . 172
10.2 Sp1 and glycosylation . . . 174
10.2.1 HK-2 cell Sp1 abundance and glycosylation *in vitro* . . . 174
10.2.2 HK-2 cell *O*-GlcNAc transferase abundance *in vitro* . . . 175
10.2.3 Discussion . . . 177

Chapter 11 Intracellular thiamine metabolite concentration and transketolase activity in PTECs *in vitro* 178
11.1 Concentration of intracellular thiamine . . . 178
11.1.1 Primary PTEC intracellular thiamine metabolite concentration *in vitro* 178
11.1.2 HK-2 cell intracellular thiamine metabolite concentration *in vitro* . . . 179
11.1.3 Discussion . . . 181
11.2 Transketolase activity . . . 184

11.2.1 Primary PTEC transketolase activity *in vitro* . . . 184
11.2.2 HK-2 cell transketolase activity *in vitro* . . . 184
11.2.3 Discussion . . . 185

Chapter 12 Thiamine uptake and handling in PTECs *in vitro* 187
12.1 Primary PTEC monolayer transport studies *in vitro* . . . 187
12.1.1 Primary PTEC monolayer integrity . . . 187
12.1.2 Monolayer [^{3}H]thiamine transport studies in primary PTECs *in vitro* 187
12.1.3 Discussion . . . 190
12.2 Rate of uptake of thiamine by HK-2 cells *in vitro* . . . 190
12.2.1 Discussion . . . 191
12.3 Rate of release of thiamine from HK-2 cells *in vitro* . . . 192

Chapter 13 Double blind placebo-controlled trial of thiamine supplementation in patients with type 2 diabetes and microalbuminuria 196
13.1 Patient characteristics . . . 196
13.1.1 Clearance rate definition . . . 199
13.2 Effect of therapy with high-dose thiamine on type 2 diabetes patients . . . 199

Chapter 14 General discussion 205
14.1 Comparison of model systems . . . 205
14.2 Experimental and analytical decisions . . . 208
14.2.1 Cell culture methods . . . 209
14.2.2 Discrepancies between the HK-2 cell and the primary cell cultures . . 210
14.3 Effects of hyperglycaemia on PTECs *in vitro* . . . 211
14.3.1 Alternative hypotheses . . . 212
14.4 Effect of high thiamine supplementation . . . 215
14.5 Benfotiamine intervention trials . . . 217

Chapter 15 Conclusions 220
15.1 Further work . . . 222

Appendix A Supplementary statistical data 224

Appendix B Primer sequences 230

Appendix C Other experiments undertaken 231
C.1 *In vivo* thiamine metabolism . . . 231
C.2 Residual binding domain computation . . . 232

References 233

List of Figures

1.1 Metabolic syndrome . . . 2
1.2 A histological section through a normal glomerulus . . . 10
1.3 A histological section through a diabetic glomerulus . . . 10
1.4 Electron micrograph of thickening of the glomerular basement membrane . . . 10
1.5 Ophtalmogram showing details of proliferative diabetic retinopathy . . . 16
1.6 Ophtalmogram showing scatter photocoagulation scars . . . 17
1.7 The reactions of the polyol pathway . . . 19
1.8 The reactions of the hexosamine biosynthesis pathway . . . 23
1.9 Structures of the eight active forms of vitamin E . . . 26
1.10 The structure of α-lipoic acid . . . 26

2.1 The structure of thiamine and thiamine phosphate esters . . . 32
2.2 The mechanism of thiamine ylid formation . . . 32
2.3 The mechanisms of thiamine hydrolysis and oxidation . . . 34
2.4 The structures of thiamine analogues . . . 35
2.5 The mechanism of Benfotiamine conversion to TMP and THM . . . 36
2.6 The metabolism of thiamine and its phosphate esters . . . 38
2.7 Schematic summary of the pentose phosphate pathway . . . 42
2.8 Sequence of the *SLC19A2* minimal promoter region . . . 50
2.9 THTR-1 localisation . . . 54
2.10 THTR-2 localisation . . . 55

3.1 Schematic of known *O*-Linked sugar-peptide bonds . . . 57
3.2 Structure of *O*-Linked *N*-Acetylglucosamine modification . . . 58
3.3 UDP-GlcNAc precursors . . . 60
3.4 Extent of *O*-GlcNAc in HeLa cells . . . 61
3.5 Structures of Sp1 to Sp4 . . . 65
3.6 Roles of Sp1 *O*-GlcNAcylation . . . 67

4.1 Diabetic thiamine deficiency . . . 72
4.2 Thiamine therapy hypothesis . . . 76

5.1 Project hypothesis overview . . . 79

6.1 Cells from a human kidney digest separated in Percoll . . . 88
6.2 Microscopic image of a monolayer of human PTECs . . . 88
6.3 Schematic showing thiamine oxidation to thiochrome . . . 89
6.4 The reaction scheme for chloroethylthiamine synthesis . . . 91
6.5 Thiamine assay example chromatogram . . . 96
6.6 Example standard curve for thiamine analysis . . . 97

6.7 Example standard curve for thiamine monophosphate analysis 97
6.8 Example standard curve for thiamine pyrophosphate analysis 98
6.9 Thiamine assay single analyte analysis 99
6.10 Hexosamine pathway intermediate assay mobile phase gradient 103
6.11 Hexosamine pathway intermediate assay example chromatogram 103
6.12 Example standard curve for UDP-glucose analysis 104
6.13 Example standard curve for UDP-*N*-acetylglucosamine analysis 104
6.14 BioMix Red PCR cycling conditions 108
6.15 Primer quality control example gel image 108
6.16 qPCR example control amplifications 109
6.17 qPCR example product melt curves 110
6.18 Example primer efficiency determination curve 111
6.19 SYBR green qPCR cycling conditions 113
6.20 qPCR example sample amplification 114
6.21 Example standard curve for NADH 121
6.22 Example transketolase assay reaction curve 122
6.23 Schematic of a Transwell insert 125

7.1 Aqp-1 staining in cells from Percoll density gradient (top fraction) 134
7.2 Aqp-1 staining in cells from Percoll density gradient (middle fraction) 134
7.3 Aqp-1 staining in cells from Percoll density gradient (bottom fraction) 135
7.4 UMOD staining in cells from Percoll density gradient (top fraction) 135
7.5 UMOD staining in cells from Percoll density gradient (middle fraction) 136
7.6 UMOD staining in cells from Percoll density gradient (bottom fraction) . . . 136
7.7 Aqp-1 staining in human kidney 137
7.8 Aqp-1 staining in human kidney cortex 137
7.9 Aqp-1 staining in human kidney medulla 138
7.10 UMOD staining in human kidney 138
7.11 UMOD staining in human kidney cortex 139
7.12 UMOD staining in human kidney medulla 139
7.13 IHC negative control for kidney extract cells 140

8.1 THTR-2 staining in human kidney cortex (1) 144
8.2 THTR-2 staining in human kidney cortex (2) 144
8.3 THTR-2 staining in human kidney cortex (3) 145
8.4 THTR-2 staining in human kidney cortex (4) 145
8.5 THTR-2 staining in human kidney cortex (5) 146
8.6 THTR-2 staining in human kidney medulla 146
8.7 THTR-2 staining in smooth muscle 147
8.8 THTR-1 staining in human kidney cortex (1) 147
8.9 THTR-1 staining in human kidney cortex (2) 148
8.10 THTR-1 staining in human kidney cortex (3) 148
8.11 THTR-1 staining in human kidney medulla 149
8.12 IHC negative control slide for kidney sections 149
8.13 THTR-1 staining in HK-2 cells 152
8.14 THTR-2 staining in HK-2 cells 152
8.15 THTR-1 staining in primary PTECs (−G−T) 153
8.16 THTR-1 staining in primary PTECs (−G+T) 153
8.17 THTR-1 staining in primary PTECs (+G−T) 154
8.18 THTR-1 staining in primary PTECs (+G+T) 154
8.19 THTR-2 staining in primary PTECs (−G−T) 155

8.20 THTR-2 staining in primary PTECs (−G+T) 155
8.21 THTR-2 staining in primary PTECs (+G−T) 156
8.22 THTR-2 staining in primary PTECs (+G+T) 156

9.1 Thiamine transporter gene expression in primary PTECs *in vitro* 158
9.2 Hexosamine pathway-related gene expression in primary PTECs *in vitro* . . . 159
9.3 Hyperglycaemia-related gene expression in primary PTECs *in vitro* 160
9.4 Thiamine transporter gene expression in HK-2 cells *in vitro* 161
9.5 Hexosamine pathway-related gene expression in HK-2 cells *in vitro* 162
9.6 Hyperglycaemia-related gene expression in HK-2 cells *in vitro* 162
9.7 Gene expression in HK-2 cells *in vitro* compared to human kidney cortex . . 163
9.8 THTR-1 abundance in primary PTECs cultured in low thiamine *in vitro* . . . 164
9.9 THTR-1 abundance in primary PTECs cultured in high thiamine *in vitro* . . 165
9.10 THTR-1 abundance in HK-2 cells cultured in low thiamine *in vitro* 166
9.11 THTR-1 abundance in HK-2 cells cultured in high thiamine *in vitro* 166
9.12 THTR-1 HK-2 cell immunoblot specimen bands 167
9.13 THTR-1 primary PTEC immunoblot specimen bands 167
9.14 Confocal fluorescence microscopy of THTR-1 immunostaining 168
9.15 THTR-1 immunoblot positive control 168
9.16 Densitometry analysis of a THTR-1 western blot 168

10.1 Hexosamine pathway metabolite abundance in primary PTECs *in vitro* . . . 171
10.2 Hexosamine pathway metabolite abundance in HK-2 cells *in vitro* 172
10.3 UDP-GlcNAc in HK-2 cells supplemented with glucosamine *in vitro* 173
10.4 UDP-GlcNAc in HK-2 cells supplemented with glucotamine *in vitro* 173
10.5 Glycosylation status of Sp1 in HK-2 cell nuclear extracts *in vitro* 175
10.6 Abundance of Sp1 in HK-2 cell nuclear extracts *in vitro* 176
10.7 Abundance of OGT in HK-2 cells cultured in 4 nM thiamine *in vitro* 176
10.8 Abundance of OGT HK-2 cells cultured in 26 mM glucose *in vitro* 177

11.1 Intracellular thiamine content of primary PTECs *in vitro* 179
11.2 Intracellular thiamine pyrophosphate content of primary PTECs *in vitro* . . . 180
11.3 Intracellular thiamine content of HK-2 cells *in vitro* 180
11.4 Intracellular thiamine monophosphate content of HK-2 cells *in vitro* 181
11.5 Intracellular thiamine pyrophosphate content of HK-2 cells *in vitro* 182
11.6 Transketolase activity in primary PTECs *in vitro* 184
11.7 Transketolase activity in HK-2 cells *in vitro* 185

12.1 P_{app} for thiamine at different concentrations in primary PTECs *in vitro* . . . 188
12.2 P_{app} values for forward and reverse [^{3}H]thiamine transport *in vitro* 189
12.3 P_{app} ratios forward:reverse *in vitro* 189
12.4 [^{3}H]thiamine uptake rate into HK-2 cells *in vitro* 191
12.5 [^{3}H]thiamine content of HK-2 cells *in vitro* before release window 193
12.6 [^{3}H]thiamine absolute release rate from HK-2 cells *in vitro* 194
12.7 [^{3}H]thiamine release rate constant from HK-2 cells *in vitro* 195

13.1 Effect of high-dose thiamine on plasma thiamine concentration *in vivo* 200
13.2 Effect of high-dose thiamine on UAE in type 2 diabetes patients 201
13.3 Individual UAE changes in patients receiving thiamine therapy or placebo . . 202
13.4 Effect of ACE-I/ARB therapy on UAE in patients receiving thiamine therapy 203

14.1 Thiamine deficiency spiral 216

List of Tables

1.1 Drugs available to treat diabetes 7

2.1 Thiamine composition of the diet 39

6.1 Thiamine assay standard calibration data 91
6.2 Thiamine assay low concentration standard composition 93
6.3 Thiamine assay high concentration standard composition 94
6.4 Thiamine assay mobile phase gradient 96
6.5 Thiamine assay intra- and inter-batch CVs 97
6.6 Thiochrome half lives 98
6.7 Thiamine assay limits of detection 99
6.8 Hexosamine pathway metabolite assay standard preparation 101
6.9 Hexosamine pathway analyte recoveries 102
6.10 Gel components for SDS-PAGE gels 118
6.11 Transketolase assay standards 121

12.1 [^{3}H]thiamine handling in HK-2 cells *in vitro* 194

13.1 Pakistan trial patient characteristics 198

A.1 Supplementary statistical information 224

B.1 Primer sequences 230

Acknowledgments

I am very grateful to my supervisor Paul Thornalley for his guidance and expertise throughout my project. It has been thoroughly enjoyable working with members of the Disease Mechanisms and Therapeutics Research Group as well as other researchers and colleagues within the Clinical Sciences Research Institute and I wish to thank them for all their help and friendship. In particular, special thanks must go to Fang Zhang and Lisa Godfrey who have brightened many an early morning in the lab and been cheery work companions throughout the most stressful of times. Thanks must also go to Daniel Zehnder, without whom many research ideas would never have come about and who stepped in with the offer of a human kidney available for research. I am very grateful for the patient help of Sean James in all manners immunohistochemical and histological, especially for cutting countless kidney sections without so much as a breath of complaint. I am, of course, also immensely thankful for the support and unconditional love of my wife, Sarah, and the rest of my family, especially during the writing of this thesis.

James Larkin, November 2010.

Dedication

To my Dad, without whose inspiration, my life would be but a fraction of what it now is.

22nd Feburary 1946—17th January 2010.

Declarations

I declare that all the work presented in this thesis, except where specifically stated, was original research performed by myself under the supervision of Professor Paul J Thornalley. None of this work has been previously submitted to any other degree. All sources of information have been acknowledged by means of reference.

Excerpts from papers on which I am co-author are included within this thesis. These are reproduced with with kind permission from Springer Science+Business Media: Diabetologia, "High-dose thiamine therapy for patients with type 2 diabetes and microalbuminuria: a randomised, double-blind placebo-controlled pilot study", 52(2) 2009 208–212, N. Rabbani and S. S. Alam and S. Riaz and J. R. Larkin and M. W. Akhtar and T. Shafi and P. J. Thornalley, © Springer-Verlag 2008 and "Thiamine in diabetic nephropathy: a novel treatment modality? Reply to Alkhalaf A, Kleefstra N, Groenier KH et al. [letter]", 52(6) 2009 1214–1216, N. Rabbani and S. Alam and S. Riaz and J. Larkin and M. Akhtar and T. Shafi and P. Thornalley, © Springer-Verlag 2009. My experimental contribution to these papers was analysis of thiamine concentrations in urine and plasma and determination of sVCAM-1 concentrations in plasma.

James Larkin

Copyright Permissions

Figure 1.1 adapted with permission from Macmillan Publishers Ltd: Nature [Zimmet et al., 2001], © 2001. Figures 1.2, 1.3, 1.4 reprinted with permission from Macmillan Publishers Ltd: Modern Pathology [Lai et al., 2004], © 2004. Figure 2.2 adapted with permission from the American Chemical Society [Washabaugh and Jencks, 1989], © 1989. Figure 2.3 adapted with permission from Academic Press, Inc. [Washabaugh et al., 1993], © 1993. Figure 2.8 adapted with permission from Elsevier [Reidling et al., 2002], © 2002. Figures 2.9 and 2.10 adapted with permission for non-commercial work from the American Society for Biochemistry and Molecular Biology [Subramanian et al., 2003] and [Subramanian et al., 2006] respectively, © 2003 and 2006 respectively. Figure 3.1 adapted with permission from Oxford University Press [Spiro, 2002], © 2002. Figure 3.6 adapted with permission from Elsevier [Özcan et al., 2010], © 2010. Figure 4.1 adapted with kind permission from Springer Science+Business Media: Diabetologia [Thornalley et al., 2007], © 2007.

Abstract

Diabetes is a chronic epidemic compounded by a burden of vascular complications including diabetic nephropathy. Diabetic nephropathy affects ∼40% of patients and is characterised by increased urinary albumin excretion and decreased glomerular filtration rate.

Diabetic patients exhibit ∼75% decreased plasma thiamine concentration, linked to increased renal thiamine clearance. In streptozotocin-induced diabetic rats, decreased plasma thiamine concentration was also associated with a reduction in expression and activity of transketolase. Transketolase is a thiamine pyrophosphate-dependent enzyme and a critical component of the reductive pentose phosphate pathway, a metabolic pathway leading from glycolysis involved with the synthesis of ribose sugars. It is proposed that increasing the relative flux of glucose through the pentose phosphate pathway can ameliorate hyperglycaemic damage. This thesis investigates mechanisms mediating the increased renal thiamine clearance and the effects of thiamine therapy on type 2 diabetic patients with nephropathy. The hypothesis that hyperglycaemia increases flux through the hexosamine pathway, leading to increased *O*-glycosylation of the transcription factor Sp1 and subsequent decreased expression of thiamine transporters is investigated.

Thiamine transporters in normal human kidney sections were found to be localised to the proximal tubule. Investigations in primary cultures of human proximal tubule epithelial cells and the HK-2 cell line have shown that there is a decreased expression (−48 to −80%) and abundance (−52 to −77%) of thiamine transporters in cells cultured in high glucose concentrations (26 mM) with respect to low glucose concentrations (5 mM). There is only limited evidence supporting the involvement of the hexosamine pathway in these decreases.

A double-blind, placebo-controlled study investigated the effect of thiamine supplementation on type 2 diabetic patients with microalbuminuria. Thiamine therapy restored plasma thiamine concentrations from 11 nM to 98 nM, exceeding the published median concentration observed in normal patients (64 nM). After three months, thiamine therapy, but not placebo, caused a decrease in the urinary albumin excretion rate relative to baseline ($-18\,\mathrm{mg\,day^{-1}}$). These results show promise for thiamine as a therapy for diabetic nephropathy.

Abbreviations and Symbols

−G−T 5 mM glucose, 4 nM thiamine
−G+T 5 mM glucose, 4 µM thiamine
+G−T 26 mM glucose, 4 nM thiamine
+G+T 26 mM glucose, 4 µM thiamine
A Adenine
$\boldsymbol{A_x}$ Absorbance at wavelength x nm
ABC Avidin-biotin complex
ACCORD Action to Control Cardiovascular Risk in Diabetes
ACD Advanced Chemistry Development
ACE Angiotensin-converting enzyme
ACE-I Angiotensin-converting enzyme inhibitor
ACS American Chemical Society
ACTION Aminoguanidine Clinical Trial In Overt diabetic Nephropathy
AD Anno Domini
ADA American Diabetes Association
ADP Adenosine diphosphate
AEBSF 4-(2-aminoethyl)benzenesulphonyl fluoride
AER Albumin excretion rate
AGE Advanced glycation endproduct
α-KGDH Alpha ketoglutarate dehydrogenase
AMP Adenosine monophosphate
ANOVA Analysis of variance
ANT-2 Adenine nucleotide translocase 2
AP-1 Activator protein 1
AP-2 Activator protein 2
APS Ammonium persulphate
Aqp-1 Aquaporin 1
AR Aldose reductase
Ara Arabinose
ARB Angiotensin receptor blocker
Asn Asparagine
ATP Adenosine triphosphate
AU Absorbance units or arbitrary units
BBGD Biotin-responsive basal ganglia disease
BLAST Basic local alignment search tool

BMI Body mass index
bp Base pairs
BP Blood pressure
BSA Bovine serum albumin
°C Degress centigrade
$^{n}C_{m}$ Combinations choosing m from n
C Cytosine
C/EBP CCAAT/enhancer-binding protein
CA California
cAMP Cyclic adenosine monophosphate
CD Cluster of differentiation
CET Chloroethylthiamine
CH Carbohydrazide
CHD Coronary heart disease
cm Centimetres
CoA Coenzyme A
CREB Cyclic AMP response element binding protein
$\mathbf{C_t}$ Threshold cycle
CT Connecticut
CTGF Connective tissue growth factor
CTRI Clinical Trials Registry—India
CV Coefficient of variance
CVD Cardiovascular disease
δ or Δ Delta—difference between
D *Dextro*-rotatory
Da Daltons
DAB 3,3'-Diaminobenzidine
DAG Diacylglycerol
DAPI 4',6-diamidino-2-phenylindole
DC Detergent compatible
DCCT Diabetes Control and Complications Trial
DDP-IV Dipeptidyl-peptidase 4
DE Delaware
DHAP Dihydroxyacetone phosphate
DiAcTridH 2,4,-diacetamido-2,4,6-trideoxyhexose
DMEM Dulbecco's modified Eagle medium
DMSO Dimethyl sulphoxide
DN Diabetic nephropathy
DNA Deoxyribonucleic acid
dNTP Deoxynucleoside triphosphate
DPP-IV Dipeptidyl peptidase IV
DPX Distyrene and plasticisers in xylene
ε Molar extinction coefficient
$\varepsilon_{1\%}$ Extinction coefficient of a 1% solution
ε_{x} Molar extinction coefficient at x nm

E4P Erythrose-4-phosphate
E-64 *N*-(trans-epoxysuccinyl)-L-leucine 4-guanidinobutylamide
EC Enzyme Commission
ECL Enhanced chemiluminescence
ECM Extracellular matrix
EDTA Ethylenediaminetetraacetic acid
(E)GFP (Enhanced) green fluorescent protein
ELISA Enzyme-linked immunosorbent assay
eNOS Endothelial nitric oxide synthase
ER Endoplasmic reticulum
ESRD End-stage renal disease
ET-1 Endothelin 1
F6P Fructose-6-phosphate
FAD Flavin adenine dinucleotide
$FADH_2$ Flavin adenine dinucleotide reduced form
FBS Foetal bovine serum
FM4-64 *N*-(3-triethylammoniumpropyl)-4-(4-diethylaminophenylhexatrienyl)pyridinium dibromide
Fuc Fucose
FucNAc *N*-acetylfucosamine
g Grams
g Standard gravitational force of acceleration ($9.81\,\mathrm{m\,s^{-2}}$)
G Guanine
G3P Glyceraldehyde-3-phosphate
G-6-P Glucose-6-phosphate
Gal Galactose
GalNAc *N*-acetylgalactosamine
GAPDH Glyceraldehyde-3-phosphate dehydrogenase
GDH Glycero-3-phosphate dehydrogenase
GDP Guanosine diphosphate
GE General Electric
GFAT-1 Glutamine fructose-6-phosphate amidotransferase 1
GFR Glomerular filtration rate
GKLF Gut enriched Krupple-like Factor
Glc Glucose
GlcN-6P Glucosamine-6-phosphate
GlcNAc *N*-acetylglucosamine
GlcNAc-1P *N*-acetylglucosamine-1-phosphate
GlcNAc-6P *N*-acetylglucosamine-6-phosphate
GLO Glyoxalase
GLP-1 Glucagon-like peptide 1
GLUT-1 Glucose transporter 1
GPI Glycosylphosphatidylinositol
GSH Glutathione
^{3}H Tritium

H&E Haematoxylin and eosin
$HbA_{1(c)}$ Haemoglobin $A_{1(c)}$ fraction
HBP Hexosamine biosynthesis pathway
HDL High-density lipoprotein
HEK Human embryonic kidney
HeLa Henrietta Lacks
HEPES 4-(2-hydroxyethyl)-1-piperazineethanesulfonic acid
HIV/AIDS Human immunodeficiency virus/acquired immunodeficiency syndrome
HK-2 Human kidney 2
HPLC High performance/pressure liquid chromatography
HPV Human papilloma virus
HRP Horseradish peroxidase
HSD Honestly significant difference
HSP Heat shock protein
HUVEC Human umbilical vein endothelial cell
Hyl Hydroxylysine
Hyp Hydroxyproline
IBM International Business Machines
IEC Ion exchange chromatography
IFG Impaired fasting glucose
IGF-1 Insulin-like growth factor 1
IGT Impaired glucose tolerance
IHC Immunohistochemistry
IL Illinois
IL-1β Interleukin 1 beta
IPA Isopropanol
IS Internal standard
kDa Kilodaltons
KEGG Kyoto Encyclopedia of Genes and Genomes
k_{cat} Enzyme turnover number
k_{cat}/K_m Enzyme specificity constant ratio
KIM-1 Kidney injury molecule 1
K_m Michaelis constant
λ Wavelength
λ_{max} Wavelength at maximum absorption or emission
L *Levo*-rotatory
L Litres
LC-MS/MS Liquid chromatography with tandem mass spectrometry
LC-SAX Liquid chromatography, solid anion exchange
LDL Low-density lipoprotein
LOD Limit of detection
µg Micrograms
µm Micrometres
µmol Micromoles
µM Micromoles per litre

µL Microlitres
m Metres
M Moles per litre
mA Milliamps
MA Massachusetts
Man Mannose
MCPHA Amish lethal microcephaly
MDCK Madin Darby canine kidney
mg Milligrams
MGEA5 Meningioma expressed antigen 5
MIM Mendelian Inheritance in Man
min Minutes
mL Millilitres
mm Millimetres
mmol Millimoles
mM Millimoles per litre
MMP Matrix metalloproteinase
MN Minnesota
MO Missouri
mol Moles
mRNA Messenger RNA
MW Molecular weight
NAD^+ Nicotinamide adenine dinucleotide oxidised form
NADH Nicotinamide adenine dinucleotide reduced form
$NADP^+$ Nicotinamide adenine dinucleotide phosphate oxidised form
NADPH Nicotinamide adenine dinucleotide phosphate reduced form
NCBI National Center for Biotechnology Information
NCOAT Nuclear cytoplasmic *O*-GlcNAcase and acetyltransferase
NCV Nerve conduction velocity
ND NanoDrop
NF-κB Nuclear factor of kappa light chain gene enhancer in B (bursa of Fabricius) cells
NF-Y Nuclear factor Y
ng Nanograms
NHS National Health Service
NJ New Jersey
nm Nanometres
nM Nanomoles per litre
nmol Nanomoles
NMR Nuclear magnetic resonance
NOS Nitric oxide synthase
NRK Normal rat kidney
Ω Ohms
o Ortho
$O_2^{\cdot -}$ Superoxide
***O*-GlcNAc** *O*-linked *N*-acetylglucosamine

OGT Uridine diphospho-*N*-acetylglucosamine:polypeptide β-*N*-acetylglucosaminyltransferase
PAGE Polyacrylamide gel electrophoresis
PAI-1 Plasminogen activator inhibitor 1
PAP Peroxidase anti-peroxidase
$\boldsymbol{P_{app}}$ Apparent permeability
PARP Poly (ADP-ribose) polymerase
PASM Periodic acid-silver methenamine [Doyle and Campbell, 1976]
PBS Phosphate buffered saline
PCR Polymerase chain reaction
PDGF Platelet derived growth factor
PDH Pyruvate dehydrogenase
PDR Proliferative diabetic retinopathy
PGO Peroxidase and glucose oxidase
pH Power of hydrogen
pI Isoelectric point
$\mathbf{P_i}$ Inorganic phosphate
$\mathbf{PP_i}$ Inorganic pyrophosphate
PI3K Phosphoinositol 3-kinase
$\boldsymbol{pK_a}$ Acid dissociation constant
PKC Protein kinase C
pmol Picomoles
PPAR-γ Peroxisome proliferator-activated receptor-gamma
PPP Pentose phosphate pathway
pRb Retinoblastoma protein
Pse Pseudaminic acid (5,7-diacetamido-3,5,7,9-tetradeoxy-L-glycero-L-manno-nonulosinic acid)
PTEC Proximal tubule epithelial cell
PVDF Polyvinylidene fluoride
PVP Polyvinylpyrrolidone
Q Glutamine
qPCR Quantitative polymerase chain reaction
q.s. *Quantum sufficit*—As much as is necessary
R5P Ribose-5-phosphate
RAAS Renin-angiotensin-aldosterone system
RBC Red blood cell
RDI Reference daily intake
REC Regional ethics committee
RFC-1 Reduced folate carrier 1
RNA Ribonucleic acid
ROS Reactive oxygen species
RT Reverse transcriptase
s Seconds
S7P Sedoheptulose-7-phosphate
SD Standard deviations
SDS Sequence Detection System or sodium dodecyl sulphate
Ser Serine

SL2 Schneider line 2
SOD Superoxide dismutase
Sp1 Specificity protein 1 or stimulating protein 1
SP2 Service pack 2
SPE Solid phase extraction
SPSS Statistical Package for the Social Sciences
SUMO Small ubiquitin-like modifier
sVCAM-1 Soluble vascular cell adhesion molecule 1
T Thymine
$t_{1/2}$ Half life
$t_{5\%}$ Time for a 5% decay
TAF TBP-associated factors
TBP TATA binding protein
TBS-T Tris buffered saline with 0.1% v/v Tween-20
TCA Trichloroacetic acid
TEMED *N*,*N*,*N*',*N*'-tetramethylethylenediamine
TFA Trifluoroacetic acid
TGF-α or -β Transforming growth factor alpha or beta
TGFR Transforming growth factor receptor
THF Tetrahydrofuran
THM Thiamine
Thr Threonine
THTR-1 Thiamine transporter 1
THTR-2 Thiamine transporter 2
TIMP Tissue inhibitor of metalloproteinases
TK or TKT Transketolase
TMP Thiamine monophosphate
TPI Triose phosphate isomerase
TPP Thiamine pyrophosphate
Tris Tris(hydroxymethyl)aminomethane
TRMA Thiamine-responsive megaloblastic anaemia
TTFD Thiamine tetrahydrofurfuryl disulphide (Fursultiamine)
TTP Thiamine triphosphate
Tween-20 Polyethylene glycol sorbitan monolaurate
TX Texas
TXNIP Thioredoxin interacting protein
Tyr Tyrosine
U Enzyme units
UAE Urinary albumin excretion
UCP1 Uncoupling protein 1
UCSF University of California, San Francisco
UDP Uridine 5'-diphosphate
UDP-Glc Uridine 5'-diphosphoglucose
UDP-GlcNAc Uridine 5'-diphospho-*N*-acetylglucosamine
UK United Kingdom

UKPDS United Kingdom Prospective Diabetes Study
UMOD Uromodulin
USA United States of America
UTP Uridine 5'-triphosphate
UV Ultraviolet
v Version
V Volts
v/v Volume for volume
VA Virginia
VEGF Vascular endothelial growth factor
vWF von Willebrand factor
W Watts
WHO World Health Organisation
WHR Waist-hip ratio
w/v Weight for volume
w/w Weight for weight
X5P Xylulose-5-phosphate
Xyl Xylose
ZDF Zucker diabetic fatty

Chapter 1

Introduction to diabetes

1.1 Definition and classification

Diabetes mellitus is a chronic disease of sugar metabolism relating to the hormone insulin. It is increasing in incidence to epidemic proportions globally and is divided into two main subtypes. Type 1 diabetes is insulin-dependent and occurs when the body does not produce insulin or produces a defective insulin; type 2 diabetes is traditionally non-insulin-dependent and occurs when the body becomes less responsive to available insulin. In both types, the outcome is an increased fasting plasma glucose concentration from between 3–7 mM to 7–30 mM [American Diabetes Association, 2010a].

1.2 Aetiology and prevalence

Type 1 diabetes is characterised by an auto-immune mediated destruction of pancreatic β-cells, often developing early in life. Pre-clinical histological analysis of the diabetic pancreas reveals a state of insulitis, characterised by the infiltration of a large population of mononuclear lymphocytes responsible for attacking the β-cells [Gepts and Lecompte, 1981; Qu et al., 2003]. Most of the attacking cells are T-cells (some $CD4^+$ with a majority of $CD8^+$) along with a small subset of macrophages and B-cells (reviewed by Bach [1994]). Despite this sustained attack on the only cells capable of producing insulin, over 80% of β-cells must be destroyed before clinical symptoms become apparent [Gepts, 1984]. The cause of this auto-immune attack is not clear. There is a sizeable genetic element to the disease—studies with twins and type 1 diabetes have consistently shown that there is a

higher concordance rate for monozygotic than dizygotic twins [Kyvik et al., 1995; Kaprio et al., 1992; Lo et al., 1991]. However, monozygotic concordance is only 40% which leaves a substantial non-genetic environmental component to the disease. Genetic susceptibility to type 1 diabetes is not only linked to autoimmune attack of the β-cells. Kida [1999] demonstrated that the insulin gene (chromosome 11p15.5) is linked to type 1 diabetes with symptoms arising through the manufacture of a defective insulin, not through destruction of the β-cells.

Type 2 diabetes is not traditionally a disease of young people and tends to develop later in life. Its progression is more gradual than type 1 diabetes and clinical symptoms often follow a period of symptom-free pre-diabetes. Pre-diabetes is often associated with impaired glucose tolerance (IGT), impaired fasting glucose (IFG) and other risk factors which combine in a state called the metabolic syndrome. Metabolic syndrome is a collection of risk factors for coronary heart disease (CHD) and there is a strong link between these risk factors and incidence of type 2 diabetes. Its World Health Organisation (WHO) definition is outlined in Figure 1.1. Despite its use as an educational concept, a recent WHO working party concluded that the metabolic syndrome has limited practical use as a diagnostic or clinical management tool [Simmons et al., 2010].

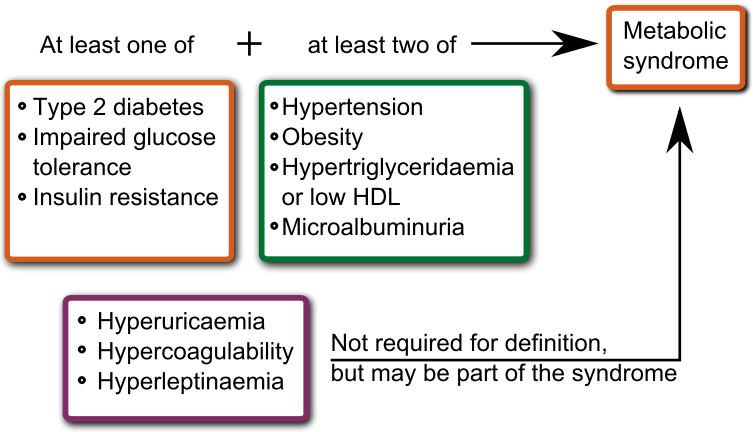

Figure 1.1: Metabolic syndrome as defined by the World Health Organization [1985]. Insulin resistance is defined as being within the highest quartile for the relevant population. Hypertension is defined as blood pressure (BP) $\geq$140/90 mmHg. Obesity is defined as a body mass index (BMI) $\geq$30 kg m^{-2}, or a waist-hip ratio (WHR) >0.90 for males and WHR >0.85 for females. Hypertriglyceridaemia is defined as $\geq$1.7 mM triglycerides. Low high-density lipoprotein (HDL) is defined as <0.9 mM for men; <1.0 mM for women. Microalbuminuria is a urinary albumin excretion (UAE) rate $\geq$20 µg min^{-1} or an albumin creatinine ratio $\geq$30 mg mmol^{-1}. Adapted with permission from Zimmet et al. [2001].

The number of diagnosed diabetes patients in the UK has increased from around 1.4 million in 1996 to 2.6 million today, around 4.3% of the population [Diabetes UK, 2010]. By 2025, Diabetes UK estimates that there will be around 4 million diagnosed diabetes patients. Most of these patients will have type 2 diabetes driven by an ageing population and an increasing incidence of obesity [Dixon, 2010]. Indeed, Thomas et al. [2005] have estimated that one fifth of older men and women in the UK (aged 60–79) currently have either impaired glucose tolerance or undiagnosed diabetes. Within the UK, 90% of adult diabetic patients have type 2 diabetes and only 10% have type 1 diabetes. Children of age 17 and under have predominantly type 1 diabetes with 97% of diagnosed diabetic children being type 1 patients. The prevalence of type 1 diabetes in UK children is around one case per 700–1000 population for a total of around 21 500 under-18s with type 1 diabetes. Type 2 diabetes has historically not been evident in children but this trend is changing recently. The first cases of type 2 diabetes in children were diagnosed in overweight girls aged 9–16 of Indian, Pakistani or Arabic ethnic origin [Ehtisham et al., 2000] with the first cases in Europid children being diagnosed two years later [Drake et al., 2002]. Children of South Asian origin are 13 times more likely to have type 2 diabetes than white children [Ehtisham et al., 2004].

Globally, the estimated diabetes prevalence is 285 million (4.3% of the population, as in the UK) and is expected to rise to affect 438 million people by 2030 with the economic and social impact expected to be greatest in developing countries [Diabetes UK, 2010; International Diabetes Federation, 2009]. In response to the predicted scale of the epidemic, the United Nations has passed a resolution which declared that diabetes is an international public health issue [Atkins and Zimmet, 2010]. Within the UK, 10% of the NHS budget is now spent on diabetes care. This figure is around £9 billion per year, equivalent to £286 per second or £150 per capita per annum.

1.3 Historical perspective

Diabetes was known to antiquity with the Greeks first coining the term diabetes, $\delta\iota\alpha\beta\acute{\eta}\tau\eta\varsigma$, meaning "siphon" and referring to the large quantities of urine produced by diabetic patients [Kirchhof et al., 2008]. In 1675, Thomas Willis added the suffix *mellitus* meaning honey to signify the sweet taste of the urine. Diabetes insipidus is the other main form of diabetes and has similar symptoms including increased urination (polyuria) and increased thirst (polydipsia). However, diabetes insipidus is caused by hormonal imbalances producing more

urine directly e.g. antidiuretic hormone deficiency [Onuigbo and Skalski, 2010]. Due to the lack of glucose, urine produced by in this manner is not sweet. The distinction between type 1 and type 2 diabetes was first made by Harold Himsworth who recognised the difference between insulin-sensitive and insulin-insensitive diabetes pathologies [Himsworth, 1936].

Despite knowledge of the symptoms, diabetes remained difficult to treat. Before the differentiation of type 1 and type 2 diabetes, they were identified and treated as one disease. Various dietary treatments were used with limited success throughout the 19th century. The role of the pancreas in glucose metabolism was not understood until 1889 when two Germans, Joseph von Mering, a doctor, and Oskar Minkowski, a scientist, removed the pancreas from a dog and discovered that it developed all the symptoms of diabetes before dying shortly after [v. Mering and Minkowski, 1890]. By 1910, Edward Sharpey-Schafer had made progress with understanding the function of the pancreas. He had discovered that the islets of Langerhans within it produced the chemical used to control glucose metabolism which he called insulin from "insula", the Latin for "island". This was followed by the 1921 discovery in Canada by Frederick Banting and Charles Best that an extract of islets from a healthy dog could cure a diabetic dog of its disease. Their subsequent work led to the purification of insulin which was first injected as a treatment into a diabetic patient in 1922 [Banting et al., 1991]. Fourteen year old Leonard Thompson, who received the insulin, lived for 21 more years after his first treatment due to regular dosing with insulin—an outcome not previously imaginable.

1.4 Diagnosis and symptoms

In modern times, type 1 diabetes is often diagnosed early in life after patients have presented with symptoms such as increased thirst, increased urine production or unexplained weight loss. Criteria established by the World Health Organization [1999] allow diagnosis based on one of several characteristics including a fasting plasma glucose $\geq$7 mM or a plasma glucose $\geq$11.1 mM two hours after an oral glucose tolerance test (glucose loads vary for children at 1.75 g per kg body mass with a standard 75 g dose for adults). Additional diagnosis criteria are recommended by other organisations. For example, the American Diabetes Association recently suggested that an HbA_{1c} of $\geq$6.5% is also a valid diagnostic criterion [American Diabetes Association, 2009, 2010b].

The primary symptoms of diabetes noticeable to a patient are polydipsia coupled with a dry mouth, polyuria, weakness and fatigue, loss of weight and blurred vision. As the

disease progresses, secondary complications arise including nephropathy, retinopathy and neuropathy (Sections 1.6.2, 1.6.4 and 1.6.3). It is these secondary complications which are the main burden of the disease, not only on the patient but also on the economy.

1.5 Therapy

Therapies for diabetes are wide-ranging and address associated risk factors such as dyslipidaemia and hypertension as well as attempting to maintain a normal blood glucose concentration. Maintaining good glycaemic control is key in reducing the risk of microvascular complications [The Diabetes Control and Complications Trial Research Group, 1993; UK Prospective Diabetes Study (UKPDS) Group, 1998; Stratton et al., 2000; Stolar, 2010]. To achieve this goal a variety of therapeutic strategies are employed.

The therapy of type 1 diabetes is dependent on the administration of insulin. Modern therapy uses recombinant human insulin produced in *E. coli* or yeast rather than insulins purified from animals. Insulin therapy has advanced considerably over time and there is now a wide range of insulins available for different uses. Despite this, there has been no effective therapy developed that provides normal glycaemic control for patients with type 1 diabetes. Until that time, insulin therapy supplemented with careful diet control will remain the most important strategy.

For some type 2 diabetes patients it may be possible to maintain adequate glycaemic control through dietary restriction alone, especially if diagnosed early [Gross et al., 2005]. More often, pharmacological intervention is required. The United Kingdom Prospective Diabetes Study (UKPDS) group have shown that more intensive control of blood glucose is key in controlling microvascular complications in patients with type 2 diabetes. Patients studied over a ten year period showed a significant 12% reduction in risk with intensive glycaemic control when compared to conventional therapy for any diabetes endpoint [UK Prospective Diabetes Study (UKPDS) Group, 1998]. This 12% decrease corresponded to a change in HbA_{1c} from a median of 7.9% to 7.0%. The UKPDS also showed a strong link between glycaemic control and microvascular complications: a 1% decrease in HbA_{1c} across the cohort decreased microvascular complications by 37% [Stratton et al., 2000]. Thus, a key target for pharmacological intervention is a reduction in the plasma glucose concentration and it is upon this premise that many diabetic therapies are based.

Treatment of type 2 diabetes often starts with a single oral agent before progressing as the need arises to multiple agents, possibly including insulin [Blonde, 2009]. There

are many classes of drugs available for clinicians to choose from and these are summarised in Table 1.1. Often, drugs are combined to form a more convenient therapy such as the GlaxoSmithKline product Avandamet which combines the thiazolidinedione rosiglitazone with metformin. Recently there have been problems highlighted regarding the use of tight glycaemic control as a target for therapy. The Action to Control Cardiovascular Risk in Diabetes (ACCORD) trial investigated the effects of intensive glycameic control versus regular glycaemic control in 10 250 type 2 diabetic patients over a mean 3.5 years of follow-up. The ACCORD group concluded that relative to the regular therapy group, the intensive therapy group had an increased relative and absolute risk of mortality during the follow-up period with no decrease in risk of cardiovascular events [Action to Control Cardiovascular Risk in Diabetes Study Group et al., 2008]. They propose that this increased risk in mortality may be due to increases in hypoglycaemic episodes, effects of the multiple drugs in combination required to lower the plasma glucose and unforseen effects of rapidly lowering plasma glucose. More recently, the ACCORD group also concluded that targeting systolic blood pressure to lower than 120 mmHg compared to lower than 140 mmHg did not reduce a composite outcome of fatal and non-fatal cardiovascular events [ACCORD Study Group et al., 2010]. There has also been controversey over the use of some thiazolidinediones as therapies in type 2 diabetic patients. Both rosiglitazone [Nissen and Wolski, 2007] and to a lesser extent pioglitazone have been linked to an increased risk of cardiovascular events in type 2 diabetes patients due to increased water retention (reviewed by Stafylas et al. [2009]). Only recently, pioglitazone was looked upon as a promising agent to lower risk of cardiovascular events due to its favourable effect on patient lipid profiles [Betteridge, 2007]. Even now, the situation is not clear because the beneficial effects of pioglitazone may outweigh the harmful effects [Erdmann et al., 2009].

1.6 Chronic complications of diabetes mellitus

1.6.1 Micro and macro-vascular complications

Since the introduction of insulin therapy, chronic diabetic complications have been the major cause of morbidity and mortality associated with the disease [Deckert et al., 1978]. Diabetic complications can be broadly divided into categories based on the size of blood vessels affected. Macrovascular complications affect larger vessels and include coronary heart disease (CHD) and stroke. Microvasular disease affects tissues which rely on the non-insulin-dependent glucose transporter GLUT-1 for their glucose uptake. These tissues are prone to

Drug class	Description	Example drugs
Biguanides	Biguanides are a class of drugs that lower hepatic gluconeogenesis and increase peripheral insulin sensitivity, thereby lowering plasma glucose [Kirpichnikov et al., 2002]. The more modern metformin is associated with a much lower risk of lactic acidosis than the now withdrawn phenformin. Unlike other therapies, biguanides do not raise the risk of hypoglycaemia and are not associated with weight gain.	Metformin
Sulpohonylureas	Sulphonylureas stimulate pancreatic insulin production thereby lowering plasma glucose. They may be associated with hypoglycaemia and weight gain through decreased glycosuria and increased caloric intake to combat hypoglycaemia.	Glimepiride, chlorpropamide
Meglitinides	Meglitinides (including D-phenylalanine derivatives) are taken prior to food and stimulate the pancreas to produce more insulin by binding to and inhibiting an ATP-dependent K^+ channel. This is similar to the sulphonylureas but at a separate binding site. The binding to the K^+ channel leads ultimately to an opening of voltage-dependent Ca^{2+} channels and concomitant release of insulin. Due to their similar mode of action, they share side-effects with the sulphonylureas including hypoglycaemia and weight gain. Meglitinides are known together with sulphonylureas as insulin secretagogues.	Repaglinide, nateglinide
Thiazolidinediones	Thiazolidinediones are insulin sensitizers and increase insulin sensitivity in muscle, adipose tissue and the liver. Hypoglycaemia is uncommon but weight gain due to re-distribution of adipose tissue and fluid retention is relatively common. Other side effects include congestive heart failure, anaemia and an increased risk of pregnancy, even with contraceptive pills.	Pioglitazone, rosiglitazone
α-Glucosidase inhibitors	α-Glucosidase inhibitors are administered with food and decrease the post-prandial glucose spike by reducing the digestion speed of disaccharides. This lowered speed increases the quantity of carbohydrate which enters the lower intestine where gut flora act on it to produce relatively large quantities of gas. Other side effects include bloating, stomach pain and diarrhoea [Godbout and Chiasson, 2007]	Miglitol, acarbose
Insulin	Insulin and its analogues are the most direct and effective antihyperglycaemic agents available. They are given by injection since oral administration leads to digestion and low bio-availability. The risk of hypoglycaemia is relatively high and they often lead to significant weight gain. [Purnell and Weyer, 2003]	Insulin, recombinant insulins e.g. insulin glargine
Dipeptidyl peptidase (DDP) IV inhibitors	Dipeptidyl peptidase IV plays a major role in glucose metabolism because of its role degrading incretins such as glucagon-like peptide 1 (GLP-1). DPP-IV inhibitors work by raising levels of insulin production and lowering glucagon release, both of which lower blood glucose concentrations [McIntosh et al., 2005]. Side effects include a runny nose, a sore throat and a headache.	Sitagliptin, saxagliptin
Incretin mimetics	Exenatide is a GLP-1 receptor agonist and shares many of the same glucoregulatory properties of endogenous GLP-1. It is injected daily. [Stonehouse et al., 2008; Drucker, 2006]	Exenatide

Table 1.1: Drugs available to treat diabetes subdivided by class of action

high intracellular glucose concentrations during periods of hyperglycaemia and include the retina and the kidney (sites of retinopathy and nephropathy respectively) which have dense networks of capillaries. Other tissues with poor circulation through capillary beds are also affected e.g. the extremities of the limbs where neuropathy is common.

The macrovascular cardiovascular disease (CVD) is the largest single cause of morbidity and mortality amongst diabetic patients: it is cited as the cause of diabetic mortality in 65% of cases in the USA [Engelgau et al., 2004]. The UKPDS group also observed that macrovascular complications were over twice as common and 70 times more likely to be fatal as microvascular complications in diabetes patients after 9 years of follow-up [Turner et al., 1996]. This means that whilst preventing macrovascular complications is likely to extend lives, unless the microvascular complications are also addressed, the quality of those lives is likely to be lower than necessary or desired.

1.6.2 Diabetic nephropathy

Diabetic nephropathy (DN) is a pathology of the kidney which is defined symptomatically by an increase in albumin excretion in the urine without the presence of other renal diseases. DN affects approximately 40% of type 1 and type 2 diabetic patients throughout their lives [Gross et al., 2005], and is associated with increased morbidity and mortality from cardiovascular effects. The percentage of patients starting renal-replacement therapy due to DN-associated end-stage renal disease (ESRD) is globally variable but in the USA it is 40% [US Renal Data System, 2009] and is a maximum in Malaysia where it is 58% [Williams, 2010].

1.6.2.1 Progression

DN has a progressive pathology with the disease being categorised into different stages depending on the severity of the albumin excretion. Type 1 diabetes patients have a relatively well-defined disease progression from the mildest forms of the disease because diagnosis is during the earliest stages [Najafian and Mauer, 2009]. Type 2 diabetes patients have a less well defined progression since the diabetes, and the associated period of pre-diabetes, may have gone undiagnosed for a period of years.

The first stage is present at diagnosis and is characterised by acute renal hypertrophy and hyperfiltration. This takes the form of increased kidney and glomerular size accompanied by a 20–50% increase in glomerular filtration rate (GFR). Urinary albumin excretion (UAE) is usually in the normal range at this stage and the patient's blood pressure

is usually normal. Within the first five years after diagnosis, patients progressively develop a thickening of the glomerular basement membrane and tubular basement membrane along with accumulation of extracellular matrix (ECM; mainly fibronectin, laminin and collagens IV and VI [Bruneval et al., 1985; Ayo et al., 1990]) material in the tubulointerstitium and mesangium. This is seen histologically as a thickening of the affected areas as well as possible Kimmelstiel-Wilson nodular lesions in the mesangium ([Scheinman et al., 1978] and reviewed by Mason and Wahab [2003]). This whole process, called glomerulosclerosis, is the physical hallmark of DN. Figures 1.2 and 1.3 show the progression of glomerulosclerosis with Figure 1.4 showing the details of a thickened basement membrane. The initial increase in filtration rate seen in DN is caused by an increase in the glomerular hydrostatic pressure but as glomerulosclerosis progresses it causes scarring and progressive loss of glomerular function. This stage is still characterised by normal UAEs of $<20\,\mu g\,min^{-1}$ or $30\,mg\,day^{-1}$.

Although timings are not exact, between 7–15 years after diagnosis some patients develop microalbuminuria, or incipient nephropathy. This is defined by a UAE of $>20\,\mu g\,min^{-1}$ and $\leq 199\,\mu g\,min^{-1}$ ($>30\,mg\,day^{-1}$ and $\leq 300\,mg\,day^{-1}$). GFR is still supranormal at this stage and blood pressure is typically increasing at a rate of $3\,mmHg\,year^{-1}$. Some of these microalbuminuric patients will progress to clinically persistent proteinuria (defined as a UAE $>200\,\mu g\,min^{-1}$ or $>300\,mg\,day^{-1}$). This marks the start of clinically overt renal disease and often occurs around 15–20 years after diabetes diagnosis. At this stage, there are clear abnormalities in the kidney structure, blood pressure is often high and increasing at around $5\,mmHg\,year^{-1}$ and GFR begins to decline steadily at a variable rate with a median about $12\,mL\,min^{-1}\,year^{-1}$. Within 10 years, 50% of type 1 diabetic patients with overt nephropathy progress to end stage renal disease (ESRD). This figure rises to more than 75% by 20 years [American Diabetes Association, 2004]. During ESRD, glomerular closure is complete and the GFR is $<10\,mL\,min^{-1}$. At this stage, the patient must move onto renal replacement therapy to survive. Typically patients start with peritoneal dialysis and progress to haemodialysis as complications arise. It is, however, more common for a macroalbuminuric patient to die of cardiovascular disease in any given year than to progress to more severe forms of nephropathy requiring renal replacement therapy [Adler et al., 2003].

The UKPDS estimated the rates of progression from normoalbuminuria to microalbuminuria to macroalbuminuria to elevated plasma creatinine or renal replacement therapy as 2.0%, 2.8% and $2.3\,\%\,year^{-1}$ respectively [Adler et al., 2003]. Generally, a patient will start with microalbuminuria and progress to albuminuria before developing overt nephropathy. Patients regressing from micro- to normoalbuminuria are an exception, not the rule.

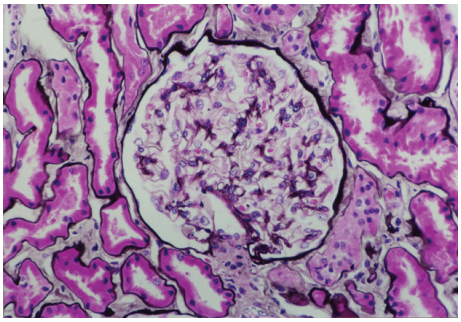

Figure 1.2: A histological section through a normal glomerulus without the diffuse thickening of the glomerular basement membrane. 240x magnification with periodic acid–silver methenamine (PASM) stain and haematoxylin and eosin (H&E) counter-stain. Reprinted with permission from Lai et al. [2004].

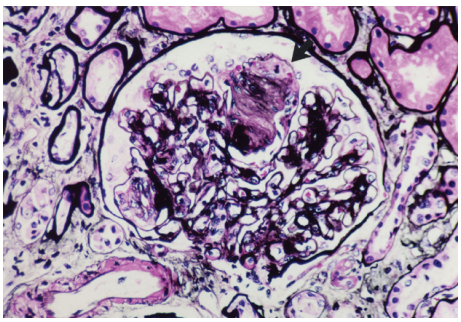

Figure 1.3: A histological section through a diabetic glomerulus exhibiting glomerulosclerosis with mesangial sclerosis and Kimmelstiel-Wilson nodule comprised of deposited mesangial matrix (arrowed). 240x magnification with PASM stain and H&E counter-stain. Reprinted with permission from Lai et al. [2004].

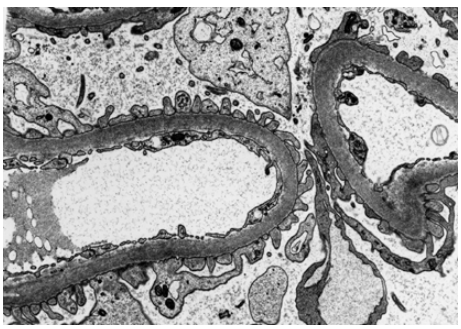

Figure 1.4: Uniform and homogeneous thickening of the glomerular capillary basement membrane. 4800x magnification using lead citrate and uranyl acetate electron microscopy. Reprinted with permission from Lai et al. [2004].

1.6.2.2 Diagnosis

The American Diabetes Association [2004] recommends that the albumin:creatinine ratio measured in a spot urine sample is used as the primary means to diagnose DN. Another method suggested is to measure the albumin content of a timed urine collection, typically 24 hours long. After diagnosis, GFR is commonly followed as a proxy for renal function. GFR may be determined by measuring the renal clearance rate of creatinine but this method is prone to overestimation due to the secretion of creatinine by the tubules. A more accurate method uses secretion of inulin, an exogenous plant-derived polysaccharide, which is completely filtered and neither re-absorbed nor secreted by the tubules. The GFR can then be suitably estimated using an equation similar to the Cockroft-Gault equation [Tsinalis and Thiel, 2009].

1.6.2.3 Risk factors

The rate of progression of DN from one stage to the next is influenced by a group of risk factors. Key members of this group include glycaemic control and arterial blood pressure. Maintaining good glycaemic control is key to lowering the risk of progression of nephropathy [The Diabetes Control and Complications Trial Research Group, 1993] and tight control of blood pressure lowers the risk of micro and macrovascular complications [UK Prospective Diabetes Study Group, 1998]. Normotensive patients have a slower rate of decline in GFR with respect to hypertensive patients [Hovind et al., 2001]. Other modifiable factors such as serum cholesterol and albuminuria act as progression markers [Hovind et al., 2001] whilst dyslipidaemia and smoking are risk factors. Non-modifiable risk factors for DN include age, a genetic predisposition and time since diagnosis of diabetes [Gross et al., 2005]. Genetic predisposition appears to be both complex and important since around 70% of type 1 and 60–75% of type 2 diabetic patients do not develop nephropathy, irrespective of glycaemic control. The genetics of DN is often based around propensity for developing certain risk factors such as hypertension and is reviewed by Schena and Gesualdo [2005].

1.6.2.4 The glomerulus

The glomerular capillary wall has three main layers: the epithelial podocyte cells face the urinary side, the endothelial cells face the circulatory side and the glomerular basement membrane with its associated mesangial cells lies in between [Steffes et al., 2001; Deen, 2004; Mathieson, 2009]. These layers act in combination to provide the complete glomerular filtration capability. The endothelial cells lining the capillary walls have large pores between

them called fenestrae which block the passage of erythrocytes and larger cells but do little to prevent passage of small molecules and proteins. Beyond the endothelial cells, the glomerular basement membrane provides the next filtration step. Secreted mainly by the mesangial cells, it is extensively covered in negatively charged glycosaminoglycans including heparan sulphate which form an effective barrier to prevent the passage of most plasma protein. Further filtration is achieved by the slit-like pores between the foot processes of the final cellular layer, the podocytes. Once past the podocytes and into Bowman's space, glomerular filtration is complete and the ultrafiltrate is free to pass down the proximal tubule.

1.6.2.5 Molecular pathology

Structural changes in the kidney during diabetes can be subdivided into early adaptive changes and later pathological changes associated with the progression of DN [Phillips, 2003]. The early changes, such as glomerular hypertrophy, are not indicative of progressive renal disease but the later changes are. The latter pathological changes are characterised by a gradual scarring of both the glomerulus and the tubulointerstitial region.

Traditionally DN was considered a predominantly glomerular disease with mesangial expansion and the thickening of the glomerular basement membrane being of primary importance. This view has changed more recently to include changes in the tubulointerstitial region as well as other cell types within the glomeruli. The hallmark of DN, the progressive deposition of extracellular matrix material, first manifests in the glomerulus before becoming more apparent in the tubulointerstitium as the disease progresses [Najafian and Mauer, 2009]. In both cases, the deposited material is predominantly made up of the ECM collagens type I, III, IV and VI and fibronectin [Mason and Wahab, 2003]. The abundance of ECM material is a function of both synthesis by mesangial cells and degradation by matrix metalloproteinases (MMPs). The synthesis rate is increased in DN, driven largely by an increase in transforming growth factor-β (TGF-β) signalling [Schena and Gesualdo, 2005] and is discussed more thoroughly below. Also, the degradation rate of ECM by MMPs is decreased in DN. Mesangial cells cultured in hyperglycaemic conditions exhibit increased expression and activity of plasminogen activator inhibitor 1 (PAI-1), decreased expression of MMPs and increased inhibition of MMPs by tissue inhibitor of metalloproteinase-1 (TIMP1) [Abdel Wahab and Mason, 1996].

There is also evidence that it is the podocytes that are key in the progression of DN, both prognostically and mechanistically. Work by Pagtalunan et al. [1997] showed that podocytes are lost in early stage DN and that each remaining podocyte spreads its foot pro-

cesses wider. Meyer et al. [1999] further showed that podocyte number is a key predictor for long term urinary albumin excretion in Pima Indians. Nakamura et al. [2000] demonstrated that DN patients had podocytes present in their urine whereas healthy volunteers did not. In 2005, evidence that experimentally-induced podocyte loss alone was sufficient to induce albuminuria and glomerulosclerosis was published by Wharram et al. [2005]. More recently, work by [Dessapt et al., 2009] demonstrated that either increased TGF-β expression or mechanical stretching is sufficient to decrease podocyte adhesion via reduced $\alpha 3\beta 1$ integrin expression. The evidence that hyperglycaemia and mechanical stress are both important factors in podocyte loss was reviewed by Lewko and Stepinski [2009].

The exact cause of the presence of albumin in the urine is not clear. Persistent albuminuria represents the result of leakage past the glomerular basement membrane at a rate that exceeds the metabolic and re-absorptive capacity of the proximal tubular epithelium. The classical view is that albuminuria is caused by a failure of the glomerular filter to retain albumin, either through loss of podocytes [Stitt-Cavanagh et al., 2009] or through changes in the glomerular basement membrane or through haemodynamic factors or a combination of all of the above [Ziyadeh, 2008]. The loss of the glomerular endothelial glycocalyx, mediated by growth factors and inflammatory cytokines in diabetes may be a key mechanism [Satchell and Tooke, 2008]. The timecourse for the regeneration of a lost glycocalyx after intevention of therapy is unkown but may be several weeks [Potter et al., 2009]. The alternative view explaining the presence of albuminuria in DN is that there could be a failure of the tubule reclamation and degradation pathways for albumin [Comper and Russo, 2008]. However, this view is controversial because there is direct evidence from two-photon microscopy that albumin is filtered very effectively in normal rat kidneys [Tanner, 2009].

1.6.2.6 The role of TGF-β

TGF-β is the collective name for a family of three multifunctional secreted proteins (TGF-β-1, TGF-β-2 and TGF-β-3) which signal through one of three membrane-bound transforming growth factor receptors (TGFRs), TGFR-1, TGFR-2 and TGFR-3. The receptors are serine/threonine kinases which collectively signal to a multidude of different down-stream processes. Importantly for DN, these down-stream processes include the deposition of ECM material during fibrosis. This process is naturally found during wound-healing after the release of TGF-β by platelets [Border and Noble, 1994] but is also found in disease states such as rheumatoid arthritis, radiation-induced fibrosis and myocarditis as well as DN [Pohlers et al., 2009].

The effects of TGF-β may be direct through the activation of a kinase cascade or propogated by induction of other factors such as connective tissue growth factor (CTGF). CTGF is an immediate early gene that can be induced by TGF-β [Grotendorst, 1997] and has been shown to be involved in both early and late-stage DN [Riser et al., 2000; Twigg et al., 2002]. Recently, CTGF has also been shown be induced by advanced glycation endproducts (AGEs) in a TGF-β-independent manner [Chung et al., 2010]. Increasing expression of TGF-β has been linked to many of the proposed pathways of hyperglycaemia-induced damage. Its expression is increased by hyperglycaemia [Murphy et al., 1999; Wahab et al., 2001], exposure to AGEs and ROS [Park et al., 2001] as well as *de novo* synthesis of diacylglycerol and subsequent activation of protein kinase C [Brosius, 2008]. Glycated proteins also appear to be partly involved in changes to the ECM: exposure of glomerular endothelial cells to glycated albumin causes increased expression of collagen IV and fibronectin [Cohen et al., 1997]. Also, podocytes and glomerular endothelial cells are less able to adhere to type IV collagen modified by methylglyoxal [Pedchenko et al., 2005; Dobler et al., 2006], potentially leading to anoikis. The proposed mechanisms behind increased ROS and AGE production are discussed in Section 1.7.

TGF-β abundance and activity in the kidney is controlled at multiple levels—trancription, translation, secretion and also by activation of the inactive form of the protein [Phillips, 2003]. Glucose is a potent stimulator of TGF-β transcription although higher abundances of the protein are often only observed after stimulation with a synergystic factor [Fraser et al., 2002]. Examples of such factors include platelet derived growth factor (PDGF) or interleukin-1β (IL-1β) [Phillips et al., 1996, 1997]. Hyperglycaemia-induced TGF-β transcription was blocked in primary rat mesangial cells by the addition of an Sp1-decoy oligodeoxynucleotide which blocks Sp1 binding to the promoter region of TGF-β [Chae et al., 2004]. TGF-β is also known to upregulate expression of glucose transporter 1 (GLUT-1) which promotes higher intracellular glucose concentrations through increased glucose upatake [Schena and Gesualdo, 2005]. Work by Heilig et al. [1995] demonstrated for the first time that overexpression of GLUT-1 in rat mesangial cells cultured in 8 mM glucose was sufficient to induce increased collagen synthesis in the same manner as culturing wild-type mesangial cells in 30 mM glucose. Follow up work demonstrated that knocking down GLUT-1 can prevent glucose-induced expression of GLUT-1 and fibronectin in mesangial cells [Heilig et al., 2001]. Most recently, Wang et al. [2010] have demonstrated that overexpression of GLUT-1 in mouse mesangial cells alone was sufficient to induce a renal disease similar to diabetic glomerulosclerosis in non-diabetic animals. This work demonstrates that

it is the intracellular, and not extracellular, concentration of glucose which is key in driving downstream effects such as the production of ECM proteins. This also introduces the idea of a positive feedback loop with hyperglycaemia inducing TGF-β expression which in turn promotes expression of GLUT-1 leading to still higher intracellular glucose concentrations.

TGF-β activity is not just found in one cell type; it has important roles throughout the glomerulus. Glomerular visceral epithelial cells exposed to hyperglycaemia upregulate both TGF-β and fibronectin expression [van Det et al., 1997]. Podocytes exposed to hyperglycaemia increase expression of the receptor TGFR-2 [de la Cruz et al., 2002] allowing for an autocrine or local paracrine signalling within the glomerulus [de la Cruz et al., 2002]. Thus the emerging picture is that TGF-β signalling is induced by hyperglycaemia and associated downstream effects, and is invovled in mediating the overproduction of ECM proteins as well as changes in cell population in the glomeruls leading to glomerulosclerosis and albuminuria.

1.6.3 Diabetic retinopathy

Diabetic retinopathy is the leading cause of new cases of blindness amongst adults aged 20–74 years [National Institute of Diabetes and Digestive and Kidney Diseases, 2008]. Its progression passes through four stages of increasing severity: mild, moderate and severe non-proliferative retinopathy followed by proliferative diabetic retinopathy (PDR). Symptoms progress in severity beginning with microaneurysms from the capillaries of the retina in mild non-proliferative retinopathy. The moderate and severe stages are both characterised by blockages in increasing numbers of retinal capillaries leading to localised ischaemia where parts of the retina are deprived of oxygen and nutrients. Eventually, larger sections of the retina become malnourished stimulating progression to proliferative retinopathy. In PDR these ischaemic sections signal for nutrient provision by the release of pro-angiogenic factors. Uncontrolled release of these factors leads to neovascularisation of the surface of the retina and vitreous humour characterised by a diffuse microvasculature with abnormally fragile walls. These new vessels do not cause blindness *per se* but because of their fragility they frequently leak blood into the humour which leads to severe vision loss.

Macular oedema is another factor which can cause vision loss associated with diabetic retinopathy. It is caused by fluid leakage into the central part of the retina, or macula, from damaged or fragile vessels leading to fatty deposits called exudate. This causes swelling in the macula and subsequently blurred central vision. In addition to these symptoms, patients may eventually experience retinal scarring or detachment. Figure 1.5 is an example image of the fundus of an eye exhibiting PDR. There are no warning symptoms of retinopa-

thy to the patient until vision begins to decline in proliferative retinopathy so frequent eye checks are recommended.

Risk factors for diabetic retinopathy include hypertension, duration since diabetes diagnosis and HbA_{1c} levels [Chatziralli et al., 2010]. Retinopathy is also more common in males than females. The best strategies for combating the advance of the disease include lowering blood pressure [Schrier et al., 2002] and tight glycaemic control [Diabetes Control and Complications Trial writing team, 2002; Prescrire Group, 2010]. In common with other diabetic complications, common pathways of damage have been implicated including protein kinase C activation, oxidative stress and increased AGE accumulation. In addition, PDR is characterised by a high level of growth factors in the vitreous humour such as insulin-like growth factor-1 (IGF-1) and vascular endothelial growth factor (VEGF) [Simó et al., 2002].

As well as minimising risk factors, early diagnosis is key to preventing vision loss. If prevention strategies do not work, retinal photocoagulation is the standard treatment for PDR. Photocoagulation was developed in the 1950s and uses a laser to denature protein and seal vessels. It causes some scotomas, or areas of visual darkening, but overall the effect on the visual field is minor compared to the total blindness which could develop in untreated PDR. Figure 1.6 is an image of a retina after photocoagulation. As well as sealing vessels, photocoagulation decreases production of vasoproliferative factors such as VEGF [Aiello et al., 1994]. Other strategies for VEGF reduction include anti-VEGF drugs including pegaptanib (Macugen™ [Cunningham et al., 2005]), bevacizumab (Avastin™ [Scott et al., 2007]) and ranibizumab (Lucentis™ [Nguyen et al., 2006]) injected intraocularly. A final strategy is to use a vitriectomy for patients with advanced vision loss.

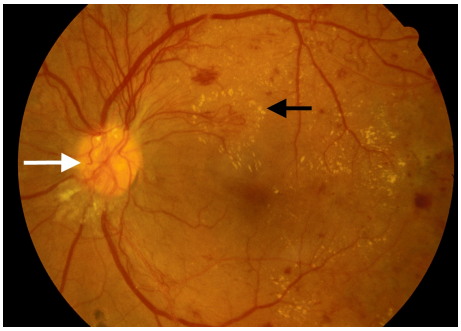

Figure 1.5: Ophtalmogram showing details of proliferative diabetic retinopathy with active neovascularisation over the optic disk (white arrow) and deposition of exudate around the neovascularisation of the macula i.e. macular oedema (black arrow) (UCSF Department of Ophthalmology)

1.6.4 Diabetic neuropathy

Diabetic neuropathy is the most common microvascular complication of diabetes, affecting high percentages of all diabetic patients (up to 50% depending on the study [Boulton, 2005]). It is a major contributor to the "diabetic foot"—a term encompassing a wide variety of problems including ulcers [Boulton, 2008]—with at least 15% of diabetic patients being affected by foot ulcers at some point [Brem and Tomic-Canic, 2007]. Diabetic neuropathy is the leading cause of non-traumatic limb amputation with around 60% of non-traumatic lower limb amputations in the US occurring in diabetic patients [National Institute of Diabetes and Digestive and Kidney Diseases, 2008].

There are four main types of neuropathy. The first and most common is peripheral neuropathy which is diffuse and starts as a loss of feeling in limbs or a lack of control. It often develops into shooting pains and numbness in the extremities although not all patients experience painful symptoms. In these cases, small wounds often go unnoticed and untreated which leads to the development of more complex lesions including ulcers [Brem and Tomic-Canic, 2007]. The second type is autonomic neuropathy which is characterised by damage to the unmyelinated nerves throughout the autonomic nervous system [Ewing and Clarke, 1982]. Symptoms include poor digestion, erectile dysfunction and incontinence. The third type, proximal neuropathy is characterised by weakness of the legs accompanied by pain in the hips and upper leg whilst the fourth type, focal neuropathy, is characterised by a sudden weakness or pain caused by a single nerve or group of nerves.

In all cases, neuropathy progression is associated with a steady lowering of nerve conduction velocities [Brown et al., 2004]. Research published by the Diabetes Control and Complications Trial writing team [2002] identifies hyperglycaemia as the main risk factor

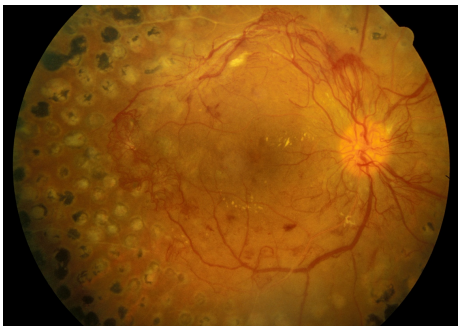

Figure 1.6: Ophtalmogram showing scatter photocoagulation scars on the fundus of an eye in a PDR patient (UCSF Department of Ophthalmology)

for neuropathy and states that tight glycaemic control is the best approach for lowering incidence and severity. Other risk factors include age, hypertension, dyslipidaemia and smoking status. As with other diabetic complications, the pathogenesis of neuropathy is connected to increased oxidative damage, increases in flux through the hexosamine and polyol pathways, increases in AGEs and the activation of protein kinase C [Brownlee, 2001]. As a specific example, glycation damage by glucose and methylglyoxal to laminin, fibronectin and collagens I and IV in the ECM around neurons leads to impairment of axon re-growth [Öztürk et al., 2006; Duran-Jimenez et al., 2009].

As a supplement to tight glycaemic control, there are several possible palliative therapies for neuropathy. These include a wide range of drugs that include local anaesthetics such as lidocaine, anticonvulsants such as gabapentin (also the gold standard for chronic pain) [Boulton, 2005], and other alternatives such as topical capsaican which depletes the tissue of substance P thereby reducing nervous transmission of pain [Zhang and Po, 1994]. Other strategies which target the pathogenesis of the disease are discussed in Section 1.8.

1.7 Biochemical theories on mechanisms of hyperglycaemia-induced damage

The five main hypotheses concerning the mechanism of glucose-induced damage in diabete are: increased polyol pathway flux; increased accumulation of advanced glycation endproducts (AGEs); activation of protein kinase C (PKC); increased flux through the hexosamine pathway and oxidative stress [Brownlee, 2001]. Each of these is outlined below.

1.7.1 Polyol pathway flux

The polyol pathway, also called the sorbitol-aldose reductase pathway, is a two step pathway that converts glucose to fructose via sorbitol (Figure 1.7). Aldose reductase (AR), which converts glucose to sorbitol, was first described as being capable of reducing glucose by Hers [1956]. Subsequently, van Heyningen [1959] showed that there is a high AR activity in rat lenses and that there is an accumulation of polyols in the lens during formation of diabetic 'sugar' cataract formation. AR has a relatively high K_{m} for glucose of around 200 mM [Jedziniak et al., 1981]. This means that at physiological concentrations (3–7 mM) there is only a small flux from glucose to fructose. This situation changes, however, in the hyperglycaemic environment found in diabetic patients where an increased intracellular

glucose concentration leads to increased production of sorbitol with a concomitant lowering in the concentration of NADPH. It is worth noting that sorbitol dehydrogenase (Figure 1.7) has a K_{m} for sorbitol of only 1.4 mM and is unlikely to limit the flux through the pathway [Jedziniak et al., 1981].

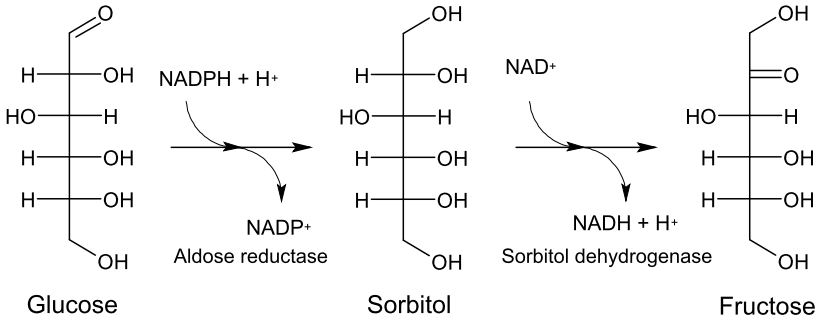

Figure 1.7: The reactions of the polyol pathway

In the hyperglycaemic state there is a relatively large flux through the polyol pathway varying from 33% of total glucose in rabbit lens to 11% in human erythrocytes [Brownlee, 2001]. There were several competing theories as to how this increased flux could be detrimental to the cells. The first was the sorbitol osmotic stress theory which proposed that sorbitol is membrane-impermeable and high concentrations of sorbitol would therefore accumulate, producing osmotic stress and damage to cells. In favour of this theory, high concentrations of sorbitol have been found in the lenses of diabetic rats. In contrast, sorbitol permeases have been found in human erythrocytes [Kracke et al., 1994], schwannoma cells [Mizisin et al., 1997] and rat renal inner medullary interstitial cells [Schüttert et al., 2002] which could potentially relieve any osmotic stress. These osmotic effects could therefore be limited to certain cell types lacking sorbitol permeases.

A more recent proposal is that the shift in the NAD^+:NADH ratio in favour of NADH, as effected by sorbitol dehydrogenase, is the resposible for the damage induced by increased polyol pathway flux. This shift in ratio would have the effect of inhibiting glyceraldehyde-3-phosphate dehydrogenase (GAPDH), an enzyme dependent on NAD^+ as a substrate. As the NAD^+ pool decreased GAPDH would become less active, which in turn would increase the concentrations of the glycolytic precursors glyceraldehyde-3-phosphate and dihydroxyacetone phosphate [Williamson et al., 1993]. These would act not only as precursors for AGE formation but also for diacylglycerol (through α-3-glycerophosphate) which activates protein kinase C; both are discussed later.

It is also proposed that the reduction in NADPH as a result of the activity of aldose reductase leads to an increase in oxidative stress: NADPH is required for the regeneration of reduced glutathione (GSH). Evidence for this theory was put forward by Lee and Chung [1999] who observed decreased concentrations of glutathione in the lenses of mice that overexpressed aldose reductase. The clinical effects of the inhibition of aldose reductase vary between different models. The aldose reductase inhibitor zenarestat increased nerve-conduction velocity in a dose-dependent manner in a double-blind placebo-controlled trial in humans [Greene et al., 1999]. The increase in oxidative stress as a result of decreased NADPH availability is a recurring theme and is also important for consideration of the pentose phosphate pathway and thiamine metabolism.

1.7.2 Advanced glycation endproducts

The second proposed mode of action of hyperglycaemia is though the production of advanced glycation endproducts (AGEs)—a term coined by Cerami [1986]. AGEs are formed when glycating agents react non-enzymatically with target molecules including proteins, lipids and nucleic acids thereby altering the shape or function of the target [Thornalley et al., 1999]. There are at least four main glycating agents in cells: glucose, glyoxal (formed from lipid peroxidation, the degradation of glycated proteins and the auto-oxidation of glucose), methylglyoxal (formed from the fragmentation of triose-phosphates, acetone metabolism and the catabolism of threonine) and 3-deoxyglucosone (formed from the degradation of glucose-modified proteins and fructosamines phosphorylated by fructosamine 3-phosphokinase).

The formation of the toxic α-oxoaldehyde methylglyoxal is an unavoidable corollary of glucose metabolism via glycolysis (the Embden-Meyerhof pathway). One of the glycolytic intermediates, dihydroxyacetone phosphate, is relatively unstable and is capable of undergoing spontaneous dephosphorylation to yield methylglyoxal [Thornalley, 2003a]. It is not possible to eliminate this conversion but its flux is diminished by keeping the steady state concentrations of triose-phosphates as low as possible. The net result is that these dicarbonyl compounds account for only 0.1–0.4% of the glycolytic flux [Thornalley, 2003a].

The glyoxalase system exists to detoxify these molecules and convert them to the relatively harmless D-lactate. The system comprises two enzymes, glyoxalases I and II (GLO1 and GLO2 respectively) along with a catalytic amount of reduced glutathione (GSH) [Lohmann, 1932]. Methylglyoxal reacts non-enzymatically with GSH to form a hemithioacetal which is then converted to *S*-D-lactoylglutathione by GLO1 [Marmstål and Mannervik, 1981]. GLO2 then recovers the GSH from the *S*-D-lactoylglutathione yielding D-lactate in

the process. The majority D-lactate is metabolised by mitochondrial 2-hydroxyacid dehydrogenase [Tubbs, 1965]. Despite the specificity constant for GLO1 ($k_{\mathrm{cat}}/K_{\mathrm{m}}$) being close to the limit of diffusion, damage to molecules can still be caused by dicarbonyl molecules escaping the system.

AGE production can damage three main classes of protein. The first is intracellular proteins. Glycation of these can affect their structure and function, often by damaging critical residues such as arginines in active sites which are more chemically reactive and more prone to glycation. Secondly, extracellular matrix proteins can be damaged. These modified proteins then interact abnormally with both other extracellular matrix proteins and with integrins on the surface of cells [Dobler et al., 2006]. The third class of proteins which can be damaged is plasma proteins. Damage here can lead to proteins which bind to receptors on endothelial, mesangial and macrophage cells causing receptor-mediated production of ROS. AGE receptor activation activates the transcription factor NF-κB which causes pathological changes in gene expression. AGEs are found in increased concentrations in streptozotocin-induced diabetic rat retinas, glomeruli and nerves as shown by mass spectrometric detection of analytes in the samples [Karachalias et al., 2003].

1.7.3 Activation of protein kinase C

The activation of protein kinase C (PKC) is the third proposed route of damage mediated by hyperglycaemia. There are at least 11 isoforms of PKC, of which 9 are activated by the same signalling molecule: diacylglycerol (DAG)—a lipid secondary messenger. The increased activity of PKC *in vivo* appears to be due to increased *de novo* DAG synthesis. DAG concentrations are chronically increased in the diabetic state because of the elevation in glucose concentration and thus elevation in the concentration of dihydroxyacetone phosphate (DHAP). DHAP is reduced to glycerol-3-phosphate before being acylated twice to yield DAG [Koya and King, 1998].

Many isoforms of PKC are activated by DAG, thus the increased DAG concentration leads to an increase in the activity of PKC (primarily the β- and δ-isoforms) which has myriad consequences within the cell: PKC isoforms are involved in a very wide range of cellular processes. A decrease in endothelial nitric oxide synthase (eNOS) and an increase in endothelin-1 (ET-1) leads to blood flow abnormalities; an increase in VEGF leads to changes in vascular permeability and increases in angiogenesis; an increase in TGF-β leads to an increase in collagen and fibronectin (two major extracellular matrix proteins) and thus capillary occlusion and increases in the thickness of the ECM; an increase in plasminogen

activator inhibitor 1 (PAI-1) leads to a decrease in fibrinolysis, thickening of the ECM and vascular occlusion; an increase in NF-κB activation leads to a pro-inflammatory gene expression response and an increase in NAD(P)H oxidases leads to an increase in reactive oxygen species which damage multiple proteins [Brownlee, 2001; Geraldes and King, 2010].

1.7.4 Activation of the hexosamine pathway

The fourth proposed mechanism of damage originated in research from the late 1990s [Sayeski and Kudlow, 1996; Kolm-Litty et al., 1998] and involves an increase in flux through the hexosamine biosynthesis pathway (HBP). The HBP is a branch of metabolism off glycolysis involved in the production of UDP-*N*-acetylglucosamine and other amino sugar products. Thse are used for the synthesis of *O*- and *N*-linked glycoproteins as well as nucleic acids (Figure 1.8). These products are used for the enzymatic addition of *O*-GlcNAc residues to proteins in a manner similar to phosphorylation. These modifications can alter the properties of the target protein dramatically and in the case of transcription factors there can be far reaching consequences in terms of gene expression. Inhibition of the first committed step in the HBP, the enzyme glutamine fructose-6-phosphate amidotransferase (GFAT), blocks hyperglycaemia-induced overexpression of TGF-α, TGF-β1 [Kolm-Litty et al., 1998] and PAI-1 [Du et al., 2000]. The role of the HBP in the alteration of transcription in cells in hyperglycaemia is considered in more detail in Chapter 3.

1.7.5 Oxidative stress

It has been proposed by Brownlee [2001] that the common theme connecting each of the four theories put forward above is oxidative stress. Each is involved in the common process of overproduction of superoxide by the mitochondrial electron transport chain. Specifically, hyperglycaemia induces high levels of electron donation from the citric acid cycle electron donors NADH and $FADH_2$ to complexes I and II respectively. This leads to an increase in mitochondrial membrane potential as protons are pumped out which inhibits complex III. This inhibition increases the half-life of free radical intermediates of ubiquinone (coenzyme Q) which leads to O_2 being reduced to superoxide ($O_2^{\cdot -}$). Above a certain threshold, the mitochondrial membrane potential-driven production of superoxide is markedly increased [Korshunov et al., 1997] from the current estimated base-rate of 0.15% of all O_2 being reduced to $O_2^{\cdot -}$ [Brand, 2010]. If manganese superoxide dismutase (MnSOD—the mitochondrial SOD) or uncoupling protein 1 (UCP1) is overexpressed in hyperglycaemic cells then the superoxide is removed more quickly or the proton gradient collapses to the point

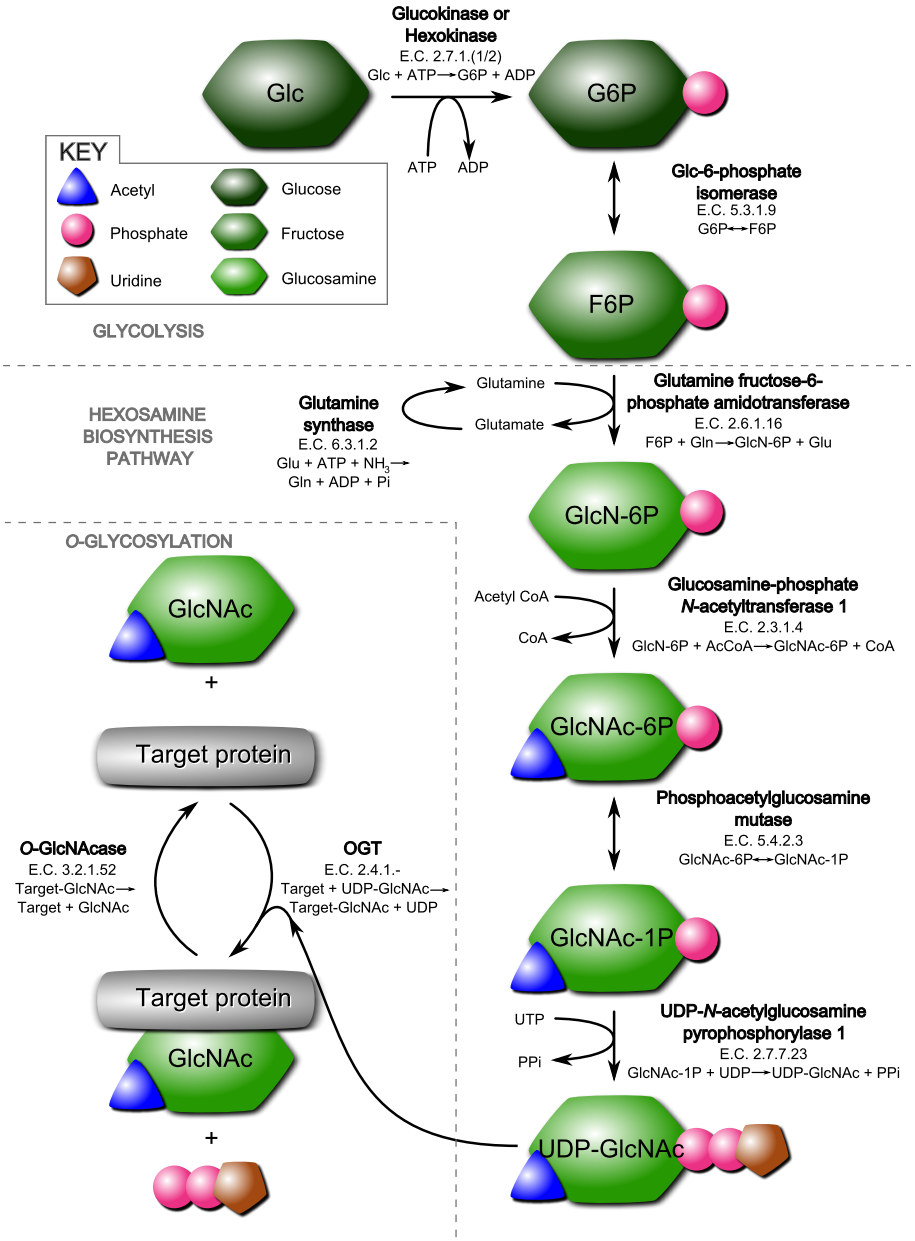

Figure 1.8: The reactions of the hexosamine biosynthesis pathway. Glc: Glucose; G6P: Glucose-6-phosphate; F6P: Fructose-6-phosphate; GlcN-6P: Glucosamine-6-phosphate; GlcNAc-6P: *N*-acetylglucosamine-6-phosphate; GlcNAc-1P: *N*-acetylglucosamine-1-phosphate; UDP-GlcNAc: Uridine diphosphate-*N*-acetylglucosamine

where superoxide production is decreased. This prevents increased polyol pathway flux, increased intracellular AGE formation, increased PKC activation and increased hexosamine pathway flux. The linking event appears to be the inhibition of glyceraldehyde-3-phosphate dehydrogenase by reactive oxygen species [Du et al., 2000]. Whether this is a direct inhibition of the enzyme or as a result of the decrease in cellular levels of NAD^+ and activation of poly (ADP-ribose) polymerase (PARP, an enzyme which poly(ADP-ribosyl)ates GAPDH) is unclear but cellular glutathione levels remain high during this inactivation. This decrease in GAPDH activity causes a build up of all glycolytic intermediates preceeding it in the Embden-Meyerhof pathway. These include the triosephosphates, precursors for methylglyoxal; fructose-6-phosphate, precursor for the hexosamine pathway; glucose, precursor for the polyol pathway and glycerol, which although not a direct glycolytic intermediate is required for PKC activation.

Further sources of ROS in the cells are NADPH oxidase (used to manufacture superoxide in macrophages and phagosomes) and uncoupled nitric oxide synthase (NOS) which forms both NO and $O_2^{\cdot -}$ or $ONOO^-$ (peroxynitrite—formed by NO reacting with $O_2^{\cdot -}$) [Sullivan and Pollock, 2006]. NADPH oxidase appears to be activated in hyperglycaemia by PKC [Nakagami et al., 2005] which could further stimulate more mitochondrial superoxide production.

Additionally, the cellular glutathione pool which is involved in sequestering and neutralising ROS is dependent on the availability of NADPH for regeneration. NADPH is produced primarily by the thiamine-dependent reductive pentose phosphate pathway. The role of thiamine in this process is discussed in more detail in Section 2.5 on page 39.

1.8 Therapeutic approaches to prevent diabetic complications

Secondary to the treatment of the underlying diabetes is the need to treat complications as they arise. Since it is the complications, not the disease *per se*, which are the main cause of morbidity and mortality such treatments are an invaluable tool in battling the disease. Several major classes of therapies are discussed below.

1.8.1 Antioxidants

Diabetes leads to an elevation in reactive oxygen species (ROS) production that is capable of overwhelming the body's natural defence systems. In such a situation, it is a logical strategy to attempt to counter this increase in ROS with antioxidant therapies. An antioxidant is any chemical which can be oxidised itself in a sacrificial manner to protect other potential targets of oxidation by ROS. These chemicals are often regenerated using enzymatic systems, for example, glutathione re-reduces ascorbic acid before itself being re-reduced by glutathione reductase. When these endogenous systems are overwhelmed, addition of further ready-reduced exogenous antioxidants helps to maintain homeostasis.

The diet is a major source of antioxidants with many fruits and vegetables containing high concentrations, for example, apples [Huber and Rupasinghe, 2009], strawberries [Azzini et al., 2010] and many other foods [Dilis and Trichopoulou, 2010]. Studies in mice with the antioxidants *N*-acetyl-L-cysteine and vitamins C and E have demonstrated that they can protect β-cells against glucose-toxicity [Kaneto et al., 1999], possibly by protecting the β-cells against glucose-induced apoptosis whilst not depressing their natural division rate.

Vitamin E is the combined name for a set of eight tocopherols and tocotrienols including the well-known α-tocopherol, the member of the group with the highest bioavailability (Figure 1.9) [Brigelius-Flohé and Traber, 1999]. Vitamin E is fat-soluble and acts by scavenging the peroxyl radical and preventing lipid peroxidation in membranes. Each member of the group has similar antioxidant properties and combined they are amongst the antioxidants shown to have a specific benefit to combat diabetes side-effects, at least in animal models. In human patients the evidence is a little less clear with further studies needed to draw significant conclusions [Pazdro and Burgess, 2010].

It is likely that not all of the effects seen upon vitamin E administration are due to its antioxidant properties. It has been shown to inhibit protein kinase C [Azzi et al., 1997] and also to influence transcription by peroxisome proliferator-activated receptor-γ (PPAR-γ) by acting as a ligand to the transcription factor [Pascale et al., 2006; Fang et al., 2010]. Also, vitamin E can exist as one of eight stereoisomers. The naturally occurring isomer is *RRR* whereas many commercial supplements are racemic at all chiral centres (all-rac). None of these steroisomers is exactly equivalent to the naturally occurring *RRR* form which may partially explain differences between supplements and diets rich in vitamin E [Brigelius-Flohé and Traber, 1999].

Another often studied antioxidant is α-lipoic acid (Figure 1.10), or thioctic acid, which is a cofactor for the E2 subunit of three mitochondrial enzyme complexes [Raddatz

and Bisswanger, 1997; Biewenga et al., 1997]. It was found to be an antioxidant when it was shown to prevent symptoms of vitamin C and E deficiency by Rosenberg and Culik [1959]. Its potential use as a therapeutic agent to treat diabetes has been considered for some time [Gandhi et al., 1985] and more recently many papers have been published specifically examining its effects on diabetic neuropathy. For example, Reljanovic et al. [1999] conducted a two year placebo controlled study of the effect of α-lipoic acid on diabetic neuropathy. They concluded that α-lipoic acid did have a beneficial effect on several attributes of nerve conduction. Other studies by Coppey et al. [2001] in streptozotocin-induced diabetic rats have shown that treatment with α-lipoic acid or hydroxyethyl starch deferoxamine can significantly improve both nerve conduction velocity and preceding characteristics such as a reduction in endoneurial blood flow.

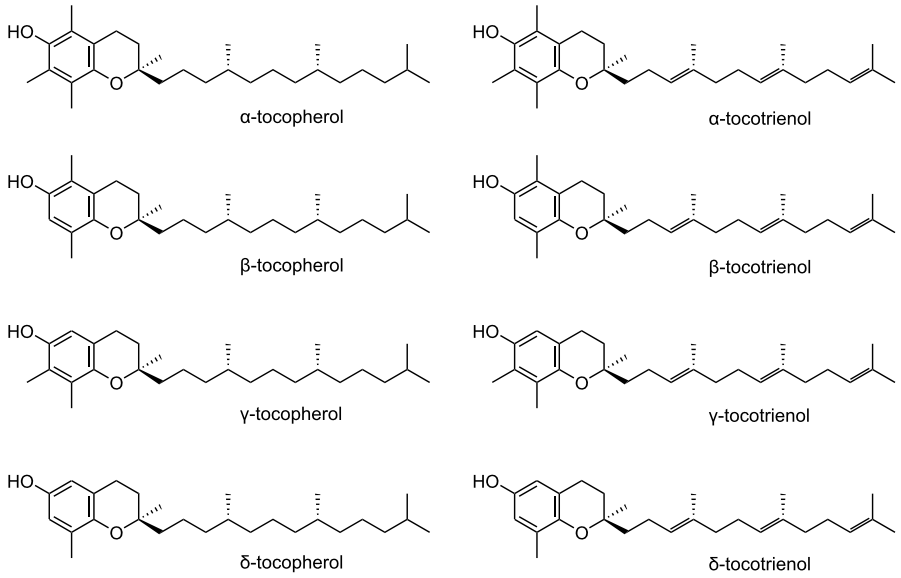

Figure 1.9: The structures of the eight biologically active forms of Vitamin E

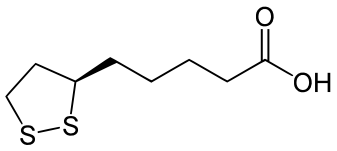

Figure 1.10: The structure of α-lipoic acid

1.8.2 Aldose reductase inhibitors

Aldose reductase (AR), the first step in the polyol pathway, was an attractive pharmacological target when considering the damage caused by excess polyol pathway flux. Soon after the discovery of the involvement of AR in diabetic cataractogenesis researchers demonstrated that AR inhibitors were capable of inhibiting cataract formation in diabetic rats [Dvornik et al., 1973] and galactose-exposed rabbits [Kinoshita et al., 1968].

Early AR inhibitors developed for human use were toxic and had poor specificity—they often inhibited other members of the aldo-keto reductase superfamily including aldehyde reductase isoforms. More recently drugs such as epalrestat have been marketed as a treatment for diabetic neuropathy yet their efficacy remains below what has been demonstrated in animal models since they are only partially effective in ameliorating symptoms [Ramirez and Borja, 2008]. This may well be due to AR being implicated in many more pathways than originally envisaged [Srivastava et al., 2005]. For example, AR may be more involved with the reduction of a wide range of aldehydes generated from lipid peroxidation than with the reduction of glucose. Inhibiting its activity may thus be increasing damage from lipid peroxidation byproducts. Moreover, antioxidant administration alone is sufficient to prevent cataractogenesis in rats, even though intra-lens polyol concentrations can be very high (80–90 mM) [Srivastava et al., 2005]. Thus a possible solution to increase AR inhibitor efficacy would be to administer AR inhibitors in combination with antioxidants.

1.8.3 Aminoguanidine

Aminoguanidine, also known as Pimagedine, is a small nucleophilic hydrazine derivative which is able to react rapidly with dicarbonyl compounds and prevent the accumulation of AGEs in the body. Aminoguanidine was noted to react with AGEs *in vitro* by Brownlee et al. [1986] and by 1989, evidence had been published that aminoguanidine lowered AGE concentrations in experimental diabetes [Nicholls and Mandel, 1989].

Based on this evidence, two clinical trials were established to investigate whether aminoguanidine was effective in preventing overt nephropathy in diabetic patients. One trial was conducted with type 1 and the other with type 2 diabetic patients (ACTION I and II respectively). The outcome was not spectacular and the ACTION II trial was stopped in 1998 because of poor efficacy and safety concerns with side effects including abnormal liver function tests and gastrointestinal disturbances [Freedman et al., 1999]. ACTION I was not stopped but failed to deliver its clinical endpoint—a decrease in the time to the doubling of

baseline serum creatinine—although there were some significant changes in lipid metabolism and urinary protein output. These underwhelming results combined with other evidence of toxicity (e.g. causing malignant tumours in rats [Oturai et al., 1996]) and off-target effects (e.g. enzyme inhibition, reviewed by Thornalley [2003b]) means that aminoguanidine is not likely to be used clinically.

1.8.4 Thiamine and Benfotiamine

The high cytosolic glucose concentrations prevalent in the diabetic state are damaging through the pathways described above. Other pathways, such as the pentose phosphate pathway (PPP) are capable of using this glucose and diverting it to less damaging metabolites such as ribose-5-phosphate. The enzyme with most control over flux through the PPP is transketolase which is dependent on the pyrophosphate form of the vitamin thiamine as a cofactor. Thus it has been proposed that treatment with thiamine or derivatives such as Benfotiamine could enhance activity of the PPP, thereby diverting glucose away from damaging pathways. Thiamine as a therapy is discussed in more detail in the following chapter, in particular also in Section 4.4.

Chapter 2

Introduction to thiamine

Thiamine, or vitamin B_1, is a water soluble vitamin which is essential in the pyrophosphate form as a cofactor for key steps in carbohydrate metabolism. Like all vitamins, the human body is unable to synthesise thiamine so it must be obtained in the diet where it can be found in a wide variety of foods including whole grains, yeast, liver, pork and many vegetables. Phosphate esters of thiamine in the diet are often hydrolysed in the gut lumen by phosphatases to yield free thiamine which is subsequently transported from the lumen of the gut into the blood stream where circulates freely. Thiamine is taken up into tissues via dedicated transporters where it is pyrophosphorlyated to form the active cofactor, thiamine pyrophosphate.

The concentration of thiamine in the body is maintained by a balance between intestinal absorption, renal clearance and thiamine catabolism and degradation. Thiamine is filtered at the glomerulus into the ultrafiltrate and is then actively re-absorbed in the proximal tubules. It is this reabsorption that is crucial in maintaining a steady concentration of the vitamin in the body.

2.1 Discovery and historical significance

Extreme thiamine deficiency in the diet gives rise to the disease beriberi (which translates as "I cannot, I cannot" from the Sinhalese language from Sri Lanka) which was known to antiquity—indeed, its symptoms were described by the Chinese physician Ch'ao-Yuan-Fang Wu Ching in the 7^{th} century AD. The disease has symptoms which include weight loss, impaired tactile sensitivity (hypesthesia), oedema, vascular damage, weakened reflexes (hyporeflexia) and in advanced cases, heart failure and death. Modern characterisation of

the disease began in Japan where it was particularly prevalent due to the diet and known locally as *kakké* (derived from two Chinese words meaning leg disease) [Carpenter, 2000]. The best description of the disease was published in 1804 by Tachibana Nan-kei. This described not only the main symptoms as above but also seasonal variations and social variations such as prevalence in the student population but not in the upper classes.

It was a Japanese naval doctor, Takaki Kanehiro, who first noted that the disease affected naval officers less than naval seamen. The former consumed a varied diet including meat and vegetables whilst the latter often consumed nothing but white rice for weeks at a time. In 1882, he arranged an experiment on identically crewed Japanese battleships. One crew was fed a more varied diet with meats, beans, barley and other ingredients whilst the other was fed only white rice. Over the course of an identical voyage, the former ship had only fourteen cases of beriberi with no fatalities where as the latter ship (with only rice in the diet) had 161 cases of beriberi out of 376 crew with 25 fatalities. Despite Takaki's work on the causes of beriberi, the majority of Japanese navy doctors still believed that beriberi was an infectious disease or caused by a toxin with the result that no program was put in place to prevent the disease.

The first Western doctor to study the condition was Christiaan Eijkman, a Dutch medical officer working in Java, who could induce polyneuritis gallinarum (a beriberi-like disease) in chickens by feeding them only polished white rice and could cure it by feeding them kitchen scraps (1893–1896). He observed a pathogenic degradation of the myelination in both the chickens and in human beriberi patients. His successor, Gerrit Grijns, also demonstrated that autoclaving food at 100–110 ℃ caused it to lose its "protective factor" [Wuest, 1962]. Grijns was so convinced of this protective factor that he made the first attempts to isolate it. However, it wasn't until ten years later that a Polish chemist, Casimir Funk, obtained a crystalline substance from rice polishings [Funk, 1912a; Carpenter, 2001]. He was convinced that he had isolated the vital ingredient in rice that prevented beriberi and also that it was an amine. To this end, he coined the word "vitamine" meaning an amine vital to life [Funk, 1912b]. As it turned out, Funk had not isolated thiamine but more likely nicotinic acid. It was the Dutch chemists Barena C P Jansen and Willem F Donath who, in 1926, first successfully isolated crystals of thiamine which they named "aneurin" (for anti-neuritic vitamin). The structure provided by Jansen and Donath omitted the crucial sulphur atom. Shortly after, the British Medical Research Council proposed the identifier vitamin B_1 for this anti-beriberi factor. By 1934, the structure of thiamine had been correctly solved by R R Williams, an American chemist who gave the vitamin the name

"thiamine" in recognition of this sulphur atom [Carpenter, 2000]. His laboratory followed this feat with the first chemical synthesis of thiamine in 1936 (reviewed by Wuest [1962]). The first commercial synthesis of thiamine took place in 1937. The cumulative outcome of this research was that in the 1920s in Japan, a culture still very much dependent on white rice as a staple food, beriberi accounted for 30% of all deaths yet by 1969, that figure had dropped to 0.5% as a result of research into thiamine [Lonsdale, 2006].

2.2 Structure and structural analogues

Thiamine is a relatively stable compound comprising a thiazolium ring and a pyrimidine ring linked by a methylene bridge (Figure 2.1). It is stable when exposed to heat in anhydrous form but is thermally-labile in foods, physiological systems and other non-anhydrous conditions [Dwivedi and Arnold, 1973]. Thiamine has a molecular mass of 300.8 Da and a full chemical name of 3-[(4-amino-2-methylpyrimidin-5-yl)methyl]-5-(2-hydroxyethyl)-4-methyl-1,3-thiazol-3-ium. It is prepared commercially as either the hydrochloride salt or the slightly less soluble mononitrate salt for fortification in foods and for pharmaceutical use [Expert Group On Vitamins and Minerals, 2000]. Synonyms for thiamine include thiamin, Aneurenin(e), Vitaneurin and other trade names [Expert Group On Vitamins and Minerals, 2000]. The polar nature of thiamine makes it highly soluble in water. Dissolving thiamine hydrochloride at a concentration of 1% (w/v) in water naturally yields an acidic solution (pH 3.13) in which the thiamine is stable at room temperature but not when heated. When pH is increased beyond 5.5, thiamine becomes increasingly unstable although the chemical half-life of thiamine at pH 7.0 and 25℃ is 47 weeks [Pachapurkar and Bell, 2005]. The biological half-life of thiamine is shorter than this due to catabolism, thiaminase, thiamine oxidase and probably also peroxidase. Thiamine has a yeast-like thiazole odour and a bitter taste.

The 2H proton of thiamine is very acidic ($pK_a = 18.0$) and is capable of abstracting to the solvent leading to the formation of the potent nucleophilic thiazolium ylid (Figure 2.2) [Haake et al., 1971; Washabaugh and Jencks, 1989]. In the active site of thiamine-dependent enzymes, this is exploited by lowering of the pK_a by the active site of the enzyme (see Section 2.5 on page 39)

Thiamine degrades through hydroxide-catalysed thiazolium ring opening, leading to the mercapto-olefinic derivative. This reaction has a half-life of 33 hours at pH 7.4 [Duclos and Haake, 1974] and is reversible [Washabaugh et al., 1993] (Figure 2.3), a fact which is

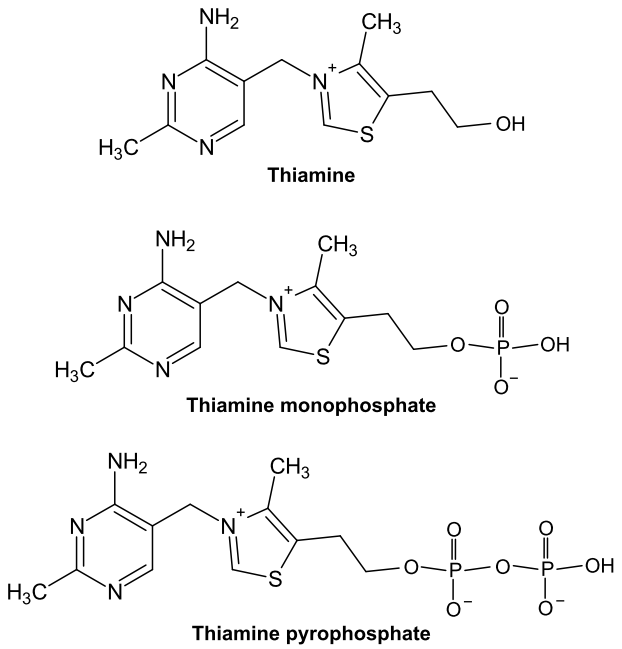

Figure 2.1: The structure of thiamine and thiamine phosphate esters.

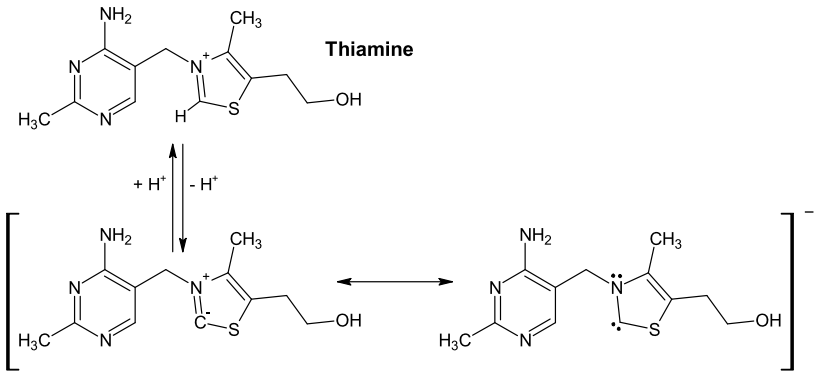

Figure 2.2: The mechanism of thiamine ylid formation. Adapted with permission from Washabaugh and Jencks [1989]

exploited in the use of any of several lipophilic allithiamine derivatives which all have a ring-opened structure that cyclises *in vivo*. Allithiamine is a lipid soluble derivative of thiamine found naturally in garlic and discovered and characterised by Fujiwara et al. [1954a,b]. Examples of prodrugs derived from allithiamine include thiamine disulphide, thiamine propyldisulphide, isobutyrylthiamine disulphide (Sulbutiamine), thiamine tetrahydrofurfuryl disulphide (Fursultiamine or TTFD) and *S*-benzoylthiamine *O*-monophosphate (Benfotiamine) (Figure 2.4). The structures of these compounds all have an open thiazolium ring which re-closes *in vivo* after hydrolysis or reduction as appropriate. In the case of Benfotiamine, the benzoyl-thioester linkage is hydrolysed by cellular and plasma non-specific esterases, releasing benzoic acid. The resulting mercapto-olefinic formamide cyclises spontaneously to form the thiazolium ring of thiamine monophosphate. Additionally, Benfotiamine can be hydrolysed by intestinal phosphatases to yield *S*-benzolythiamine. This is truly lipophilic and can be detected in plasma after oral Benfotiamine dosing. *S*-benzolythiamine is hydrolysed by esterases in tissues to yield thiamine (Figure 2.5) [Thornalley, 2005].

2.3 Metabolism of thiamine

Mammals are unable to synthesise thiamine and rely on exogenous sources of the vitamin. Many bacteria, yeast and plants can synthesise thiamine monophosphate *de novo* by fusing thiazole and pyrimidine moieties [Webb et al., 2007]; a process which was first elucidated in yeast in 1960 [Camiener and Brown, 1960a,b]. These are synthesised separately and often by quite diverse, species-specific mechanisms [Begley et al., 2008]. Research in this area is still active and far from complete. In 2004, researchers managed to re-create the complete thiazole synthesis system in a cell-free extract from *E. coli* [Leonardi and Roach, 2004] and Kong et al. [2008] recently described a new gene in *Arabidopsis thaliana* which is similar to the *E. coli* pyrimidine biosynthesis gene ThiC.

Once synthesised, thiamine cycles between one of four phosphorylation states in a process summarised in Figure 2.6. Generally, in animals, thiamine is pyrophosphorylated in one step to the active thiamine pyrophosphate (TPP). The majority of TPP will then be bound by enzymes requiring it as a cofactor. Generally around 90% of cellular TPP is contained within or associated with the mitochondria and used by the enzymes within [Bettendorff et al., 1994b]. The remaining 10% is to be found in the cytosol where it can be used as a cofactor for transketolase. Only 3–5% of cellular thiamine was found bound to transketolase in rat brains [Bettendorff et al., 1994b]. TPP is capable of being

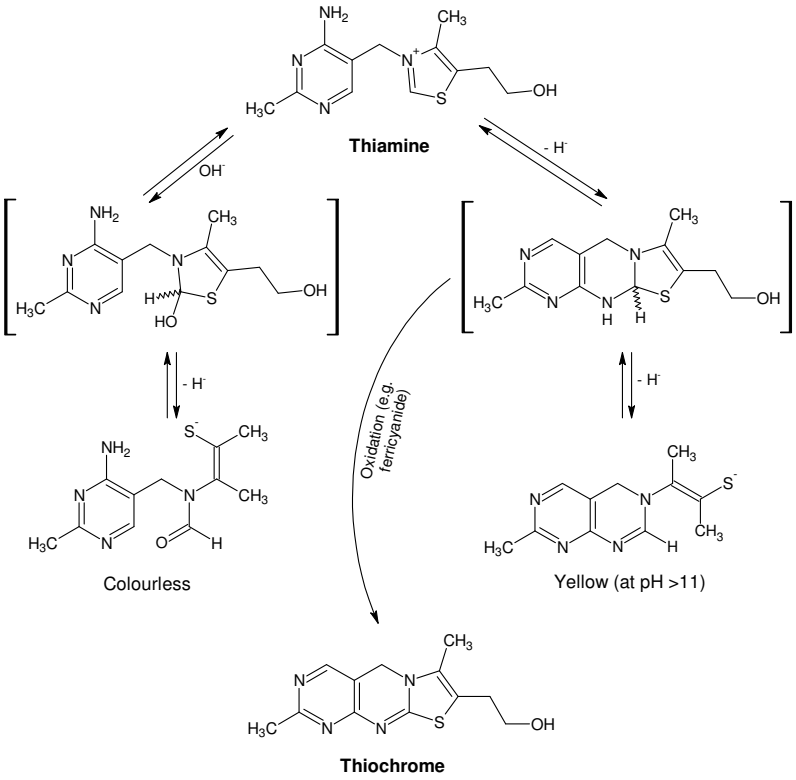

Figure 2.3: The mechanisms of thiamine reversible hydrolysis and irreversible oxidation to the highly fluorescent thiochrome. Adapted with permission from Washabaugh et al. [1993].

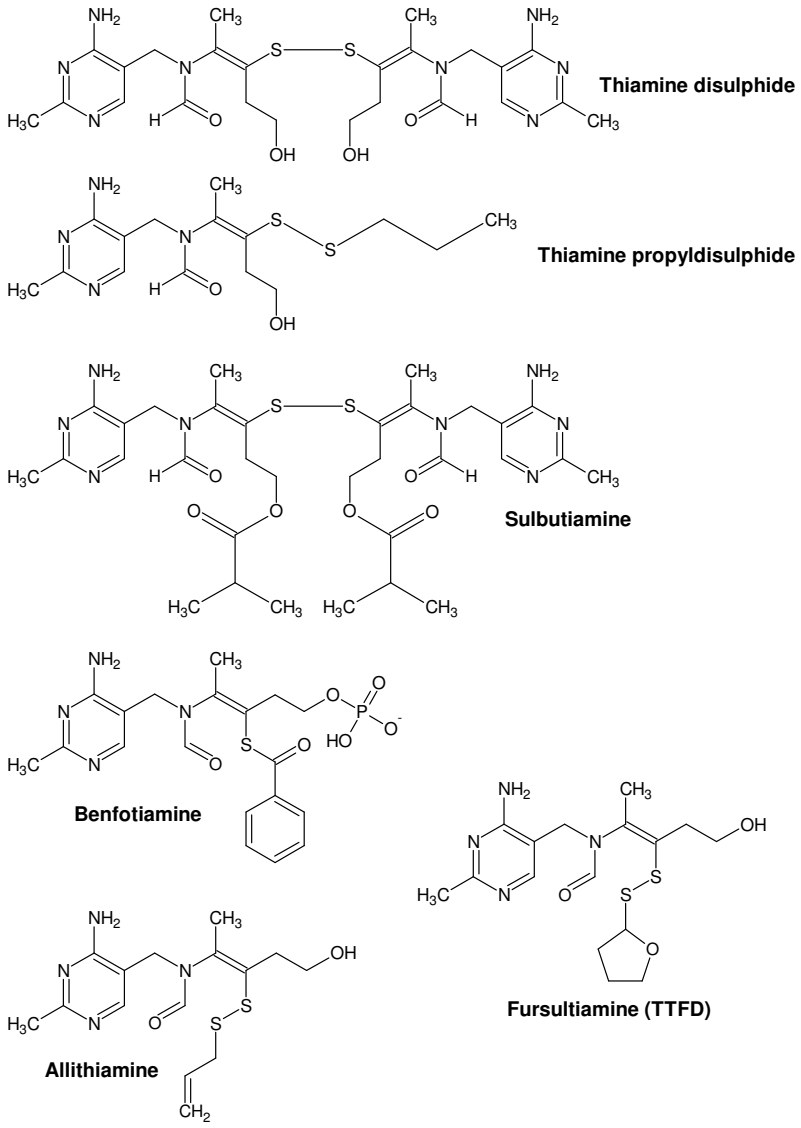

Figure 2.4: The structures of analogues of thiamine and allithiamine

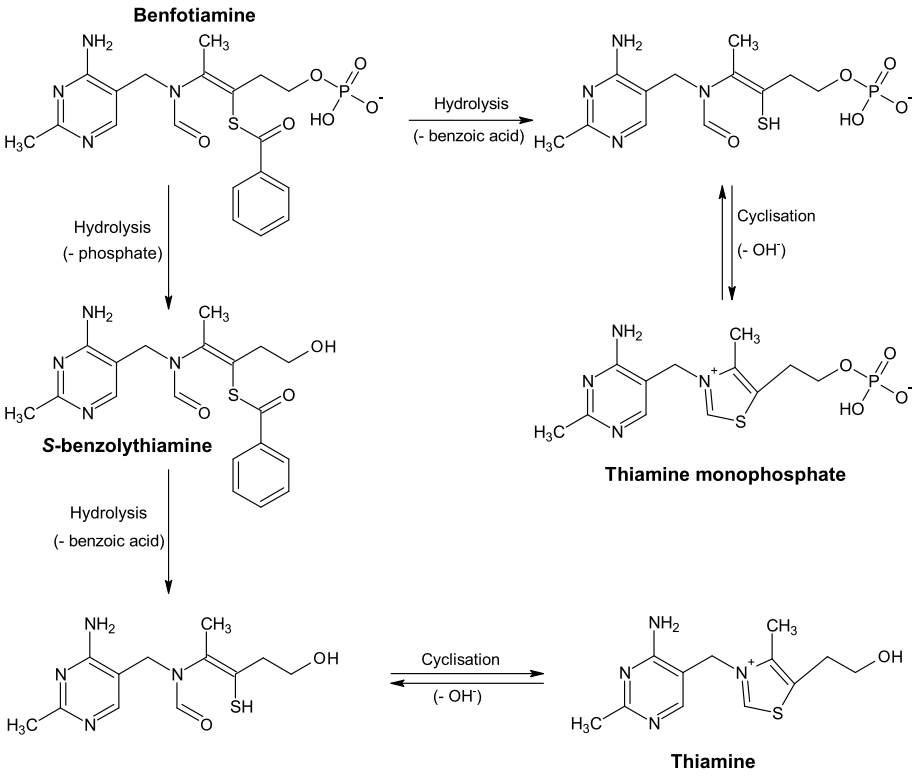

Figure 2.5: The mechanism of Benfotiamine conversion to TMP and THM

dephosphorylated in a stepwise manner via TMP back to the non-phosphorylated thiamine (Figure 2.6).

A small amount of TPP is further phosphorylated from the cytosolic pool to form thiamine triphosphate (TTP) in certain neurons [Makarchikov et al., 2003] in which it is a cofactor for an enzyme involved in the unusual phosphorylation of histidine residues [Nghiêm et al., 2000] as well as playing a part in conduction of nerve impulses [Bettendorff et al., 1994a].

2.4 Thiamine in the diet

Thiamine is widely available in the diet of higher organisms where it must be taken in at regular intervals due to its water soluble nature and low overall body storage capacity. Foods derived from whole grains of cereal crops provide the largest proportion of thiamine in the UK diet amongst young people (38%, [Gregory and Lowe, 2000; Expert Group On Vitamins and Minerals, 2000]) with vegetables, potatoes and savoury snacks accounting for an additional 26%. The data for UK adult dietary composition of thiamine was compiled by the Office for National Statistics in 2002 and a summary is given in Table 2.1. Most of the thiamine is lost from whole grains in the production of white flour or polished rice so in the UK, white flour must be fortified with thiamine to a level not less than an equivalent of 0.24 mg per 100 g flour [Expert Group On Vitamins and Minerals, 2000]. Other potent sources of thiamine in the diet include meat (particularly pork muscle), milk, legumes, fruit and eggs.

Thiamine requirements in the diet are highly dependent on carbohydrate-based energy intake which in itself is also subject to variation based on age, body weight and physical activity as well as other factors such as climate or pathological conditions [Standing Committee on the Scientific Evaluation of Dietary Reference Intakes, 1999; World Health Organization's Department of Nutrition for Health and Development, 1999; Expert Group On Vitamins and Minerals, 2000]. Patients with cancer have high glycolytic fluxes and so have increased need for thiamine but supplementation has drawbacks because the high doses of thiamine given allow for fast production of the nucleotides needed for rapid cell division via the transketolase-dependent reductive pentose phosphate pathway (see Section 2.6 on page 41) [Boros et al., 1998]. Since requirements are relative to energy usage, the expression of intake as a ratio to calories consumed is the preferred method. The recommended daily dietary intake of thiamine in the UK is virtually stable throughout life rising from 0.3 for

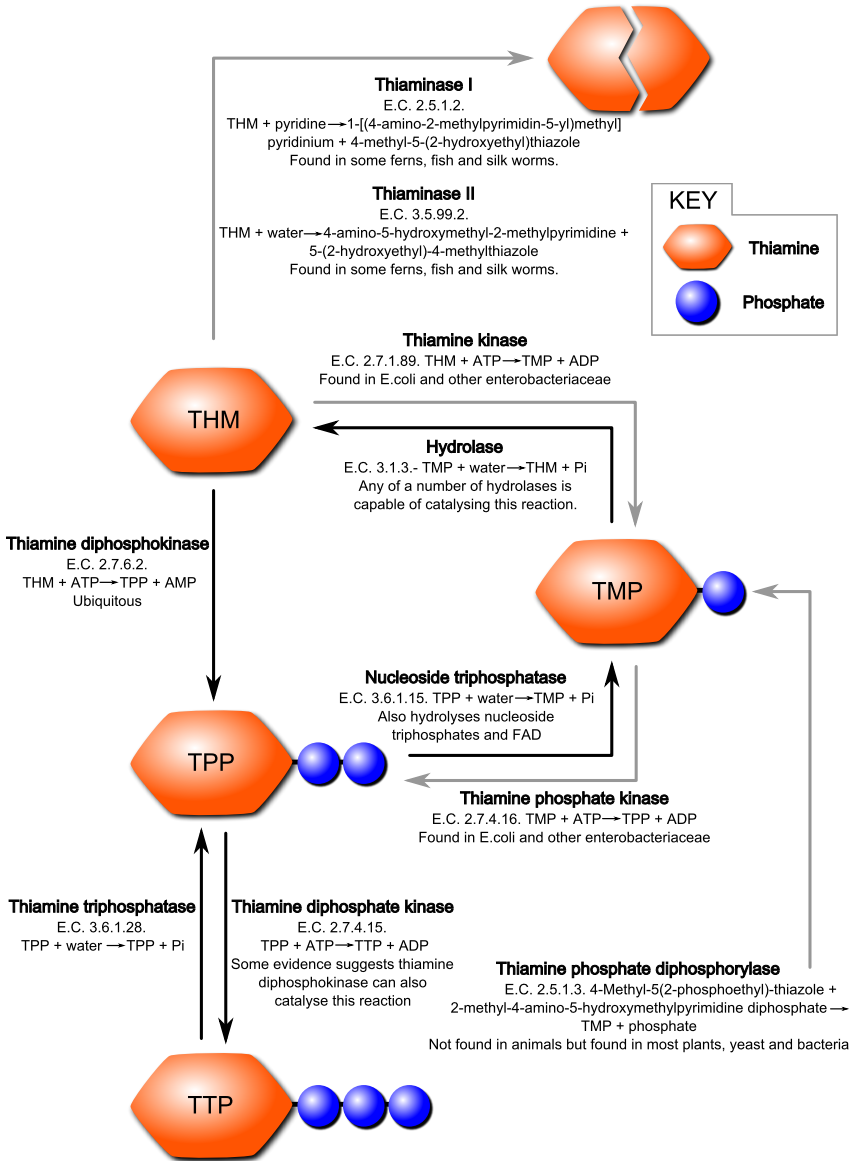

Figure 2.6: The metabolism of thiamine and its phosphate esters. Normal mammalian reactions are drawn with black arrows. Reactions common to other classes of species are drawn with grey arrows. References: thiaminase I [Fujita, 1954]; thiaminase II [Fujita et al., 1954]; thiamine diphosphokinase [Leuthardt and Nielsen, 1952]; thiamine kinase [Iwashima et al., 1972]; nucleoside triphosphatase [Brightwell and Tappel, 1968]; thiamine phosphate kinase [Nishino, 1972]; thiamine diphosphate kinase [Itokawa and Cooper, 1968]; thiamine triphosphatase [Hashitani and Cooper, 1972]; thiamine phosphate diphosphorylase [Camiener and Brown, 1960b]. Figure drawn with reference to the KEGG database available at *http://www.genome.jp/kegg/* [Kanehisa and Goto, 2000].

infants to 0.4 mg 1000 kcal^{-1} for adults [Department of Health, 1991]. This translates to a reference daily intake (RDI) of around 1 mg day^{-1} for a typical adult human. A slightly higher rate of intake is recommended by the US authorities at 0.5 mg 1000 kcal^{-1} with an increase to 0.9–1.0 mg 1000 kcal^{-1} for pregnant or breast-feeding ladies [National Research Council, 1989].

2.5 Physiological role of thiamine

The majority of thiamine is active in the body as TPP, also known as cocarboxylase, which is used as a cofactor by several enzymes. Three of these are multi-enzyme complexes involved in the dehydrogenation of α-keto acids: the pyruvate dehydrogenase complex (PDH), the α-ketoglutarate (2-oxoglutarate) dehydrogenase (α-KGDH) complex and the branched chain α-ketoacid dehydrogenase complex. In addition to these complexes, two further enzymes require TPP as a cofactor: the pentose phosphate pathway enzyme transketolase and 2-hydroxyphytanoyl-CoA lyase which is a lysosomal enzyme involved in the catabolism of phytanoic acid from chlorophyll [Foulon et al., 1999].

The three multi-enzyme complexes listed first are all large structures—larger than a ribosome—and structurally very similar to each other. They each have three subunits named E1, E2 and E3. It is the E1 subunit after which each complex is named and which requires TPP as a cofactor. The E2 subunit uses two lipoic acid molecules bound to lysine

Type of food	Percentage of dietary thiamine intake
Cereals and cereal products	34
Milk and milk products	6
Egg and egg dishes	1
Fat spreads	0
Meat and meat products	21
Fish and fish dishes	1
Vegetables (excluding potatoes)	15
Potatoes and savoury snacks	13
Fruit and nuts	3
Sugars, preserves and confectionery	1
Drinks	2
Miscellaneous	3
Average daily intake (mg)	1.77

Table 2.1: Thiamine composition of the diet from data on adults aged 19–64 years in the United Kingdom as assessed in 1990–1991 [National Diet & Nutrition Survey, 2002].

residues as cofactors (Figure 1.10 on page 26) whilst the E3 subunit uses a molecule of FAD. All E1 subunits are multimeric, each with two α and two β domains [Ciszak et al., 2003].

In the case of the PDH complex, the E1 subunit initiates the reaction with the TPP ylid attacking the electrophilic ketone of pyruvate. This results in an intermediate β-alkoxide which decarboxylates yielding an enol which is deprotonated yielding a stable intermediate bound covalently to the TPP. This undergoes reductive acetylation using the lipoamide moieties on the E2 subunit, regenerating the TPP [Ciszak et al., 2003]. The E2 subunit then adds coenzyme A forming a molecule of acetyl-CoA before being regenerated by the FAD contained in the E3 subunit.

A very similar reaction happens in the α-KGDH complex where the E1 subunit performs the decarboxylation of α-ketoglutarate yielding a succinyl-TPP complex. This complex is the precursor for the subsequent oxidation and transfer of coenzyme-A (performed by the E2 and E3 subunits respectively) to yield succinyl-CoA, the final product [Tretter and Adam-Vizi, 2005].

The third complex requiring TPP as a cofactor is that which decarboxylates the α-ketoacids derived from the degradation of the branched chain amino acids leucine, valine and isoleucine. In a manner similar to the other two complexes, the α-ketoacids are decarboxylated and activated products are formed: 3-methylbutanoyl-CoA, isobutyryl-CoA and *S*-2-methylbutanoyl-CoA from each amino acid respectively. Each of these is then passed ultimately into the citric acid cycle or biosynthetic pathways.

The reason why thiamine requirements are linked to dietary carbohydrate intake is now clear: PDH is one of the main enzymes using TPP as a cofactor and pyruvate is primarily derived from glucose metabolism. Hydrolysis of fatty acids yields acetyl-CoA subunits directly without pyruvate involvement. However, in the brain, which relies heavily on glucose (either exogenous or derived from gluconeogenic substrates during fasting) the presence of TPP is more critical for energy release from metabolites. Of course, the fasting brain relies more heavily overall on ketone bodies for energy but there is always some glucose consumption since the mitochondria (used for ketone body conversion to acetyl-CoA and subsequent oxidation by the citric acid cycle) are clustered in the cell bodies and are not found along the axons where glycolysis is the primary energy source.

Transketolase is also dependent on TPP as a cofactor. This key enzyme in the pentose phosphate pathway is discussed in more detail below.

2.6 The pentose phosphate pathway

The pentose phosphate pathway (PPP) is a key metabolic pathway with two main roles in the cell: it produces reduced NADPH and five carbon sugars, particularly ribose-based. These two roles are spread across two branches of reactions, the oxidative reactions and the non-oxidative reactions [Cabezas et al., 1999]. The PPP is also sometimes known as the phosphogluconate pathway or the hexose monophosphate shunt.

The non-oxidative reactions are primarily used to re-arrange carbon frameworks and convert five-carbon sugars to six-carbon sugars (or vice-versa) via a series of intermediates. All reactions in the non-oxidative phase are completely reversible, indeed, they are driven in "reverse" during the Calvin cycle as part of photosynthesis [Kruger and von Schaewen, 2003]. Importantly for this thesis, two reactions in the non-oxidative pathway are catalysed by the TPP-dependent enzyme transketolase (Figure 2.7). The oxidative reactions are used to generate reduced NADPH. They start with hexose sugar phosphates and convert them to ribose-5-phosphate yielding two moles of reduced NADPH and one mole of CO_2 for each mole of sugar passed down the pathway. These pentoses can then be re-converted back to hexoses by the non-oxidative branch if required. The overall reaction for the oxidative pathway is:

$$\text{Glc-6-phosphate} + 2\ \text{NADP}^+ + \text{H}_2\text{O} \rightarrow \text{Rib-5-phosphate} + 2\ \text{NADPH} + 2\ \text{H}^+$$

The overall reaction for the non-oxidative branch is:

$$6\ \text{Rib-5-phosphate} \rightleftharpoons 5\ \text{Glc-6-phosphate}$$

The first role of the PPP, as a producer of reduced NADPH in the cytosol, is critical in maintaining cellular antioxidant capabilities since reduced NADPH is a substrate for glutathione reductase, the enzyme which maintains the cellular glutathione pool in the reduced state. It also has secondary implications since NADPH is also used in metabolic processes including fatty acid synthesis and sterol synthesis: two molecules of NADPH are oxidised for the addition of each acetyl unit to a growing fatty acid chain. This role of the pathway producing NADPH is critical to cell survival, particularly in erythrocytes which have an active PPP owing to their lack of oxidative metabolism. Additionally, the ribose sugars produced by the pathway can be used as precursors for nucleotide and nucleic acid biosynthesis.

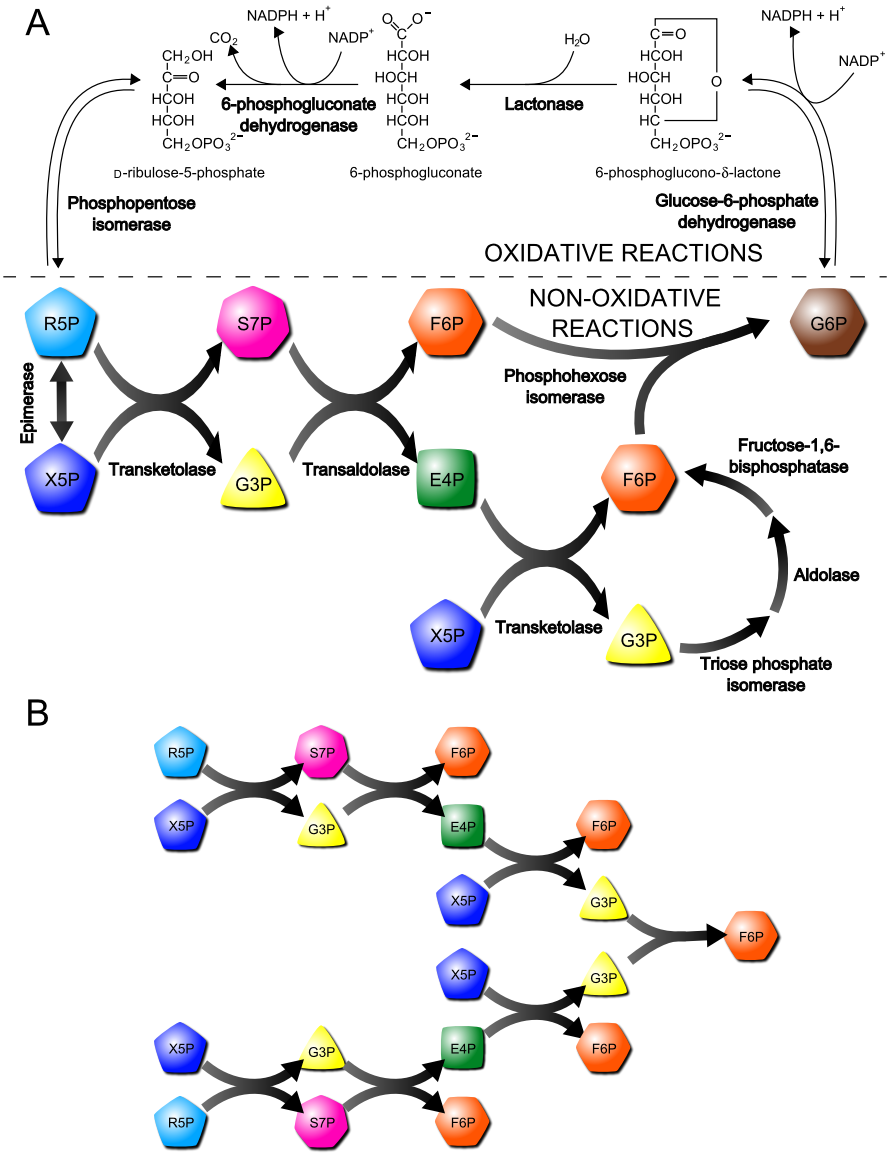

Figure 2.7: Schematic summary of the the pentose phosphate pathway. **A:** The oxidative and non-oxidative reaction pathways. All reactions in the non-oxidative part are freely reversible, as in the Calvin cycle. Single arrows are only used to indicate flux through the pathway during NADPH synthesis. The number of carbons in each sugar is indicated by the number of sides to the polygon. R5P: Ribose-5-phosphate; S7P: Sedoheptulose-7-phosphate; F6P: Fructose-6-phosphate; G6P: Glucose-6-phosphate; X5P: Xylulose-5-phosphate; G3P: Glyceraldehyde-3-phosphate; E4P: Erythrose-4-phosphate. **B:** The complete conversion of 6 riboses to 5 hexoses is shown. This is two sets of non-oxidative reactions from A in a mirror-image arrangement.

2.6.1 Control of the pentose phosphate pathway

The first oxidative reaction in the PPP, the conversion of glucose-6-phosphate (G-6-P) to 6-phosphoglucono-δ-lactone, is essentially irreversible and provides the most control over flux through this pathway. It is catalysed by the enzyme glucose-6-phosphate dehydrogenase. Genetic defects in this enzyme can have serious consequences such as the disease favism which is an intolerance to fava beans. Fava beans contain a molecule called divicine which raises cellular H_2O_2 to fatal levels when G6P dehydrogenase is inactive.

The limiting factor for flux through the pathway is the availability of the oxidised $NADP^+$. The $NADP^+$:NADPH ratio in the liver of a well fed rat is around 0.014 meaning there is a vast excess of the reduced NADPH. This is considerably lower than the NAD^+:NADH ratio in the same tissue which is around 700. Thus, NADPH is only produced as fast as it is required. In the liver or adipose tissue this rate is higher than it would be in muscle due to the high rate of lipogenesis and thus the high demand for NADPH. The non-oxidative branch of the pathway is primarily controlled by substrate availability and will flow readily in either direction.

This arrangement of oxidative and non-oxidative pathways allows for some interesting biochemistry if the cellular need arises. It is possible for cells to use the pathway in one of four ways dependent on the need for ribose-5-phosphate, NADPH and ATP. Firstly, if a cell requires much more R-5-P than NADPH—perhaps a dividing cell synthesising nucleotides—then G-6-P can be converted to fructose-6-phosphate and glyceraldehyde-3-phosphate by normal glycolytic means. Then transketolase and transaldolase can convert these to ribose-5-phosphate with the net result:

$$5\ \text{G-6-P} + \text{ATP} \longrightarrow 6\ \text{R-5-P} + \text{ADP} + \text{H}^+$$

The second mode would be if the needs for NADPH and ribose-5-phosphate are balanced. In this case, the oxidative pathway can be used on its own to produce two moles of NADPH and one mole of ribose-5-phosphate for each mole of glucose-6-phosphate:

$$\text{G-6-P} + 2\ \text{NADP}^+ + \text{H}_2\text{O} \longrightarrow \text{R-5-P} + 2\ \text{NADPH} + 2\ \text{H}^+ + \text{CO}_2$$

The third and fourth modes are similar in that the cell requires much more NADPH than ribose-5-phosphate but they differ in whether the cell requires ATP or not. If the cell does not require ATP, the glucose-6-phosphate can be completely oxidised by the PPP yielding only NADPH. If the cell requires ATP, the ribose-5-phosphate can be returned to glycolysis as pyruvate via the non-oxidative branch. This pyruvate can then be used to

either generate ATP or as a precursor for biosynthetic pathways. Both the oxidative and non-oxidative reactions are required here and the metabolites will move in a circular motion (anticlockwise on Figure 2.7 A). The reaction for option three is:

$$\text{G-6-P} + 12\ \text{NADP}^+ + 7\ \text{H}_2\text{O} \longrightarrow 6\ \text{CO}_2 + 12\ \text{NADPH} + 12\ \text{H}^+ + \text{P}_i$$

and for option four:

$$3\ \text{G-6-P} + 6\ \text{NADP}^+ + 5\ \text{NAD}^+ + 5\ \text{P}_i + 8\ \text{ADP} \longrightarrow$$
$$5\ \text{pyruvate} + 3\ \text{CO}_2 + 6\ \text{NADPH} + 5\ \text{NADH} + 8\ \text{ATP} + 2\ \text{H}_2\text{O} + 8\ \text{H}^+$$

These varied options make the PPP incredibly flexible and able to respond to cellular needs in a way that other pathways are unable to. The fact that it provides an alternative route for complete oxidation of glucose may be useful in the diabetic state, especially since diabetes is a state associated with an increase in oxidative stress and the extra NADPH generated by option three above may be useful. "Normal" oxidation of this glucose through the citric acid cycle would primarily generate ATP or increase the mitochondrial membrane potential, exacerbating the production of superoxide.

2.6.2 Transketolase

Transketolase (E.C. 2.2.1.1, TK) is a ubiquitous thiamine pyrophosphate-dependent enzyme found in all domains of life. It is a homodimer with each chain having a mass of around 68 kDa in humans. There are two active sites within each TK homodimer, each at the interface between the sub-units. Each active site requires one calcium ion and one molecule of TPP as cofactors. It catalyses two reactions within the pentose phosphate pathway. These are the interconversion of the two pentose phosphates ribose-5-phosphate and xylulose-5-phosphate with the seven-sugar sedoheptulose-7-phosphate and the triosephosphate glyceraldehyde-3-phosphate along with the interconversion of the four-carbon erythrose-4-phosphate and xylulose-5-phosphate with fructose-6-phosphate and glyceraldehyde-3-phosphate:

$$\text{R-5-P} + \text{X-5-P} \rightleftharpoons \text{S-7-P} + \text{GA3P}$$

$$\text{E-4-P} + \text{X-5-P} \rightleftharpoons \text{F-6-P} + \text{GA3P}$$

The dependence of TK on TPP and a metal ion was originally demonstrated in yeast. TPP can be removed from mammalian TK with relatively mild acidic conditions whilst the

removal of TPP from yeast and *E. coli* TK requires alkaline conditions [Datta and Racker, 1961] after which the activity is completely ablated [Saitou et al., 1974]. Only after the addition of TPP and a divalent metal ion is activity restored [Heinrich et al., 1972]. This dependence on TPP has also been demonstrated by the presence of TPP in solved crystal structures in yeast [Lindqvist et al., 1992; Nikkola et al., 1994]. The binding of TPP to TK is a two-step process [Esakova et al., 2005; Kochetov and Izotova, 1973]. The first is the binding of the TPP to the apo-enzyme in an fast and readily reversible step yielding a catalytically inactive intermediate. This is followed by a second, slow step which includes conformational changes in the apo-enzyme yielding the active holo-enzyme [Dalby et al., 2007]. In addition, TK is prone to removal of the TPP moiety when any excess is removed [Mitra et al., 1998]. This poses potential problems for the activity of TK in situations where thiamine is deficient.

The mechanism of catalysis in TK is similar to that of PDH in that there is an activated aldehyde being transferred to an acceptor which in the case of TK is an aldose and in the case of PDH is the lipoamide. In both reactions it is the C2 atom of TPP which ionises to yield the carbanion which attacks the carbonyl group of the substrate and forms an activated glycoaldehyde. This then condenses with the new aldehyde to form a ketose sugar which is released from the enzyme [Schenk et al., 1998].

2.7 Assay of thiamine

The clinical measurement of thiamine deficiency has traditionally been made by the use of an indirect method using a suitable proxy: erythrocyte transketolase activity and saturation with TPP. Erythrocytes are easily obtainable and transketolase activity in them is high because of high ROS production and concomitantly high flux through the pentose phosphate pathway. The assay involves measuring transketolase activity in fresh erythrocyte extract followed by the addition of exogenous TPP and re-measurement of the activity. These values can be used to determine the "thiamine effect", or percentage of transketolase unsaturated with TPP. A normal range for the thiamine effect in healthy human subjects is 0–15%, in mildly thiamine deficient patients 15–25% and in severely thiamine deficient patients >25% [Brady et al., 1995]. A urinary excretion rate for thiamine exceeding $0.20\,\mu mol\,day^{-1}$ or $67\,\mu g\,day^{-1}$ is considered the threshold value for evidence of dietary sufficiency of the vitamin [Finglas, 1993].

For measurement of thiamine concentration in other biological samples, an array of assay techniques have been used historically. These often involved measuring an indirect response such as rate of growth of an organism. For example, rat growth rates were used to study thiamine content of food before and after cooking [Aughey and Daniel, 1940]. Other techniques used involved assaying increased rates of alcohol production by fermenting yeast or using bacteria such as *Staphylococcus aureus*. Such methods either involved large amounts of cumbersome equipment or were subject to error due to thiamine biosynthesis pathways present. Another factor was that both the pyrimidine and thiazole moieties are active in many of these organisms [Niven and Smiley, 1943]. By 1943, a refinement of these techniques was in use. It involved measuring the rate of production of polysaccharide by *Streptococcus salivarius* when grown on a minimally defined agar medium [Niven and Smiley, 1943]. *Streptococcus salivarius* is unable to use either cleavage product alone or both combined as a substitute for thiamine.

These old techniques for assay of thiamine were vastly improved upon with the introduction of the thiochrome method. Thiochrome is a highly fluorescent molecule which can be synthesised easily by the alkaline oxidation of thiamine and its phosphate esters and then readily detected (this is further covered in the Materials and Methods chapter, particularly Figure 6.3 on page 89). This method was further refined when combined with chromatography by Sander et al. [1991] when it completely replaced prior methods of detection. Subsequent improvements led to increases in sensitivity and specificity along with reduced analysis time [Fayol, 1997; Gerrits et al., 1997]. A thorough account of a modern HPLC-based thiamine assay is given in Section 6.4 on page 89.

2.8 Thiamine transporters

There are two main proteins expressed in human cells that transport the physiologically cationic thiamine across membranes. These are human thiamine transporters 1 and 2 (THTR-1 and THTR-2). Each of these is a member of the solute carrier family of proteins, a fact represented in their gene names: *SLC19A2* and *SLC19A3* respectively. The only other member of this family of proteins is reduced folate carrier 1 (RFC-1, gene name *SLC19A1*) which transports the anionic folate across membranes. BLAST (Basic Local Alignment Search Tool) analysis of the human genome suggests that there are no further members of this family lying undiscovered [Ganapathy et al., 2004]. Homologues of these transporters are evident in the genomes of other species such as *D. melanogaster* and *C.*

elegans but the nature of the proteins in these organisms has not been studied [Ganapathy et al., 2004]. Each member of the *SLC19* gene family is expressed ubiquitously but generally with higher levels in tissues such as kidney, intestine, liver and pancreas.

2.8.1 THTR-1

Human thiamine transpoter 1 (THTR-1) was the first identified member of the thiamine transporter family. The coding region for the gene for THTR-1, *SCL19A2*, was cloned from a human foetal brain cDNA library and the protein was determined to contain 497 amino acid residues for a total molecular mass of 56 kDa and with a likely 12 transmembrane helices [Diaz et al., 1999]. After the gene had been identified as a thiamine transporter and cloned, Said reported on expression and promoter analysis of *SLC19A2* in intestinal cells [Reidling et al., 2002] and cellular and molecular aspects of thiamine uptake in cultured liver cells [Said et al., 2002]. The initial work on the intestinal cells identified that the stomach, duodenum and jejunum cells contained higher levels of *SCL19A2* mRNA relative to β-actin compared to the colon, cecum, rectum and ileum [Reidling et al., 2002] i.e. THTR-1 was more abundant in the proximal end of the digestive tract than the distal end.

Thiamine transpoter research began during study of the disease thiamine-responsive megaloblastic anaemia (TRMA, MIM (Mendelian Inheritance in Man): 249270, also known as Rogers syndrome after Lon Rogers who discovered it in 1969 [Rogers et al., 1969]). TRMA is an autosomal recessive disorder and mutations found clinically (D93H, S143F, G172D and others including insertion mutations [Bergmann et al., 2009]) are associated with impaired uptake of thiamine from the diet, thiamine deficiency, megaloblastic anaemia (abnormally large erythrocytes), sensorineural deafness and non-type 1 diabetes mellitus [Labay et al., 1999; Alzahrani et al., 2006]. Studies on some of these mutations have revealed that they are associted with decreased activity of the transporter, not a failure of the transporter to correctly express on the surface of cells [Balamurugan and Said, 2002]. TRMA is treatable by daily oral administration of pharmacological doses of thiamine to the patient (25–300 $\mathrm{mg\,day^{-1}}$ versus a normal RDI of around 1.5 $\mathrm{mg\,day^{-1}}$) [Oishi and Diaz, 2007]. Benzoyloxymethyl-thiamine, a lipophilic derivative of thiamine, has also been used in the treatment of TRMA [Valerio et al., 1998]. In each case, treatment with thiamine maintains health and corrects hyperglycaemia in pre-pubescent children but there is a chronic decline in pancreatic function after puberty with a related requirement for insulin.

Neufeld et al. [1997] studied approximately 12 families from various ethnic groups with TRMA and used the data to determine the location of the gene responsible by linkage

analysis. They concluded that the locus of the gene responsible for TRMA was 1q23.2–q23.3 but they did not identify the exact gene. The exact identity was found two years later when several groups identified mutations in the genetic sequence and characterized the protein responsible for TRMA as a thiamine transporter [Diaz et al., 1999; Dutta et al., 1999; Fleming et al., 1999; Labay et al., 1999]. This new protein was named THTR-1 and showed a 39% sequence homology to the reduced folate carrier gene, *SLC19A1*. As a result, the gene for THTR-1 was named *SLC19A2*.

2.8.2 THTR-2

Human Thiamine Transporter 2 (THTR-2) was the second identified member of the thiamine transporter family. It is a transmembrane protein comprising 496 amino acids with a molecular weight of 56 kDa. The protein undergoes no post-translational processing before reaching maturity with 12 transmembrane helices [Zeng et al., 2005]. The gene was first reported in humans by Eudy et al. [2000] who recognised its significance as a human homologue of a mouse gene which was potentially responsible for seizures in DBA/2J mice. The gene was mapped to chromosome 2q37 (later refined to 2q36.3) and assigned the name *SLC19A3* as it fell in the same solute carrier family as THTR-1 and RFC-1. The functional nature of the protein was first reported a year later by Rajgopal et al. [2001] who demonstrated that it was a highly specific thiamine transporter that did not transport folate as RFC-1 does.

THTR-2 has a high apparent structural homology with THTR-1. Both appear to have the same membrane-spanning helix configuration, have a similar molecular mass and share 53% amino acid sequence identity. THTR-2 appears to be expressed ubiquitously [Eudy et al., 2000; Zeng et al., 2005] but is found at higher levels in certain tissues e.g. placenta, liver and kidney along with discrete areas of the small intestine. Like THTR-1, it is more abundant in the proximal half of the small intestine with some expression in the more distal regions and colon [Said et al., 2004]. Tissues where THTR-2 is expressed are often the same as those with higher than average levels of THTR-1. Despite their similar localisation, there are differences in abundance between THTR-1 and THTR-2, often with a lower abundance of THTR-2 than THTR-1 in a given tissue. For example, Ashokkumar et al. [2006] have shown a level of THTR-1 mRNA several times higher than THTR-2 mRNA in HEK-293 kidney cells. The more abundant mRNA for THTR-1 does not, however, mean that it is the only protein critical for the uptake of thiamine. The importance of THTR-2 has recently been demonstrated in Japan by two brothers presenting with a Wernicke's-

like encephalopathy which responded to thiamine treatment. Wernicke's encephalopathy is characterised by impairment of short-term memory, ataxia, confusion and ophthalmoparesis. On investigation they were found to be compound heterozygotes for the K44E and E320Q mutations in *SLC19A3*, not normally found in ethnically matched control patients [Kono et al., 2009]. The authors proposed that the sub-cellular trafficking problems with the mutated protein may explain the selective lesions seen in MRI scans of the brothers. In addition, they speculated that the the up-regulation of THTR-1 in response to poor activity of THTR-2 may be responsible for preventing any further symptoms of deficiency. Furthermore, defects in THTR-2 are responsible for biotin-responsive basal ganglia disease (BBGD), a genetic recessive disease that starts in childhood and presents as a subacute encephalopathy, dysphagia and confusion. BBGD progresses to severe rigidity and dystonia and eventual death if left untreated [Zeng et al., 2005]. High doses of biotin (Vitamin B_7; a cofactor for several critical carboxylases) are able to relieve symptoms within a few days although the connection to thiamine transport remains unclear [Zeng et al., 2005].

THTR-2 has a marked polarity in its expression in *in vitro* intestinal models. It was found by Said et al. [2004] to be expressed primarily on the apical membrane of polarised intestinal Caco-2 cells with relatively little expression at the basolateral membrane. This is in contrast to THTR-1 which was found to be expressed at both apical and basolateral membranes in the same cell system, possibly with higher expression in the latter than the former membrane. In the same study Said et al. [2004] analysed the relative contributions of each transporter to the total carrier mediated thiamine transport in Caco-2 cells using siRNA knockdown techniques. For each protein they were able to specifically knock down expression and demonstrate a marked decrease in the uptake of thiamine. They concluded that the two proteins together were responsible for the total carrier-mediated thiamine uptake in this *in vitro* model. More recently, the role of THTR-2 *in vivo* has been further investigated by the same group [Reidling et al., 2010]. They used an *SLC19A3* deficient mouse strain and demonstrated in both *ex vivo* cells and intestinal loops that thiamine uptake was significantly reduced by between 70–80%. They hypothesise that the remainder of uptake is attributable to an up-regulated THTR-1.

2.8.3 Mitochondrial thiamine pyrophosphate transporter

There is a third protein which is involved in thiamine transport. The gene found at *SLC25A19* was originally thought to encode a mitochondrial deoxyribonucleotide carrier (DNC) [Dolce et al., 2001]. However, more recent studies by Lam et al. [2005] provided the

first evidence that this was unlikely, followed soon after with the discovery by Lindhurst et al. [2006] that *SLC25A19* actually encodes a mitochondrial thiamine pyrophosphate transporter. Lindhurst et al. [2006] demonstrated a decrease in mitochondrial thiamine pyrophosphate concentrations in knockout mice along with normal mitochondrial levels of ribo- and deoxyribonucleoside triphosphates—the originally proposed substrate of the DNC. In addition, Kang and Samuels [2008] have provided bioinformatic, transgenic *in vivo* and enzyme kinetic study evidence strongly in favour of *SLC25A19* being a transporter of thiamine pyrophosphate.

Mutations in this protein cause Amish lethal microcephaly (MCPHA) which is known to cause brain retardation and α-ketoglutaric aciduria. Knockout mice deficient in SLC25A19 die by embryonic day 12 with a neural tube closure defect [Lindhurst et al., 2006]. Beyond such observations, little is known about the role of *SLC25A19* and its function in cellular thiamine metabolism.

2.8.4 Promoter elements of *SLC19A2* and *SLC19A3*

Reidling et al. [2002] characterised the promoter elements of the THTR-1 gene necessary for expression. By cloning the gene and selectively removing certain upstream sections of the sequence, they identified several putative 5'-elements for regulation of the gene. Importantly, the gene was found not to have a TATA box at the expected location but instead had a CAAT box at position −305. The minimal promoter region between −356 and −36 was analysed and putative regulatory elements including Nuclear Factor-1 (NF-1), Activator Protein-1 (AP-1), Gut enriched Krupple-Like Factor-1 (GKLF) and Stimulating protein-1 (Sp1) were identified (Figure 2.8).

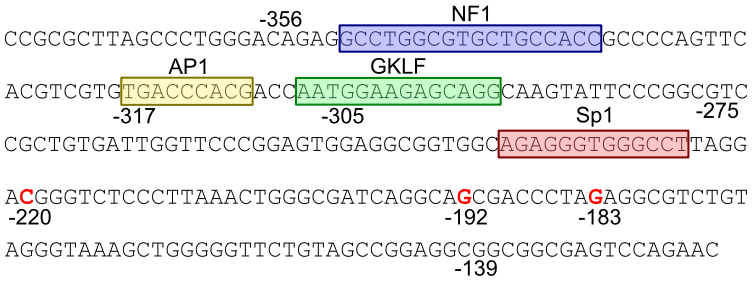

Figure 2.8: The sequence of the *SLC19A2* minimal promoter region required for basal activity. Boxes indicate putative promoter elements; red indicates transcription initiation sites. The numbers are nucleotides relative to the A of the ATG start site as 1. Adapted with permission from Reidling et al. [2002].

Further work by the same laboratory [Reidling and Said, 2003] investigated the promoter element in more detail using a variety of model systems including transgenic mouse studies and cotransfection studies using *Drosophila* SL2 cells—a well established cell line without any endogenous Sp1 activity [Courey and Tjian, 1988]. The transgenic mouse studies used full length and minimal promoter elements and showed that independent mutations of the GKLF/Sp1, NF-1 or Sp1 *cis* elements led to a decrease in *SLC19A2* promoter activity. They also established that GKLF, NF-1 and Sp1 proteins all form complexes with the DNA in the *SLC19A2* promoter. Specifically with regard to Sp1, they showed that it increases promoter activity *in vitro*. In the *Drosophila* SL2 cell studies, cells were simultaneously transfected with the *SLC19A2* promoter and an Sp1 containing vector. These studies showed a dose-dependent activation of both the minimal and full length promoter by Sp1. Taken together, these results suggest a role for three of the four transcription factors—GKLF, NF-1 and Sp1—being involved in the activation of *SLC19A2* gene expression *in vivo*. This may in turn suggest that they are important in cellular regulation of thiamine uptake and potentially whole-body thiamine homeostasis.

The role of 5'-promoter elements in the expression of *SLC19A3* was researched thoroughly by Nabokina and Said [2004] who used transiently transfected Caco-2 cells with 5'-deletion analysis conducted from a cloned 5'-regulatory region from the human *SLC19A3* gene. The minimal promoter needed for transcription was found between positions −77 and +55 bp and contained a number of putative promoter binding elements including sites for Sp1 (GC boxes at positions −48/−55 and −15/−12 bp) and NF-1. These elements were discovered by, and further investigated with, mutational analysis. Mutating all sites except the more distal (−48/−55 bp) GC box had no effect on basal transcription. Mutation of the distal GC box markedly decreased basal transcription. Supershift analysis showed that both Sp1 and the related Sp3 are capable of binding to this GC box which suggests a role for both these transcription factors and this GC box in modulating basal expression of *SLC19A3*.

2.8.5 Characteristics of thiamine transport

Thiamine transport has been studied in several different models representing different tissues. The HepG2 cell line has been used to model the liver [Said et al., 2002], jejunal basolateral membrane vesicles have been isolated and studied [Dudeja et al., 2003] and the HEK-293 cell line has been used to model certain aspects of kidney uptake [Ashokkumar et al., 2006]. More recently, a similar study was published on thiamine uptake in pancreatic β-cells [Mee et al., 2009]. Each of these studies are concordant on several points.

1) The uptake of thiamine is both temperature and energy dependent but independent of Na^+ or other metal cations such as Li^+ or K^+. Uptake is slower at temperatures lower than 37℃ and is inhibited markedly by pre-incubation of cells with inhibitors of metabolism such as 2,4-dinitrophenol, sodium azide, *p*-chloromercuriphenyl sulphonate and iodoacetate, each at 1 mM. This suggests that there is an active transport process involved which is independent of sodium translocation across the membrane.

2) The uptake is dependent on a pH gradient across the cell membrane. There is a much higher uptake rate with an alkaline or neutral buffer around cells than with an acidic buffer. That is, there must be an outwardly facing pH gradient i.e. $pH_{in} < pH_{out}$.

3) The uptake is saturable as a function of concentration with apparent K_m values in both the nanomolar and low micromolar range. This again suggests a form of active transport. The K_m values are dependent on tissue type but as an example, thiamine uptake in HEK-293 cells has an apparent K_m at 70.0±18.4 nM and another at 2.66±0.18 µM [Ashokkumar et al., 2006]. Said et al. [2004] determined that the K_m for THTR-2-mediated thiamine uptake was 27.1±7.6 nM in Caco-2 cells. Likewise, Dutta et al. [1999] determined an apparent K_m of 2.5±0.6 µM for thiamine uptake by THTR-1 alone. These two results taken with the work by Ashokkumar et al. [2006] suggest that multiple transporters with different affinities for thiamine work togather to provide overall thiamine transport capacity.

4) Thiamine transport is subject to competition and inhibition by other small molecules. The transport of [^{3}H]thiamine is *cis*-inhibited and *trans*-stimulated by unlabelled thiamine and structural analogues such as oxythiamine and amprolium but not by structurally unrelated organic cations such as tetraethylammonium and *N*-methylnicotinamide. Also, uptake of thiamine is competitively inhibited by amiloride in a dose-dependent manner with an apparent K_i of 0.6 mM in HEK-293 cells.

Collectively, these observations suggest that the thiamine is taken up by at least two carriers which are specific to thiamine and are thiamine-proton antiports. It is thus likely that each contributes to the total capacity for thiamine transport which would explain the multiple apparent K_m values observed. THTR-1 appears to be the more dominant transporter with the higher flux in liver cells [Said et al., 2002] and HEK-293 cells (between four and ten times the flux of THTR-2 [Ashokkumar et al., 2006]). It is worth noting that exposure of cells to high concentrations of thiamine leads to lower levels of transporter expression and protein abundance [Mee et al., 2009], possibly as a result of negative feedback. An alternate explanation would be the ability of thiamine to break open into an acyclic, unionised form and diffuse across the membrane at high concentrations.

2.8.6 Cellular trafficking of THTR-1 and THTR-2

Work on cellular trafficking of THTR-1 and THTR-2 was carried out and published between 2003 and 2006 [Subramanian et al., 2003, 2006]. In each case, a series of experiments was performed in duodenal epithelial cells involving successively truncated forms of the relevant target protein with enhanced green fluorescent protein (EGFP) coupled to the carboxy-terminus. Imaging of the cells after each transfection gave subcellular localisation information and allowed a certain amount of mechanistic determination to be made about sub-cellular movement of the transporters.

The full length THTR-1-EGFP-fused protein was actively expressed on the surface of the cell. When EGFP-fused truncations were studied it emerged that THTR-1 needed amino acids 19–29 in the amino-terminus *and* integrity of the transmembrane backbone polypeptide for surface expression (Figure 2.9). Removal of the carboxy-terminal region did not affect the localisation of the transporter to the surface. Notably, truncations within a region where thiamine responsive megaloblastic anaemia (TRMA) mutations are commonly found resulted in intracellular retention of the protein which may explain some of the aetiology of that disease. Confocal imaging of THTR-1 trafficking revealed that microtubules, but not microfilaments, are essential for its intracellular movement [Subramanian et al., 2003].

THTR-2, unlike THTR-1, appears to be expressed almost exclusively on the apical membrane of polarised cells [Boulware et al., 2003; Subramanian et al., 2006]. This was demonstrated in both Caco-2 cells and MDCK cells as models of the intestine and the kidney respectively. Subramanian et al. [2006] showed that around 90% of fluorescence observed from the full-length THTR-2-GFP fusion protein was seen at the apical membrane with only around 10% seen at the basolateral membrane (Figure 2.10). It is common for many nutrient transporters to be dependent on sequences within their carboxy-termini for correct polarised trafficking yet this was not the case with THTR-2. Despite its carboxy-terminus domain being quite dissimilar to that of THTR-1 and a potential source of difference between the two proteins, THTR-2-GFP fusion proteins with truncations from the carboxy-terminus region were still polarised and inserted in the membrane in the same way as the full-length protein. In a similar manner to THTR-1, modifications to the amino-terminus and the polypeptide backbone prevented correct movement from the intracellular membrane structures to the cell surface [Subramanian et al., 2006]. It is thus likely that THTR-1 and THTR-2 belong to a growing family of proteins more heavily reliant on transmembrane polypeptide sequences to direct their trafficking [Kundu et al., 1996; Lin et al., 1998; Dunbar et al., 2000].

Direct imaging of THTR-2-containing vesicles showed a rapid bi-directional traf-

ficking process to and from the cell surface. This movement of THTR-2-containing vesicles was faster than the movement of THTR-1 containing vesicles (average velocity of 2.3±0.1 versus 1.71±0.13 µm s^{-1} respectively). The movement can again be disrupted by inhibitors of microtubule, but not microfilament, formation as was found with THTR-1. Microtubular structures within MDCK cells are polarised with a minus end at the apical face and a plus end at the basolateral face. Movement along the microtubules is conducted by dyneins (to the minus end) and kinesins (to the plus end). The apical localisation of THTR-2 suggests a role for dyneins in this process but further work is needed to characterise this fully [Subramanian et al., 2006].

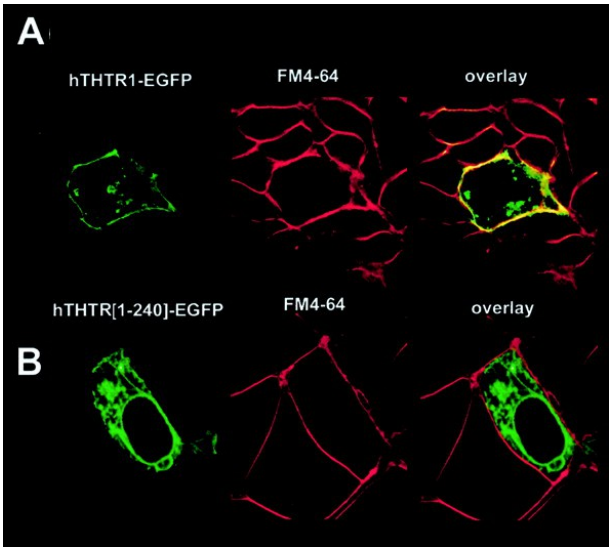

Figure 2.9: THTR-1 localisation. **A:** Left to right: Full length THTR-1-EGFP fusion product in HuTu-80 duodenal epithelium cells (green); FM4-64—a lipophilic styryl dye specific to the plasma membrane (red); Overlay of both plasma membrane and THTR-1-EGFP confirming localisation of full length protein. **B:** Left to right: Truncated THTR-1-EGFP demonstrating intracellular location; FM4-64 plasma membrane marker; overlay. Adapted with permission from Subramanian et al. [2003].

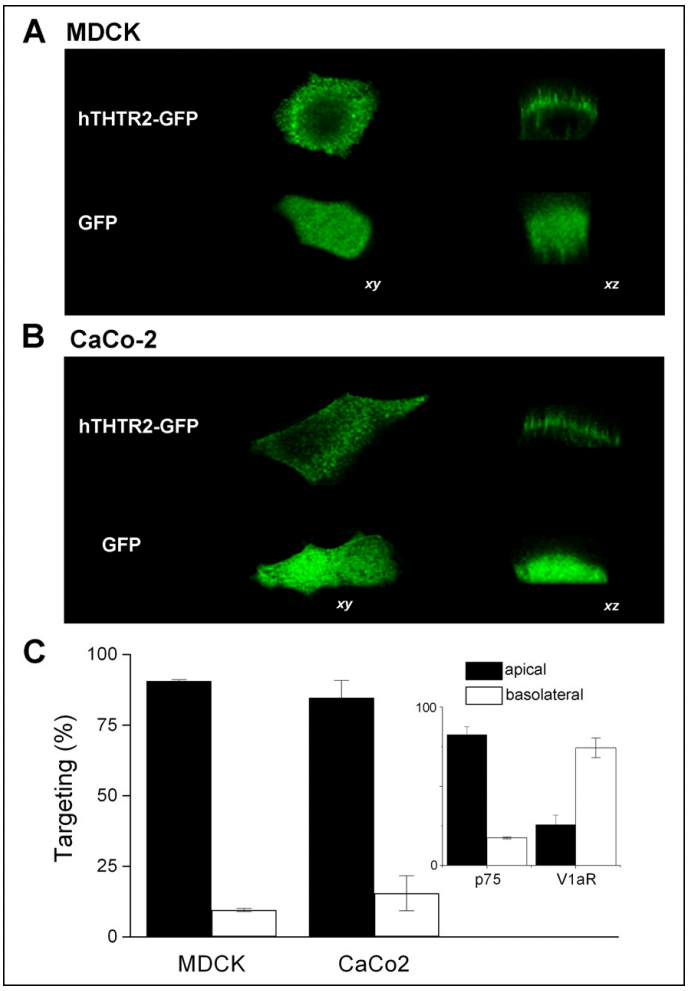

Figure 2.10: THTR-2 localisation. **A:** The targeting of THTR-2-GFP and GFP alone in single MDCK cells in lateral (*xy*, left) and axial (*xz*, right) sections. **B:** The targeting of THTR-2-GFP and GFP alone in single Caco-2 cells in lateral (*xy*, left) and axial (*xz*, right) sections. **C:** The cumulative population measurements of axial polarity of THTR-2 expression, compared with known apical (p75) and basolateral (V1aR) markers. Reproduced with permission from [Subramanian et al., 2006].

Chapter 3

Introduction to glycosylation and Sp1

Glycosylation is the process by which carbohydrate moieties, or glycans, are added to proteins forming glycoconjugate products. These moieties are added by either a co-translational or post-translational process and can range in size from a single monosaccharide unit to large multimeric complexes comprising many monosaccharides. The GlcNAc-β-Asn linkage in ovalbumin was the first glycosylation linkage described [Johansen et al., 1961] and since then the field has expanded dramatically to include a wide range of linkages and chemistries (reviewed by Spiro [2002]).

Glycans can be attached to proteins in one of several manners. An N-glycan, or N-Asn-linked oligosaccharide, as the name suggests is joined by a β-glycosylamine linkage to the nitrogen in the residual group of asparagine residues. In particular, the linkage of N-acetylglucosamine (GlcNAc) monosaccharides to this residue is the most widely distributed of all glycosylations and forms the basis of many large and complex polysaccharide moieties [Spiro, 1973]. O-glycans are linked through an active hydroxyl group in much the same manner as phosphorylations, however their variety is much wider than that of phosphorylation. They are found on every species of hydroxyl containing amino acid residue: serine, threonine, tyrosine and the non-standard amino acids hydroxyproline and hydroxylysine. They are also found in a wide variety of anomeric configurations, both α- and β-forms, and with a wide variety of carbohydrate moieties (Figure 3.1). Most O-linked glycans are based around a molecule of N-acetylgalactosamine (GalNAc) linked to a serine or threonine residue. This core is then extended into a variety of structure sub-classes. Due

to this abundance, the term *O*-glycan is commonly used in the literature to refer specifically to *O*-GalNAc-based glycans. Of course, other *O*-linked glycans exist and these are usually referred to by specific names, e.g. *O*-GlcNAc. Other major classes of glycoconjugates also exist such as C-mannosyl linkages where an α-mannosyl residue is bound to C2 of tryptophan through a carbon-carbon bond [de Beer et al., 1995], phosphoglycosyl bonds where a carbohydrate is attached to a protein via a phosphodiester linkage [Haynes, 1998] and glycosylphosphatidylinositol (GPI) anchors in which mannose residues are used with phosphoethanolamine and phosphatidylinositol to link proteins to a phospholipid membrane. These other classes of structures are beyond the scope of this thesis and will not be discussed further.

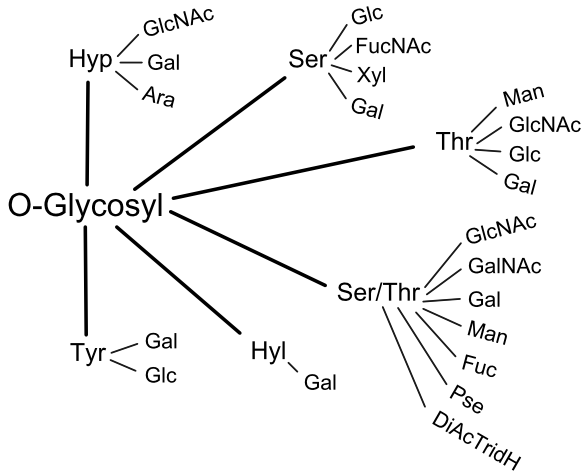

Figure 3.1: Schematic representation of known types of *O*-Linked sugar-peptide bonds. Hyp is hydroxyproline; Hyl is hydroxylysine; GlcNAc is *N*-acetylglucosamine; Gal is galactose; Ara is arabinose; Glc is glucose; FucNAc is *N*-acetylfucosamine; Xyl is xylose; Man is mannose; GalNAc is *N*-acetylgalactosamine; Pse is pseudaminic acid; DiAcTridH is 2,4,-diacetamido-2,4,6-trideoxyhexose. Adapted with permission from Spiro [2002].

3.1 The *O*-GlcNAc modification

It was the prevailing dogma for much of the last century that glycosylation occurred exclusively on proteins that were either actively excreted from the cell or were destined to be transported to the cell surface. By the mid 1980s this view was considered to be incomplete and is likely only to be true today for classical *N*-type glycans and *O*-glycans. Both of these classes of glycan are dependent on glycosyltransferases with active sites contained

within the ER or Golgi apparatus [Varki et al., 1999]. It is now evident that other types of glycosylation exist. Proteins that are not excreted but remain in the nuclear or cytoplasmic compartments can be glycosylated by a number of smaller modifications which are dynamically added and removed post-translationally. A key example of this type of modification is the addition of *N*-acetylglucosamine monosaccharide units via an *O*-linked β-linkage to serine or threonine residues within polypeptides (Figure 3.2). This modification is known as *O*-GlcNAc. It was first characterised systematically in 1983 in studies using radiolabelled UDP-galactose and highly purified bovine galactosyltransferases which were used to tag the *O*-GlcNAc residues [Torres and Hart, 1984]. These early studies were also the first to conclusively demonstrate the location of *O*-GlcNAc in intracellular locations, rather than the traditional extracellular realm of glycosylations where it is notably absent. *O*-GlcNAc presence is widespread throughout multicellular eukaryotes having been seen in virtually all studied systems [Comer and Hart, 2000]. In systems where it is present, it is essential and its ablation is fatal, for example in mouse embryonic stem cells [Shafi et al., 2000].

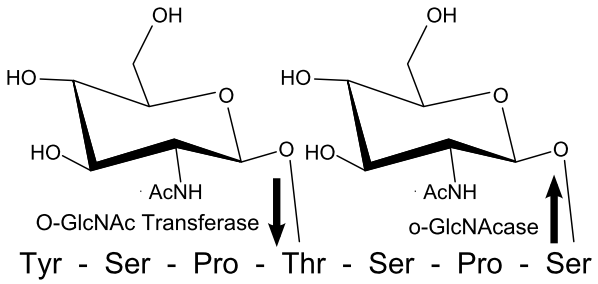

Figure 3.2: The structure of *O*-Linked *N*-acetylglucosamine. *O*-GlcNAc transferase (OGT) dynamically attaches *N*-acetylglucosamine to serine or threonine residues and *O*-GlcNAcase removes the modification. The peptide shown represents a typical attachment site, however there is no well defined consensus sequence. Adapted from Varki et al. [1999].

3.2 Control of *O*-GlcNAc cycling

The amount of *O*-GlcNAc present on serine and threonine residues in a protein, its "*O*-GlcNAcylation" status, is rapidly and dynamically altered by a pair of enzymes in a manner that is highly analogous to phosphorylation and dephosphorylation by kinases and phosphatases. These enzymes are *O*-GlcNAc transferase (OGT; uridine diphospho-*N*-acetylglucosamine:polypeptide β-*N*-acetylglucosaminyltransferase), which adds *N*-acetylglucosamine units, and *O*-GlcNAcase which removes them. Since glycosylation and phos-

phorylation can both potentially occur on the same amino acid residues, there exists a complex dynamic interplay between the two modifications, frequently with multiple sites of phosphorylation or glycosylation on the same protein, often on the same residues [Comer and Hart, 2000]. Indeed, the treatment of cells with agents which promote phosphorylation, like okadaic acid—a phosphatase inhibitor, reduce *O*-GlcNAcylation whilst inhibition of kinases leads to increased levels of *O*-GlcNAc [Griffith and Schmitz, 1999]. Unlike phosphorylation where there are many known pairs of kinases and phosphatases, the single pair of enzymes involved in *O*-GlcNAc cycling suggests that changes to the rate of addition or removal of the *O*-GlcNAc will have wide-reaching effects over the entire cell, rather than specific effects on small sections of metabolism as with phosphorylation [Varki et al., 1999].

3.2.1 *O*-GlcNAc transferase

O-GlcNAc transferase (OGT; E.C. 2.4.1.-) catalyses the addition of *N*-acetylglucosamine to serine or threonine residues within proteins using the activated precursor uridine diphosphate-*N*-acetylglucosamine (UDP-GlcNAc) forming a β-glycosidic link. Its gene is found at Xq13 in humans [Shafi et al., 2000], it was cloned for the first time in 1997 and is highly evolutionarily conserved [Kreppel et al., 1997]. The enzyme, as purified from rat liver, is a heterotrimer comprising two 110 kDa α subunits and one 78 kDa β subunit [Haltiwanger et al., 1992]. It is the α subunit which contains the active site. Each N-terminus of the α-subunits contains at least 11.5 tetratricopeptide repeats—a structural motif made of 34 amino acid residues—[Blatch and Lässle, 1999; Kreppel et al., 1997] which facilitate the formation of large complexes, not only containing the α and β-subunits but also other proteins which can modify the activity and target specificity of the complex [Comer and Hart, 2000].

OGT activity is critically dependent on the abundance of its substrate UDP-GlcNAc. UDP-GlcNAc occupies a unique central position in cellular metabolism with many key pathways combining to produce the molecule (Figure 3.3). It is because of this central position and dependence on UDP-GlcNAc concentration that OGT is so exquisitely sensitive to the metabolic status of the cell. In addition to the central position of UDP-GlcNAc in cellular metabolism, OGT is capable of being *O*-GlcNAcylated itself as well as phosphorylated on tyrosine residues (which appears to activate the enzyme) [Kreppel et al., 1997]. It is inhibited by UDP, in a potent negative feedback loop, and is sensitive to a range of UDP-GlcNAc/UDP ratios which span the entire physiological range of nucleotide sugars. These factors combine to add a further level of complexity to the regulation of the enzyme and *O*-GlcNAcylation itself.

3.2.2 *O*-GlcNAcase

A purified enzyme fraction which could catalytically remove *O*-GlcNAc from proteins was isolated from rat spleen cytosol in by [Dong and Hart, 1994]. The enzyme activity was specific to *O*-GlcNAc and was not affected by the presence of *O*-GalNAc, either as an inhibitor or as a substrate. The enzyme was shown to have two subunits: a 54 kDa α subunit and a 51 kDa β subunit. The apparent mass of the catalytically active enzyme indicates that the molecule is an $\alpha\beta$ heterodimer. The enzyme was first referred to as hexosaminidase C and was observed to have a neutral pH dependence, as opposed to the acidic dependence of the more extensively studied lysosomal hexosaminidases A and B [Varki et al., 1999]. More recently, researchers studying the cytosolic hyaluronidase MGEA5 (meningioma expressed antigen 5) deduced that this enzyme shared the same sequence as the enzyme with the *O*-GlcNAcase activity and that the two proteins were splice variants [Comtesse et al., 2001]. Thus it is common in the literature for the protein to be referred to as *O*-GlcNAcase or MGEA5. The term bifunctional protein NCOAT (nuclear cytoplasmic *O*-GlcNAcase and acetyltransferase) is now also commonly used since the protein has multiple catalytic roles including the acetylation of lysine residues in histone tails.

The nature of the regulation of *O*-GlcNAcase is not fully understood. It appears to be found in protein complexes which often include OGT itself, particularly in the case of transcription complexes. *O*-GlcNAcase also interacts with a large number of other proteins within the cell but little detail is understood. What is known is that its activity is tightly regulated in order to prevent futile cycling of *O*-GlcNAcylation within these complexes.

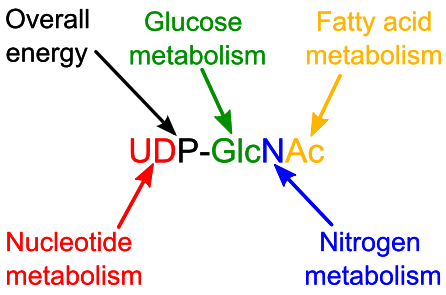

Figure 3.3: UDP-GlcNAc precursors. UDP-GlcNAc biosynthesis is crucially dependent on many diverse areas of cellular metabolism. This unique position means that as a substrate for OGT, it is sensitive to changes in many of these metabolic pathways. Adapted from Varki et al. [1999].

3.3 Functions of *O*-GlcNAc

The role of the *O*-GlcNAc modification is dependent on its exact location and the function of the protein to which it is attached, much as is the case for phosphorylation. Understanding of the role of the *O*-GlcNAc modification began to accelerate once researchers could reliably detect the modification *in situ*. Early research was impeded because *O*-GlcNAc is particularly labile and was frequently lost during ionisation procedures used during mass spectrometery. Early strategies to combat this problem included direct chemical derivatisation of *O*-GlcNAc [Vocadlo et al., 2003] and enzyme-linked derivatisation with a ketone-biotin tag [Khidekel et al., 2003, 2004]. These techniques were complemented by the development of a specific antibody against the *O*-GlcNAc modification which showed the true extent of modification on cellular proteins. Figure 3.4 illustrates *O*-GlcNAcylation in an extract from HeLa cells.

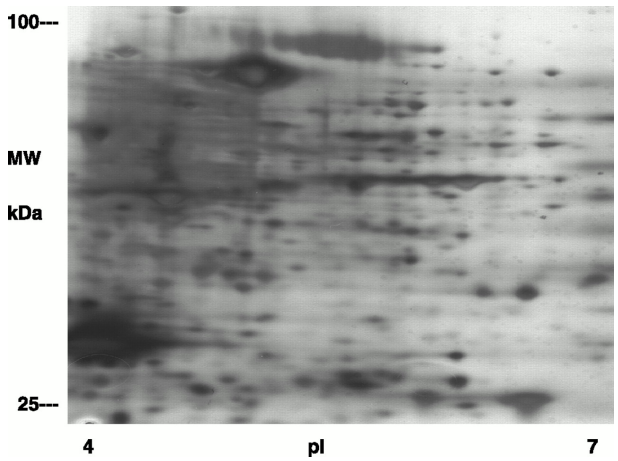

Figure 3.4: An extract from HeLaS3 cells were immunopurified using an *O*-GlcNAc specific antibody. The resultant protein mix was separated using 2D gels and then silver-stained. Large numbers of individual proteins can be seen to be *O*-GlcNAcylated. Reproduced from Wells et al. [2001]

There are several known systems in which *O*-GlcNAc plays a part, some of which are more relevant to this thesis than others. *O*-GlcNAc is known to be important in regulating protein trafficking. For example, in neurons, *O*-GlcNAcylation of synapsin appears to prevent the release of neurotransmitter-containing vesicles from the cytoskeleton, thereby delaying or preventing neurotransmission [Cole and Hart, 1999]. Research on the role of *O*-GlcNAc on synapsins began in 1991 [Lüthi et al., 1991] and is still an active area of research today with recent papers being published on the potential role of *O*-GlcNAc in

synaptic plasticity in the hippocampus e.g. [Tallent et al., 2009]. As an aside to this, *O*-GlcNAc has also been implicated in the pathogenesis of several neurodegenerative diseases. The locus for the OGT gene, Xq13, has been linked to Parkinson's dystonia [Graeber et al., 1992] and the *O*-GlcNAcase locus, 10q24.1 has been linked to late onset Alzheimer's disease. Direct inhibition of *O*-GlcNAcase appears to block tau phosphorylation *in vivo* [Yuzwa et al., 2008] and tau *O*-GlcNAcylation itself appears to be important in development of aggregated tau bundles [Gong et al., 2006].

Protein turnover is also affected by *O*-GlcNAcylation. Several core parts of the 26S proteasome are *O*-GlcNAcylated which appears to inhibit ATPase activity of the proteasome, thereby lowering proteolytic capacity e.g. [Zhang et al., 2007]. Also, there is a definite link between *O*-GlcNAc and ubiquitination itself; the two processes aren't completely antagonistic but ubiquitination appears to be modulated by *O*-GlcNAcylation with E1, the ubiquitin activating enzyme, being *O*-GlcNAcylated [Guinez et al., 2008]. Reduced glycosylation of the transcription factor Sp1 has been shown to be associated with increased proteasome susceptibility [Han and Kudlow, 1997].

Perhaps most importantly, *O*-GlcNAc modification is heavily involved with the regulation of transcription and translation. The direct *O*-GlcNAcylation of several transcription factors is important to modify their function. Such modified transcription factors include NF-κB, p53, c-Myc, CREB and Sp1 [Zachara and Hart, 2004]. In addition, basal transcription factors such as the eukaryotic initiation factor 4A1, parts of the ribosome and RNA polymerase II are modified [Zachara and Hart, 2004; Jackson and Tjian, 1989]. This opens up a massive potential for cellular regulation by *O*-GlcNAcylation.

3.4 *O*-GlcNAc in diabetes

O-GlcNAc levels are intrinsically linked to the availability of UDP-GlcNAc which in turn is dependent on the availability of glucose. Flux through the hexosamine biosynthesis pathway (HBP) which produces the UDP-GlcNAc normally accounts for 2–5% of the total glycolytic flux. Under conditions of elevated glucose or glycolytic inhibition (for example, increased free fatty acid metabolism inhibits pyruvate oxidation [Hawkins et al., 1997]) higher absolute fluxes pass through the HBP leading to elevated UDP-GlcNAc levels and higher rates of *O*-GlcNAcylation. This provides a link between elevated *O*-GlcNAc levels with diabetes, in which glucose levels are inherently unstable and hyperglycaemia is common, and increased flux through the HBP which has long been implicated in hyperglycaemic toxicity [Brownlee,

2001]. There is much evidence that hyperglycaemia is responsible for increased flux through the HBP in a wide variety of systems. Pang et al. [2004] report how HBP flux is increased in neonatal rat cardiomyocytes in hyperglycaemia and Rajamani and Essop [2010] also report that hyperglycaemia induces the HBP leading to apoptosis in the myocardium. Pantaleon et al. [2010] ascribe the toxic effects of hyperglycaemia on early mouse embryos to increased flux through the HBP and James et al. [2002] propose that hyperglycaemia causing increased flux through the HBP is responsible for determining transcription of NF-κB-dependent genes in mesangial cells.

The ultimate effect of increased flux through the HBP is increased *O*-GlcNAcylation. A multitude of studies have been published which attempt to link increased *O*-GlcNAcylation with the complications of diabetes. Teo et al. [2010] reviewed studies demonstrating that increased HBP flux in adipocytes leads to an impairment in insulin-dependent glucose uptake i.e. insulin resistance. Further studies increased the HBP flux by a variety of means including glucosamine infusion (bypassing the flux-controlling GFAT at the start of the HBP pathway, [Virkamäki et al., 1997; Rossetti et al., 1995]), GFAT transgenic mice [Hebert et al., 1996; Hazel et al., 2004] and OGT transgenic mice [McClain et al., 2002]. In each case, levels of *O*-GlcNAc increased and insulin resistance was observed. In addition, McClain et al. [2002] found deoxynorleucine, an inhibitor of GFAT, prevented this observed insulin resistance, confirming that it is the combination of OGT and UDP-GlcNAc that is important. Work conducted by Fülöp et al. [2007] on the myocardium in Zucker diabetic fatty (ZDF) rats showed elevated cellular UDP-GlcNAc and concomitant *O*-GlcNAcylation. However, there was no change in OGT expression suggesting that it is increased flux through the HBP that is crucial in this model. The myocardium was observed to exhibit several characteristics typical of type 2 diabetic cardiomyopathy including delayed calcium sequestration and impaired mechanical relaxation. More recently, research with kidney sections from patients suffering from diabetic nephropathy by Degrell et al. [2009] has shown that the number of nuclei which stain positive for *O*-GlcNAc in diabetic glomeruli is significantly higher than for control kidneys.

In summary, it is now clear that hyperglycaemia, hyperlipidaemia and insulin can all affect *O*-GlcNAcylation and that the dysregulation of this important means of modification of cellular transcription is likely to be a key culprit in the aetiology of diabetic complications [Hart et al., 2007; Dias and Hart, 2007].

3.5 The Sp family of transcription factors

The Sp family of transcription factors constitutes half of a major group of transcription factors called the Sp/KLF family (KLF: Krüppel-like factor, so named because of its homology to the *Drosophila* protein Krüppel). There have been eight members of the Sp family discovered to date. The first, Sp1, was characterised in 1987 after an earlier discovery [Dynan and Tjian, 1983; Kadonaga et al., 1987, 1988] whilst more recently discovered members of the family have been numbered incrementally. The name Sp originally referred to the purification scheme for the protein which included Sephacryl and phosphocellulose columns. However, more recently other expansions have been attached to the abbreviation including "specificity protein" and "stimulating protein". Each member of the family contains three highly conserved Cys_2His_2 zinc-finger domains for binding specific sequences of DNA known as GC boxes (consensus sequence 5'–GGGGCGGGG–3') or GT boxes (consensus sequence 5'–GGTGTGGGGG–3') [Letovsky and Dynan, 1989; Philipsen and Suske, 1999]. Not all members of the Sp family have been studied equally; Sp1 and Sp3 have been more thoroughly studied compared to other members of the family. Sp2 appears to be expressed ubiquitously but there is little data on specific tissue expression levels [Kingsley and Winoto, 1992]. Sp4 is found only in the developing testes and the brain, Sp7 is involved in osteoblast differentiation [Nakashima et al., 2002] and the expression characteristics of the other members of the family have yet to be investigated thoroughly [Waby et al., 2008].

3.5.1 Sp1 transcription factor

As a key ubiquitous transcription factor, Sp1 expression is essential for life: Sp1 null mice die around embryonic day 11 after a period of retarded development [Marin et al., 1997]. Sp1 has a molecular mass of around 81 kDa and shares structural similarity with other members of the Sp family (Figure 3.5). Both Sp1 and Sp3 have been shown to be bifunctional as transcriptional regulators. Whether they activate or repress transcription of a particular gene depends on the cell type and the promoter although the mechanisms behind this process are poorly understood. As an example, Sp1 has been shown to repress transcription of the human adenine nucleotide translocase-2 (ANT2) promoter [Zaid et al., 2001] yet it promotes transcription of the thiamine transporters THTR-1 and THTR-2 [Reidling and Said, 2003; Nabokina and Said, 2004]. The situation isn't clear even when a gene has been determined as "activated" or "repressed" by Sp1 since the influence of other factors can change the activity of Sp1 in a given situation; the presence of platelet-activating factor prevents the

repression of MMP-9 expression by Sp1 in human corneal epithelial cells [Taheri and Bazan, 2007].

Sp1 is capable of synergistic activation where a promoter element contains multiple Sp1 binding sites. Sp1 appears to achieve this through a direct protein-protein interaction which loops the intervening DNA, something that Sp3 is incapable of [Mastrangelo et al., 1991; Su et al., 1991]. Sp1 also appears to play a key role in regulating the methylation pattern of genes by maintaining methylation-free CpG islands for many promoter elements, mainly house-keeping genes. Sp1 exerts transcriptional control over a large number of genes spread over virtually the entire genome but with strong emphasis on genes involved in the synthesis and metabolism of nucleotides along with cell cycle-related genes. Importantly for this thesis, the promoter elements for the thiamine transporters contain Sp1 binding sites.

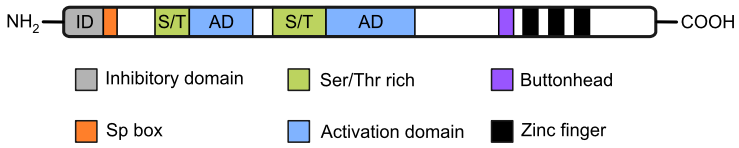

Figure 3.5: Structure of the Sp family from Sp1 to Sp4. This figure shows the structure of the lower part of the Sp family with key domains highlighted. The two activator domains are each capable of stimulating transcription when bound to DNA through a DNA-binding zinc-finger domain. The serine and threonine rich regions are involved with most post-translational modification, especially phosphorylation and glycosylation. The buttonhead domain is in a highly charged region of the protein and is used for synergistic activation by sterol-regulatory element-binding proteins. [Li et al., 2004; Solomon et al., 2008].

Notably, the promoter elements for genes regulated by Sp1 are often missing the TATA box for binding TATA-binding protein (TBP) and recruitment of the associated TBP-associated factors (TAFs) [Kadonaga et al., 1987]. Instead, Sp1 is capable of binding to transcription factor TFIID via TATA binding protein associated factors TAFII130 and TAFII55 before recruiting the RNA polymerase RNAPolII directly [Gill et al., 1994; Solomon et al., 2008]. It has been estimated by Letovsky and Dynan that there are between 5000 and 10 000 copies of Sp1 within a mammalian cell which corresponds to an intranuclear concentration of between 1.25–2.5 $\times 10^{-7}$ M [Letovsky and Dynan, 1989].

3.5.2 Sp1 post-translational modifications

The fact that Sp1 is capable of being *O*-GlcNAcylated was first demonstrated by Jackson and Tjian [1988] who noted that Sp1 could be purified using its affinity for wheat germ

agglutinin. We now know that members of the Sp family can accept a wide range of post-translational modifications with residues spread throughout their structures that can accept phosphorylation, *O*-GlcNAcylation, acetylation, ubiquitination and SUMOylation (small ubiquitin-like modifier). Sp1 is capable of being glycosylated on at least eight different residues with sites scattered throughout the structure. Some are located in the serine and threonine rich regions highlighted in Figure 3.5 but others are located in regions such as the zinc finger domains. Despite being thought of as a basal transcription factor, the large number of post-translational modifications that the Sp1 can accept means that it is a perfect candidate for modulating gene expression in response to hormonal and other factors (reviewed by Solomon et al. [2008]).

Before discussing modifications in detail, one important factor which should be reiterated is that serine and threonine residues are potential targets for both glycosylation and phosphorylation. This conflict is not hypothetical but very real. A common conclusion in the Sp1 field is that this competition is key and that both phosphorylation and *O*-GlcNAcylation occur on the same residues at different times (reviewed by Wells et al. [2001]).

Modifications to Sp1 appear to alter its function in several ways. Often, a modification will alter the sub-cellular location of the transcription factor, thereby altering its transcriptional activities. Alternatively, the modifications either promote or inhibit protein-protein interactions with varied consequences. In many cases, these modifications are driven by an external factor such as insulin. These will be discussed in turn below.

3.5.3 Translocation of Sp1 to the nucleus

Like many transcription factors, Sp1 can be found both in the nucleus, where it can be active, and the cytosol, where it is transcriptionally inactive. Its location appears to be determined by its phosphorylation and glycosylation status. Studies in liver cells have shown that insulin treatment leads to *O*-GlcNAcylation of Sp1 followed by a translocation to the nucleus within 30 minutes. By 240 minutes, *O*-GlcNAcylated Sp1 in the nucleus had diminished to negligible levels. Meanwhile, phosphorylated Sp1 levels increased in the nucleus during the same time period. The researchers concluded that *O*-GlcNAcylation is critical for nuclear translocation followed by phosphorylation (often on the same residues) for activation of its transcription factor functions [Majumdar et al., 2004, 2006]. Other studies such as work on rat lymphoma cells by Dauphinee et al. [2005] have also linked *O*-GlcNAcylation of Sp1 with nuclear translocation. This potential mode of action is shown in Figure 3.6A.

3.5.4 Insulin and Sp1

Insulin not only appears to affect short term glycosylation of Sp1; it also modulates long-term Sp1 abundance. Studies on insulin deprivation in H-411E hepatocyte cells by Pan et al. [2001] showed a drop in Sp1 concentration. Furthermode, low basal levels of liver Sp1 were markedly increased upon administration of insulin in the streptozotocin-induced diabetic rat [Pan et al., 2001]. Paradoxically, glucagon also has a similar effect on Sp1 concentrations. Glucagon would normally be expected to be an antagonist to the actions of insulin but in the same H-411E hepatocyte system, glucagon treatment led to an increase in Sp1 steady-state concentrations although this appears to be through a cAMP dependent pathway [Keembiyehetty et al., 2002]. Additionally, Walgren et al. [2003] demonstrated that hyperglycaemia and insulin are both capable of increasing the glycosylation of Sp1 with each re-enforcing the actions of the other.

This means that insulin not only affects the short-term glycosylation status of Sp1 (and thus its subcellular location and activity) but also its long-term abundance in the cell. This appears to be where the actions of insulin and glucagon differ because only insulin, and not glucagon, is capable of altering the glycosylation status of Sp1 [Keembiyehetty

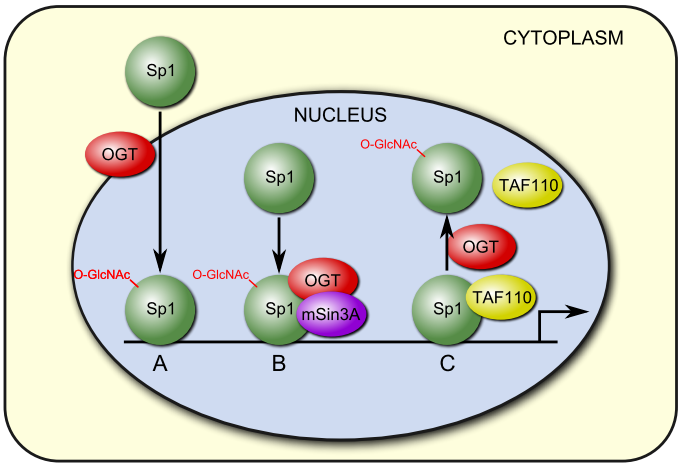

Figure 3.6: The roles of *O*-GlcNAcylation of Sp1. The conflicting roles of Sp1 *O*-GlcNAcylation are shown in this figure adapted from Özcan et al. [2010]. **A:** *O*-GlcNAcylation of Sp1 has been shown to promote nuclear translocation and activation of transcription [Majumdar et al., 2004, 2006]. **B:** Sp1 *O*-GlcNAcylation can also lead to repression of transcription by recruitment of the co-repressor protein mSin3A by OGT [Yang et al., 2002]. **C:** Other studies have shown that modification of Sp1 by *O*-GlcNAc can disrupt its interaction with TAF110, thereby repressing transcription. [Roos et al., 1997]

et al., 2002]. In summary, the action of insulin on Sp1 appears to increase long-term Sp1 levels and also short-term *O*-GlcNAcylation which leads to nuclear translocation of Sp1 and subsequent activation of transcription.

3.5.5 Other effects of Sp1 glycosylation

The nuclear translocation of Sp1 by glycosylation is in contrast to other functions of *O*-GlcNAcylation of Sp1. Whereas translocation to the nucleus would appear to increase transcription, Yang et al. [2002] have shown that OGT recruitment to Sp1 in the nucleus can glycosylate Sp1 and simultaneously recruit the corepressor mSin3A which represses transcription (Figure 3.6B).

O-GlcNAc has also been implicated in the susceptibility of Sp1 to proteolytic degradation. Han and Kudlow [1997] artificially altered the glycosylation status of many proteins in normal rat kidney (NRK) cells and MDA-468 breast cancer cells with 5 mM glucosamine. This bypassed the enzyme with most control over flux into the hexosamine biosynthesis pathway and led to hyperglycosylated Sp1. Complementarily, they used glucose starvation coupled with cAMP stimulation of the same cells to induce a hypoglycosylated state with nearly all Sp1 being non-glycosylated. After this depletion of glycosylation, Sp1 became very susceptible to proteolytic degradation by the proteasome. Additional work by Kudlow's group [Roos et al., 1997] has shown that *O*-GlcNAcylation of Sp1 blocks its ability to interact with TAF110 which represses its transcriptional activation abilities (Figure 3.6C).

Kang et al. [2003] used 2-deoxyglucose, a non-metabolizable glucose analogue which mimics glucose starvation. In this system they showed that despite mimicking a low glucose environment in the cells, Sp1 was counter-intuitively *hyper*-glycosylated yet its Sp1-dependent gene expression was lower. The Sp1 field is full of controversey similar to this and in a recently published review on glycosylation of transcription factors, Özcan et al. [2010] highlight how little we fully understand about how the glycosylation of Sp1 affects its activity. The exact result of glycosylation in any given circumstance appears to be difficult to predict and empirical data needs to be sought for any given situation. In addition to these complex observations, little work has been done on the sites of glycosylation. It may be that the effects are very much site-dependent, something not seen in studies to date.

3.5.6 Sp1 phosphorylation

A large number of studies have been performed on the effects of phosphorylation on Sp1. The consensus opinion is that phosphorylation leads to a higher affinity of Sp1 for DNA—

and with it more active transcription of the target gene—whilst dephosphorylation leads to a decreased affinity for DNA and decreased transcription. Often the phosphorylation sites occur within the zinc finger domains which has lead to suggestion that the phosphorylation is altering the structure of the zinc finger and increasing its affinity for the DNA [Waby et al., 2008].

Recent work by Chuang et al. [2008] has shown that the phosphorylation of Sp1 appears to be important for its stability during mitosis. This is contrary to much evidence which says that overall, phosphorylation of Sp1 appears to target it for proteolytic degradation, specifically phosphorylation on serine 7 with proteolytic processing being regulated by phosphorylation on serine 59 [Spengler et al., 2008]. In contrast, Vicart et al. [2006] suggest that it is *dephosphorylation* of Sp1 that is important for its stability and activity during transcription of genes involved in cell division. It is clear from the controversy in the literature that the understanding of the function of phosphorylation on Sp1 is incomplete.

3.5.7 Sp1 and the thiamine transporter genes

Analysis of the promoter elements of each member of the *SLC19Ax* family, which includes the thiamine transporters, has demonstrated that each contains at least one GC box which binds Sp1 and other members of the Sp family. In each case, analysis showed that the presence of Sp1 was essential for basal transcription of the gene with an almost complete ablation of promoter activity following introduction of GC-box sequence oligonucleotides to compete for the available Sp1 (*SLC19A1*: 3 GC boxes [Tolner et al., 1999]; *SLC19A2*: 1 GC box [Reidling and Said, 2003]; *SLC19A3*: 2 GC boxes [Nabokina and Said, 2004]). Likewise, the basal expression of each of the genes for THTR-1 and THTR-2 could be diminished by mutating the GC-box sequence in each promoter element [Reidling and Said, 2003; Nabokina and Said, 2004]. Studies in the Sp-deficient *Drosophila* SL2 cell line showed that either Sp1 or Sp3 could activate *SLC19A3* transcription in a dose-dependent manner [Nabokina and Said, 2004]. Therefore it remains unclear which protein is required *in vivo* as either may perform the activation. None of these studies investigated the effects of glycosylation of Sp1 on the efficiency of induction of transcription.

Chapter 4

Project-specific background

4.1 Thiamine deficiency in diabetes

Chronic thiamine deficiency is associated with the classical diseases beri-beri [Tanphaichitr et al., 1970] and Wernicke-Korsakoff syndrome (which comprises Wernicke's encephalopathy and Korsakoff's associated psychosis) [Butterworth, 2003; Pannunzio et al., 2000]. These are only observed in patients who have a severe, chronic deficiency of thiamine which could be due to a diet lacking the vitamin (i.e. malnutrition), chronic alcoholism (the most common reason for presentation with severe thiamine deficiency in the developed world) or increased clearance of thaimine in renal dialysis or HIV/AIDS (reviewed by Thornalley [2005]). Thiamine deficiency is conventionally assessed by means of the thiamine effect, or percentage unsaturation of transketolase with its cofactor TPP (Section 2.7). None of the likely reasons for a severe thiamine deficiency are are associated with diabetes mellitus but a mild thiamine deficiency may well be present in the diseased state. This has been considered for a long time [Janes and Brady, 1948] but only recently has more detailed study been undertaken.

The evidence for a mild thiamine deficiency in diabetic patients has mounted since the 1960s from a series of small observation trials. A Norwegian study conducted by Haugen [1964] demonstrated a 27% decrease in whole blood thiamine in 21 type 1 diabetes patients but no decrease in 12 type 2 diabetes patients. A Japanese survey of thiamine status in 7 type 1 and 39 type 2 moderately well controlled diabetic patients was conducted [Saito et al., 1987]. It concluded that 79% of diabetic patients had an erythrocyte TK activity below the normal minimum and 76% had a plasma thiamine concentration lower than the normal min-

imum. An Israeli study of 100 type 2 diabetic patients with a mean HbA_1 of 9.2% showed that erythrocyte TK activity was below the normal minimum in 18% of patients [Havivi et al., 1991]. In addition, a small study conducted by Valerio et al. [1999] in Italy examined the thiamine status of 10 type 1 diabetic patients and found that plasma thiamine concentration was 34% lower than normal controls and could be normalised in a placebo-controlled trial with 50 mg day^{-1} of the thiamine derivative benzoxymethyl-thiamine. Furthermore, a study in Hungary conducted by Jermendy [2006] investigated erythrocyte transketolase activity in seventy five diabetic patients (13 type 1 and 62 type 2 with a mean HbA_{1c} of 9.6%) and showed that the thiamine effect was significantly higher in diabetic patients that controls (14%±1% versus 8%±2%). Five of the patients were treated for seven days with 320 mg Benfotiamine daily and a significant decrease in their thiamine effect was observed (10%±3% versus 2%±2%) [Jermendy, 2006] suggesting therapy with thiamine derivatives may be beneficial.

Most recently, our laboratory studied the thiamine status of 26 type 1 and 48 type 2 diabetic patients with and without microalbuminuria in the Colchester region along with 20 normal healthy control volunteers [Thornalley et al., 2007]. We found that the plasma thiamine concentration, as measured by HPLC, was decreased 76% in type 1 diabetic patients and 75% in type 2 diabetic patients (median concentrations (95% confidence intervals): normal volunteers 64.1 nM (58.5–69.7 nM), type 1 diabetic patients 15.3 nM (11.5–19.1 nM; $p < 0.001$) and type 2 diabetic patients 16.3 nM (13.0–19.6 nM; $p < 0.001$); Figure 4.1). This decrease in plasma thiamine concentration was linked to a marked increase in renal clearance and fractional excretion of thiamine in the diabetic state. Renal clearance rates were increased 24-fold in type 1 diabetes and 16-fold in type 2 diabetes (median clearance rates were 3.7, 86.5 and 59.8 mL min^{-1} in control, type 1 and type 2 diabetic patients respectively) and fractional excretion was increased 25-fold in type 1 diabetic patients and 15-fold in type 2 diabetic patients (median fractional excretion was 2.8%, 71.2% and 41.6% in control, type 1 and type 2 diabetic patients respectively). There was no evidence of a nutritional deficiency of thiamine as judged by urinary thiamine in the normal range (> 0.20 µmol day^{-1} [Finglas, 1993]). Rather, plasma thiamine concentration negatively correlated with both renal clearance and fractional excretion of thiamine suggesting that the plasma thiamine deficiency was linked to renal mis-handling of filtered thiamine i.e. a substantial decline in tubular re-uptake of thiamine in diabetes. Additionally, plasma thiamine concentration and urinary excretion of thiamine negatively correlated with the concentration of soluble vascular cell adhesion molecule 1 (sVCAM-1), a marker of vascular dysfunction.

Interestingly the same study revealed why clinical thiamine deficiency in diabetes has gone unreported: erythrocyte TK activity, the primary clinical measure of thiamine deficiency [Haas, 1988], was not significantly different between control patients and diabetic patients, that is all patient values were below 15%. Further investigation showed that the plasma deficiency was masked by increased abundance of THTR-1 and the TMP-transporter RFC-1 in erythrocyte membranes which maintained intracellular thiamine concentrations despite the low plasma abundance. These transporters are likely up-regulated in erythrocyte precursors in reponse to the low thiamine concentration in plasma. In confirmation, direct analysis of intra-erythrocyte thiamine concentrations by HPLC showed no difference between diabetic patients and control volunteers, confirming that the higher abundance of transporter protein was masking plasma thiamine deficiency.

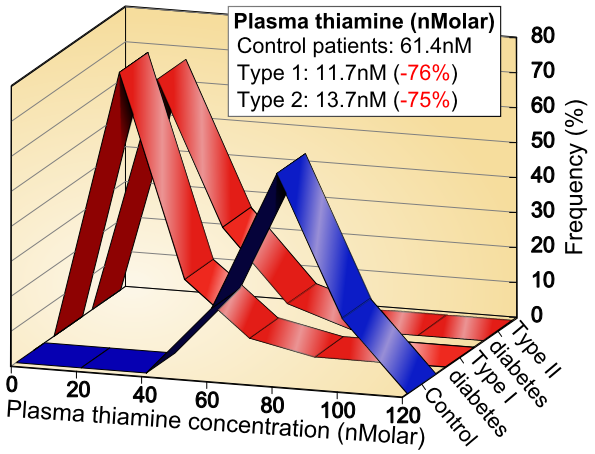

Figure 4.1: Diabetic thiamine deficiency. This frequency distribution shows that diabetic patients have marked plasma thiamine deficiency. Data in the inset represent median values for 20, 26 and 48 patients for control, type 1 and type 2 diabetes respectively. Adapted with permssion from Thornalley et al. [2007].

A small study in Australia published by Vindedzis et al. [2008] surveyed the thiamine intake status of 113 diabetic patients with both type 1 and 2 diabetes. They found that only 15.7% of patients not taking thiamine supplements had a low level of intra-erythrocyte thiamine. Vindedzis et al. [2008] concluded that supplementation with thiamine at approximately three times the recommended daily intake rate (>4 mg daily in Australia) was significantly correlated with normal erythrocyte thiamine levels but that adequate thiamine intake within the normal dietary range was not.

4.2 Thiamine and biochemical dysfunction *in vitro*

The effects of hyperglycaemia on human erythrocytes was studied by Thornalley et al. [2001]. They noted that supplementation with thiamine alleviated some of the hyperglycaemia-induced biochemical dysfunction. Specifically, incubation of the cells with 50–500 µM thiamine led to an increase in the activity of transketolase, a decrease in the concentration of the triosephosphate pool, a decreased rate of formation and concentration of methylglyoxal and increases in the concentrations of two pentose phosphate pathway intermediates, sedoheptulose-7-phosphate and ribose-5-phosphate. This effect was explained by the stimulation of the pentose phosphate pathway and a concomitant increase in activity of the non-oxidative branch of the PPP by thiamine in a manner as described above (Section 4.4 and Figure 4.2).

Other studies exposed bovine aortal endothelial cells to hyperglycaemic conditions and researchers noted an increase in membrane-localised PKC activity along with activation of poly (ADP-ribose) polymerase [Du et al., 2003], increases in intracellular UDP-GlcNAc and AGE concentration and activation of NF-κB, a transcription factor sensitive to oxidative damage. Each of these pathways of damage was blocked by the addition of 50–100 µM Benfotiamine (*S*-benzoylthiamine *O*-monophosphate) to the culture conditions [Hammes et al., 2003; Mabley et al., 2004]. Further work in bovine aortal endothelial cells has demonstrated that thiamine can prevent hyperglycaemia-induced delay in replication [Selva et al., 1996] and increase in von Willebrand factor [Ascher et al., 2001].

Work by Porta's group on bovine retinal pericytes and human umbilical vein endothelial cells (HUVECs) *in vitro* has shown that both thiamine and Benfotiamine act to prevent hyperglycaemia-induced decreases in replication, increases in apoptosis and increases in AGE accumulation [Beltramo et al., 2004; Selva et al., 1996]. In addition, in human retinal pericytes, both treatments prevented apoptosis induced by hyperglycaemia-conditioned extracellular matrix [Beltramo et al., 2009], corrected the increase in matrix metalloproteinase-2 (MMP-2) caused by hyperglycaemia and also increased the expression of tissue inhibitor of metalloproteinase-1 (TIMP-1) [Tarallo et al., 2010]. In HUVECs, thiamine and Benfotiamine both ameliorate the hyperglycaemia-induced activation of the polyol pathway by mediating an increase in transketolase activity and a decrease in aldose reductase mRNA and expression [Berrone et al., 2006].

4.3 Thiamine intervention therapy *in vivo*

In 2003, Babaei-Jadidi et al. [2003] published the results of a study of both thiamine and Benfotiamine supplements at both a low and high concentration (7 or 70 $\mathrm{mg\,kg^{-1}\,day^{-1}}$) given to streptozotocin-induced diabetic rats receiving low-dose insulin to moderate the diabetes for six months. They demonstrated that both thiamine and Benfotiamine were capable of preventing the onset of diabetic nephropathy as judged by the prevention of microalbuminuria. Thiamine and Benfotiamine were also effective in lowering the accumulation of AGEs in renal glomeruli, retina, sciatic nerve, urine and plasma [Karachalias et al., 2010a]. This result was achieved without affecting plasma glucose concentration or glycated haemoglobin. Benfotiamine also prevented hyperfiltration in diabetic animals relative to control diabetic animals. Both thiamine and Benfotiamine also corrected increased renal clearance of thiamine, glucosuria and increased diuresis. Whilst investigating the mode of action, they noted that both thiamine and Benfotiamine supplementation increased the plasma thiamine concentration in all tested groups which subsequently increased transketolase activity; transketolase abundance was only increased in the 70 $\mathrm{mg\,kg^{-1}\,day^{-1}}$ group. This diverted triosephosphates to ribose-5-phosphate and led to a decrease in PKC activity, a decrease in AGEs and a decrease in oxidative stress as measured by plasma thiol concentration. A plasma thiamine deficiency of 50–70% was also noted in the unsupplemented diabetic rats relative to the normal control rats: plasma thiamine concentration was 50–70% lower in diabetic rats.

Hammes et al. [2003] investigated the effects Benfotiamine on the development of retinopathy in Wistar rats as judged by the increase in formation of retinal acellular capillaries. High dose supplementation at 80 $\mathrm{mg\,kg^{-1}\,day^{-1}}$ was sufficient to prevent significant increase in the number of capillaries compared to control animals.

Further studies in streptozotocin-induced diabetic Wistar rats have investigated the progression of neuropathy as judged by decreased nerve conduction velocity (NCV). Therapy with high dose thiamine and Benfotiamine (70 and 100 $\mathrm{mg\,kg^{-1}\,day^{-1}}$ respectively) prevented the decrease in NCV along with preventing accumulation of AGEs [Stracke et al., 2001]. Diabetic neuropathy has also been studied in humans. Diabetic patients ($n = 24$) received Benfotiamine at 80 $\mathrm{mg\,day^{-1}}$, pyridoxine at 180 $\mathrm{mg\,day^{-1}}$ and cyanocobalamin at 0.5 $\mathrm{mg\,day^{-1}}$ for two weeks followed by a ten week period at half dosages showed a significant increase in NCV relative to placebo [Stracke et al., 1996]. Of course, the results in this study may not be specific to Benfotiamine.

Thiamine and Benfotiamine supplements have also been evaluated for their effect

against cardiomyopathy [Ceylan-Isik et al., 2006; Kohda et al., 2008]. Thiamine treatment prevented decline in glycaemic control of streptozocin-induced diabetic rats in a manner linked to residual β-cell function [Karachalias et al., 2010b]. Thiamine reduced plasma glucose and leptin concentration in drug naïve type 2 diabetic patients [González-Ortiz et al., 2010]. Also, the Hoorn study linked low dietary thiamine to progression of patients to impaired glucose tolerance (IGT) and type 2 diabetes [Bakker et al., 1998]. Thus there may be beneficial effects of thiamine therapy in the prevention of loss of glycaemic control in IGT and early stage type 2 diabetes.

4.4 Mode of action for thiamine therapy

There are several theories that attempt to explain the link between hyperglycaemia and diabetic complications. As previously discussed, these include increased flux through the polyol pathway, increased production of AGEs, activation of protein kinase C and activation of the hexosamine biosynthesis pathway. All of these pathways are likely to be linked through an overproduction of superoxide by the mitochondria. The common feature behind each of these theories is the accumulation of intracellular glucose in endothelial cells, mesangial cells and podocytes which have high expression of the glucose transporter GLUT1 [Heilig et al., 1995; Coward et al., 2005]. This high intracellular glucose concentration then leads to an increase in glycolytic intermediates and in particular a build-up of triosephosphates. These accumulating glycolytic intermediates are the driving force behind each of the theories explaining dysfunction.

Thiamine therapy uses a novel approach to potentially address this increase in intermediate accumulation. By increasing the activity of the cytosolic enzyme TK, it boosts flux through the reductive pentose phosphate pathway. The reductive PPP allows an alternative route for diversion of these intermediates and thus increasing its activity diverts potentially damaging glycolytic intermediates such as glyceraldehyde-3-phosphate into relatively low reactivity metabolic products such as ribose-5-phosphate (Figure 4.2). It is through this pathway that thiamine therapy is proposed to act.

4.5 The HK-2 cell line

The HK-2 cell line is used in this project as an *in vitro* model of the human proximal tubule epithelium. It was produced by Ryan et al. [1994] from a primary culture grown

from normal human adult male renal cortex. The culture was exposed to a recombinant retrovirus containing the human papilloma virus (HPV 16) E6 and E7 genes. This method of transduction has been shown to immortalise many diverse types of epithelial cells without changing their function (e.g. [Halbert et al., 1991; Hawley-Nelson et al., 1989]). The E6 and E7 gene products bind to DNA regulation proteins and promote cell proliferation without causing deviation from normal controls on growth such as cell-cell adhesion and anchorage dependency. This means that cells immortalised in this manner are more like the original cells than many highly transformed cell lines.

Ryan et al. verified the identity of their stably transfected cell line by comparison to primary cultures of the same cells. Adenylate cyclase activity in response to parathormone and antidiuretic hormone was measured—proximal tubules respond with an increase in adenylate cyclase activity to parathormone but not to antidiuretic hormone. α-methyl glucopyranoside cell uptake (a marker of glucose transport) was assessed in the presence of sodium chloride and phlorizin (uptake is sodium dependent and inhibited by phlorizin) and found to be similar to primary cultures of proximal tubule epithelium cells.

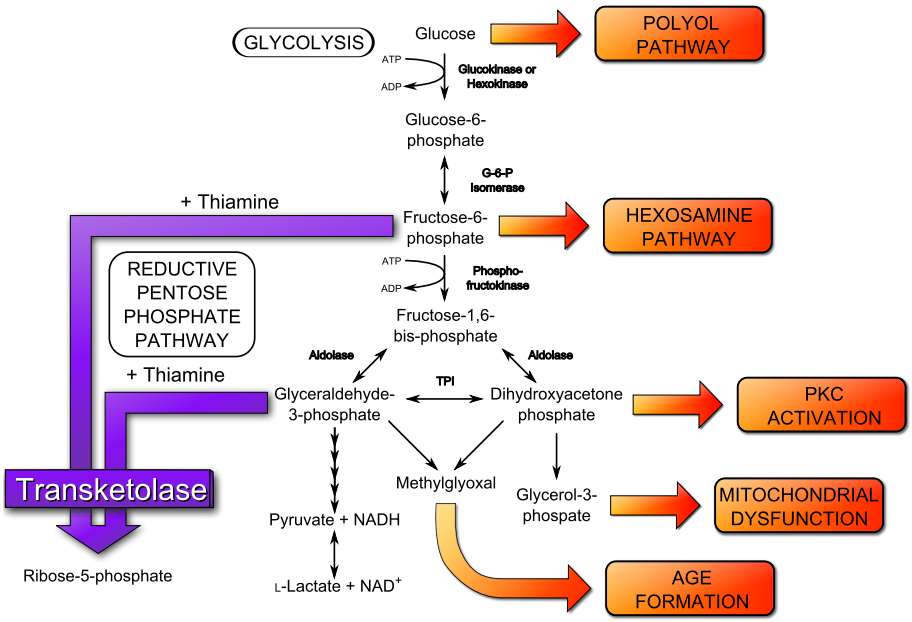

Figure 4.2: Schematic showing the hypothesis behind high-dose thiamine therapy and alleviation of symptoms of hyperglycaemia.

Chapter 5

Aims and hypotheses

Previous research by this group has shown that diabetic patients have a marked decrease in plasma thiamine concentration and a concomitant increase in renal clearance of the vitamin [Thornalley et al., 2007]. It is the primary aim of this project to identify and attempt to characterise the mechanism behind this plasma thiamine deficiency. It is the hypothesis of this thesis that it is this increased renal clearance which is responsible for the reduced plasma thiamine concentration.

To examine the increased renal clearance of thiamine, the project will follow several *in vitro* strategies. Firstly, the location of the thiamine transporters THTR-1 and THTR-2 in the human kidney will be determined. These are responsible for the salvage of filtered thiamine and are thus of crucial importance. No prior work has demonstrated the location of these transporters in human kidney sections. Work studing the MDCK canine cell line and rabbit proximal tubules suggests that the transporters are located in the proximal tubule [Mahajan and Acara, 1994]. The high degree of similarity between all mammalian systems suggests that the location will be similar in humans but this will be verified with normal human kidney samples. Formalin-fixed and paraffin-embedded human kidney sections will be stained using immunohistochemistry and antibodies against human THTR-1 and THTR-2 to demonstrate the location of the transporters.

The mechanism behind the increased renal clearance will also be investigated. The working hypothesis is that the increased renal clearance is due to decreased uptake of thiamine from the glomerular ultrafiltrate. This hypothesis is consistent with known facts. Thiamine, as a small molecule, is filtered through the glomerular basement membrane and into the ultrafiltrate. Once in the proximal tubule, it is only the activity of transporter

proteins which maintains plasma levels of key metabolites that are filtered by the glomeruli. Thus two scenarios are possible; either thiamine is more prone to filtration in the diabetic state or its re-uptake into the plasma is impaired. If the first scenario were true and filtration were increased at the glomerulus, it would stand to reason that this would be concomitant with an increase in GFR since there is no active excretion of thiamine (or any other small metabolite) in the glomerulus. Despite the increase in GFR often seen in diabetes patients, this does not account for the increased excretion so the second scenario has been adopted as a working hypothesis i.e. that there is a failure in re-uptake of the vitamin. This work will be conducted in both an immortalised proximal tubule epithelial cell (PTEC) model cell line and in primary PTECs from a normal human kidney.

The proposed mechanism behind the expected decrease in re-uptake of thiamine is based upon the transcription factor Sp1 and the products of the hexosamine biosynthesis pathway. In the diabetic state, an excess of available glucose drives a higher flux through many pathways, including the HBP ([Brownlee, 2001] and Section 3.4). Increased flux through the HBP leads to increased concentrations of UDP-*N*-acetylglucosamine, the precursor for enzymatic glycosylation. This in turn leads to elevated levels of *O*-GlcNAc on cellular proteins (Section 3.4). One such protein which is likely to be glycosylated to a higher extent in the diabetic state is the transcription factor Sp1 which is one of the factors responsible for the initiation of transcription of the thiamine transporters THTR-1 and THTR-2. It is the hypothesis of this thesis that the increased levels of glycosylation of Sp1 lead to a decrease in the expression of the thiamine transporters with a concomitant decrease in thiamine re-uptake in the kidney. Sp1 glycosylation is known to be important for the transcription of many genes but has not been demonstrated for the thiamine transporters. This hypothesis will be investigated by assessing mRNA and protein abundance of proteins involved in *O*-GlcNAcylation as well as assessing the glycosylation status of the Sp1 transcription factor. Hexosamine pathway product concentrations will also be assayed in low and high glucose concentrations. The hypothesis is summarised in Figure 5.1.

A secondary, and complementary, aim of this thesis is to investigate the pharmacological effect of thiamine on microalbuminuria in 40 type 2 diabetes patients in a double-blind placebo-controlled trial. Type 2 diabetes patients have a 75% decreased plasma thiamine concentration and a 16-fold increase in renal clearance rates of thiamine compared to normal controls [Thornalley et al., 2007]. It will be determined if an oral pharmacalogical intervention can restore plasma thiamine concentration to normal. The study will continue by assessing the effect of thiamine intervention on the rate of urinary albumin excretion.

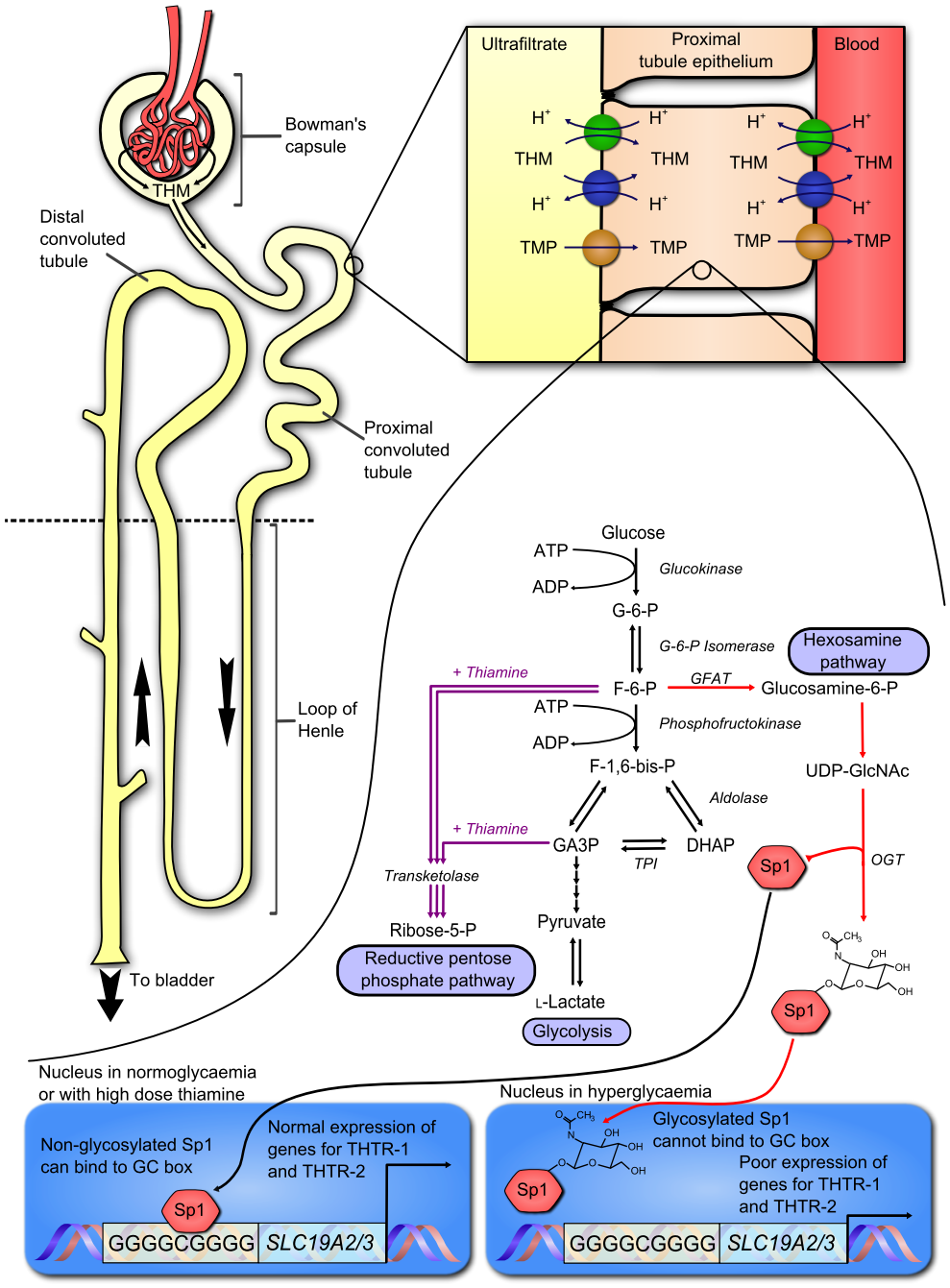

Figure 5.1: Project hypothesis overview. This encapsulates the mechanistic theory behind why we believe plasma thiamine concentrations are decreased in the diabetic state.

Chapter 6

Materials and methods

6.1 Materials

6.1.1 Cells and tissues

The human renal proximal tubule epithelial HK-2 cell line [Ryan et al., 1994] was obtained from ATCC (Manassas, VA, USA). Human kidney proximal tubule epithelial cells (PTECs) were isolated from a 25 year old female human kidney donated for transplantation but found to be unsuitable and used for renal research with consent. This study was approved by the Coventry National Health Service Regional Ethics Committee (NHS-REC): applicant Dr Daniel Zehnder.

6.1.2 Cell culture reagents

HK-2 cells and human PTECs in primary culture were cultured in a 1:1 mixture of Dulbecco's modified Eagle medium (DMEM) and Ham's F-12 nutrient supplement prepared in-house without thiamine or glucose (Biological Sciences, University of Warwick). Trypsin-ethylenediaminetetraacetic acid (EDTA) solution (0.25% trypsin w/v and 0.02% EDTA w/v in Hank's balanced salt solution, 0.22 µm sterile-filtered) was purchased from Sigma-Aldrich (Poole, UK). Foetal bovine serum (FBS) was from Biosera (Ringmer, UK).

L-Glucosamine (99%), β-D-glucose (tissue-culture grade), Lucifer yellow carbohydrazide (CH), dipotassium salt, penicillin-streptomycin solution (10 000 units mL^{-1} penicillin and 10 mg mL^{-1} streptomycin), sodium carbonate ($\geq$99.0%) and thiamine hydrochloride were purchased from Sigma-Aldrich. 4-(2-hydroxyethyl)-1-piperazineethanesulfonic acid (HEPES), sodium salt was from Fisher Scientific (Loughborough, UK).

6.1.3 Enzymes, substrates, cofactors and inhibitors

Type II collagenase (EC 3.4.24.3, 125 units mg^{-1} from *Clostridium histolyticum*) was purchased from Worthington Biochemical Corporation (Lakewood, NJ, USA). Triosephosphate isomerase (EC 5.3.1.1, Type III-S, $\geq$4000 units per mg protein) and α-glycerophosphate dehydrogenase (EC 1.1.1.8, 100–300 units per mg protein) were both purified from rabbit muscle and supplied as an ammonium sulphate suspension from Sigma-Aldrich. SensiMix SYBR green Low-Rox Kit for quantitative polymerase chain reaction (qPCR), Biomix Red PCR mix and BioScript reverse transcriptase (a Moloney murine leukaemia virus reverse transcriptase modified to have low RNAse H activity, thereby increasing yields) were purchased from Bioline (London, UK). Peroxidase and glucose oxidase (PGO) caplets each containing glucose oxidase (EC 1.1.3.4, 500 units from *Aspergilus niger*), peroxidase (EC 1.11.1.7, 100 purpurogallin units from horseradish) and buffer salts were purchased from Sigma-Aldrich.

D-Ribose-5-phosphate, disodium salt (98–100%), o-dianisidine dihydrochloride, thiamine pyrophosphate hydrochloride and β-nicotinamide adenine dinucleotide, reduced form (β-NADH, 98%) were from Sigma-Aldrich. Protease inhibitor cocktail in DMSO for mammalian cell and tissue extracts and containing 4-(2-aminoethyl)benzenesulfonyl fluoride (AEBSF) hydrochloride, aprotinin, bestatin hydrochloride, [*N*-(trans-epoxysuccinyl)-L-leucine 4-guanidinobutylamide] (E-64), leupeptin hemisulphate salt and pepstatin A was also from Sigma-Aldrich. RiboSafe RNAse inhibitor (a proprietary recombinant protein which competitively inhibits RNAses A, B and C) was purchased from Bioline.

6.1.4 Antibodies

Mouse monoclonal horseradish peroxidase (HRP)-conjugated antibodies to β-actin (mAbcam 8226, ab20272), mouse monoclonal antibodies to peptide sequence GQVEEYDLDDDINSRVEMKPK, residues 249–269 of human aquaporin 1 (Aqp-1; ab9566), rabbit polyclonal antibodies to human lamin A (ab26300) and specificity protein 1 (Sp1; ab13370), and goat polyclonal antibody to human *O*-linked *N*-acetylglucosamine transferase (OGT; ab59135) were purchased from Abcam (Cambridge, UK). Mouse polyclonal antibodies to uromodulin (UMOD; B01P) were purchased from Abnova (Taipei City, Taiwan).

Rabbit polyclonal antibodies to human thiamine transporter 1 (THTR-1; THTR11-A and THTR12-A) and human thiamine transporter 2 (THTR-2; THTR22-A) were purchased from Alpha Diagnostic International (San Antonio, TX, USA). Mouse monoclonal

antibodies to human THTR-1 (5B10) were purchased from Abnova. Rabbit polyclonal antibodies to THTR-1 (HPA016599) were purchased from Sigma-Aldrich. Goat polyclonal antibodies to THTR-1 were purchased from Santa Cruz Biotechnology (Santa Cruz, CA, USA).

Mouse monoclonal antibodies to *O*-GlcNAc residues (HGAC85, ab2735) were from Abcam. Mouse monoclonal antibodies to *O*-GlcNAc (MAb CTD 110.6) were purchased as part of an analytical kit from Pierce (Thermo Scientific, Rockford, IL, USA). Anti-mouse, -rabbit and -goat HRP-conjugated secondary antibodies were purchased from Abcam.

6.1.5 Analytical and preparative kits

Bradford assay dye reagent and the detergent compatible (DC) protein assay kit were purchased from BioRad (Hemel Hempstead, UK). Liquid chromatography solid anion exchange (LC-SAX) solid phase extraction (SPE) cartridges (quaternary amine bonded to silica with a chloride counter-ion, 500 mg per 3 mL cartridge) were from Supelco (Sigma-Aldrich). RNeasy Mini Kits for RNA preparation were purchased from Qiagen (Crawley, UK). Enzyme-linked immunosorbent assay (ELISA) kits for soluble vascular cell adhesion molecule 1 (sVCAM-1) were purchased from R&D Systems (Abingdon, UK).

6.1.6 Chromatographic materials

Methanol, acetonitrile, isopropanol (IPA), tetrahydrofuran and 35% ammonia solution (all HPLC-grade) were purchased from Fisher Scientific. Formic acid (≥96.0%) and trifluoroacetic acid (TFA, spectrophotometric grade 99+%) were purchased from Sigma-Aldrich.

Anion exchange HPLC was performed with an HEMA-IEC Bio-Q column (200 mm × 4.6 mm, 10 µm particle size) with a guard column made of the same material from Alltech (Carnforth, UK). Reversed phase HPLC was performed with a C18 X-Bridge column (150 mm × 3 mm, 3.5 µm particle size) with guard columns of the same material from Waters (Milford, MA, USA).

6.1.7 Immunohistochemistry materials

Moist chambers for maintaining high humidity around slides were from Raymond Lamb (Thermo Scientific). Xylene, isopropanol, formaldehyde solution (37% w/v), EDTA and citric acid, trisodium salt (all analytical grade) were purchased from Fisher Scientific. Water-repellent peroxidase anti-peroxidase (PAP) pens and phosphate-buffered saline (PBS)-Tween

rinsing solution (10 mM sodium phosphate at pH 7.4 plus 0.01% Tween-20) were purchased from A Menarini Diagnostics (Florence, Italy). Buffers A and C for antigen retrieval (propietary mixes at pH 6.0 and 4.5 respectively) were purchased from PickCell Laboratories BV (Amsterdam, The Netherlands). Distyrene and plasticiser in xylene (DPX) mountant, Mayer's haematoxylin solution and hydrogen peroxide solution (3% w/w) were purchased from Sigma-Aldrich. Vectastain Universal Quick Kit and Avidin/Biotin blocking kit were purchased from Vector Laboratories (Peterborough, England). LiquidDAB (3,3'-diaminobenzidine) reagent was purchased from BioGenex (San Ramon, CA, USA).

6.1.8 Analytical standards

Uridine 5'-diphosphoglucose (UDP-Glc, ≥98% disodium salt from *Saccharomyces cerevisiae*), uridine 5'-diphospho-*N*-acetylglucosamine (UDP-GlcNAc, ≥98%, sodium salt), guanosine 5'-diphospho-D-mannose (GDP-Man, ∼98% from *Saccharomyces cerevisiae*) and thiamine monophosphate hydrochloride dihydrate were purchased from Sigma-Aldrich. Chloroethylthiamine was synthesised in-house by a colleague (see Section 6.4.3.1).

6.1.9 Other reagents and consumables

For western blotting, β-mercaptoethanol, ammonium persulphate (ACS reagent grade), *N*,*N*,*N*',*N*'-tetramethylethylenediamine (TEMED; ≥99% electrophoresis grade), Tween 20, bovine serum albumin (BSA, initial fractionation by heat shock; fraction V: minimum 98%), 3',3'',5',5''-tetrabromophenolsulfophthalein sodium salt (bromophenol blue, electrophoresis grade), glycerol (molecular biology grade) and hydrochloric acid (25% w/w solution, analytical grade) were purchased from Sigma-Aldrich. Coomassie Brilliant Blue G250 (analytical grade) was purchased from Fluka (Poole, UK). Acrylamide:bis-acrylamide solution (30% w/v, 37.5:1, Ultrapure grade) was purchased from National Diagnostics (Hessle, UK). Sodium dodecyl sulphate (SDS; electrophoresis grade), acetic acid (glacial), tris(hydroxymethyl)aminomethane base, EDTA, glycine, methanol and sodium chloride (all analytical grade) were all purchased from Fisher Scientific. Instant dried skimmed milk powder was purchased from Tesco (Cheshunt, UK). Polyvinylidene fluoride (PVDF) membrane (Hybond-P) and X-ray film (Hyperfilm) were purchased from GE Healthcare (Little Chalfont, UK). Filter paper, grade 1, was purchased from Whatman (Little Chalfont, UK). Enhanced chemiluminescence (ECL) reagent kit was purchased from Pierce. Molecular mass ladder (10–250 kDa, #SM1811) was purchased from Fermentas (York, UK).

For other solutions, calcium chloride, ethanol (molecular biology grade), L-glutamine

solution (200 mM, tissue culture grade), magnesium sulphate heptahydrate, perchloric acid solution (60% w/v), potassium chloride, potassium ferricyanide ($K_3Fe(CN)_6$, >99%), trichloroacetic acid (TCA, ≥99.5%) and Triton X-100 were purchased from Sigma-Aldrich. Orthophosphoric acid (85%+), disodium hydrogen phosphate, sodium dihydrogen phosphate, potassium dihydrogen phosphate (anhydrous), dipotassium hydrogen phosphate trihydrate, sodium hydroxide (98+%), potassium hydroxide and sodium acetate salt (all analytical grade) were purchased from Fisher Scientific. Tritiated thiamine ($10\,\mathrm{Ci\,mmol^{-1}}$, $1\,\mathrm{mCi\,mL^{-1}}$, 50 µCi aliquot) was purchased from American Radiolabeled Chemicals (St. Louis, MO, USA). Percoll (15–30 nm colloidal silica particles coated with polyvinylpyrrolidone (PVP), 23% w/w in water) for density centrifugation was purchased from Fluka. Ultima Gold scintillation fluid was purchased from Perkin Elmer (Seer Green, UK).

Primers were ordered from the Invitrogen custom primer service (Paisley, UK) in lyophilised form. Nuclease-free water was purchased from Qiagen. Oligo $d(T)_{18}$ primers ($270\,\mathrm{ng\,\mu L^{-1}}$ in water), deoxyribonucleotide triphosphate (dNTP) mixes (lithium salts, 100 mM each) and agarose powder (electrophoresis grade) were purchased from Bioline. Ethidium bromide solution ($10\,\mathrm{mg\,mL^{-1}}$ in water, for molecular biology) was purchased from Sigma-Aldrich.

UV transparent microplates and microspin filters (0.22 µm pore size, cellulose) were purchased from Corning Life Sciences (Amsterdam, The Netherlands). HPLC vials, inserts and caps were purchased from Chromacol (Welwyn Garden City, England). All other general laboratory consumables and sundries not individually detailed (including test tubes, glass slides, cover slips and tissue culture plastic-ware) came from either Greiner Bio-One (Stonehouse, England) or Fisher Scientific.

6.1.10 Instrumentation

All water used for assays had a resistivity ≥18.2 MΩ cm at 25℃ and a total organic carbon content $\leq 2\,\mathrm{\mu g\,L^{-1}}$ (filtered by an Advantage A10 Milli-Q system (Watford, UK)). Absorbance and fluorescence-based microplate assays were performed using a Fluostar Optima microplate reader (BMG Labtech, Aylesbury, England). All HPLC was performed on an UltiMate 3000 series HPLC system from Dionex (Camberley, UK) comprising a four-channel degasser, binary pumps with high pressure gradient mixing and low pressure solvent selectors for each pump, thermostatic split-loop autosampler, thermostatic column compartment with two 6-port switching valves, photodiode array and fluorescence detector. RNA quantitation and quality control was performed using an ND 1000 spectrophotometer from NanoDrop

(Wilmington, DE, USA). Ultracentrifugation was performed in a CS150GXL micro ultracentrifuge made by Hitachi Koki (Tokyo, Japan) with an S55-A rotor and polycarbonate tubes from Sorvall (Loughborough, UK). Gels were imaged on a ChemiGenius^2 transilluminator and imaging system from Syngene (Cambridge, England). Real-time qPCR was performed with a 7500 Fast Real-Time PCR System from Applied Biosystems (Warrington, UK). Immunohistochemistry slides were digitized using a Mirax Midi slide scanner from Carl Zeiss (Jena, Germany).

Other laboratory equipment included a chilled microcentrifuge from Hettich (Tuttlingen, Germany), a large chilled centrifuge from Sorvall, electrophoresis equipment and power supplies from Amersham Biosciences, (Little Chalfont, UK), a Vibra-cell sonicator (75 W) from Sonics & Materials (Newtown, CT, USA), a 2100 Retriever antigen retrieval unit from Prestige Medical (Blackburn, UK), an ImageScanner transparent film scanner from Amersham Biosciences and a Uvikon UV/visible spectrophotometer from NorthStar Scientific (Potton, UK). A stainless steel sieve (212 µm aperature) was purchased from Fisher Scientific.

6.1.11 Software

HPLC chromatogram integration was performed using Chromeleon software v6.80 SP2 (Dionex). Statistical tests were performed in either SPSS v18 (IBM, Chicago, IL, USA) or GraphPad Prism v5 (GraphPad Software, La Jolla, CA, USA). qPCR analysis was performed with Sequence Detection System (SDS) software v2.0.1 (Applied Biosystems). Scanned slides were viewed and cropped using Mirax Viewer v1.12.22 (Carl Zeiss). Primers were designed using the Primer 3 software based at the National Center for Biotechnology Information (NCBI) website (www.ncbi.nlm.nih.gov/nuccore). X-ray film image scanning was performed using LabScan software (Amersham Biosciences). Densitometry was performed using ImageJ (rsbweb.nih.gov/ij). Figures for this thesis were prepared using Gnumeric v1.9.14 (www.gnome.org/gnumeric) and Inkscape v0.47 (www.inkscape.org). Chemical structures were drawn with Chemsketch v10 (ACD/Labs, Toronto, Canada). This thesis was typeset using LaTeX 2_ε typesetting software (www.latex-project.org).

6.2 Cell culture methods

HK-2 cell line PTECs and freshly isolated human PTECs were both cultured in the same manner in a 37℃ incubator with a 5% CO_2 95% air water-saturated atmosphere. The medium used was DMEM/F-12 supplemented with 2.5% FBS, 1% penicillin/streptomycin solution (final concentrations 100 U mL^{-1} penicillin and 100 µg mL^{-1} streptomycin), 20 mM $NaHCO_3$, 15 mM HEPES at pH 7.4. Media were supplemented with glucose and thiamine to achieve final concentrations of 5 mM or 26 mM glucose and 4 nM or 4 µM thiamine. Samples of medium were assayed to test final glucose and thiamine concentrations.

Cells were cultured in sterile polystyrene culture vessels with no additional coating necessary for cell adhesion. Cells were passaged when at around 80–90% confluence and were never allowed to reach confluence unless monolayer formation was required for the experiment. Passaging was achieved by aspirating culture medium and adding approximately 1 mL per 25 cm^2 0.25% trypsin-EDTA to each flask. The flasks were returned to a 37℃ incubator for 3–5 min until the cells had detached. The activity of the trypsin was neutralised by adding culture medium including FBS to the flask and the cells were then diluted to the target concentration in new flasks.

Immortalised cells were revived from liquid nitrogen storage every three months to ensure that cells did not drift genetically over long periods of time. After removal from cold storage, cells were grown exponentially for a minimum of two weeks to allow them to become accustomed to the new 5 mM glucose, 4 nM thiamine medium before use.

For experimental procedures, four different combinations of glucose and thiamine concentration were used. These were: (i) 5 mM glucose and 4 nM thiamine (−G−T), (ii) 5 mM glucose and 4 µM thiamine (−G+T), (iii) 26 mM glucose and 4 nM thiamine (+G−T) and (iv) 26 mM glucose and 4 µM thiamine (+G+T). Cells were routinely cultured in −G−T medium and were seeded into the four experimental media simultaneously from the same stock for the duration of an experimental incubation. HK-2 cell passage number was unknown; primary cells were used at passage number 4 or earlier.

6.3 Proximal tubule epithelial cell extraction

There has been much work performed since the 1950s on isolating cellular fractions from kidneys. Early work used magnetic particles of iron oxide which lodged in glomeruli during perfusion and were subsequently used to separate glomeruli using magnetic attraction [Cook and Pickering, 1958]. This method was not chosen because of the potential for oxidative

damage caused by the iron particles. Other methods advocate differential sieving or other mechanical means [Weiland et al., 2007; Obatomi and Bach, 1996; Luhe et al., 2003; Rudolfs K. Zalups, 1996] or enzymatic techniques [Elliget and Trump, 1991; Frye and Patrick, 2002; Terryn et al., 2007]. The enzymes chosen for digestion can vary quite widely with most people using collagenase and others using additives such as BSA or secondary enzymes including dispase (a bacillus-derived matrix metalloproteinase which cleaves fibronectin and collagen IV and to a lesser extent collagen I but not collagen V or laminin). More elaborate methods include using antibodies to a unique epitope on the cell of interest followed by a secondary antibody conjugated with a magnetic particle. Separation can thus be achieved using a powerful magnet [van Beijnum et al., 2008] in a manner similar to Cook and Pickering [1958]. Several enzymatic techniques included the use of density gradient centrifugation [Peñaranda et al., 1996; Pietruck et al., 2006, 2003; Weinberg et al., 1987; Zager and Foerder, 1992; Zager et al., 1993]. The method presented herein represents a combination of published methods refined to work well on rat PTECs and then adapted for human PTECs.

The donor human kidney was kept on ice between removal and arrival at our laboratory (less than 24 hours). Sections of cortex from the decapsulated kidney were used for PTEC isolation. Approximately 1–1.5 cm^3 of cortex tissue was cut up finely using a scalpel in a Petri dish on ice. The diced cortex was transferred to a large beaker and collagenase solution added (100 mL 0.1% type II collagenase in PBS with 5 mM $CaCl_2$). The beaker was covered and incubated and digested for 40 min at 37°C in a shaking water bath at 180 revolutions per minute. After incubation the partially digested material was poured over a stainless steel sieve (212 µm aperature size). The material collected on the sieve contained undigested cortex and was retained for use later. The material collected below the sieve contained the tubule fragments and was sedimented by centrifugation (2 min, $30 \times g$, 4 °C). After sedimentation, the supernatant was discarded and the pellet of cellular material resuspended in ice-cold DMEM/F12 medium supplemented with 1% penicillin/streptomycin, 20 mM $NaHCO_3$, 15 mM HEPES at pH 7.4, 5 mM glucose and 4 nM thiamine in the absence of FBS. The resuspended tubule fragments were sedimented once more by centrifugation (2 min, $30 \times g$, 4 °C). The wash was repeated a total of three times for each digest to remove cellular debris.

The washed tubule fragments were then separated by density-gradient centrifugation in a self-forming 31% Percoll gradient with a final osmolarity of 300 mOsmolar made up with sodium chloride and water. The mixture of Percoll, sodium chloride, water and cellular digest fragments was homogeneous before centrifuguation. By centrifuging (30 min, $30\,000 \times g$,

4 ℃ with gentle acceleration (3/10) and no braking) a density gradient was formed and the fragments separated into three discrete fractions (Figure 6.1), of which the lower comprised the bulk of the proximal tubule fragments.

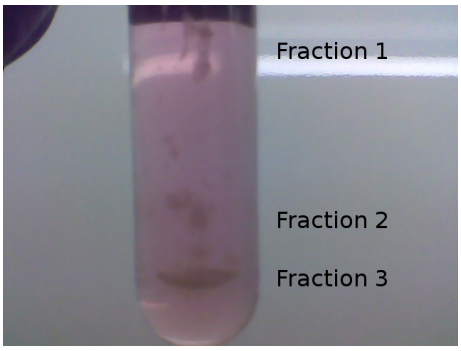

Figure 6.1: Cells from a human kidney digest separated in Percoll. Fractions 1, 2 and 3 were universally visible. Fraction 3 contained the majority of proximal tubule fragments.

All similar fractions from multiple separations were pooled and topped up to 50 mL with ice-cold medium before collecting the cellular material by centrifugation (5 min, 130 × g, 4 ℃). The supernatant was discarded to remove the Percoll. Each fraction was resuspended in 37℃ DMEM/F-12 medium as described above and further supplemented with 2.5% FBS before seeding at an estimated confluence of 10–20% in tissue culture flasks.

To further increase the yield of the extraction procedure, the material previously collected on top of the stainless steel sieve was pooled and re-digested with collagenase. All further steps were identical to the procedure described above. Figure 6.2 shows an example of a confluent monolayer of these cells under light microscopy. The identity of the cells was confirmed by immunohistochemistry.

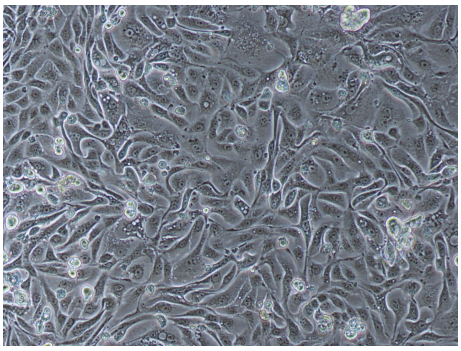

Figure 6.2: Microscopic image of a monolayer of human PTECs in primary culture

6.4 Thiamine assay

6.4.1 Principle of assay

The assay of thiamine is based on the alkaline oxidation of thiamine and its phosphate esters to highly fluorescent thiochrome and thiochrome phosphate esters respectively (Figure 6.3)—a technique first described by [Jansen, 1936]. Modern methods such as the one described herein separate the fluorescent thiochromes using reverse phase HPLC. A pre-column derivatisation technique using sodium hydroxide (15% w/v) and potassium hexacyanoferrate ($K_3Fe(CN)_6$—1% w/v) was used. Due to instability once mixed, reagents were mixed freshly at a ratio of 4:1 before an aliquot of the combined reagent was mixed with the sample. The derivatisation formed the thiochromes which were separated by HPLC and their presence detected by their strong fluorescence.

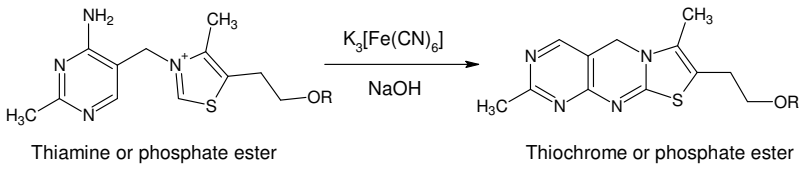

Figure 6.3: The alkaline oxidation of thiamine and its phosphate esters to the respective thiochrome by sodium hydroxide and potassium ferricyanide. R represents either H for thiamine, phosphate for thiamine monophosphate or pyrophosphate for thiamine pyrophosphate.

6.4.2 Chromatographic conditions

A Waters XBridge C18 reverse phase column as described above was chosen because high concentrations of sodium hydroxide were used for derivatisation and it has increased resistance to high pH relative to traditional silica-based C18 columns. The column was 150 mm × 3 mm with a 3.5 µm particle size and the HPLC system used was the Dionex UltiMate 3000 series system described above (see Section 6.1.10).

The mobile phases used were 10 mM KH_2PO_4 pH 8.4 in water for solvent A, 10 mM KH_2PO_4 pH 8.4 in 50% methanol for solvent B, water for rinsing in solvent line C and 30% IPA with 0.1% TFA in solvent line D for column cleaning.

The column was equilibrated with 95% A and 5% B (i.e. 2.5% methanol). Separation was carried out over 20 min from injection by raising the mobile phase linearly from 5% B to 100% B. Fluorimetric detection was carried out using an excitation wavelength of 365 nm and an emission wavelength of 439 nm.

After each injection, the column was cleaned by flushing with 10 column volumes of water followed by 10 column volumes of 30% IPA + 0.1% TFA before re-rinsing the column using 10 column volumes of water followed by 8 min re-equilibration with 95% A and 5% B at 1 mL min^{-1}.

6.4.3 Assay standardization

The assay was standardized by use of chloroethylthiamine as an internal standard. Chloroethylthiamine is not naturally occurring and exhibits a great structural similarity with thiamine and its derivatives which means that it derivatises under the same conditions yet can be chromatographically resolved. By integrating the peak area for the internal standard and the peak area for the analyte it is possible to express the analyte as a percentage of the internal standard and deduce the amount present by reference to a standard curve.

6.4.3.1 Chloroethylthiamine synthesis

Chloroethylthiamine was prepared in-house by a colleague by nucleophilic substitution of the hydroxyl group on the 5'-(2-hydroxyethyl) group on the thiazolium ring with chloride. This is facilitated by the sulphonylchlorination (-SOCl) of the hydroxyl group by thionyl chloride which is then susceptible to nucleophilic attack by chloride ions (Figure 6.4).

Thiamine chloride (1 g, 3 mmol), was added to 20 mL of thionylchloride and refluxed for three hours at 80–85 °C. The excess thionylchloride was then removed by distillation at 85–90 °C and the residual solid washed with diethyl ether (5 mL × 2). The remaining solid was purified by recrystallisation from ethanol (5 mL), filtered under aspiration and dried under a vacuum. The product was characterized by mass spectrometry and ^{1}H and ^{13}C NMR spectroscopy.

6.4.4 Calibration of stock solutions

Stock solutions of thiamine (THM), thiamine monophosphate (TMP) and thiamine pyrophosphate (TPP) were calibrated spectrophotometrically prior to use as standards. Each analyte was dissolved in 10 mM H_3PO_4 at pH 2.15 and kept on ice. The standards were

diluted in 10 mM H_3PO_4 at pH 2.15 and readings of absorbance at λ_{max} 247 nm were made, ensuring readings lay between 0.5 and 1 absorbance units by adjusting the dilution factor. The concentration of each solution was calculated with reference to Table 6.1. The calibrated stock solutions were kept at −80 °C and diluted in 10 mM sodium acetate, pH 4.5 to make working solutions of 100 µM which were kept at −80 °C or −20 °C for short term use.

Analyte	λ_{max} at pH 2.15 (nm)	ε ($M^{-1}\,cm^{-1}$)
THM	247 [Dawson et al., 1986]	14 200 [Dawson et al., 1986]
TMP	247 [Al Ali, 2006]	15 300 [Al Ali, 2006]
TPP	247 [Dawson et al., 1986]	13 000 [Dawson et al., 1986]

Table 6.1: Absorbance characteristics of thiamine assay standards

6.4.5 Preparation of standard curves

Standard curves for assay calibration were prepared in the range of 0.1–2.5 pmol of each analyte for analysis of cell extracts or plasma (the low standard curve) and in the range of 1–20 pmol for analysis of urine (the high standard curve). Each standard on the low curve contained 2.5 pmol CET as an internal standard (IS) and each standard on the high curve contained 20 pmol CET. A working stock of 0.1 µM and 0.01 µM or 1.0 µM and 0.1 µM thiamine metabolites was prepared by dilution into 10 mM sodium acetate buffer (pH 4.5)

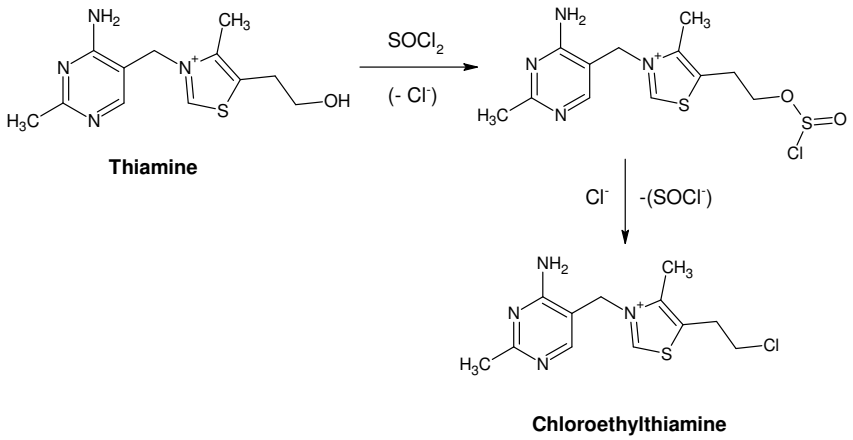

Figure 6.4: The reaction scheme for the synthesis of the internal standard, chloroethylthiamine

from the calibrated stock solutions prepared above. All preparation was carried out on ice to prevent sample degradation. Reagent volumes used for standard preparation are presented in Tables 6.2 and 6.3. For each standard tube, internal standard was combined with 20% TCA (w/v) dissolved in 0.9% sodium chloride (w/v). The thiamine metabolite mix was added to each tube and the volume made up to 40 µL with water. 10 µL of 2 M sodium acetate was added to each tube to neutralise the TCA and return the pH to approximately 4.5 (volumes determined empirically).

Each tube was mixed thoroughly by vortexing and the contents filtered through a cellulose spin filter (0.22 µm pore size, 10 min, $4000 \times g$, 4 °C). 40 µL of each filtrate was then dispensed into HPLC vials prior to analysis. Samples were not stored for longer than 48 hours at 4 °C before analysis.

6.4.6 Preparation of samples

Plasma samples (50 µL) were deproteinised with 20% TCA in 0.9% saline (20 µL) and 2.5 pmol internal standard was added (5 µL, 0.5 µM). The samples were mixed and placed on ice (10 min) to allow complete precipitation before sedimentation of the precipitate by centrifugation (10 min, $20\,000 \times g$, 4 °C). The supernatants (50 µL) were removed and the pH adjusted to 4.5 by addition of 2 M sodium acetate (8.5 µL—volume determined empirically). Samples were spin-filtered (0.22 µm pore size) and 40 µL was used for thiamine analysis.

Urine samples were diluted 10-fold in water before analysis. Dilute urine samples (25 µL) were deproteinised with 20% TCA in 0.9% saline (10 µL) and 20 pmol internal standard was added (10 µL, 2 µM). The samples were mixed and placed on ice (10 min) to allow complete precipitation before sedimentation of the precipitate by centrifugation (10 min, $20\,000 \times g$, 4 °C). The supernatants (44 µL) were removed and the pH adjusted to 4.5 by addition of 2 M sodium acetate (10 µL—volume determined empirically). Sample were spin-filtered (0.22 µm pore size) and 40 µL was used for thiamine analysis.

Cell samples were collected by trypsinisation from a T-75 flask near confluence. Cells were washed twice in successive steps in ice-cold PBS in order to ensure complete removal of thiamine present in the growth medium. The cells were resuspended in lysis buffer (200 µL, 10 mM sodium acetate pH 4.5 with 0.02% Triton X-100) at an approximate density of 8×10^5 cells in 50 µL—a density previously determined to be suitable for thiamine analysis. The samples were kept on ice at all times so that the low pH and the low temperature ensured analyte stability.

The samples were sonicated on ice (10 seconds, 75 W) and transferred to ice-cold

Standard (pmol)	0.5 µM Internal Standard (µL)	20% TCA (µL)	0.1 µM Thiamine metabolite mix (µL)	0.01 µM Thiamine metabolite mix (µL)	Water (µL)	2 M Sodium acetate (µL)	Total volume (µL)
0.1	5	10	-	10	15	10	50
0.25	5	10	-	25	-	10	50
0.5	5	10	5	-	20	10	50
1.0	5	10	10	-	15	10	50
1.5	5	10	15	-	10	10	50
2.0	5	10	20	-	5	10	50
2.5	5	10	25	-	-	10	50

Table 6.2: Thiamine assay low concentration standard composition (0.1–2.5 pmol analyte per standard)

Standard (pmol)	2 µM Internal Standard (µL)	20% TCA (µL)	1.0 µM Thiamine metabolite mix (µL)	0.1 µM Thiamine metabolite mix (µL)	Water (µL)	2 M Sodium acetate (µL)	Total volume (µL)
1	10	10	-	10	10	10	50
2	10	10	-	20	-	10	50
5	10	10	5	-	15	10	50
10	10	10	10	-	10	10	50
15	10	10	15	-	5	10	50
20	10	10	20	-	-	10	50

Table 6.3: Thiamine assay high concentration standard composition (1–20 pmol analyte per standard)

microcentrifuge tubes before sedimenting membranes by centrifugation (30 min, 20 000 × g, 4 ℃). The cytosolic supernatant was used for thiamine analysis and protein concentration determination (BioRad DC protein assay). For thiamine analysis, the supernatants (50 µL) were deproteinised with 20% TCA in 0.9% saline (10 µL) and 2.5 pmol internal standard was added (5 µL, 0.5 µM). The samples were mixed and placed on ice (10 min) to allow complete precipitation before sedimentation of the precipitate by centrifugation (10 min, 20 000 × g, 4 ℃). The supernatants (60 µL) were removed and the pH adjusted to 4.5 by addition of 2 M sodium acetate (8 µL—volume determined empirically). Sample were spin-filtered (0.22 µm pore size) and 40 µL was used for thiamine analysis.

6.4.7 Chromatography of samples

After preparation, samples were stored in a 4 ℃ autosampler immediately prior to analysis. The autosampler needle drew 40 µL 15% NaOH and 10 µL 1% $K_3Fe(CN)_6$ and dispensed them into a clean vial. The derivatising agent was mixed by 3 repeats of drawing and dispensing in the vial. 10 µL was drawn from the derivitising agent solution and dispensed into the 40 µL of sample. The sample was mixed thoroughly by 3 repeats of drawing and dispensing. 25 µL of the derivatised sample was drawn up and injected onto the column already equilibrated with 95% A and 5% B (see Section 6.4.2 for details of the mobile phase). The gradient described in Table 6.4 was run to first separate the analytes, then displace the phosphate salts before cleaning and re-equilibrating the column.

The fluorescence chromatogram obtained was integrated using the Chromeleon software and concentrations of thiamine metabolites determined by reference of the thiochrome peak area ratio (analyte/internal standard) to the standard curve. An example chromatogram is given in Figure 6.5. Example standard curves are given in Figures 6.6 (THM), 6.7 (TMP) and 6.8 (TPP).

6.4.8 Assay validation

Intra- and inter-batch coefficients of variance (CV) were determined by repeated measures of 1 pmol standards containing all three analytes. 12 identical replicates were run consecutively to determine the intra-batch CV. 12 replicates made separately and analysed with separate standard curves were used to determine the inter-batch CV. The results are given in Table 6.5.

Thiochrome half life was determined by a colleague [Al Ali, 2006] by manually derivatising a standard sample and then injecting aliquots at regular intervals and moni-

Time (min)	A (10 mM KH_2PO_4 pH 8.4 in water)	B (10 mM KH_2PO_4 pH 8.4 in 50% methanol)	C (Water)	D (30% IPA + 0.1% TFA)	Flow (mL min^{-1})
0	95	5	0	0	0.5
20	0	100	0	0	0.5
20.01	0	0	100	0	0.5
22	0	0	100	0	1.0
31	0	0	100	0	1.0
31.6	0	0	0	100	0.4
44	0	0	0	100	0.4
44.01	0	0	100	0	0.4
46	0	0	100	0	0.4
48	0	0	100	0	1.0
55	0	0	100	0	1.0
55.01	95	5	0	0	1.0
70	95	5	0	0	1.0
70.5	95	5	0	0	0.5

Table 6.4: Thiamine assay mobile phase gradient

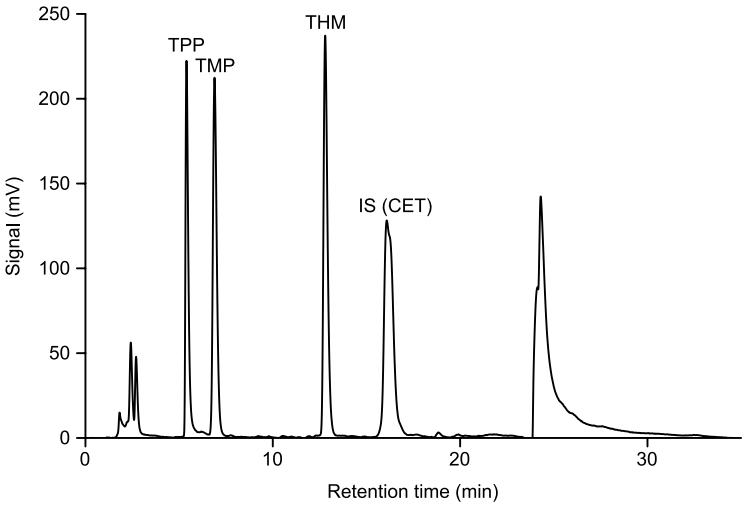

Figure 6.5: Thiamine assay example chromatogram. This is a chromatogram obtained for a 1 pmol standard for THM, TMP and TPP. The internal standard has 2.5 pmol present as for all samples and standards.

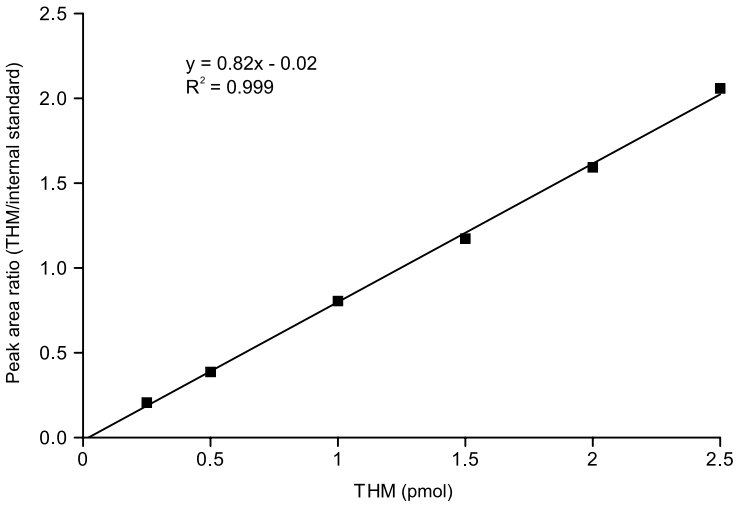

Figure 6.6: Example standard curve for thiamine analysis. This is a typical standard curve in the range of 0.25 to 2.5 pmol.

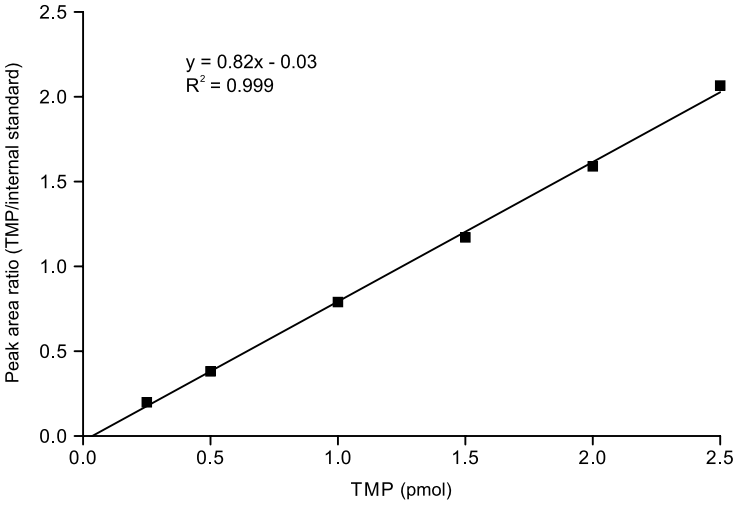

Figure 6.7: Example standard curve for thiamine monophosphate analysis. This is a typical standard curve in the range of 0.25 to 2.5 pmol.

Analyte	Intra-batch CV (%)	Inter-batch CV (%)
THM	1.1	3.2
TMP	2.4	3.0
TPP	2.0	3.7

Table 6.5: Thiamine assay intra- and inter-batch CVs ($n = 12$)

toring fluorescence. The results in Table 6.6 show that the fluorescence is stable for the duration of the assay. It also underlines the necessity to derivatise each sample individually prior to analysis, especially considering that complete oxidation is achieved within 15 seconds [Wielders and Mink, 1983].

Analyte	$t_{1/2}$ (hours)	$t_{5\%}$ (hours)	$t_{5\%}$ (min)
THM	3.4	0.25	15
TMP	4.3	0.32	19
TPP	5.0	0.37	22
IS	3.4	0.25	15

Table 6.6: Thiochrome half lives after derivatisation

To confirm that analytes did not interconvert during sample preparation or derivatisation, 2 pmol standards were prepared which contained only one analyte. These were analysed sequentially separated by blank samples to test for carryover from one to the next. No carryover was observed indicated by blank chromatograms with no observable peaks. Results in Figure 6.9 show that only TPP has a small peak for TMP (3.6% the size of the TPP peak) and no other analytes are present as contaminants. This small TMP peak may be present as a contaminant in the commercially available TPP (repeated assays with fresh TPP gave the same chromatograpy) or it may be due to degradation of TPP to TMP during sample handling. Fresh plasma spiked with known amounts of THM, TMP or TPP show a

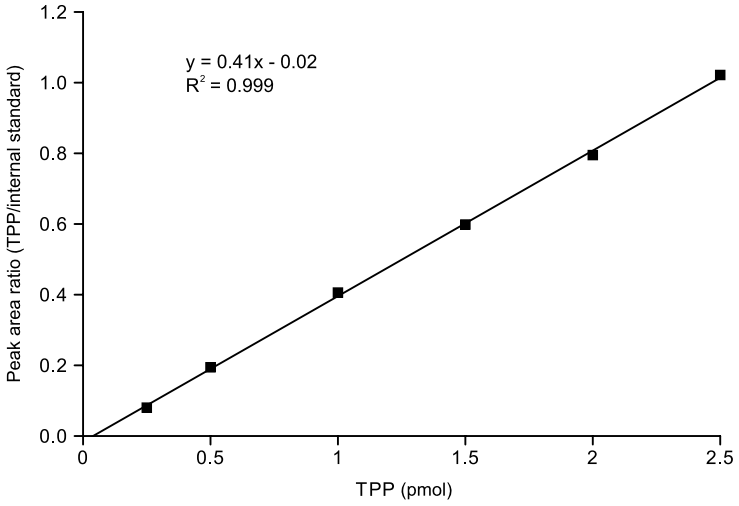

Figure 6.8: Example standard curve for thiamine pyrophosphate analysis. This is a typical standard curve in the range of 0.25 to 2.5 pmol.

similar pattern with recoveries of the analytes between 96–103%.

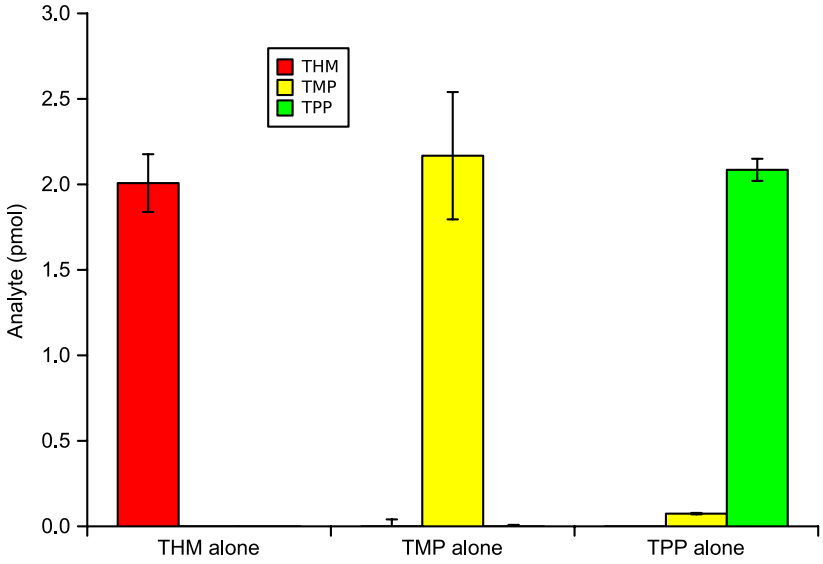

Figure 6.9: Thiamine assay single analyte analysis. In each case, 2 pmol analyte were assayed, $n = 3$

Limits of detection (LOD) for analytes were determined according to the definition of the Environmental Protection Agency (defined in 40 CFR §136, [EPA, 2010]). A low 0.5 pmol standard was assayed 10 times and the LOD determined from LOD $= t_{(n-1,1-\alpha=0.99)} \times S$ where $t_{(n-1,1-\alpha=0.99)}$ is the Student's t value appropriate for a 99% confidence level and a standard deviation estimate with $n-1$ degrees of freedom and S is the standard deviation of the replicate analyses. LODs are given in Table 6.7. If the protocol for the HPLC machine were to be modified for maximum injection of analyte and not optimised for speed, the limits of detection could be lowered to 40% of their current values. This sensitivity was not required for any analysis so the assay was optimised for speed.

Analyte	LOD (fmol)
THM	32
TMP	6.7
TPP	94

Table 6.7: Thiamine assay limits of detection. $n = 10$

6.5 Hexosamine pathway intermediate assay

6.5.1 Aim and principle

This assay was designed to separate by HPLC and quantify hexosamine biosynthesis pathway intermediates by UV absorbance. Specifically, the assay quantified levels of uridine diphosphate-*N*-acetylglucosamine (UDP-GlcNAc) and uridine diphosphate-glucose (UDP-Glc). Samples were initially prepared by anion exchange solid phase extraction before separation on an anion exchange HPLC column. Guanosine 5'-diphospho-D-mannose (GDP-mannose) was chosen as an internal standard due to its low abundance in human cells and tissues.

This method was based on the work initially validated by Robinson et al. [1995] who adapted an original assay developed in 1985 [Wice et al., 1985]. This method was improved herein by eliminating the need for ozone-depleting solvents and reducing spurious peaks present on the chromatogram by adding solid phase extraction based on previous work by Span et al. [2001]. Other methods (e.g. capillary zone electrophoresis [Lehmann et al., 2000]) have been published to determine the concentration of these metabolites but HPLC was chosen due to equipment availability and prior experience with the technique.

6.5.2 Standard preparation

Authentic standards for the assay were calibrated and used to prepare standard curves for sample quantitation. Both UDP-Glc and UDP-GlcNAc were prepared in 10 mM KH_2PO_4 at pH 7.0 before spectrophotometric calibration at 262 nm (ε_{262} =10 000 $M^{-1}\,cm^{-1}$ at pH 7.0 [Dawson et al., 1986]). For standard use, a mixture of UDP-Glc and UDP-GlcNAc was prepared with both analytes at a concentration of 150 µM. Standards were prepared as described in Table 6.8. Each of the standards was subjected to solid phase extraction in a manner identical to that of the samples.

6.5.3 Sample preparation

Cells were grown in each test medium for five days. Cultured cells close to confluence from one T-175 tissue culture flask ($\sim 7.5 \times 10^6$ cells) were removed by trypsinisisation and sedimented by centrifugation (5 min, $125 \times g$, 4 °C) for each sample. The supernatant was discarded and the cell pellet washed by resuspension in ice-cold PBS followed by re-sedimentation. Ice-cold lysis buffer comprising 100 mM KCl, 1 mM EDTA and 50 mM

KH_2PO_4 at pH 7.5 (1 mL) was added to each cell pellet. All steps from this point forward were performed on ice.

The cells in the pellet were lysed by sonication (10 s, 75 W) and the membranes clarified from the lysate by centrifugation (30 min, 20 000 × *g*, 4 °C). The membrane pellet was discarded and the supernatant collected. 50 µL of the supernatant was reserved for protein assay and 700 µL was used for the remaining assay steps.

Each 700 µL supernatant aliquot was mixed with 700 µL 1.2 M perchloric acid to precipitate protein and 10 µL 1 mM GDP-mannose (10 nmol) added as an internal standard. The samples were mixed by brief vortexing and allowed to stand on ice for 10 min to allow complete precipitation. The protein precipitate was sedimented by centrifugation (10 min, 13 500 × *g*, 4 °C) and the supernatant reserved (approximately 1.3 mL supernatant was recovered in each case). 10 times the volume of each supernatant of KH_2PO_4 at pH 2.5 was added to each supernatant before beginning solid phase extraction.

6.5.4 Solid phase extraction

The solid phase extraction (SPE) used Supelclean LC-SAX anion exchange cartridges (3 mL capacity, 500 mg packing material each). A vacuum manifold was used to speed up sample permeation through the packing material but for optimal binding of analytes to the substrate, the flow rate was never allowed to exceed 5 mL min^{-1}. Prior to use the columns were conditioned by applying the following to each cartridge in turn, in each case leaving 0.5–1 mm of solvent on top of the frit after each application: 2 mL methanol, 2 mL water, 2 mL 10 mM KH_2PO_4 at pH 2.5. After conditioning, the samples were loaded onto and drawn through the SPE cartridges. The cartridges were washed with 5 × 1 mL 10 mM KH_2PO_4 at pH 2.5 followed by 2.5 mL 50 mM KH_2PO_4 at pH 2.5 and finally 0.5 mL 150 mM KH_2PO_4

Standard (nmol)	1 mM GDP-mannose (µL)	150 µM standard mix (µL)	10 mM KH_2PO_4 at pH 2.5 (mL)
1	10	6.67	12.98
5	10	33.33	12.96
10	10	66.67	12.92
20	10	133.3	12.86
35	10	233.3	12.76
50	10	333.3	12.66

Table 6.8: Standard curve preparation details for the hexosamine pathway metabolite assay.

at pH 7.5. All eluates were discarded. The compounds of interest were eluted using 2 × 0.75 mL 150 mM KH_2PO_4 at pH 7.5. The tubes were left to run dry and the entire volume of eluate was collected. The samples were spin-filtered (0.22 µm pore size, 10 min, 4000 × *g*, 4 ℃) and transferred to HPLC vials ready for injection. Samples were stored at 4℃ prior to analysis.

6.5.5 HPLC conditions

The HPLC column used was a 200x4.6 mm HEMA-IEC Bio-Q anion exchange column with a 10 µm particle size. The mobile phases were 15 mM ammonium formate, pH 3.8 (A) and 1 M ammonium formate, pH 4.5 (B). Water and 30% IPA were used for rinsing salt from the system and cleaning the column after sample runs. The column was held in a thermostatic column oven at 25 ℃. The mobile phase increased from 0% to 50% B over 25 min using a concave gradient (slope 8 in the Chromeleon software) and is shown in Figure 6.10. The mobile phase was held at 50% B for 2.5 min before returning to 100% A for equilibration (7.5 min). The flow rate was 2 mL min^{-1} and detection was by UV absorbance at 262 nm. The autosampler was thermostatically controlled at 4℃ and the injection volume was 100 µL. The needle was washed before every injection using water. The column was washed with 100% B prior to 30% IPA in water. An example chromatogram is given in Figure 6.11. Example standard curves generated using the peak area ratio of the analyte peak/internal standard peak are given in Figures 6.12 and 6.13. Analyte recoveries after SPE are given in Table 6.9.

Analyte	Recovery (%)
UDP-Glc	90.1%
UDP-GlcNAc	86.4%
GDP-Man	75.4%

Table 6.9: Hexosamine pathway analyte recovery percentages after solid phase extraction.

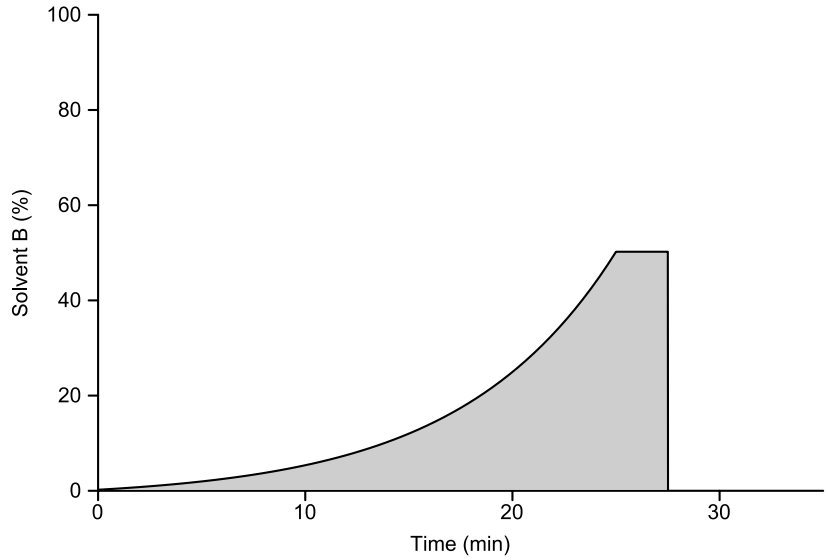

Figure 6.10: Hexosamine pathway intermediate assay mobile phase gradient

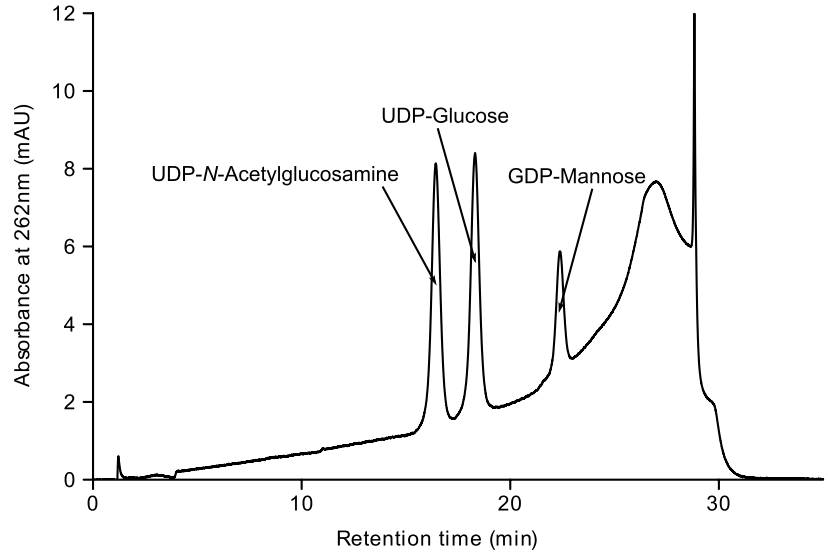

Figure 6.11: Hexosamine pathway intermediate assay example chromatogram. This chromatogram shows peaks for UDP-Glucose and UDP-*N*-acetylglucosamine (5 nmol each) as well as the internal standard, GDP-mannose (10 nmol).

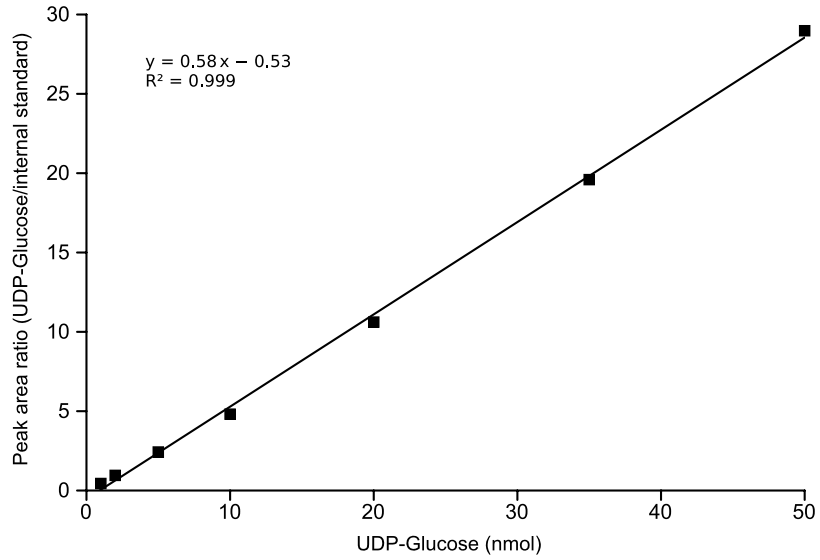

Figure 6.12: Example standard curve for UDP-glucose analysis. This is a typical standard curve in the range of 1 to 50 nmol.

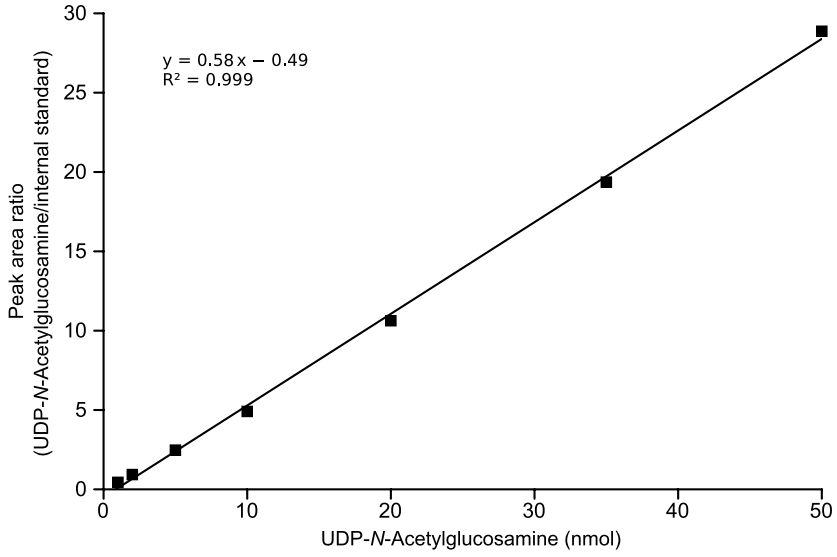

Figure 6.13: Example standard curve for UDP-*N*-acetylglucosamine analysis. This is a typical standard curve in the range of 1 to 50 nmol.

6.6 Real-time quantitative PCR

6.6.1 Principle of assay

Real-time quantitative PCR (qPCR) was used for assaying the relative copy numbers of mRNA transcripts in cells and tissues. Briefly, the cellular RNA was extracted and reverse-transcribed to yield cDNA. The cDNA was then amplified in a normal PCR reaction whilst the amplification was quantified at every cycle by measuring the fluorescence of the reaction as it prodeeded. The fluorescence was generated using the SYBR green dye which is highly fluorescent when bound to double-stranded, but not single-stranded, DNA (i.e. the amplification product). This technique was chosen above other chemistries such as TaqMan (which relies on cleavage of a dual-labelled probe during amplification to separate free fluorophore from the quencher) due to its ease of use and price.

6.6.2 Primer design

Good quality primers were designed for the qPCR in a manner similar to other PCR reactions. Criteria for choosing a good primer were that the primer should be between 18 to 22 base pairs in length, have a target melting temperature of around 60°C, have a GC content of 40–60%. The presence of a GC clamp at the 3' was advantageous. Primer design attempted to avoid potential secondary structure formation, excessive repeats, and runs of more than four bases of a kind to avoid mis-priming.

In addition to following the good primer design principles above, the following principles specific to qPCR were also applied. Amplicon lengths were designed to be short(around 100 base pairs) to allow for quick amplification. If it was possible, primers were designed to span an exon-exon junction or so that the amplicon bridged an intron completely *i.e.* for the product to pass an exon-exon junction in the cDNA. This was to enforce an additional element of quality control on the assay. If cDNA had been prepared from a total RNA extract which had not been treated with DNAse enzymes, there may have been genomic DNA present which would have provided an additional template for the primers. A primer which bridged an exon-intron junction was not likely to prime on genomic DNA whilst an amplicon that spanned an entire intron would produce a longer product than expected, often not amplifying completely in the time available.

Following the criteria above, the following technique was used to generate primers for qPCR. The gene of interest was retrieved from the NCBI nucleotide database available online at *www.ncbi.nlm.nih.gov/nuccore*. The correct mRNA sequence was selected from the

database results. By using an mRNA sequence, the database was pre-annotated with exon-exon junctions which made primer design quicker and more efficient. Using the accession number for the chosen mRNA sequence, the NCBI Primer-Blast tool was used to generate primers (*www.ncbi.nlm.nih.gov/tools/primer-blast*). Primer-Blast is based on the Primer3 software for generation of primers [Rozen and Skaletsky, 2000]. The subsequent basic local alignment search tool (BLAST) step compared the primers with the Refseq RNA database. This step determined the specificity of the primers by seeing if they were likely to mis-prime on alternate targets.

Of the possible primers returned by the NCBI Primer-Blast tool, one or two pairs were chosen based on their specificity to the target sequence, their exon-exon junction spanning characteristics, their T_m, their amplicon length and their GC%. All primer sequences used are presented in Table B.1 in Appendix B. The process for testing primers once purchased is described below.

6.6.3 RNA extraction

Cellular RNA should be of high quality for accurate quantitation by qPCR. Cellular RNA is not stable and the extraction of RNA was carefully carried out to avoid problems with RNAse degradation of the samples. RNAses are exceptionally stable and active enzymes that do not generally require cofactors for their function. To avoid degradation of RNA, all samples were snap-frozen in a dry ice and ethanol bath before storage at −80℃ prior to extraction—a temperature at which RNAses are inactive. The only other alternative would have been to immediately denature all protein in the samples, an approach not as practical as snap-freezing.

RNA extraction was carried out using the microspin-based Qiagen RNeasy Mini Kit following the protocol provided by the manufacturer. Briefly, the sample was lysed completely by addition of a buffer containing both a high concentration of guanidine-thiocyanate, a chaotropic agent, and β-mercaptoethanol to reduce di-sulphide bridges; a technique first used in 1979 [Chirgwin et al., 1979]. Cellular samples were lysed by pipetting up and down whilst tissue samples such as kidney were lysed by brief sonication. Ethanol was added according to the supplied protocol to allow for required binding conditions for the silica-based spin-column. The sample was passed through the spin-column and total RNA was bound with high efficiency, provided that the column was not overloaded. The sample was washed with a series of buffers, each containing high concentrations of ethanol before eluting the concentrated and purified RNA using 30–50 µL water.

6.6.3.1 RNA quality control

The RNA was analysed spectrophotometrically to provide information on quality and concentration. This was performed using a NanoDrop 1000 spectrophotometer using 1.5 µL of RNA per sample. The A_{260} reading was used to determine concentration of the RNA given that a value for A_{260} of 1 is equal to an RNA concentration of 44 µg RNA mL^{-1}. The ratio between the A_{260} and A_{280} values was used to determine RNA quality with respect to contaminants that absorb in the UV spectrum such as protein. Pure RNA would give an expected A_{260}/A_{280} ratio of between 1.9–2.1.

In addition to spectrophotometric analysis, spot samples of RNA were separated on a 2% agarose gel with ethidium bromide. Two peaks for the 28S rRNA and 18S RNA were clearly visible and appeared in the approximate ratio of 2:1. Smearing of these bands indicated unwanted RNAse activity and a likely degradation of all RNA in the sample. Any samples with degraded RNA were discarded and replaced with freshly derived samples.

6.6.4 Reverse transcription

After extraction of total RNA, reverse transcription was used to generate cDNA. 5 µg template RNA and 0.5 µg oligo-dT primers were added to an RNAse-free tube. Nuclease-free water was added to a final volume of 12 µL. The samples were heated to 70°C for 5 min before chilling on ice. Subsequently, 1 µL 10 mM dNTP mix, 4 µL 5× reaction buffer (provided with the BioScript enzyme), and 0.5 µL RNAse inhibitor were added to each sample. The samples were mixed by pipetting before 1 µL BioScript enzyme was added. The reverse transcriptase was thoroughly mixed into the sample by pipetting and the samples were incubated at 40°C for 60 min. The reaction was stopped by heating to 70°C for 10 min followed by chilling on ice. The cDNA was stored at −20°C without repeated freeze-thawing.

6.6.5 Testing of primers

Primers were ordered lyophilised and were reconstituted on arrival in water to a concentration of 100 µM. Pairs of primers were then diluted together to a working solution of 5 µM of each primer in water. Before use, primers were tested to ensure that they amplified a specific product of the correct mass. Reaction tubes for each primer containing 1 µL template cDNA from the reverse transcription step, 1 µL primer mix at 5 µM in water, 8 µL water and 10 µL BioMix Red mix including DNA polymerase, dNTPs, buffers, salts and loading dye. The reaction tube was thoroughly mixed and cycled through the conditions shown in

Figure 6.14 in a PCR thermocycler.

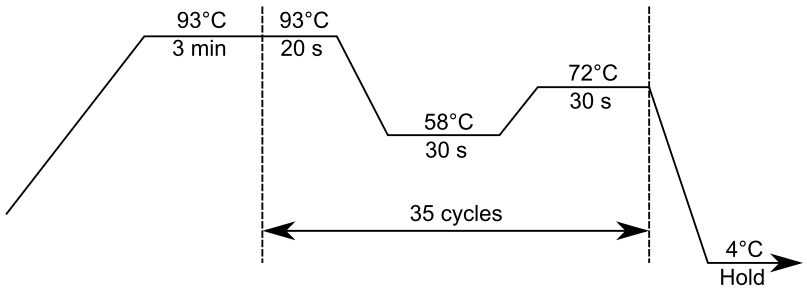

Figure 6.14: BioMix Red PCR cycling conditions

The reaction products were separated on a 2% agarose gel. This gel was prepared by dissolving 2% w/v agarose in tris-acetate-EDTA (TAE) buffer (final concentrations 20 mM tris base, 10 mM acetic acid and 1 mM EDTA.Na_2, pH 8.0) by careful heating in a microwave oven. Ethidium bromide was added from a 10 mg mL^{-1} stock to a final concentration of 0.5 µg mL^{-1} and the gel allowed to set before submerging in TAE buffer. 15 µL of each 20 µL PCR product was transferred to a well on the gel and a voltage of between 90–110 V was applied to the gel for 1–2 hours to separate the reaction products. The gel was said to be finished once the dye front had moved approximately 5 cm from the loading wells. The gel was viewed and photographed in a UV transilluminator (see Figure 6.15). Any primer pair which did not amplify with a single clean product was substituted for an alternative pair of primers for the same product. An additional technique to test primer quality not employed here would be to digest each product with a known restriction enzyme and to re-run the products on a second gel. The size ratio would indicate if the sequence of the amplified section is likely correct.

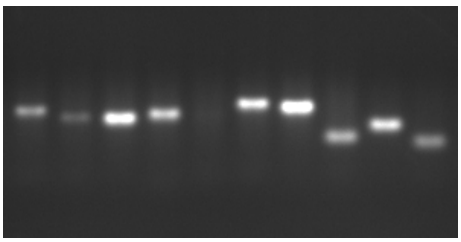

Figure 6.15: Primer quality control example gel image. Each lane represents a PCR reaction product. All lanes have produced a single product at the correct mass (as determined by including a molecular mass ladder on the gel) except lane 5 which has not amplified adequately.

6.6.6 Assay controls

All qPCR assays were thoroughly controlled to ensure reliability of the quantitative results. Water blank qPCR amplifications were performed in which the template was substituted for water and "RT−" amplifications were performed in which the template was prepared using a reverse transcription step with water substituting for the reverse transcriptase. Amplification in the water blank would indicate contamination of the experiment by exogenous material whilst amplification in the RT− blank is usually due to amplification from the genomic DNA present in the sample.

Example traces for a properly conducted experiment are shown in Figure 6.16. In cases where the water blank amplified at all, it did so very late (usually past 35 cycles). The gap between the amplification of the target and the RT− control indicated the relative abundance of genomic DNA to cRNA. For example, amplification 7 cycles later represents $1/2^7$ or 0.7% of the target being present in the form of genomic DNA. Amplification 9 cycles later would represent 0.2%. At this stage, other errors become more significant and the effect of the genomic DNA can be ignored. It is not possible to perform a water blank amplification for every well so it was assumed that if the water blank on a plate did not amplify then the quality of the plate preparation was such that the rest of the plate was also free of contamination.

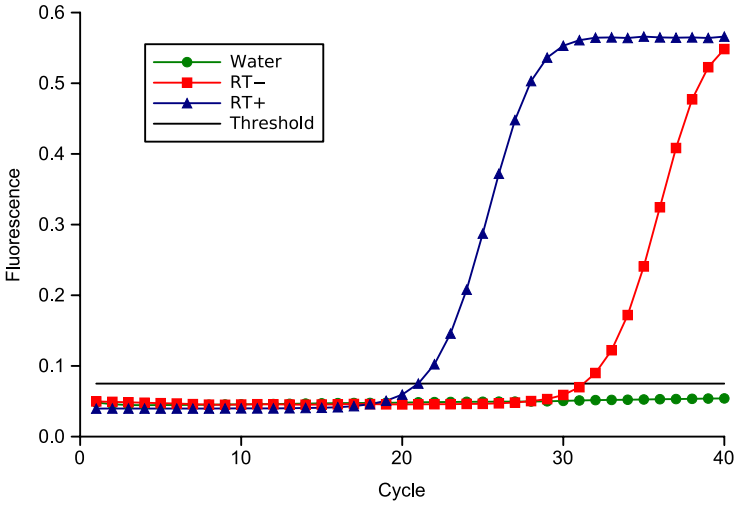

Figure 6.16: qPCR example control amplifications for THTR-1. This is an example of a properly conducted experiment. The RT+ sample crosses the threshold first at around 21 cycles. The RT− sample crosses much later at around 31 cycles meaning that it has an abundance of approximately $1/2^{10}$ or $1/1000$ of the RT+ sample. The water blank does not cross the threshold indicating that there has been no contamination of the well.

In addition to these controls, a melt curve was prepared at least onece for each primer pair and target. This was achieved using the PCR machine to increase the temperature of the sample in small steps from a relatively low temperature (e.g. 65℃) to a relatively high temperature (e.g. 90℃) over a range that incorporated the melting temperature of each product. The fluorescence decreased gradually as the products melted. By plotting the first order differential of the fluorescence against temperature, peaks were derived that corresponded to products. Figure 6.17 is an example plot containing two peaks. The good qPCR reaction has only one sharp peak corresponding to a single product and the bad qPCR reaction contains a split peak indicating the presence of primer dimers or other artefacts of amplification. Reactions with poor peak shape had their primers re-designed.

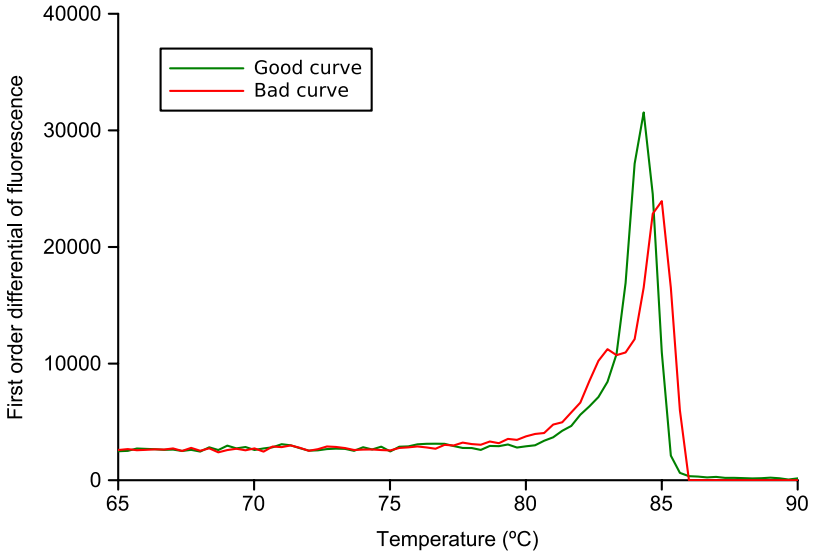

Figure 6.17: qPCR example product melt curves. The green curve represents a good quality PCR reaction with a single product. The red curve represents the product obtained from a RT− control which is of poor quality with two discernible peaks.

6.6.7 Primer efficiency

Since only relative levels of expression were required it was not necessary to construct a standard curve of the type required for absolute quantitation. The traditional comparative C_t method or the $\Delta\Delta C_t$ method is an approximation method that assumes that each PCR reaction is a perfect doubling. The ΔC_t between reference gene and target gene is calculated for both the control condition and the test condition. The difference between these ΔC_t values is the $\Delta\Delta C_t$. The fold-change in expression of the gene of interest relative to the

reference gene is then given by $2^{\Delta\Delta C_t}$. I used a more accurate method for quantitation described by Pfaffl [2001] which used pre-determined efficiencies for PCR reactions to produce higher quality results.

Detemining efficiencies for the Pfaffel method was achieved by constructing a standard curve based on serial dilutions of template DNA over several orders of magnitude. A typical curve extended from 10 to 0.01 ng RNA. The samples was amplified following the cycling conditions to be used for the assay and the C_t values were determined for each concentration. The C_t values were plotted against the logarithm of the amount of RNA (ng) and a straight line was fitted to the data. Figure 6.18 shows a typical standard curve obtained. The efficiency was determined according to Equation 6.1 where m is the gradient of the efficiency plot. Convention varies but I used a value of 1 to mean a perfectly efficient reaction with a doubling of product every cycle. Efficiencies should be between 0.9 and 1.1 for properly functioning primers. Efficiencies that were outside this range were often due to off-target amplification or poor annealing and were solved by re-designing primers.

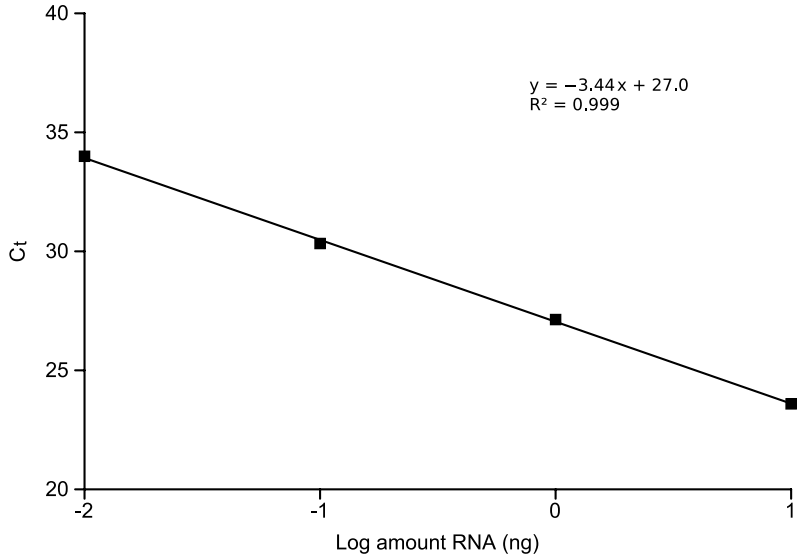

Figure 6.18: Example primer efficiency determination curve. This example curve was obtained for primers for the gene TXNIP. The gradient of the line can be used to determine efficiency using Equation 6.1.

$$\text{Efficiency} = 10^{-1/m} - 1 \tag{6.1}$$

Once primer efficiency had been determined, the ratio of relative expression levels of the genes of interest in treated versus control conditions was determined according to Equation 6.2, assuming β-actin as the loading control [Pfaffl, 2001].

$$\text{Ratio} = \frac{(1 + \text{Efficiency}_{\beta\text{-actin}})^{\Delta \text{C}_{t\beta\text{-actin}}(\text{control}-\text{treated})}}{(1 + \text{Efficiency}_{\text{target}})^{\Delta \text{C}_{t\text{target}}(\text{control}-\text{treated})}} \tag{6.2}$$

6.6.8 Design of experiments

Each primer pair was thoroughly tested prior to analysis of samples to determine efficiency and specificity by the methods described above. An RT− control was used with a typical template to determine whether the genomic DNA present would amplify at a similar rate to cDNA species. No cDNA species were sufficiently rare to amplify near the genomic DNA so further RT− controls for each primer pair were not performed to save space on plates. The loading control chosen for each experiment was β-actin, a commonly used house-keeping gene. Using a single reference gene is potentially problematic if its expression varies with experimental conditions. It would be beneficial to use multiple genes (e.g. GAPDH, 5S RNA) simultaneously to ensure that the normalisation is correct and appropriate.

Experiments were designed to fit onto the minimum number of plates possible. A given biological replicate was assayed for all genes of interest on one 96-well plate with three technical replicates for each gene.

6.6.9 Sample analysis

After plate layout design, the plates were constructed and run on a real-time cycler. To simplify preparation of the plates, a concentrated SYBR green-containing master mix was purchased (SensiMix SYBR Low-Rox kit). This master mix contained a hot-start *Taq* polymerase which was modified to cause complete inactivation before exposure to a high temperature (95℃ for 10 min), thereby minimising primer-dimer formation and non-specific amplification which could potentially be caused during sample set-up and handling.

Each well contained a final volume of 20 µL comprising 1 µL primer solution at 5 µM for each primer in water, 1 µL template DNA, 8 µL water and 10 µL 2x SYBR green reaction master mix. To minimise pipetting errors, the primer solution and the SYBR green solution were combined into a single solution (11 µL well^{-1}) and the template DNA was diluted with water to allow a pipetting volume of 9 µL well^{-1}.

After dispensing reagents, the plates were sealed with transparent plate seals and mixed by vortexing. The plates were centrifuged briefly to sediment droplets of liquid

in the wells and to eliminate frothing and bubbling caused by mixing. The plates were transferred to the real-time cycler immediately if possible or stored at 4℃ for a maximum of 24 hours before analysis. Each plate was cycled according to Figure 6.19 and fluorescence measured each cycle during the extension phase. Fluorescence of the passive dye ROX was also recorded each cycle and used by the machine to normalise signal fluorescence. Not all plates were subjected to a dissociation stage since these are time-consuming. Instead, each primer pair was tested thoroughly beforehand to ensure that the products were of a known quality.

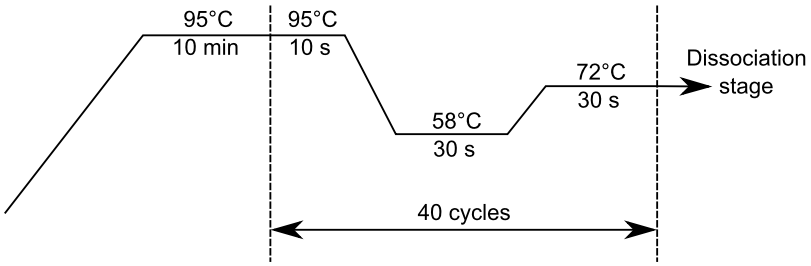

Figure 6.19: qPCR cycling conditions with SensiMix SYBR green reagents

6.6.10 Interpretation and analysis of amplification data

Analysis was undertaken only after all plates in an experimental set had been amplified. All plates that formed part of one experiment were analysed together with the same analysis conditions such as baseline and threshold values. The threshold is the fluorescence level, past which a target is considered amplified; the baseline is the period at the start of the cycling when there is little or no fluorescence. This was chosen to start after the initial fluorescence reading had stabilised and stop before fluorescence due to amplification was noticeable. It was crucial that the machine-generated values for thresholds be discarded as they could lead to varying C_t values due to inter-plate variation. An example amplification plot is given in Figure 6.20 to demonstrate choice of these values.

Relative gene expression was determined using the Pfaffl equation above and the pre-determined primer efficiencies. Statistical analysis was performed on relative gene expression before normalisation. Finally, relative gene expression was normalised to the control condition (5 mM glucose and 4 nM thiamine; −G−T).

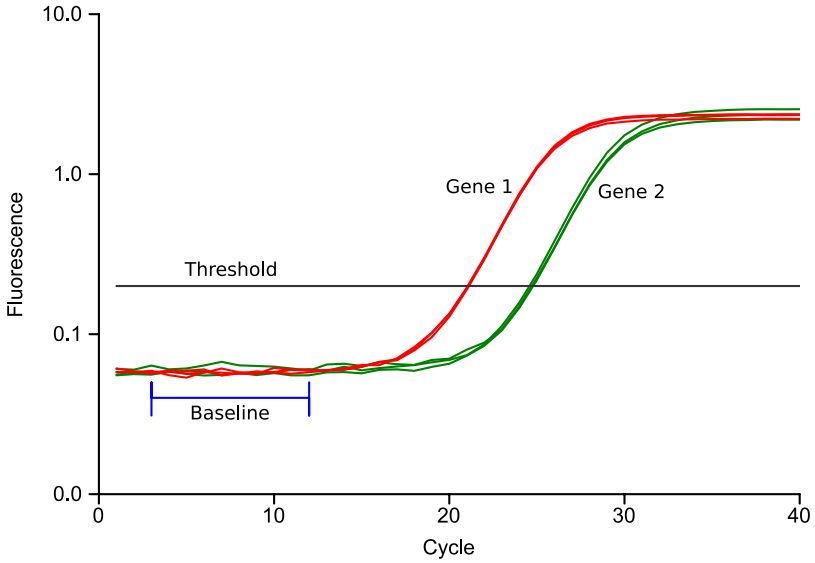

Figure 6.20: qPCR example sample amplification showing two genes in triplicate with threshold and baseline values shown. The y-axis uses a logarithmic scale which means that exponential amplification follows a straight line. Thus a threshold value of 0.2 has been chosen since this lies within the exponential portion of amplification for both genes. The baseline was adjusted from the common value of 3–15 to 3–12 so as to avoid the very early amplification of gene 1.

6.7 Immunohistochemistry

The immunohistochemistry studies were based on the Avidin-Biotin Complex (ABC) method which uses the oxidation of 3,3'-diaminobenzidine (DAB) by a peroxidase linked antibody to yield a brown stain. Nuclei were counterstained blue using Mayer's haematoxylin.

Tissue was embedded in paraffin wax and 2–3 µm sections were cut using a microtome and laid on the surface of water at 39 °C to remove creases. The sections were floated onto silane-coated slides and dried in an oven at 60 °C, a temperature just below the melting point of the wax. Cut sections were stored at room temperature in the dark before use.

Before use, the paraffin sections were de-waxed by soaking in xylene for 5 min prior to sequential transfer through baths of 100% isopropanol, 90% isopropanol and distilled water for 5 min each. The dewaxed sections were subjected to antigen retrieval to break some of the formalin crosslinks at either pH 4.5 ("Buffer C"), pH 6.0 ("Buffer A") or pH 7.8 (4.13 mM tris base, 1.71 mM EDTA, 1.24 mM citric acid, pH 7.8 with sodium hydroxide) in a bench-top antigen retrieval unit for 20 min. pH 7.8 was found to be optimal in all cases. Following antigen retrieval, sections were delineated on the surface of the slides with a hydrophobic PAP pen before being washed twice in PBS-tween wash buffer at pH 7.4 for 5 min each. The slides were soaked in a 1.5% w/w H_2O_2 solution in PBS-tween to quench endogenous peroxidase activity. The slides were washed twice more for 5 min in PBS-tween.

Normal blocking serum (3 drops—150 µL) diluted in PBS (Vectastain Universal Quick Kit) was added to each slide and left to incubate for 20 min at room temperature before being drained off. To block the high endogenous levels of biotin in the kidney sections, an avidin-biotin blocking kit was used. The slides were incubated for 15 min in avidin-D solution and PBS-tween was used to rinse the slides prior to the addition of biotin solution and a further 15 min incubation. The slides were finally rinsed with PBS-tween (2 × 5 min).

The primary antibody was diluted to an empirically pre-determined concentration (between 1:50 to 1:750; 20–1.3 µg mL^{-1}) in PBS-tween and 200 µL was applied to each slide before an overnight incubation at 4 °C. The slides were subsequently washed with PBS-tween (2 × 5 min) prior to incubation with the biotinylated secondary antibody (Vectastain Universal Quick Kit) for 30 min at room temperature.

Following the secondary antibody step, the slides were washed in PBS-tween (2 × 5 min) before incubation with the streptavidin-peroxidase complex in PBS (Vectastain Universal Quick Kit) for 30 min at room temperature. The slides were washed in PBS-tween (2 × 5 min) prior to the addition of the peroxidase substrate (DAB) which was left to react for 7 min at room temperature. The sections were sequentially briefly rinsed in distilled

water (to prevent DAB precipitation) and PBS-tween. Mayer's haematoxylin solution was added to the slides for counterstaining (60 seconds, room temperature). The slides were rinsed in distilled water prior to being allowed to "blue up" in the alkali PBS-tween wash buffer for 2–3 min.

The stained slides were thoroughly dehydrated by passing them through baths of distilled water, 90% isopropanol, 100% isopropanol and xylene before mounting in DPX mountant. The DPX was allowed to harden under a coverslip and the slides observed by light microscopy.

For immunohistochemical analysis of cells, glass slides were irradiated in a UV-crosslinker for 2 hours to sterilise them. Sterile slides were transferred to a class II hood and a 1 mL drop of medium containing cells was placed on each slide. The drop spread over around one-half to two-thirds the surface of the slide with a final cell confluence between 5–20%. Each slide was returned within a sterile container to a humidified 37°C incubator with a 5% CO_2, 95% air atmosphere. Cells adhered to the slides within a few hours and were left to culture until harvested.

On the day of cell fixation, slides were placed in a slide rack and rinsed three times in PBS to remove traces of medium. Slides were then transferred to a solution of 4% formaldehyde in PBS and left overnight at room temperature to fix. Slides were rinsed free of formaldehyde in water and left to air-dry. Slides were stored at room temperature in the dark before use. Antigen retrieval and subsequent steps were used in a manner identical to tissue paraffin-embedded tissue sections.

Negative control slides were prepared by replacing the primary antibody with PBS during the overnight incubation step.

6.8 Immunoblotting

Individual protein abundance levels were quantified by immunoblotting with subsequent chemiluminescent detection.

Protein samples were harvested or prepared by other procedures described herein before mixing 1:1 with 2× loading buffer (1.25 mL 1 M tris.HCl pH 6.8, 3 mL glycerol, 1 g SDS, 1 mL 10 mM EDTA, 500 µL β-mercaptoethanol, 10 mg bromophenol blue, *q.s.* to 10 mL with water). After mixing, the protein was denatured at 95 °C for 10 min. SDS-PAGE gels were prepared to the specifications in Table 6.10. Gel density was chosen empirically based on the molecular mass of the proteins of interest. Gels were mounted into a gel-running tank

and anode and cathode buffer was added (24.7 mM tris base—3 g L^{-1}, 192 mM glycine—14.4 g L^{-1} and 3.46 mM SDS—1 g L^{-1}). Samples were loaded into the wells (at a maximum volume of 20 µL $well^{-1}$) and then stacked at 80 V for 40 min. The gels were run at 110–130 V until the dye front had almost migrated to the base of the gel.

The separated proteins were transferred to polyvinylidene fluoride (PVDF) membrane using a semi-dry method. In detail, eight pieces of Whatman number 1 filter paper were cut to the same size as the gel and soaked in transfer buffer (38.6 mM glycine—2.9 g L^{-1}, 23.1 mM tris base—2.8 g L^{-1} and 20% v/v methanol in water). One piece of PVDF membrane was cut the same size as the gel and first soaked in 100% methanol before soaking in transfer buffer. The gel was removed from the cassette and soaked briefly in ice-cold transfer buffer. The transfer unit carbon electrodes were wetted with transfer buffer and then the following were built up from bottom to top: positive electrode, four sheets of Whatman number 1 filter paper, the PVDF membrane, the gel, four more pieces of filter paper and then the negative electrode. The stack was rolled gently with a glass rod to remove air bubbles before starting transfer. The proteins were transferred from gel to membrane by setting up a current of 120–150 mA through the stack at up to 12 V for 90–150 min depending on gel size.

After transfer, the membrane was removed from the stack and blocked overnight at 4°C in 2% BSA or 5% non-fat milk powder in tris buffered saline with tween (TBS-T: 0.8% NaCl w/v, 20 mM tris.HCl, pH 7.5—2.42 g L^{-1} and Tween 20 0.1% v/v). Validation studies were completed to ascertain experimental conditions such as the choice of blocking agent, primary and secondary antibody concentrations and incubation time. After blocking, the membrane was incubated in primary antibody solution prepared in blocking agent in TBS-T using the pre-determined concentration and time. The membrane was removed from the primary antibody solution and rinsed several times in TBS-T before incubation in an animal-specific horseradish peroxidase-linked secondary antibody solution. The membrane was rinsed thoroughly in TBS-T several times. Finally, the membrane was covered evenly with freshly mixed enhanced chemiluminescence (ECL) solution, left to stand for one minute and then sandwiched between two layers of cling film and exposed to X-ray film until bands appeared. Exposed films were developed, fixed and rinsed in water before drying. Bands were quantified by scanning the film using an Amersham Biosciences ImageScanner and densitometry was performed using ImageJ software.

If necessary, the membranes were then stripped of antibody by rinsing for one hour at room temperature in stripping buffer (6.25 mL tris.HCl pH 6.8, 2 g SDS and 714 µL

Component	12% Resolving gel (mL)	8% Resolving gel (mL)	5% Stacking gel (mL)
Distilled water	6.59	18.5	13.68
1.5 M Tris-HCl, pH 8.8	5	10	0
1.0 M Tris-HCl, pH 6.8	0	0	2.5
30% Acrylamide/bis-acrylamide	8	10.66	3.4
10% SDS	0.2	0.4	0.2
10% APS	0.2	0.4	0.2
TEMED	0.015	0.03	0.015
Total volume	20	40	20

Table 6.10: Gel components for SDS-PAGE gels

β-mercaptoethanol per 100 mL). After stripping, the membrane was washed in TBS-T, re-blocked and re-probed with a second antibody.

6.8.1 Enrichment of membrane proteins

For immunoblot analysis of membrane proteins, an enriched membrane-containing fraction was prepared using a method adapted from Bahia et al. [2003] before separation by electrophoresis. Cells under culture were washed twice with ice-cold PBS. A cell pellet was harvested by scraping cells from a tissue culture flask and then sedimenting them by centrifugation in PBS (5 min, $125 \times g$, 4 ℃). The supernatant was discarded and the cells were disrupted by sonication in lysis buffer(50 mM tris-HCl, pH 7.4 at 4℃, 50 mM EDTA and protease inhibitor cocktail) for 10 seconds on ice. The membranes were collected by centrifugation (30 min, $20\,000 \times g$, 4 ℃) and were resuspended by brief sonication in resuspension buffer (50 mM tris-HCl, pH 7.4 at 4℃, 3 mM $MgCl_2$ and 2% SDS) before analysis by immunoblotting.

6.9 Enzyme-linked immunosorbent assay

sVCAM-1 analysis was carried out using a sandwich ELISA kit. Plasma samples were diluted 20-fold and 100 µL added to the wells of a 96-well microplate according to instructions from the manufacturer. The secondary enzyme-linked antibody was added to the well (100 µL) and the plate sealed and allowed to incubate for 90 min at room temperature. Each well was aspirated and washed with wash buffer (4×100 µL) before colour reagent (100 µL) was added to each well. The hydrogen peroxide and the chromogen (tetramethylbenzidine) in the colour regent are catalysed by the peroxidase for 20 min in the dark at room temperature to yield a blue colour. The reaction is stopped by the addition of stop solution (2 N H_2SO_4, 50 µL) which yields a yellow colour. The plate was read within 30 min at 450 nm with reference wavelength correction at 540 nm.

For each plate, standards were added to the plate in the range 6.25–200 ng mL^{-1}. A standard curve was constructed and sVCAM-1 concentrations deduced with reference to the curve.

6.10 Transketolase activity assay

The activity of transketolase was measured by an enzymatic kinetic method originally developed by Smeets et al. [1971] which couples the formation of glyceraldehyde-3-phosphate (G3P) from ribose-5-phosphate (R5P) and xylulose-5-phosphate (X5P) to the oxidation of NADH using triose phosphate isomerase (TPI) and glycero-3-phosphate dehydrogenase (GDH). The method was further improved by Tate and Nixon [Tate and Nixon, 1987] who modified the concentrations of the linking enzymes to reduce the lag inherent to the assay. The version of the assay used for this work is based on the work of Chamberlain et al. [1996] which involved further optimisations for a stable reaction mixture.

$$\text{R-5-P} + \text{X-5-P} \xrightarrow{\text{Transketolase}} \text{Sedoheptulose-7-phosphate} + \text{G3P}$$

$$\text{G3P} \xrightarrow{\text{TIM}} \text{DHAP}$$

$$\text{DHAP} + \text{NADH} + \text{H}^{+} \xrightarrow{\text{GDH}} \text{Glycerophosphate} + \text{NAD}^{+}$$

Approximately 1×10^6 cells were trypsinised and washed thoroughly in ice-cold PBS to remove traces of medium and trypsin before sonication for 10 s in 100 µL 10 mM sodium phosphate buffer and 1% protease inhibitor cocktail. The membranes were sedimented by centrifugation (30 min, 20 000 × *g*, 4 ℃) and the cytosolic supernatant assayed for transketolase activity. The sample to be analysed was incubated with the assay cocktail and the reduction in absorbance at 340 nM due to removed NADH was monitored.

6.10.1 Calibration standard curve

An NADH standard curve for calibration of the assay was prepared in the range of 0–6 nmol NADH per microplate well (Table 6.11). An example standard curve is given in Figure 6.21.

6.10.2 Preparation of assay cocktail

A 10 mL assay cocktail sufficient for 50 assays was prepared by mixing the following (final concentrations are listed in parentheses): 5 mL 500 mM tris-HCl, pH 7.8 (250 mM); 1 mL 148 mM ribose-5-phosphate (14.8 mM); 253 µL 10 mM NADH (253 µM); triose phosphate isomerase (185 U ml^{-1}); glycerol-3-phosphate dehydrogenase (6 U ml^{-1}) and water to a final volume of 10 mL.

Amount of NADH (nmol)	500 mM Tris-HCl pH 7.8 (µL)	100 µM NADH (µL)	Water (µL)	Total volume (µL)
0	115	0	115	230
1	115	10	105	230
2	115	20	95	230
3	115	30	85	230
4	115	40	75	230
5	115	50	65	230
6	115	60	55	230

Table 6.11: Transketolase assay NADH standards preparation volumes

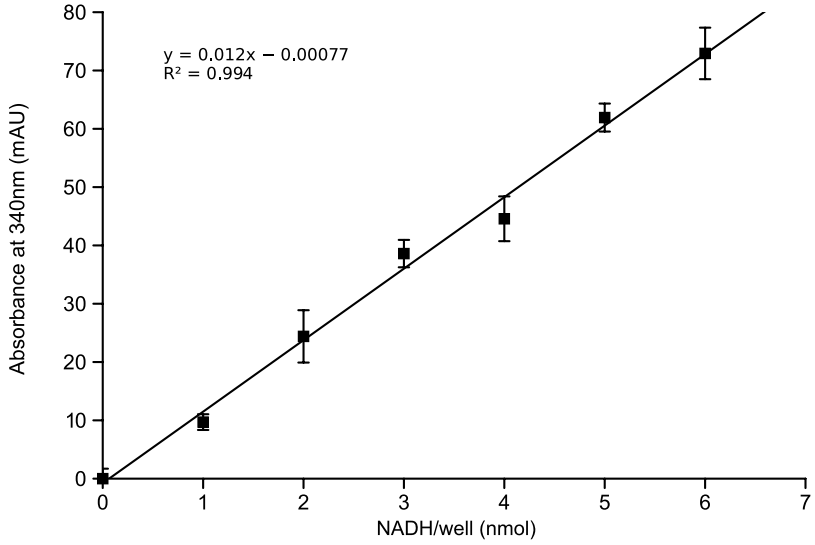

Figure 6.21: Example standard curve for NADH typically observed during a transketolase assay. The range is from 0–6 nmol well^{-1} in a total volume of 230 µL.

6.10.3 Analysis of samples

Two wells in a 96-well microplate were used for analysis of each replicate of each sample. Both wells had 200 µL assay cocktail added and then one had 10 µL water added to it to assay native transketolase activity whilst the other had 10 µL 8 mM thiamine pyrophosphate added to it to saturate the transketolase and measure the "thiamine effect"—or percentage unsaturated transketolase. The wells were mixed thoroughly by pipetting and 10 µL 5-fold diluted cell lysate was added to each well before mixing again. The absorbance was monitored at 340 nm every 2 min for 3 hours at 37 °C with regular orbital shaking prior to each read cycle in a microplate reader. The order of addition proved critical with samples giving spurious and poorly reproducible results when added in other orders.

The A_{340} was plotted against time for each sample and the linear portion of the plot (Figure 6.22) was used for determination of the gradient of the data. The time-frame for the linear portion was chosen so that for all samples analysed, the curve was linear within that range. The rate of decrease of NADH was quantified using the standard curve and was converted into transketolase activity normalised to protein concentration. Data were expressed as units of transketolase activity per mg protein.

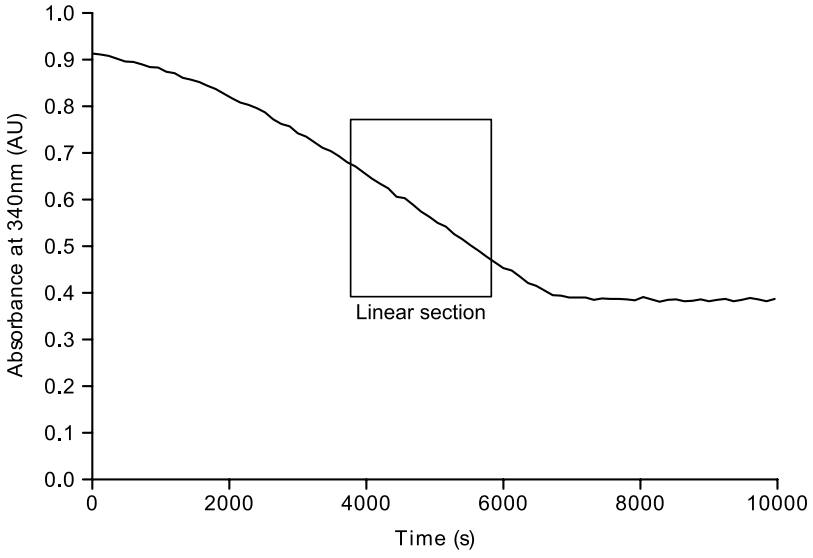

Figure 6.22: Example transketolase assay reaction curve. This typical curve shows the initial accelerating decrease in absorbance with a central linear section and a terminal plateau. The linear section was used for analysis of rate of reaction

The thiamine effect is the percentage unsaturation of transketolase with thiamine pyrophosphate and is determined using Equation 6.3 where ΔA_{340} TPP^- is the change in

absorbance for the sample incubated without thiamine pyrophosphate (i.e. apoenzyme not active) and ΔA_{340} TPP^+ is the change in absorbance for the sample incubated with thiamine pyrophosphate (i.e. apoenzyme has been saturated with cofactor and is now active).

$$\text{Thiamine effect (\%)} = \frac{\Delta A_{340}\ TPP^- - \Delta A_{340}\ TPP^+}{\Delta A_{340}\ TPP^+ \times 100} \tag{6.3}$$

6.11 Thiamine transport studies

Tritiated thiamine can be used as a tracer to follow the movement of thiamine introduced to cells. Two sets of experiments were performed using tritiated thiamine. The first was a simple uptake or release experiment. For uptake, the cells were exposed to tritiated thiamine for a set time and the amount taken up quantified. For release, the cells were pre-loaded with tritiated thiamine then release was measured during a subsequent timed release period. In both cases, transport rates relative to amount of protein can be determined. The second measured *in situ* transport across the membrane by culturing the cells on a semi-permeable support. By introduction of the labelled compound on one side of the membrane, its movement to the other side over a period of time could be measured.

6.11.1 Tritiated thiamine uptake study

The simple uptake experiment was performed using the HK-2 cell line. Cells were seeded in advance in 6-well plates and cultured for five days in one of four conditions: 5 mM glucose and 4 nM thiamine (−G−T), 5 mM glucose and 4 µM thiamine (−G+T), 26 mM glucose and 4 nM thiamine (+G−T) or 26 mM glucose and 4 µM thiamine (+G+T). At the commencement of the study, each well was washed three times with 2 mL Krebs-Ringer solution at 37℃. Krebs-Ringer solution contained 133 mM NaCl, 4.93 mM KCl, 1.23 mM $MgSO_4$, 0.85 mM $CaCl_2$, 5 mM glucose, 5 mM glutamine and 20 mM HEPES at pH 7.4 at 37℃ and 4℃. After rinsing, each well had 1 mL 15 nM ^{3}H thiamine solution added in Krebs-Ringer solution. The fluid was evenly dispersed over the cells and the plates were incubated at 37℃ for 10 min. After incubation, the plates were removed from the 37℃ heating chamber and placed on a bed of ice. The supernatant containing the bulk of the ^{3}H thiamine was discarded. The cells were washed three times with 2 mL ice-cold Krebs-Ringer solution to remove extracellular thiamine. The cells were lysed by addition of 1 mL 1 M NaOH. The lysates were transferred to microcentrifuge tubes and the lysate was clarified by centrifugation (2 min, 1000 × *g*, 21 ℃). 0.5 mL clarified cell lysate was mixed

thoroughly with 4 mL scintillation fluid. Each sample was counted for 5 min in a scintillation counter. A portion of the remaining cell lysate was used to determine protein concentration using the Bradford assay.

Having determined the radioactivity present in the scintillation tube, it was possible to determine the total radioactivity present in the cells in the well. A blank value for the radioactivity was determined from an uptake experiment with only non-radioactive thiamine and subsequently subtracted from each of the results. By combining knowledge of the specific activity of the thiamine, radioactivity in the cells and protein present in the well it was possible to determine an uptake rate in fmol $10\,\mathrm{min}^{-1}\,\mathrm{mg\,protein}^{-1}$.

6.11.2 Tritiated thiamine release study

Proximal tubule cells will, *in vivo*, transport thiamine from the proximal tubule lumen to the vasculature. This means that they both take up and release thiamine. Thus, in addition to studying uptake rate of tritiated thiamine, the release rate from cells pre-loaded with ^{3}H thiamine was also studied. HK-2 cells were prepared in 6-well plates in the four conditions described above. All cells were pre-cultured for 5 days before experimentation. On the day of the experiment, the cells were rinsed free of medium using 3x2 mL Krebs-Ringer solution at 37°C. The cells were then pre-loaded with ^{3}H thiamine for 5 hours by incubating cells with 1 mL DMEM/F-12 medium containing either 5 mM or 26 mM glucose as relevant and 15 nM ^{3}H thiamine. The cells were placed at 37°C in a 5% CO_2 humidified incubator for duration of the incubation. After the uptake period had elapsed, the cells were processed as quickly as possible. The incubation medium was discarded and the cells were rinsed with 2x2 mL Krebs-Ringer solution at 37°C, taking care to aspirate fully after each addition. Only two wash steps were used since the original thiamine concentration was only 15 nM and two rinses would be sufficient to lower that to effectively 0 nM whilst minimising the time when the cells are releasing thiamine in an unmeasured manner. After rinsing, each well had 1 mL Krebs-Ringer solution added at 37°C and the plates were returned to a 37°C heating chamber for 10 min. After this time had elapsed, the plates were chilled on ice and the 1 mL supernatant collected. The cells were rinsed three times with 2 mL ice-cold Krebs-Ringer buffer and the cells were lysed in 1 mL 1 M NaOH. The lysates were collected in micro-centrifuge tubes and clarified by centrifugation (2 min, $1000 \times g$, 21 °C). 0.8 mL lysate supernatant or 0.75 mL ^{3}H thiamine release supernatant was mixed with 4 mL scintillation fluid and mixed thoroughly. Each sample was counted for 5 min in a scintillation counter. The Bradford assay was used to determine protein concentration.

The scintillation results and the protein analysis were used to determine the amount of intracellular thiamine and the amount of thiamine released from the cells into the supernatant over 10 min.

6.11.3 Transwell inserts

Transwell inserts allow monolayers of cells to grow with access to both apical and basal chambers. A schematic is shown in Figure 6.23. The microporous membrane in the inserts used was made from polycarbonate and had 0.4 µm pores at a density of 1×10^8 pores cm^{-2}. The inserts fitted into the wells of a 12-well microplate and had a total area of 1.12 cm^2 each. Cells were seeded onto the inserts at 30–50% confluence.

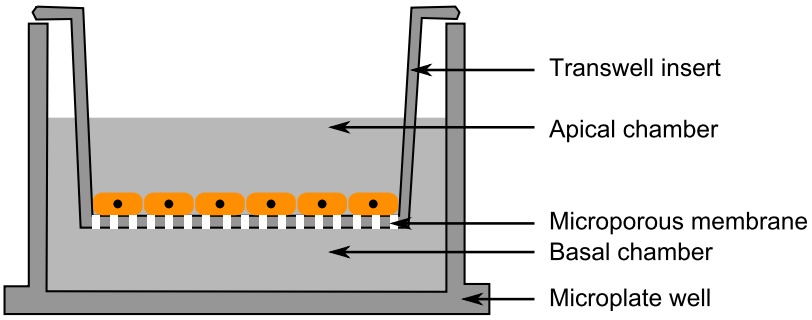

Figure 6.23: Schematic of a Transwell insert

6.11.4 Lucifer yellow permeability

The confluence and integrity of epithelial monolayers grown on Transwell inserts was determined using trans-epithelial transport rates of Lucifer yellow dye. Confluent and undamaged monolayers normally allow only low levels of Lucifer yellow to pass via the paracellular route. Damaged monolayers allow much higher transport rates. The methods for this type of assay are well established for use in the 21-day old Caco-2 monolayer system—a human colon carcinoma cell line—as a model for gut epithelial transport [Lindhardt and Bechgaard, 2003; Hubatsch et al., 2007; Konsoula and Barile, 2005].

The rate of transport of Lucifer yellow is expressed as an apparent permeability coefficient (P_{app}) which can be calculated according to the the formula displayed in Equation 6.4 [van de Waterbeemd and Testa, 2008]. P_{app} (units of $\mathrm{cm\,s}^{-1}$) is calculated from dQ/dT which is the steady state flux across the membrane ($\mu\mathrm{mol\,s}^{-1}$), A which is the surface area of the filter (cm^2) and C_0 which is the initial concentration in the donor chamber (in

µmol cm^{-3}). It is assumed that the sink concentration never exceeds 10% of the donor concentration i.e. the sink conditions are fulfilled.

$$P_{app} = \left(\frac{dQ}{dT}\right)\left(\frac{1}{A.C_0}\right) \tag{6.4}$$

A reference value for P_{app} for Lucifer yellow across intact monolayers of kidney proximal tubule cells is not known. Most published estimates are from companies specialising in transport assays across monolayers of Caco-2 cells. These estimates are around 1.1×10^{-6} cm s^{-1} e.g. [NoAb BioDiscoveries, 2009; Marine Biotechnology Research Centre, 2009] for Caco-2 monolayers and from 1–9 $\times 10^{-6}$ cm s^{-1} for *ex vivo* intestine membranes [Huynh et al., 2002]. Estimates for Madin-Darby Canine Kidney cell monolayers are much higher, for example 30×10^{-6} cm s^{-1} [NoAb BioDiscoveries, 2009].

Cells to be assayed were seeded at around 30–50% confluence on the Transwell membranes as described in the instructions from the manufacturer. The cells were allowed to grow to confluence and then left for 7 days post-confluence with bi-daily medium changes to allow complete tight junction formation. To assess the integrity of the membrane, the medium in the apical compartment was replaced with medium supplemented with Lucifer yellow dye (1 mg mL^{-1}). The inserts were transferred to wells containing fresh medium and placed on an orbital shaker at 120 revolutions min^{-1} in a humidified incubator at 37℃ for 1 hour. Following incubation, the contents of the apical and basal chambers were collected, the cells washed once with warm medium to remove excess dye and then placed in new wells with fresh medium to allow continued growth.

The apical and basal media collected were diluted to within the standard range into fresh medium and pipetted in triplicate in wells in a black 96-well microplate. A standard curve was constructed in the microplate in triplicate in the range of 0–0.25 mg mL^{-1} Lucifer yellow in medium. Fluorescence was measured with an excitation at 410 nm ($\lambda_{\max} = 425$ nm) and emission at 520 nm ($\lambda_{\max} = 528$ nm). A double reciprocal standard curve was plotted with the reciprocal of fluorescence against the reciprocal of the standard concentration and the LY concentrations of each sample deduced accordingly. As an additional check, the mass balance (i.e. the total recovered Lucifer yellow in apical and basal chambers) was calculated as a percentage of the total Lucifer yellow introduced to the system. Mass balances between 90–110% were considered acceptable. Wells with mass balances outside this range were discarded from analysis.

Using the concentrations in each chamber and the time elapsed for transport, the P_{app} for Lucifer yellow for the cells was deduced in accordance with Equation 6.4.

6.11.5 Epithelial transport studies

Monolayers of primary cells were grown as described above in each of four conditions (−G−T, −G+T, +G−T and +G+T). On the day of assay, the Lucifer yellow test was carried out as described above to ensure that the cells had formed confluent monolayers. Medium was removed and the monolayers rinsed twice apically and basally in sterile Krebs-Ringer solution at 37°C to remove excess thiamine. Krebs-Ringer solution with a known concentration of tritiated thiamine was placed in the freshly aspirated apical chamber and the insert placed in a well of a 12-well plate with fresh Krebs-Ringer solution at 37°C. The plate was returned to a 37°C incubator and placed on a rotating platform at 120 revolutions min^{-1}. At 15 min, a 10 µL sample was removed from the apical chamber and the insert moved to a second fresh well of Krebs-Ringer solution. The plate was again returned to the incubator. This procedure was repeated at time points at 30, 45 and 60 min. Following the last time point, the monolayers were rinsed with Krebs-Ringer solution and the procedure repeated with a second concentration of thiamine in the apical chamber. 6 concentrations were assayed: 10, 25, 50, 100, 150 and 200 nM—a range which significantly surpasses the expected K_{m} of transport, 70 nM [Ashokkumar et al., 2006]. Each well was used for all concentrations with the lowest concentration first, rising to the highest concentration.

A simplified version of the same experiment was conducted in forward and reverse orientations to compare transport in both directions (i.e. from basal to apical and *vice versa*). The simplified version was chosen because it is not possible to replace the apical chamber fluid repeatedly on such a short time-scale without excessive damage to the monolayer. 15 nM ^{3}H-thiamine was placed in the apical chamber and the accumulation of ^{3}H-thiamine in the basal chamber monitored over 20 min. The membranes were then rested for 30 min at 37°C in Krebs-Ringer solution with no thiamine present before 15 nM ^{3}H-thiamine was placed in the basal chamber and the apical chamber accumulation monitored over 20 min. The solutions collected from the apical and basal chambers were mixed with scintillation fluid and the radioactivity counted. The P_{app} values for each well in each direction were determined.

6.12 Protein assays

Protein concentration was assayed by one of two techniques. The majority of samples were assayed using the Bradford technique and a minority assayed using the DC protein assay kit where reagents were incompatible with the Bradford dye (e.g. high SDS concentration).

6.12.1 Bradford assay

The Bradford protein assay is an absorbance assay based on the colour shift of the Coomassie dye from a red form to a blue protein-bound form [Bradford, 1976]. Bradford dye was purchased as a concentrate and was diluted prior to use according to the instructions from the manufacturer.

Protein samples to be analysed were diluted to an within the standard range (between 0.1–1.2 mg mL^{-1}) and 20 µL pipetted in triplicate into the wells of a 96-well microplate. Standard solutions of bovine serum albumin (BSA) in the range above were also pipetted in triplicate into the plate. BSA solutions were previously calibrated by UV absorption at 280 nm using an $\varepsilon_{1\%}$ value of 6.6. Diluted Bradford dye (200 µL) was pipetted into each well and mixed thoroughly. Absorbance at 595 nm was read immediately. A standard curve was constructed and the concentration of protein in each sample deduced accordingly.

6.12.2 DC protein assay

Where buffer composition was incompatible with the Bradford dye, the BioRad DC protein assay was used which is based on Lowry detection of protein using alkaline copper tartrate solution and Folin reagent [Lowry et al., 1951]. This is also an absorbance-based assay with three reagents which are combined according to protocol supplied by the manufacturer. A diluted sample was pipetted into the wells of a 96-well microplate in triplicate. A standard curve was constructed in the range of 0.2–1.5 mg mL^{-1} in the same buffer as the samples. The DC protein assay kit reagents were pipetted into the wells and a blue colour developed in proportion to the concentration of protein present. The absorbance of the plate was measured at 690 nm immediately, a standard curve was constructed and the concentration of protein in each sample deduced accordingly.

6.13 Glucose assay

Glucose concentration was assayed by an end-point enzymatic assay based on peroxidase and glucose oxidase (PGO). The two sequential reactions shown below (Equations 6.5 and 6.6) produce the chromophore oxidised o-dianisidine in direct correlation with the concentration of glucose.

$$\text{Glucose} + 2H_2O + O_2 \xrightarrow{\text{Glucose oxidase}} \text{Gluconic acid} + 2H_2O_2 \tag{6.5}$$

$$H_2O_2 + \text{o-dianisidine (colourless)} \xrightarrow{\text{Peroxidase}} \text{Oxidised o-dianisidine (coloured)} \qquad (6.6)$$

A combined enzyme-colour reagent was prepared by dissolving one capsule of PGO enzymes into water (100 mL) and adding o-dianisidine dihydrochloride solution (1.6 mL at 2.5 mg mL^{-1}) according to the instructions from the manufacturer. Samples were diluted to within the standard range (0–1.2 mM glucose) and 25 µL of each diluted samples was incubated in triplicate with 225 µL combined enzyme-colour reagent at room temperature for 45 min in the well of a 96-well microplate. The absorbance was measured at 450 nm with the absorbance at 690 nm measured as a reference wavelength. A standard curve was constructed and the concentration of glucose in each sample deduced.

6.14 Thiamine supplementation trial

Diabetic patients from the Diabetes Clinic at the Sheikh Zayed Hospital, Lahore, Pakistan were recruited between October and December 2006 for a trial on the effects of thiamine on diabetic nephropathy. The main inclusion criteria were type 2 diabetes with persistent microalbuminuria (albumin excretion rate (AER) 30–299 mg $24\,h^{-1}$), age 35–65 years, a diabetes duration ≥5 years, HbA_{1c} ≤12.5% and a BMI 19–40 kg m^{-2}. The main exclusion criteria were significant comorbidities, known allergy or intolerance to thiamine, use of thiamine supplements, participation in an intervention study within 30 days, recipients of renal or pancreatic transplants, women who were pregnant or breastfeeding or of child bearing age not using adequate contraceptive precautions.

Forty patients were recruited and randomly assigned (by random number table method) to receive either placebo or 3 × 100 mg thiamine tablets per day for 3 months followed by a 2 month washout period. Despite this dose of thiamine exceeding the RDI by 200 times, no adverse effects were expected due to the very low oral toxicity of thiamine. Side effects have been observed with doses above 7000 mg day^{-1} [Expert Group On Vitamins and Minerals, 2003] and sometimes with parenteral administration of the vitamin [Haake et al., 1971; Wrenn and Slovis, 1992; Wrenn et al., 1989]. Any potential adverse effects of the thiamine treatment were assessed by kidney function (serum creatinine and urea nitrogen) and liver function (serum alanine transaminase, aspartate transaminase and alkaline phosphatase activities and bilirubin) tests.

Twenty four hour urine and fasting blood samples were collected with informed

consent from participants. Plasma and erythrocytes were separated by centrifugation and stored at −80℃ immediately following collection and prior to analysis for thiamine metabolites and other blood biochemistry markers. The trial was registered at the Clinical Trials Registry—India (CTRI/2008/091/000112) and ethical approval for the study was given by the Ethical/Protocol/Synopsis Committee of Sheikh Zayed Federal Postgraduate Medical Institute, Lahore, Pakistan (Eth/P609/FPGMI/2006) [Rabbani et al., 2009].

6.15 Statistical analysis

For statistical purposes, n is considered to be a biological replicate which was treated separately during the course of an experiment and analysed separately. The limit to which interpretation of n as a concept can go is ambiguous. No-one expects multiple different vials of cells or reagents to be ordered from a supplier or multiple pieces of equipment to be used for each assay yet obviously experiments need to be repeatable. It is to avoid ambiguity that I have defined my use of n here.

In addition to biological replicates, some assays used technical replicates e.g. multiple wells for a biological replicate in a microplate for a transketolase activity assay. In these cases, a repeated measures ANOVA was used with appropriate *post hoc* tests to correctly analyse the data produced.

For single comparisons between two sets of parametric data, a Student t-test was conducted to determine significance. For multiple group comparisons, an ANOVA was performed followed by either a Bonferroni or Tukey HSD *post hoc* tests for individual comparisons. The Bonferroni adjustment was chosen when only a limited number of comparisons were being made or when unequal sample sizes prevented use of the Tukey comparison. All statistical comparisons were made in SPSS, Gnumeric or GraphPad Prism.

For the Pakistan supplementation trial, statistical tests were all two-sided (<0.05). Significances of differences between mean and median analytes of thiamine treatment and placebo groups were determined using Student's t-test and a Mann-Whitney U test, respectively. Significances of differences from baseline and post-therapy and post-washout period mean and median analytes were determined using a paired samples t-test and a Wilcoxon signed-rank test, respectively. Correlation analysis was performed by calculating the Spearman rho statistic. Significance of difference of proportions was made by reference to Finney's 2×2 contingency tables [Rabbani et al., 2009].

All data are presented as means ± standard deviation unless otherwise specified.

Results and Discussion

Chapter 7

Immunohistochemistry characterisation of human kidney cells

The phenotypes of freshly isolated human proximal tubule epithelial cells (PTECs) were characterized by immunohistochemistry (IHC). After kidney digestion and Percoll density-gradient centrifugation, as described in Section 6.3, three fractions of cells were obtained. Cells from each fraction were seeded onto glass slides, allowed to adhere, fixed with formaldehyde and then stained independently for aquaporin-1 (Aqp-1) and Tamm-Horsfall protein (uromodulin or UMOD). In all cases, nuclei were stained blue by Meyer's haematoxylin and the antigen of interest was stained brown using DAB.

Aqp-1 is considered a marker for the proximal convoluted tubule and the descending loop of Henle [Tanaka et al., 2008] and is not found in the distal tubules. UMOD is considered a marker for the thick ascending limb of the loop of Henle [Sikri et al., 1981; Allen and Tisher, 1976] and is not found in proximal tubule cells or the glomeruli [Baer et al., 1997]. A qualitative assessment of the abundance of staining on each slide was made as quantitative data were unnecessary to correctly identify cell populations. Aqp-1 immunostaining was weak in the top fraction of the Percoll density gradient with only a few cells stained (Figure 7.1). The middle fraction had a higher percentage of cells staining for Aqp-1 but still <30%, likely due to contamination from the lower band of cells or from cells from the proximal portion of the loop of Henle (Figure 7.2). Contamination is likely to have arisen due to the

diffuse banding evident after Percoll centrifugation (Figure 6.1, page 88). A longer density-gradient separation could have been used to provide more discrete fractions but was not used because the longer centrifugation would lead to decreased cell viability with only a marginal increase in the yield of PTECs. Near universal, high-intensity staining for Aqp-1 was evident in the lower fraction of cells (Figure 7.3). UMOD staining was absent or at very low levels in all three fractions obtained (Figures 7.4, 7.5 and 7.6) which is consistent with the absence of the medulla boundary zone (thick ascending loop of Henle).

To corroborate the location specificity of Aqp-1 and UMOD as reported in the literature, paraffin-embedded sections of normal human kidney were stained for each protein. Figure 7.7 shows the immunostaining pattern of Aqp-1 in normal human kidney. There was heavy staining in the cortex and very little staining in the medulla. Figures 7.8 and 7.9 are details of normal human cortex and medulla respectively. These show that Aqp-1 staining was specific to the proximal tubules and not glomeruli or distal tubules. A series of similar experiments with immunostaining for UMOD indicated that UMOD was mainly found in the medulla (Figure 7.10). Closer examination of the cortex and the medulla (Figures 7.11 and 7.12 respectively) indicated a complete absence of staining in the cortex, including both glomeruli and tubules, whilst staining is present in the medulla in the ascending limb of Henle.

A negative control was performed for each culture condition, cell fraction or kidney section assayed by immunohistochemistry by omitting the primary antibody from the overnight incubation step. Negative controls gave no significant staining, see Figure 7.13. By combining the staining patterns of UMOD and Aqp-1 in whole kidney sections with the staining patterns in the cells from the different fractions of the Percoll density gradient, the bottom fraction of cells could be identified as containing predominantly PTECs.

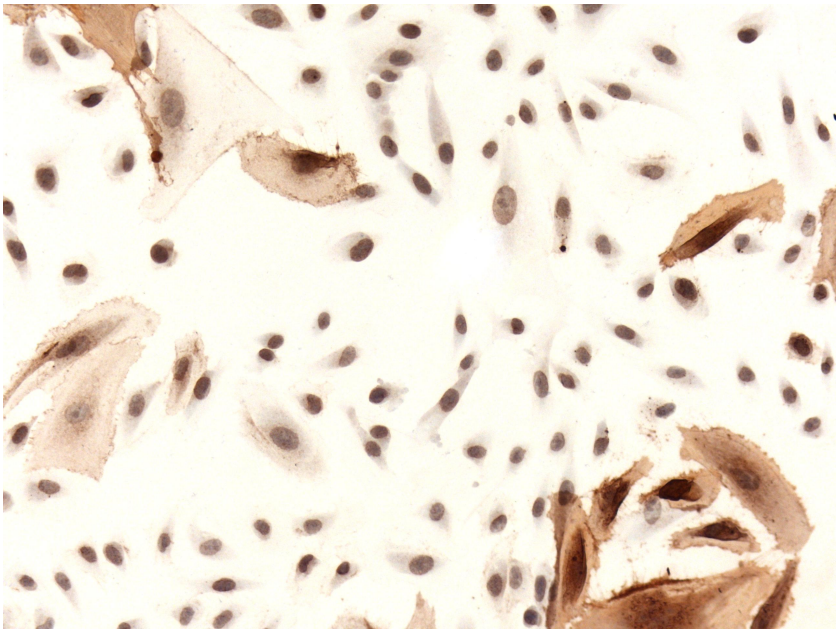

Figure 7.1: Aqp-1 immunostaining in cells from the top fraction of the Percoll density gradient. Stained cells are a small minority of the population. Magnification is 200x.

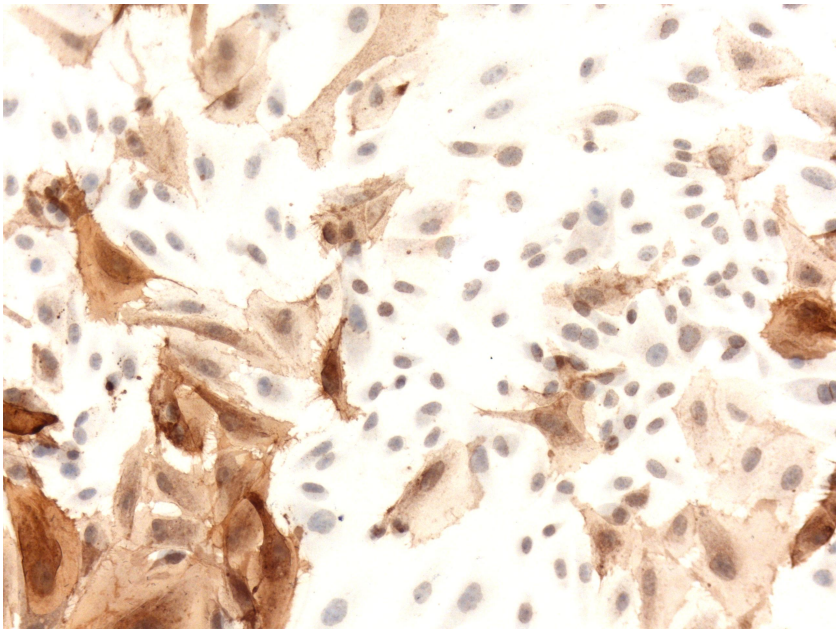

Figure 7.2: Aqp-1 immunostaining in cells from the middle fraction of the Percoll density gradient. Stained cells comprise the minority of cells (possible contamination from the bottom fraction). Magnification is 200x.

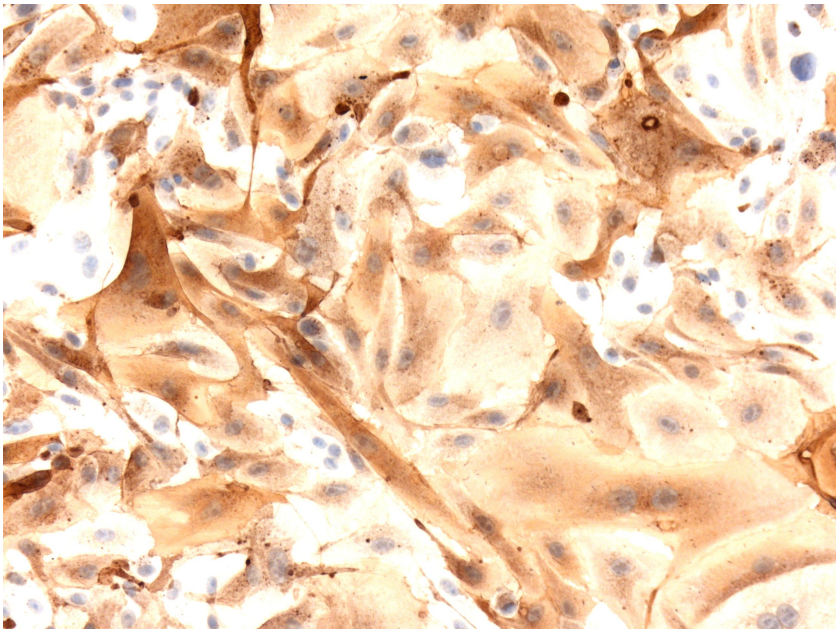

Figure 7.3: Aqp-1 immunostaining in cells from the bottom fraction of the Percoll density gradient. The staining is intense and near universal confirming this cell population is PTECs. Magnification is 200x.

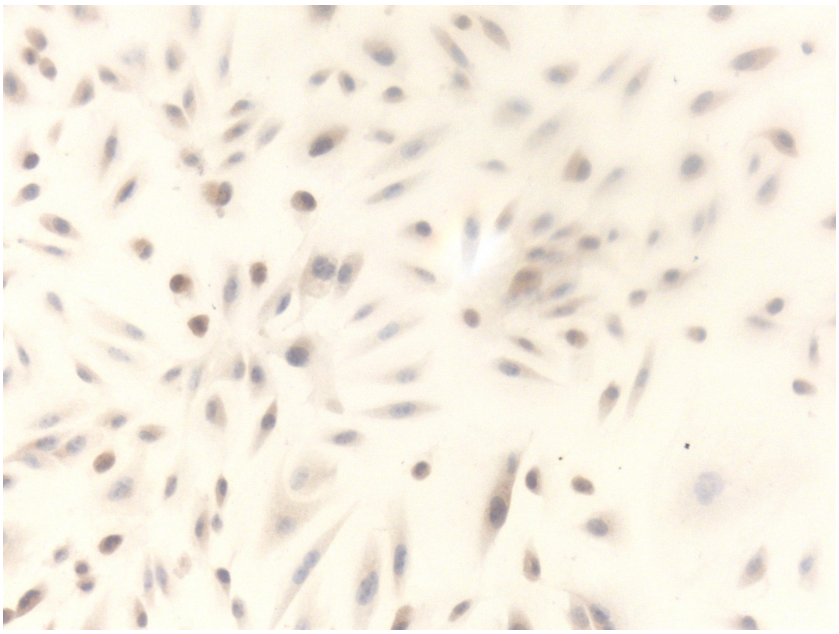

Figure 7.4: UMOD immunostaining in cells from the top fraction of the Percoll density gradient. Staining is very weak. Magnification is 200x.

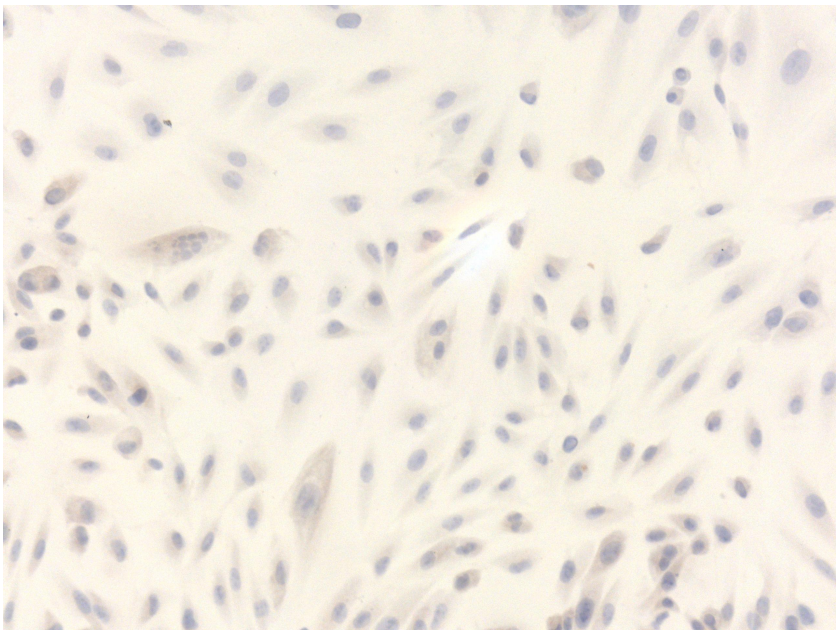

Figure 7.5: UMOD immunostaining in cells from the middle fraction of the Percoll density gradient. Staining is very weak. Magnification is 200x.

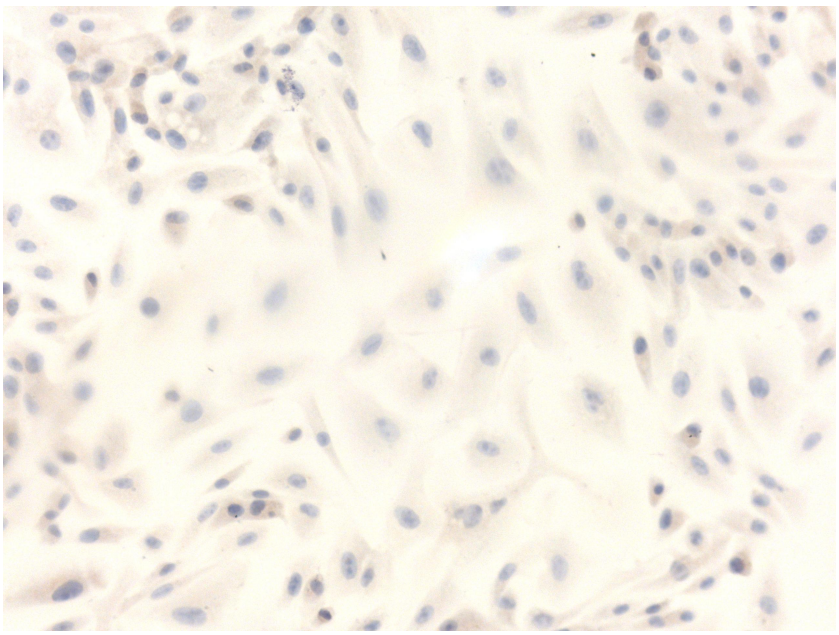

Figure 7.6: UMOD immunostaining in cells from the bottom fraction of the Percoll density gradient. Staining is very weak. Magnification is 200x.

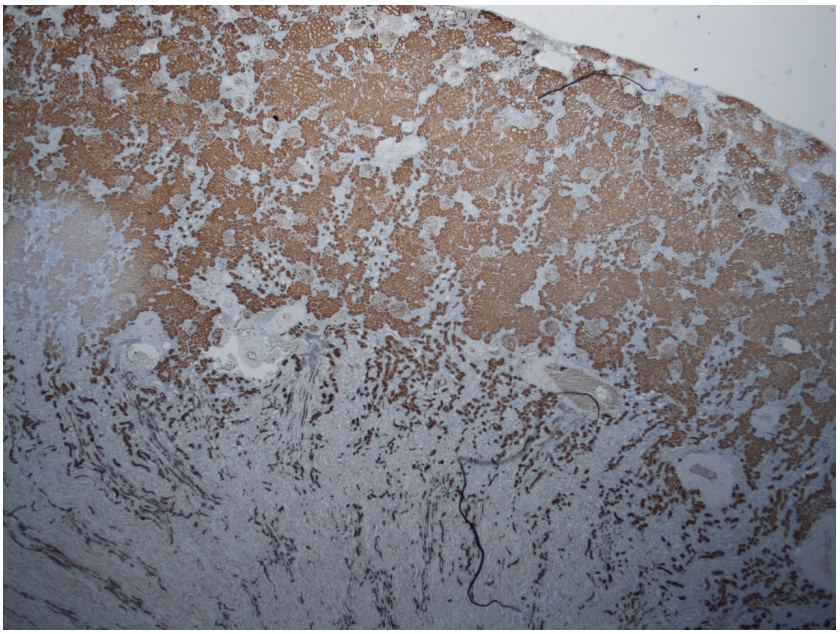

Figure 7.7: Aqp-1 immunostaining in a normal human kidney section. The cortex and the medulla are clearly delineated with heavy staining in the cortex and little in the medulla. Magnification is 16x.

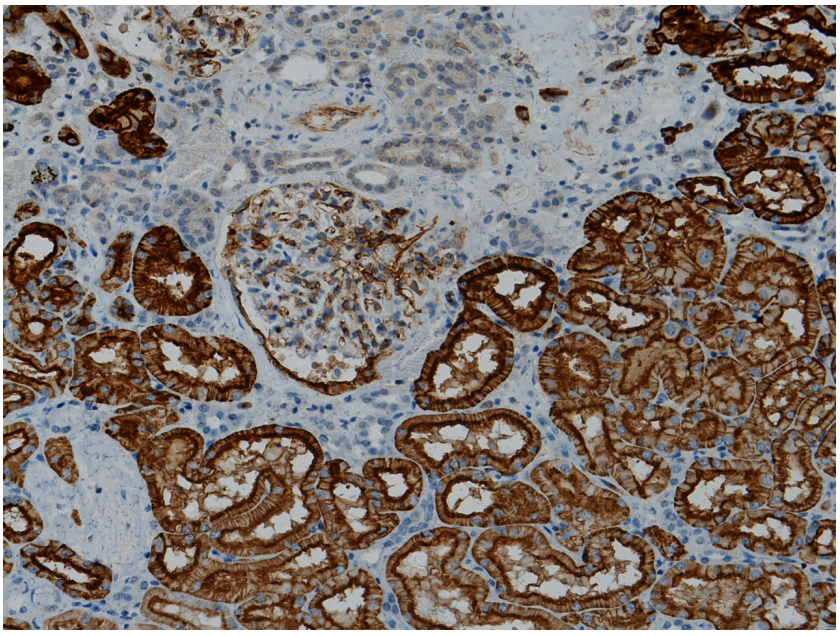

Figure 7.8: Aqp-1 immunostaining in a normal human kidney cortex section. There is heavy staining in the proximal tubules, especially in the brush border. There is comparatively little staining in the glomeruli. Magnification is 200x.

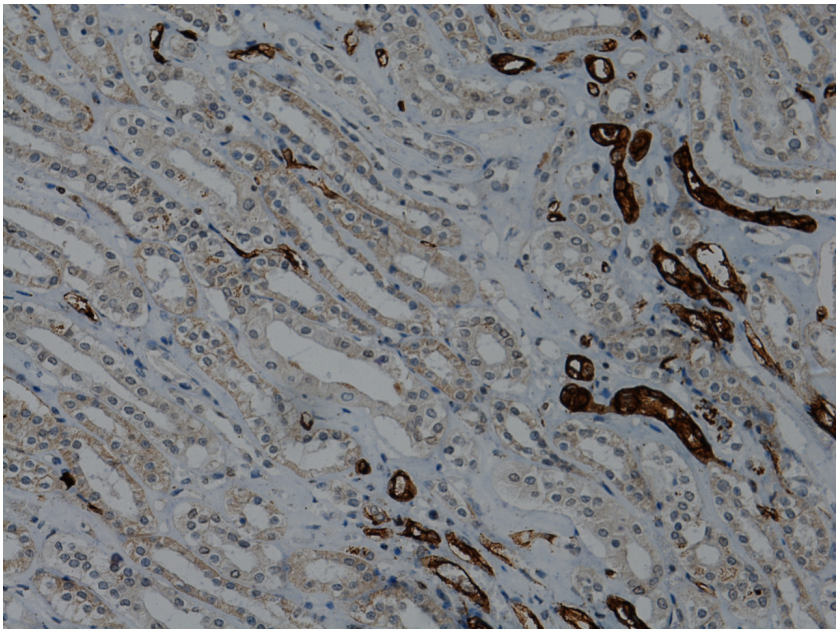

Figure 7.9: Aqp-1 immunostaining in a normal human kidney medulla section. Staining is very weak in the distal tubules and loops of Henle. Magnification is 200x.

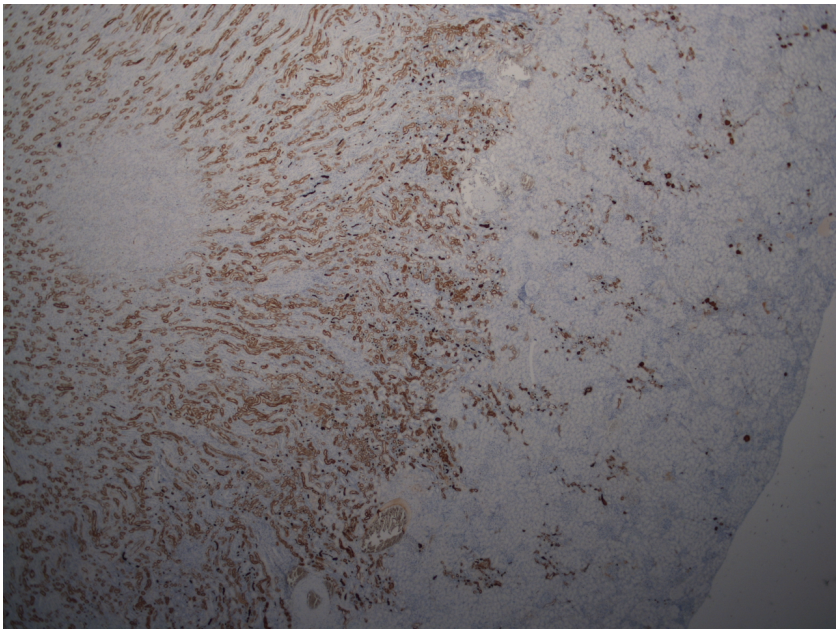

Figure 7.10: UMOD immunostaining in a normal human kidney section. The cortex and the medulla are clearly delineated with heavy staining in the medulla and absence of staining in the cortex. Magnification is 16x.

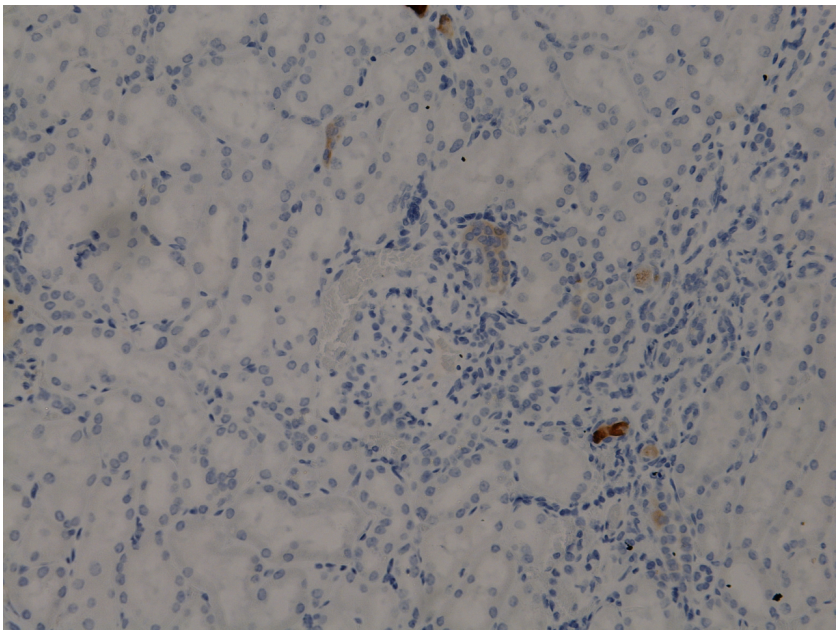

Figure 7.11: UMOD immunostaining in a normal human kidney cortex section. There is no significant staining in any part of the cortex. Magnification is 200x.

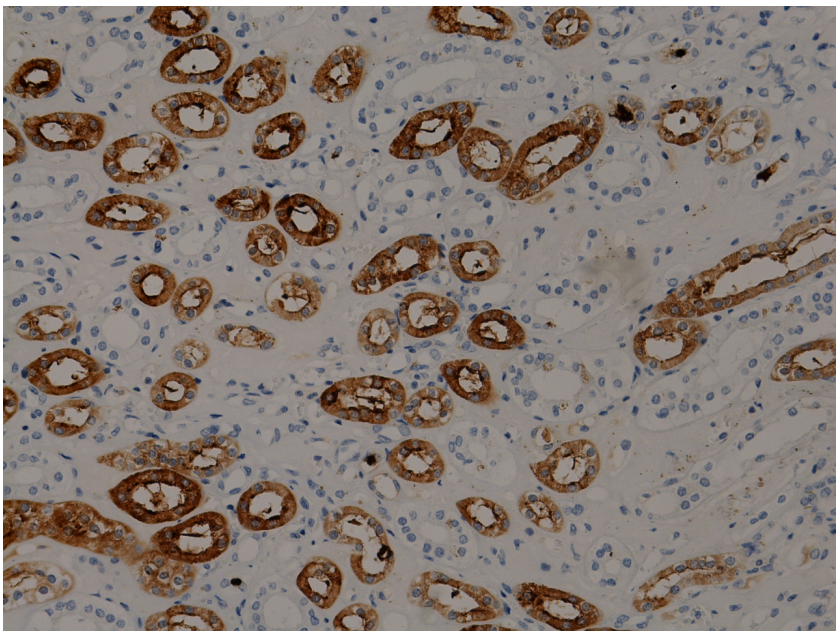

Figure 7.12: UMOD immunostaining in a normal human kidney medulla section. Staining is strong in the ascending limbs of Henle. Magnification is 200x.

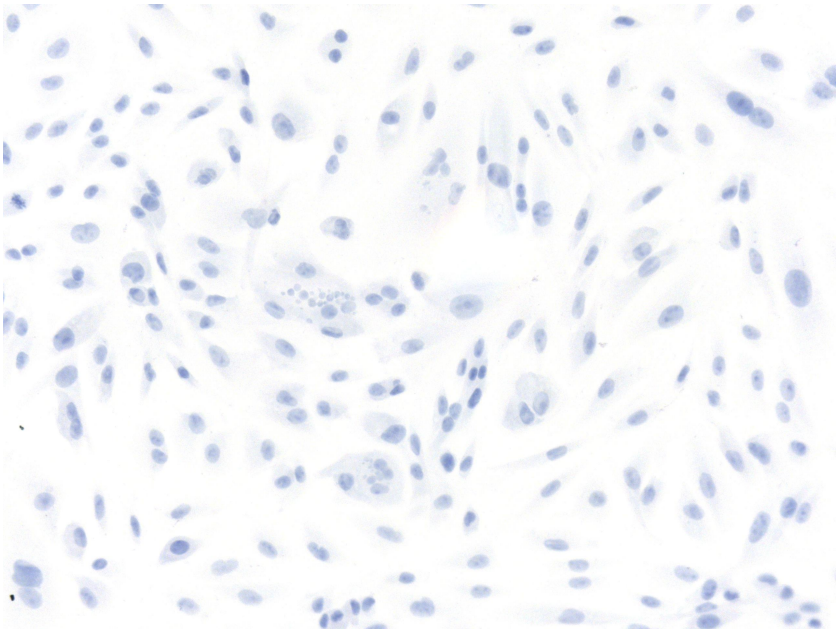

Figure 7.13: Kidney extract cell culture IHC negative control sample image. No immunostaining was evident in any negative control slide. Magnification is 200x.

Chapter 8

Immunohistochemistry thiamine transporter staining

8.1 Immunostaining of kidney thiamine transporters

A qualitative assessment of the location of the thiamine transporters THTR-1 and THTR-2 throughout the kidney was made in sections taken from five paraffin-embedded normal human kidneys.

The typical immunostaining pattern observed for THTR-2 was for strong staining in the proximal tubules, with the most intense staining at the apical membrane brush border. There was no staining observed in the distal tubules and only very weak staining observed in the glomeruli. Generally, only weak staining was seen at the basal membrane of PTECs. In most PTECs, the cytoplasm stained to an intermediate intensity for THTR-2. This cytoplasmic stain was often polarised, with darker staining towards the apical membrane of the cells and lighter staining towards the basal membrane. This would be consistent with the synthesis of THTR-2 and transport to the apical, but not the basal, membrane. Example images from three different kidneys are given in Figures 8.1, 8.2 and 8.3. A wider field of view of staining for THTR-2 in a kidney cortex is given in Figure 8.4. A more magnified image of the staining in a fourth kidney cortex is given in Figure 8.5.

The immunostaining for THTR-2 in the medulla was much weaker than the staining in the cortex. There was some weak apically-aligned staining in the epithelial cells of some tubules, probably the proximal section of the descending loops of Henle. There was also some weak and diffuse cytoplasmic staining in other tubules in the medulla. An image of

THTR-2 staining in the medulla of a normal kidney is given in Figure 8.6. There was only poor staining in smooth muscle lining arterioles in the kidney (Figure 8.7).

Work by Subramanian et al. [2006] in cell culture systems indicated that THTR-2 is more predominantly located on the apical membranes of polarised cells. Also, the proximal tubule is the region of the nephron responsible for re-absorption of the majority of valuable small molecules from the ultrafiltrate. Thus the hypothesised location for THTR-2 is the brush border of PTECs with little staining elsewhere. The observed staining patterns for THTR-2 in the kidney sections corroborate this hypothesis. There is a strong apical polarity for THTR-2 with high intensity staining evident on the apical faces of proximal tubule cells and to a much lower extent, some cells in the medulla.

The typical staining pattern observed for THTR-1 was different to that observed for THTR-2. The staining in the glomeruli was weak or absent and there was strong staining in the proximal tubule epithelial cells, both similar to the staining patterns for THTR-2. In contrast to the staining patterns for THTR-2, the proximal tubule epithelia were not as markedly polarised although apical polarisation was still prominent in large numbers of tubules. There was relatively strong cytoplasmic staining in the proximal tubule epithelia. Strong staining was also seen in many distal tubule sections. Often this staining was observed to occur on every other cell around the circumference of a tubule section (e.g. Figure 8.8). Example staining patterns for THTR-1 in normal human kidney cortex sections from three different kidneys are presented in Figures 8.8, 8.9 and 8.10. In the inner medullary region, the loops of Henle did not stain for either THTR-1 or THTR-2 but the collecting ducts stained strongly for THTR-1 but not THTR-2, see Figure 8.11.

Work by Subramanian et al. [2003] in cell culture systems indicated that THTR-1 is more likely to be localised to both apical and basal membranes in polarised cells. THTR-1 should also be predominantly located in the proximal tubule. This is not the case when examining kidney sections. The localisation of THTR-1 in the distal tubules and the collecting ducts was unexpected. Work by Mahajan and Acara [1994] used rat kidney sections and reported that there was measurable thiamine uptake by the medulla although this report may not be reliable as it was published before the discoveries of THTR-1 and THTR-2 and says that there is no active uptake of thiamine in the kidney sections, either cortical or medullary. In the cortex, there are cells at the most distal region of the ascending limb of Henle that have extensive coverings of villi [Allen and Tisher, 1976] and it may be these that are expressing THTR-1 in addition to the proximal tubules.

Negative control slides for every kidney stained were prepared by omitting the pri-

mary antibody from the overnight incubation step. No staining was seen on any negative control slide, see Figure 8.12.

Although it is possible to deconvolute multiply stained images such as these into separate channels [Ruifrok and Johnston, 2001], these images cannot be used for secure quantitation of antigen [van der Loos, 2008], because: (i) multiple steps of chromogen production in the triple-stepped development are non-stoichiometric for antigen; and (ii) the DAB chromophore does not follow the Beer-Lambert law—DAB colour is due to a scattering of light rather than to absorbance. These limitations notwithstanding, qualitative analysis of the images may still be performed.

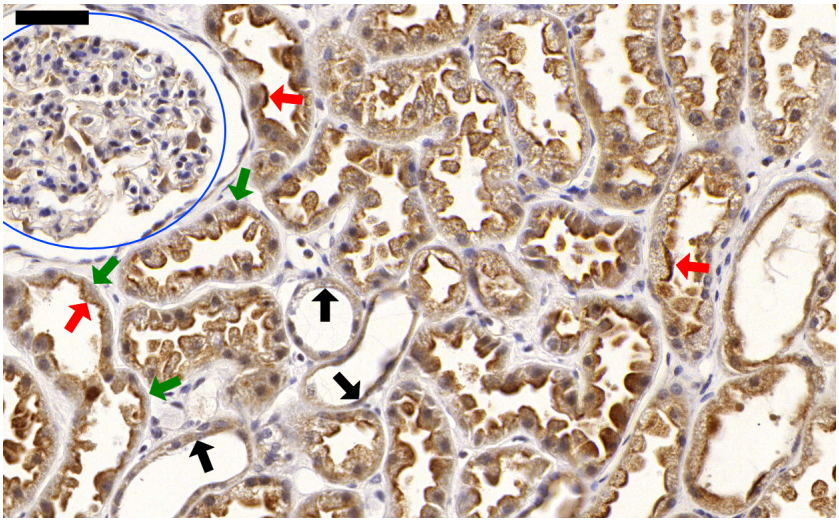

Figure 8.1: THTR-2 immunostaining in a normal human kidney cortex. Staining is relatively weak in the glomerulus (blue circle) and the distal tubules (black arrows). There is heavy staining in the crenellated brush borders in the proximal tubule epithelial cells (red arrows) but relatively weak staining of the basal membrane of the same cells (green arrows). Scale bar represents 100 µm.

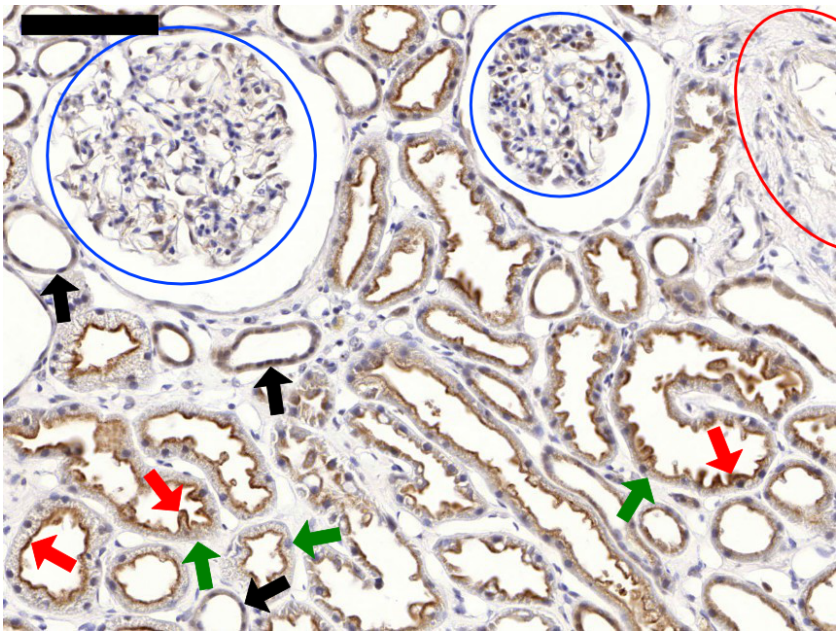

Figure 8.2: THTR-2 immunostaining in a second normal human kidney cortex. The staining pattern is very similar to that seen in Figure 8.1. There is staining in the brush borders of the proximal tubule epithelial cells (red arrows). There is no staining in the glomeruli (blue circles), distal tubules (black arrows), smooth muscle (red circle) or the basal membranes of the PTECs (green arrows). Scale bar represents 100 µm.

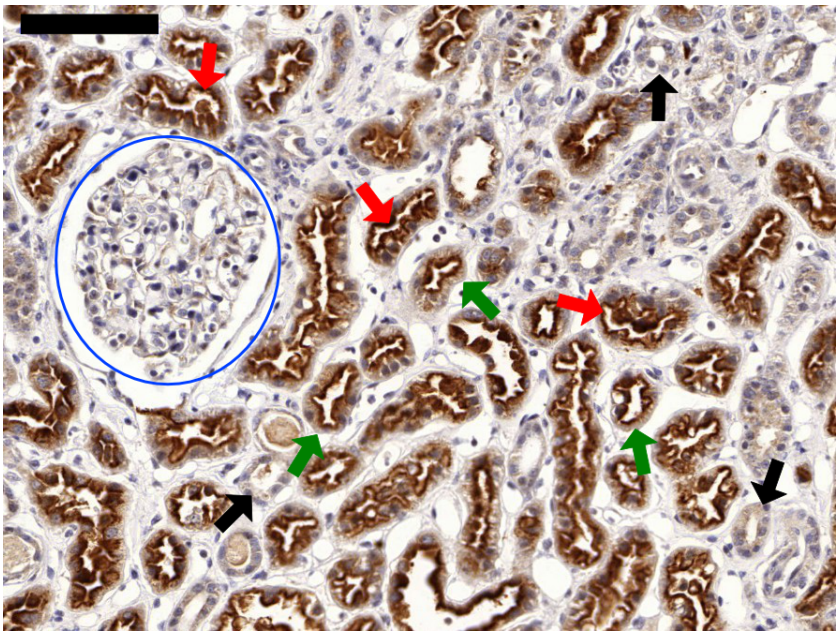

Figure 8.3: THTR-2 immunostaining in a third normal human kidney cortex. Staining similar to Figures 8.1 and 8.2 although stronger. Blue circle: glomerulus; red arrows: PTEC brush border; green arrows: PTEC basal membrane; black arrows: distal tubules. Scale bar represents 100 µm.

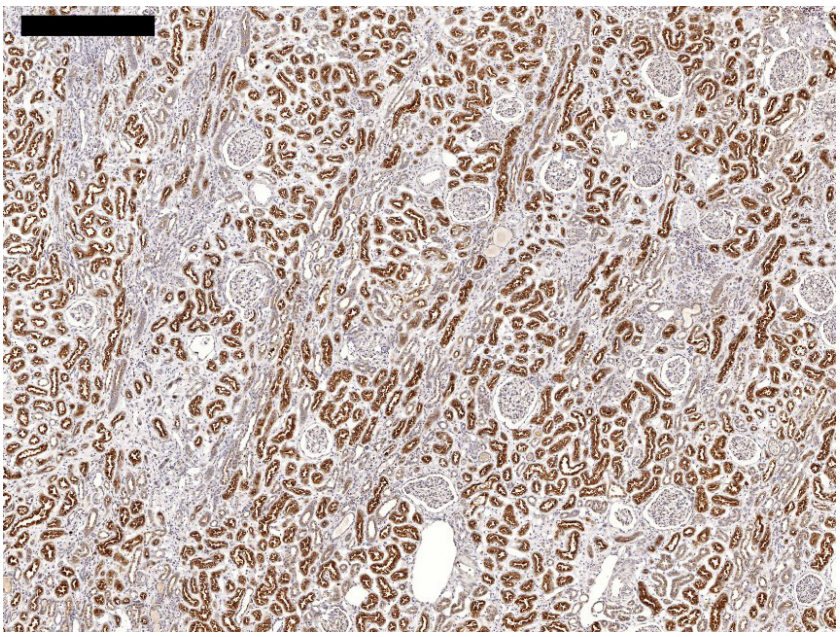

Figure 8.4: THTR-2 immunostaining in a third normal human kidney cortex. This image is from the same kidney as Figure 8.3 but with a larger field of view. The staining pattern is clear at this magnification. Scale bar represents 500 µm.

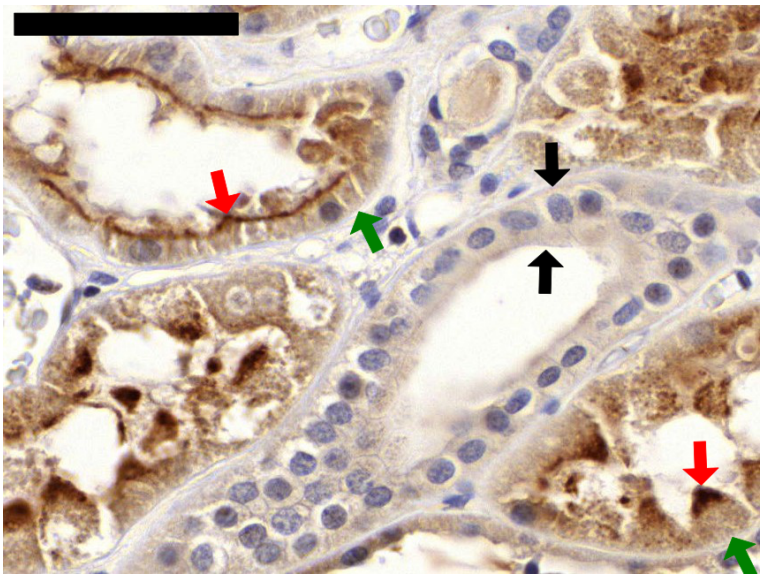

Figure 8.5: THTR-2 immunostaining in a fourth normal human kidney cortex. There is strong staining for THTR-2 in the apical membrane of the PTECs (red arrows). There is no staining in the distal tubules (black arrows) or on the basal membrane of the proximal tubule epithelium (green arrows). Scale bar represents 50 µm

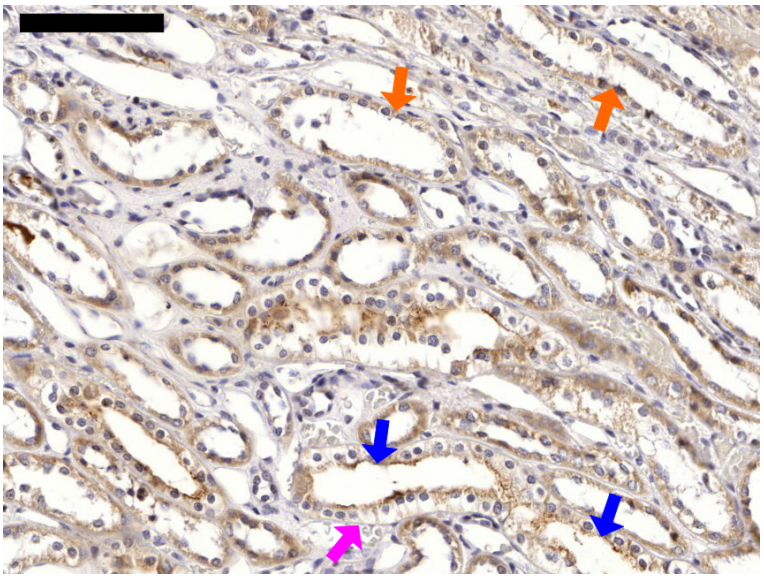

Figure 8.6: THTR-2 immunostaining in a normal human kidney medulla. The staining for THTR-2 in the medulla is much weaker than in the cortex. There is weak staining present on the apical membrane of some tubules (blue arrows), possibly the proximal portions of the descending loops of Henle. There is no staining on the basal membranes of cells where apical staining is present (pink arrow). Some other tubules have cytoplasm that stains weakly and diffusely for THTR-2 (orange arrows). Scale bar represents 100 µm.

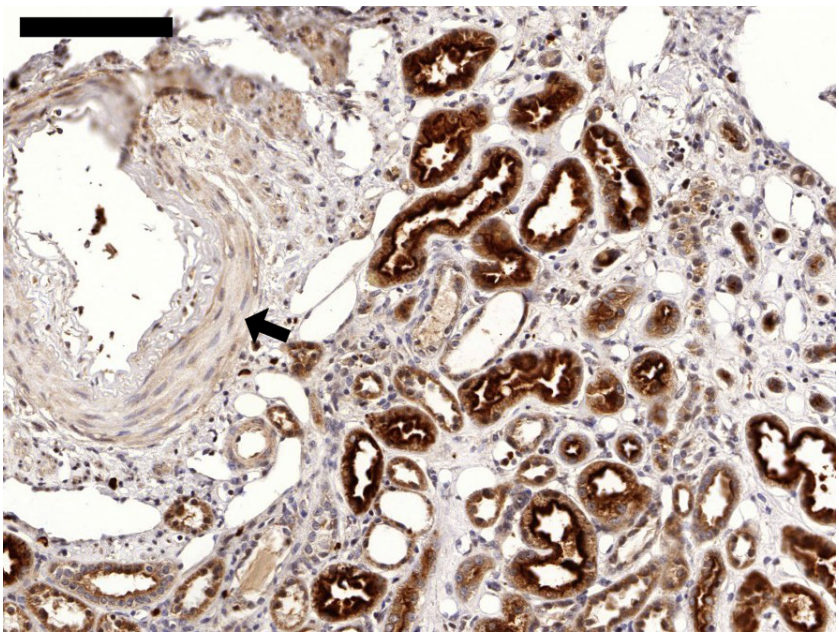

Figure 8.7: THTR-2 immunostaining in smooth muscle in the kidney. There is only weak staining in the smooth muscle that lines the arterioles within the kidney (black arrow). There is strong staining in the adjacent proximal tubules. Scale bar represents 100 µm.

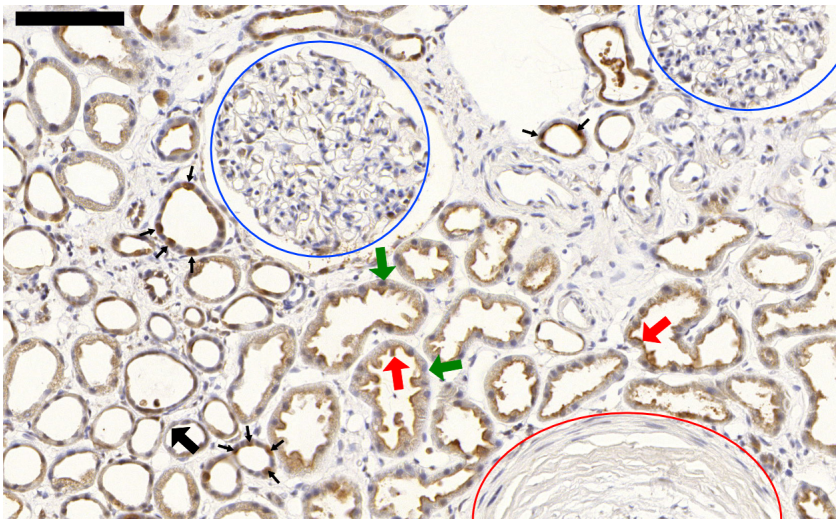

Figure 8.8: THTR-1 immunostaining in normal human kidney cortex. There is staining for THTR-1 on the apical membranes of the PTECs (red arrows). There is no staining on the basal membranes of the same PTECs (green arrows). Some distal tubules have stained weakly for THTR-1 (e.g. thick black arrow) but others stain for THTR-1 in a cell-specific manner (thin black arrows). There is no staining for THTR-1 in glomeruli (blue circles) or smooth muscle (red circle). Scale bar represents 100 µm.

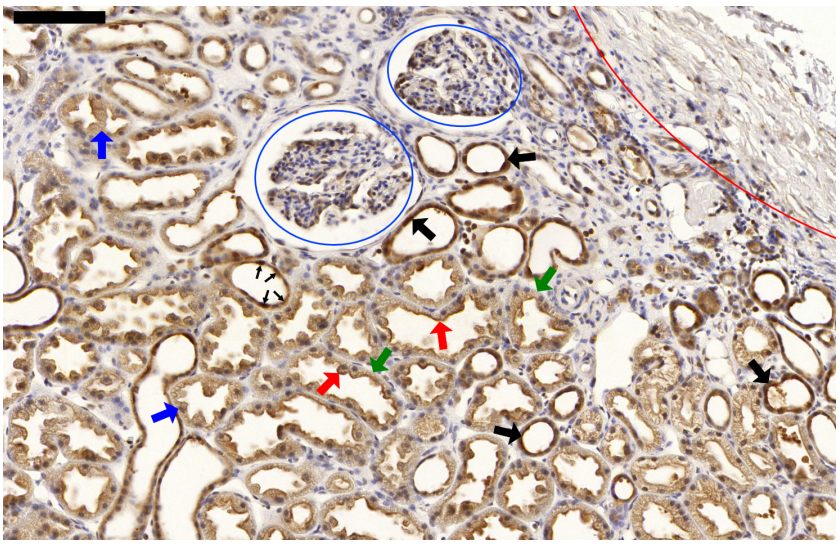

Figure 8.9: THTR-1 immunostaining in a second normal human kidney cortex. The smooth muscle did not stain (red arc) and the glomeruli (blue circles) were weakly stained, although to a higher intensity than in Figure 8.8. The proximal tubules stained for THTR-1 with more intense staining at the apical membranes (red arrows) than the basal membranes (green arrows). In some proximal tubules the polarity of staining was more difficult to discern (blue arrows). A high percentage of smooth-lumened tubules stained for THTR-1 (large black arrows) and in some cases, staining was cell-specific, as in Figure 8.8 (small black arrows). Scale bar represents 100 µm.

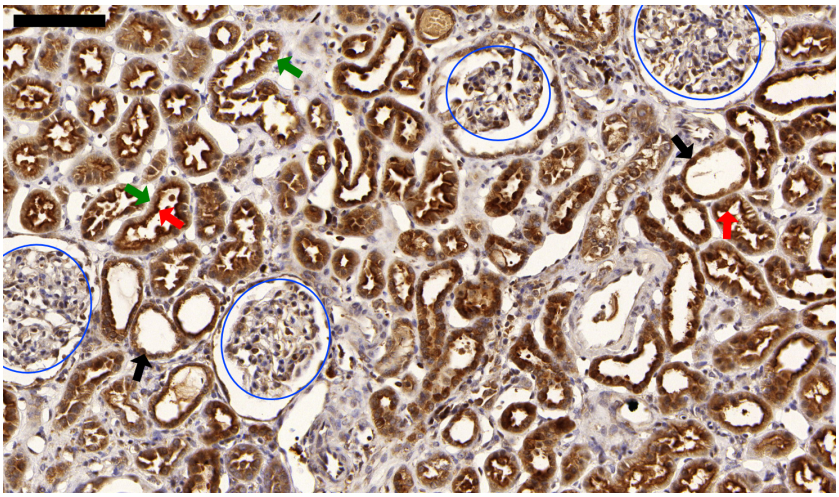

Figure 8.10: THTR-1 immunostaining in a third normal human kidney cortex. There was relatively weak staining in the glomeruli (blue circles) but heavy staining in the proximal tubules. There was some polarisation evident in the PTECs but the difference between staining intensity at the apical membranes (red arrows) and basal membranes (green arrows) was not as clear as for the THTR-2 staining. The distal tubules have stained for THTR-1 in most cases (black arrows). The possibility of non-specific staining must be considered for this image as the mean intensity is high. Scale bar represents 100 µm.

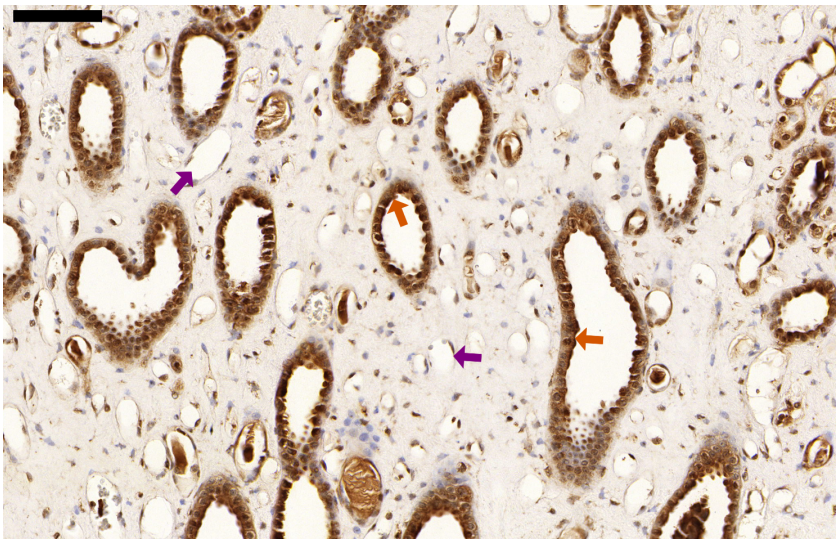

Figure 8.11: THTR-1 immunostaining in a normal human kidney inner medullary region. The loops of Henle (purple arrows) have not stained but the collecting ducts (orange arrows) have stained for THTR-1. The staining in the collecting duct epithelia does not appear to be polarised. Scale bar represents 100 µm.

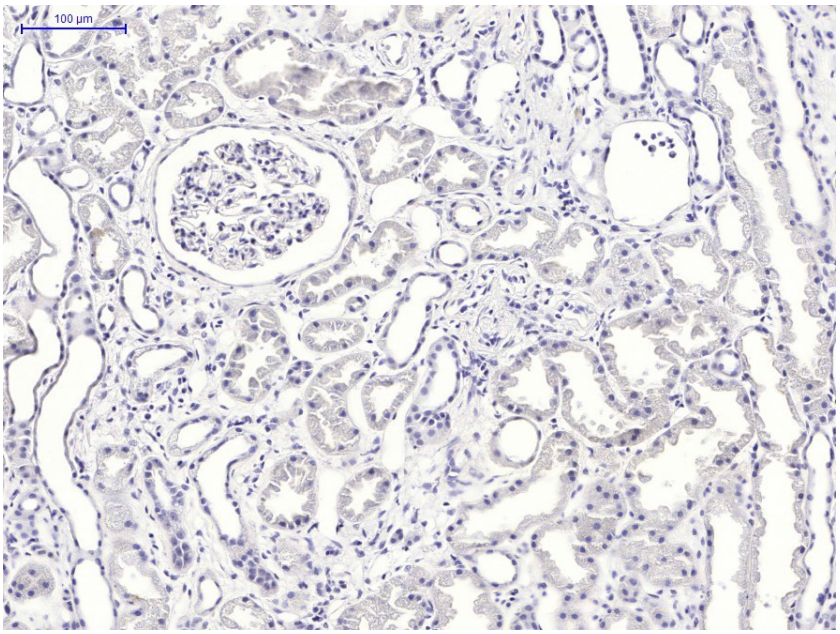

Figure 8.12: Kidney negative control slide. No immunostaining was observed in any region of any negative control slide.

8.2 Immunostaining of thiamine transporters in primary PTECs

In addition to observing the staining pattern of transporters within whole kidney sections, cultured cells were also stained. Human PTECs were grown in primary culture in four combinations of glucose and thiamine concentration to compare subcellular localisation of thiamine transporters as well as to gain a qualitative overview of expression in these conditions. HK-2 cells were also stained for THTR-1 and THTR-2 to compare morphology with the primary proximal tubule cell cultures.

The four conditions used for the primary cells were 5 mM glucose and 4 nM thiamine (−G−T), 5 mM glucose and 4 µM thiamine (−G+T), 26 mM glucose and 4 nM thiamine (+G−T) and 26 mM glucose and 4 µM thiamine (+G+T). After three days in each of these conditions, cells were seeded onto sterile glass slides and grown for two more days for a total of five days' culture in each condition. The HK-2 cells were grown only in −G−T conditions. Cells were fixed in formaldehyde before staining for THTR-1 and THTR-2.

The HK-2 cells stained for THTR-1 in a diffuse manner over the plasma membrane but with a heavier nuclear stain. The cells also show very heavy sub-nuclear staining areas, probably nucleoli (Figure 8.13). There was no staining for THTR-2 evident in HK-2 cells (Figure 8.14). Positive control normal kidney slides stained at the same time as the HK-2 cell slides stained as expected. This suggests that there is very little or no THTR-2 present in the HK-2 cells; a result corroborated by western blot and mRNA quantitation (Section 9.1.2 on page 159).

Human PTECs in primary culture stained for both THTR-1 and THTR-2. Figures 8.15, 8.16, 8.17 and 8.18 give examples of staining patterns for THTR-1 in −G−T, −G+T, +G−T and +G+T conditions respectively. Figures 8.19, 8.20, 8.21 and 8.22 are staining patterns under the same conditions for THTR-2. Four slides for each antigen in each condition were stained with representative slides shown here. The differences between these images are not bold enough for strong conclusions to be drawn in a qualitative manner. It could be argued that there is more nuclear stain relative to cytoplasmic stain in the cells cultured in the low glucose conditions. Since the intensity of stain is not directly proportional to amount of protein, such assertions are likely insecure from these images. The images indicate no large difference in immunostaining location in the four conditions. Notably, though, whilst there is some sub-nuclear compartmentalization of the staining in the PTECs in primary culture, it is much diminished relative to the HK-2 cell images. Also,

there is THTR-2 staining in the PTECs in primary culture where as there is no THTR-2 staining in the HK-2 cells.

All the cells in culture exhibited increased numbers of densely staining nucleoli relative to cells in kidney sections. Nucleoli are sub-regions of the nucleus where ribosomes are manufactured [Raška et al., 2006]. They fragment into 10 sections before mitosis, disappear during DNA replication and then reform after cell division around 10 nuclear organising regions—where clusters of rRNA genes are located—before rapidly coalescing into a single entity. There are two factors which explain the increase in nucleoli in cultured cells: (i) 2 µm sections cut tangentially though tissues with 10 µm diameter nuclei are likely to miss small nucleoli whereas cells in culture are present in their entirety on the slide and, (ii) cells in culture are dividing more rapidly than cells in a whole tissue which means increased rates of protein synthesis and increased demand for ribosome synthesis leading to larger nucleoli. The nucleoli stain more heavily than the surrounding nucleus with the basophilic haematoxylin stain. The significance of the heavy nucleolar staining with the brown DAB chromophore is unclear.

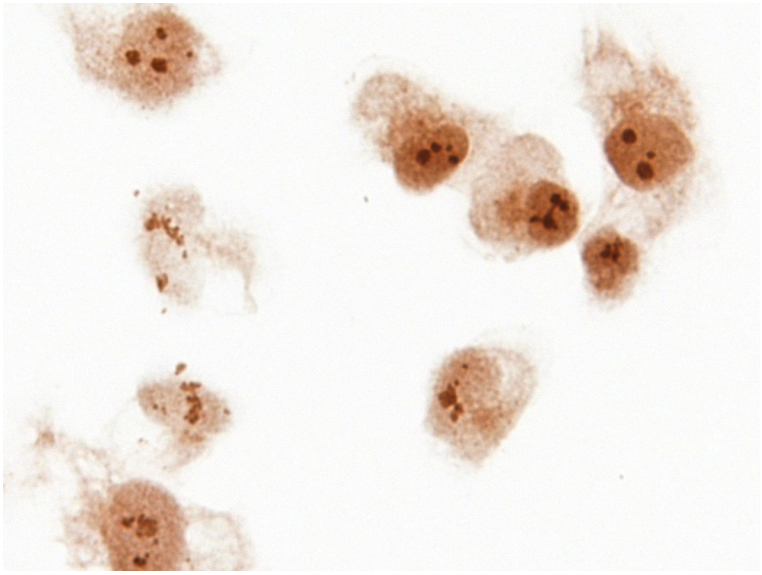

Figure 8.13: THTR-1 immunostaining in HK-2 cells. There is some plasma membrane staining but the majority of staining is nuclear and there are specific dark patches within the nuclei. Magnification 630x.

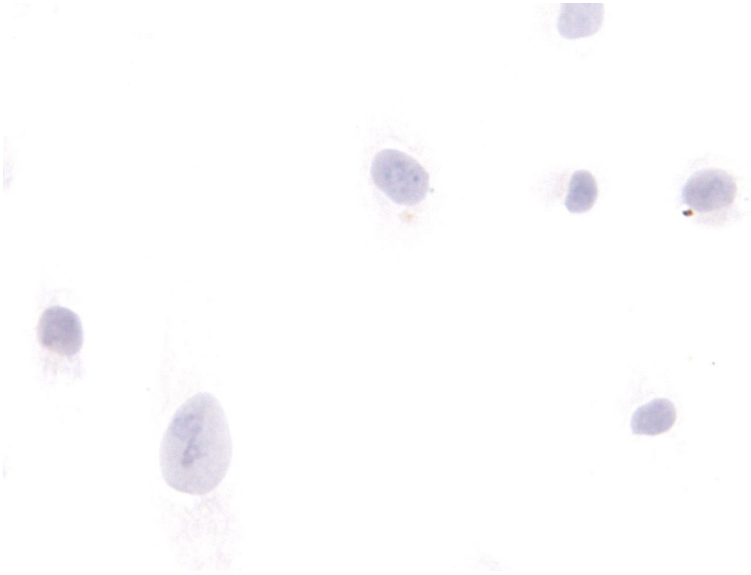

Figure 8.14: THTR-2 immunostaining in HK-2 cells. No staining was evident in any HK-2 cell slide stained for THTR-2. Magnification 630x.

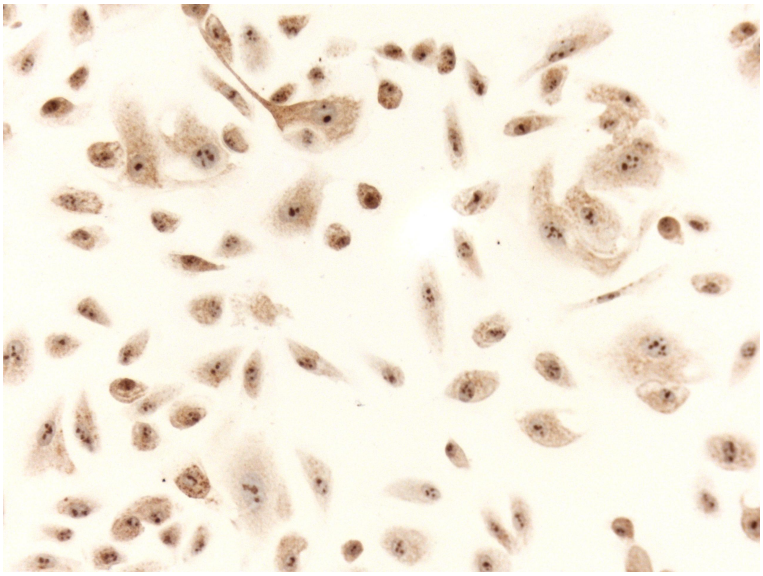

Figure 8.15: THTR-1 immunostaining in human PTECs in primary culture in 5 mM glucose and 4 nM thiamine conditions (−G−T). Magnification 200x.

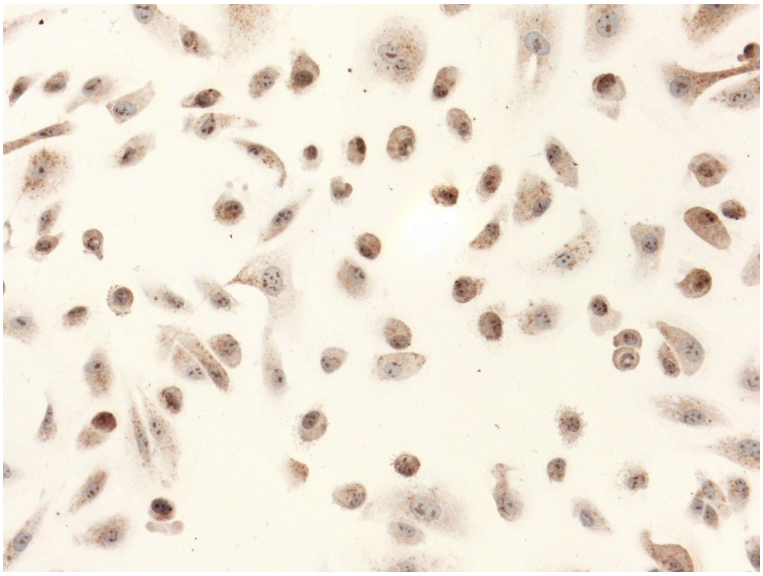

Figure 8.16: THTR-1 immunostaining in human PTECs in primary culture in 5 mM glucose and 4 µM thiamine conditions (−G+T). Magnification 200x.

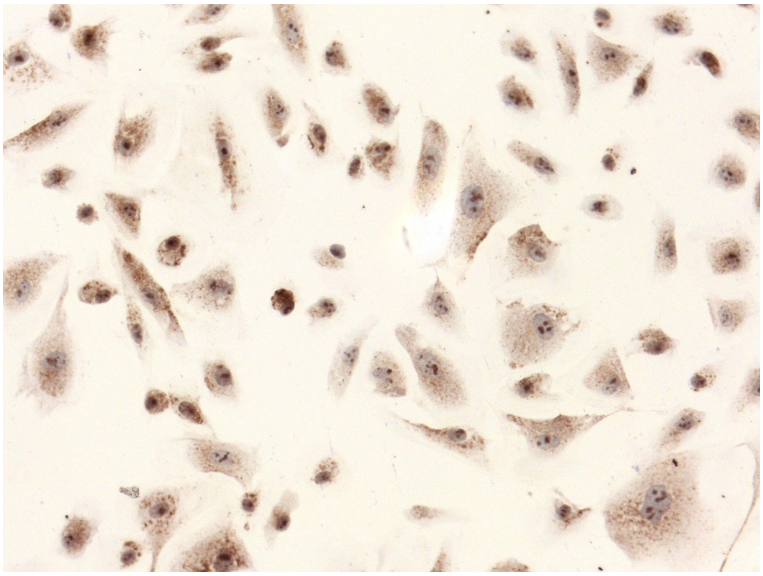

Figure 8.17: THTR-1 immunostaining in human PTECs in primary culture in 26 mM glucose and 4 nM thiamine conditions (+G−T). Magnification 200x.

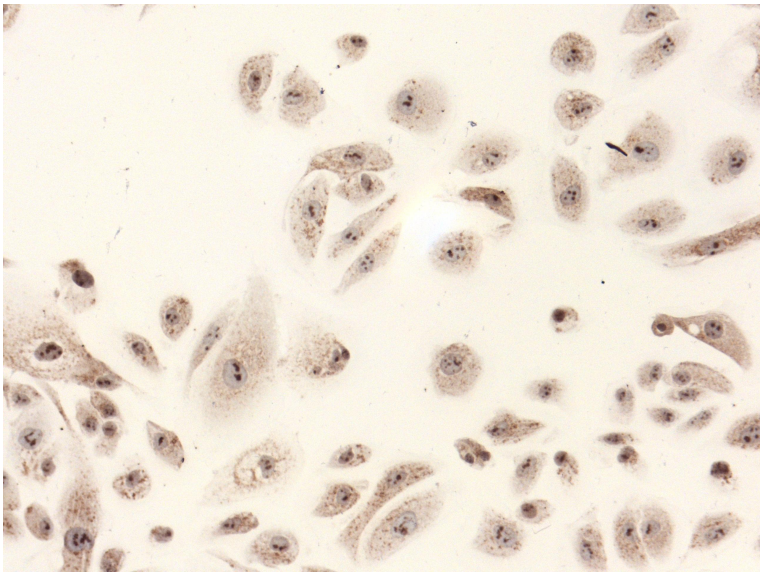

Figure 8.18: THTR-1 immunostaining in human PTECs in primary culture in 26 mM glucose and 4 µM thiamine conditions (+G+T). Magnification 200x.

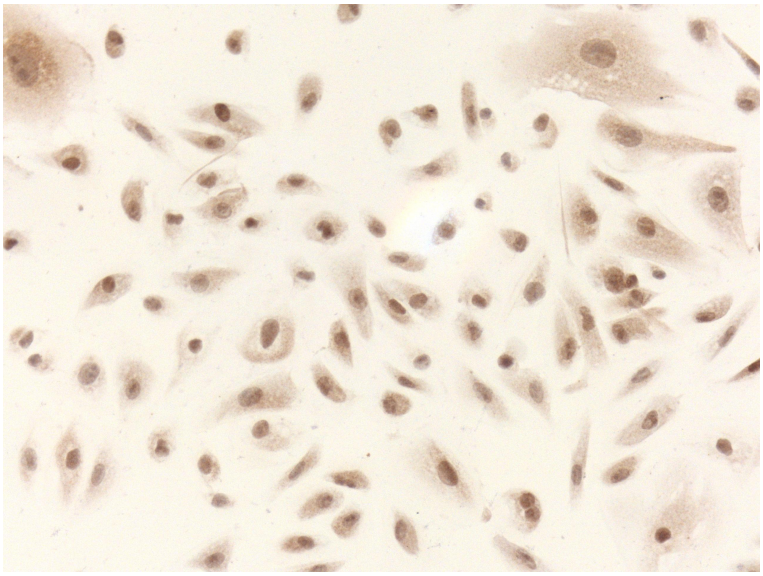

Figure 8.19: THTR-2 immunostaining in human PTECs in primary culture in 5 mM glucose and 4 nM thiamine conditions (−G−T). Magnification 200x.

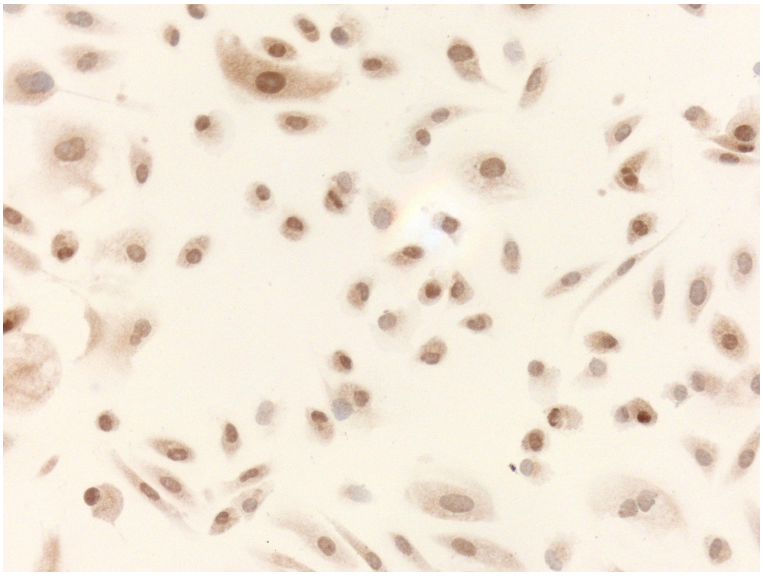

Figure 8.20: THTR-2 immunostaining in human PTECs in primary culture in 5 mM glucose and 4 µM thiamine conditions (−G+T). Magnification 200x.

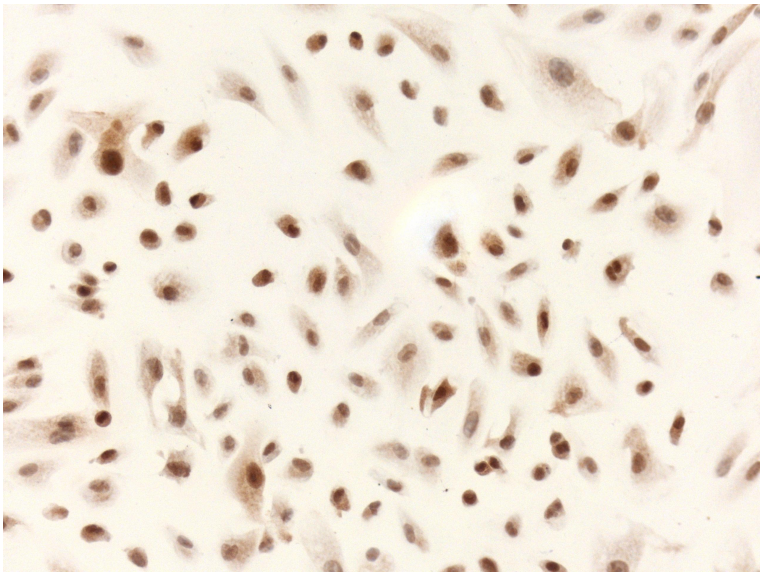

Figure 8.21: THTR-2 immunostaining in human PTECs in primary culture in 26 mM glucose and 4 nM thiamine conditions (+G−T). Magnification 200x.

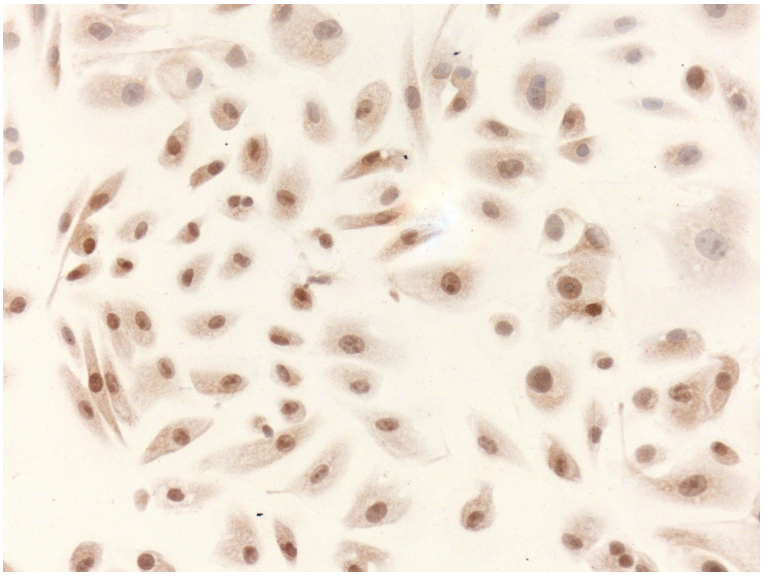

Figure 8.22: THTR-2 immunostaining in human PTECs in primary culture in 26 mM glucose and 4 µM thiamine conditions (+G+T). Magnification 200x.

Chapter 9

mRNA and thiamine transporter protein abundance in PTECs *in vitro*

9.1 mRNA quantitation

Primary PTECs and immortalised HK-2 cells were cultured for five days in four different conditions: −G−T, −G+T, +G−T and +G+T. Cells were harvested, RNA was isolated and mRNA was quantified by real-time qPCR. In each case, gene expression was normalised to β-actin as a control using the Pfaffl method of quantitation [Pfaffl, 2001]. All ratios relative to β-actin were then normalised to the −G−T control condition.

9.1.1 Primary PTEC mRNA quantitation *in vitro*

Figure 9.1 gives the relative gene mRNA abundance in the four conditions for the thiamine transporters, THTR-1 and THTR-2, and the reduced folate carrier, RFC-1. For THTR-1, there was a slight and significant decrease in expression level when the low glucose condition was supplemented with excess thiamine (-19%; $p < 0.01$) which may be attributed to down-regulation of the transporter in an abundant environment. THTR-1 and THTR-2 expression were both significantly decreased in the high glucose conditions with respect to the low glucose conditions (THTR-1: -70 to -80%; $p < 0.001$. THTR-2: -48 to -54%; $p < 0.001$). For both THTR-1 and THTR-2, additional thiamine did nothing to reverse

the decrease in expression in the high glucose conditions. RFC-1 expression was decreased in all conditions with respect to −G−T: −G+T, −24%; +G−T, −39%; +G+T, −32% ($p < 0.001$). RFC-1 expression was also decreased 19% in +G−T with respect to −G+T ($p < 0.01$). No other significant changes were observed.

The lower mRNA abundance of the transporters, particularly THTR-1 and THTR-2, in the hyperglycaemic conditions supports the hypothesis that hyperglycaemia is causing a decrease in thiamine re-absorption in the kidney. The fact that high thiamine supplementation does nothing to ameliorate the decline is discussed in further detail in Section 14.4.

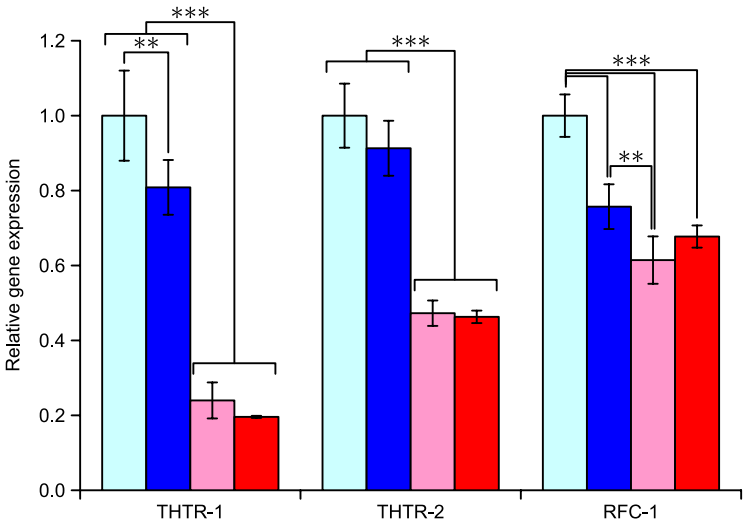

Figure 9.1: Thiamine transporter gene expression in primary PTECs *in vitro*. □−G−T; ■−G+T; □+G−T; ■+G+T. $** = p < 0.01$; $*** = p < 0.001$. $n = 5$ for all samples.

Gene expression of components of the hexosamine pathway-based hypothesis of reduction in renal thiamine reabsorption were also studied (Figure 9.2). The expression of *O*-linked *N*-acetylglucosamine (*O*-GlcNAc) transferase (OGT) was decreased 19% in −G+T with respect to −G−T ($p < 0.05$). Decreases in OGT expression of 55–64% were observed in both high glucose conditions with respect to both low glucose conditions ($p < 0.001$). *O*-GlcNAcase expression was significantly increased in +G+T with respect to −G−T (+52%; $p < 0.05$). Glutamine fructose-6-phosphate amidotransferase (GFAT-1) expression was slightly decreased in −G+T with respect to −G−T (−24%; $p < 0.05$). GFAT-1 was more markedly decreased by 90–93% in the high glucose conditions with respect to the low glucose conditions ($p < 0.001$). Sp1 also showed a marked decrease in expression in the

high glucose conditions with respect to the low glucose conditions—decreased by 71–77% ($p < 0.001$). Transketolase (TKT) expression was markedly decreased in all conditions with respect to −G−T: −G+T, −38%; +G−T, −62%; +G+T, −59% ($p < 0.001$). There was a significant decrease in TKT expression in +G−T (−39%) and +G+T (−34%) with respect to −G+T ($p < 0.001$).

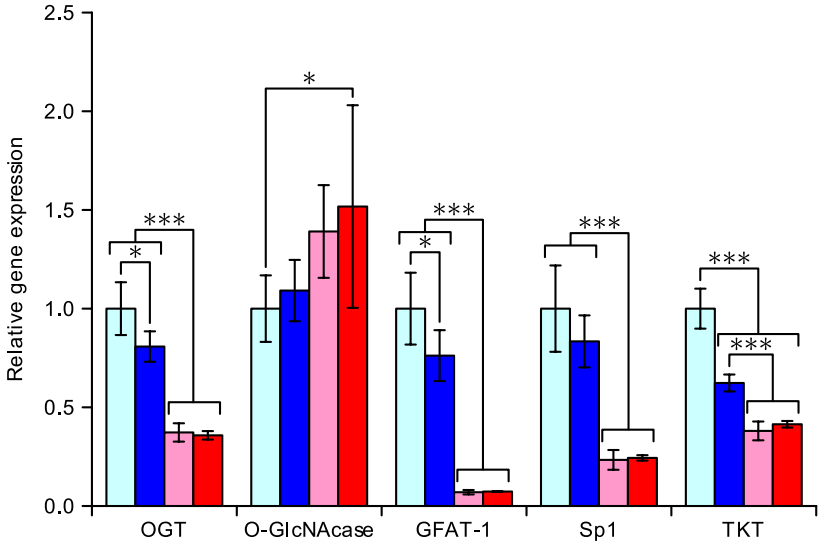

Figure 9.2: Hexosamine pathway-related gene expression in primary PTECs *in vitro*. □−G−T; ■−G+T; □+G−T; ■+G+T. $* = p < 0.05$; $*** = p < 0.001$. $n = 5$ for all samples.

Gene expression was also studied in genes that had previously been found to be responsive to hyperglycaemia (Figure 9.3). There was no significant difference between collagen expression in the hyperglycaemic conditions and −G−T. Expression of collagen IV was increased in the hyperglycaemic conditions with respect to −G+T (+G−T, +28%; +G+T, +32%; both $p < 0.05$). Thioredoxin interacting protein (TXNIP) was profoundly up-regulated in the hyperglycaemic conditions relative to the normoglycaemic conditions—increased by 48–65 fold ($p < 0.001$); there was a slightly higher response in (+21%) in +G+T versus +G−T ($p < 0.05$).

9.1.2 HK-2 cell mRNA quantitation *in vitro*

HK-2 cells were cultured for five days in four conditions (−G−T, −G+T, +G−T and +G+T), as described above. Figure 9.4 gives relative gene expression for thiamine transporter genes in HK-2 cells cultured in the four conditions. In contrast to the primary PTECs,

there was a slight increase in relative expression of THTR-1 in the hyperglycaemic conditions relative to the normoglycaemic conditions (increased 19–29%; $p < 0.05$ for all, $p < 0.01$ for two comparisons and $p < 0.001$ for the increase from −G+T to +G−T). There were no significant differences in expression of THTR-2 between any of the conditions. RFC-1 expression was unaffected by changing conditions with the exception of an increase of 15% in +G−T with respect to −G+T ($p < 0.01$).

The results for THTR-1 expression are counter-intuitive, especially considering the decreased abundance of THTR-1 protein seen in the HK-2 cells in the same conditions (Section 9.2, page 164). The absence of change in THTR-2 expression is not unexpected given that there appears to be little or no THTR-2 present in HK-2 cells, as indicated by immunohistochemistry. The counter-intuitive nature of many of the HK-2 cell results is discussed in detail in Chapter 14.

Hexosamine pathway-related gene expression was also investigated in HK-2 cells (Figure 9.5). OGT expression was increased slightly in hyperglycaemic conditions with respect to normoglycaemic conditions (increased 22–28%; $p < 0.01$). oGlcNAcase expression levels were increased in +G+T with respect to both −G−T and −G+T (+15% and +16% respectively; $p < 0.05$). Expression of GFAT-1 was increased in hyperglycaemic conditions with respect to normoglycaemic conditions (increased 31–36%; $p < 0.01$, except −G−T to +G+T, $p < 0.05$). Neither Sp1 nor transketolase expression was changed in any condition.

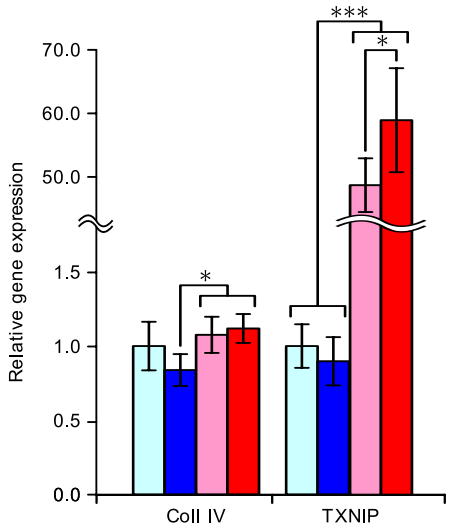

Figure 9.3: Hyperglycaemia-related gene expression in primary PTECs *in vitro*. □−G−T; ■−G+T; □+G−T; ■+G+T. $* = p < 0.05$; $*** = p < 0.001$. $n = 5$ for all samples.

These results are markedly different from those obtained in the primary PTECs. In the HK-2 cells, OGT expression is increased in hyperglycaemia; in the primary cells OGT expression is decreased in hyperglycaemia. The same is true for GFAT-1 expression: it is increased in hyperglycaemia in the HK-2 cells yet profoundly decreased in the primary PTECs under the same conditions. Sp1 and TKT are unaffected by hyperglycaemia in the HK-2 cells yet both are down-regulated under the same conditions in the primary PTECs. The only gene which has similar expression patterns in both HK-2 cells and primary PTECs is *O*-GlcNAcase. The significance of these differences is discussed in more detail when considering the different models of the diabetic kidney used in Chapter 14.

The expression of genes related to hyperglycaemia was also investigated (Figure 9.6). Expression of collagen IV was unchanged in any condition. TXNIP expression was increased in the hyperglycaemic conditions with respect to the normoglycaemic conditions (increased 59–71%, $p < 0.001$). The increase in TXNIP expression follows the same trend in HK-2 cells as in primary PTECs but the responses in the HK-2 cells are of much lower magnitude. The TXNIP expression in primary PTECs was increased 48–65 *fold* in hyperglycaemic conditions.

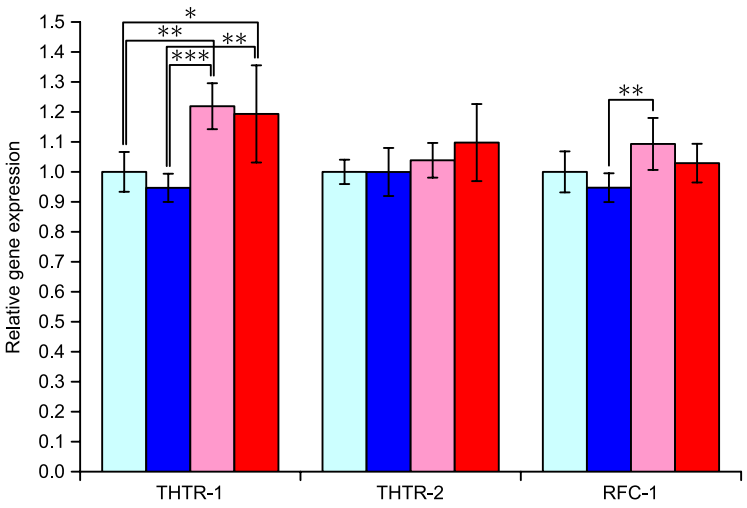

Figure 9.4: Thiamine transporter gene expression in HK-2 cells *in vitro*. □ −G−T; ■ −G+T; □ +G−T; ■ +G+T. $* = p < 0.05$; $** = p < 0.01$; $*** = p < 0.001$. $n = 4$ for all samples.

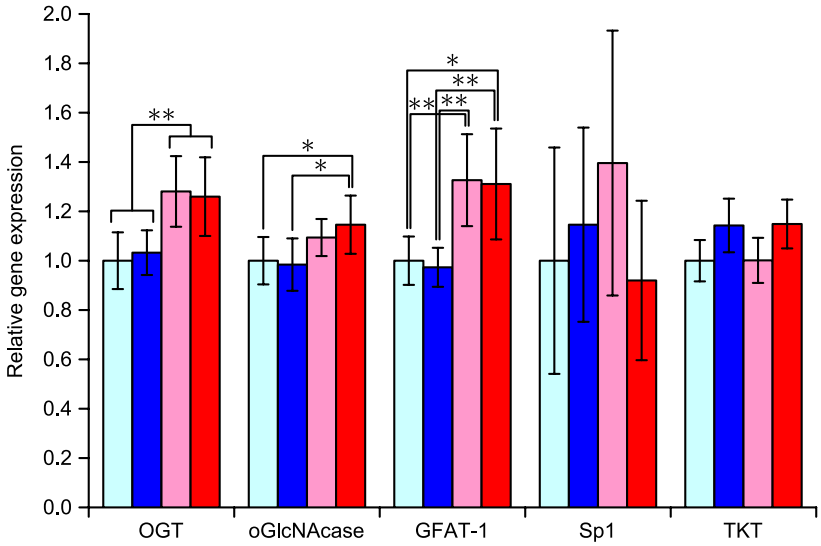

Figure 9.5: Hexosamine pathway-related gene expression in HK-2 cells *in vitro*. −G−T; −G+T; +G−T; +G+T. $* = p < 0.05$; $** = p < 0.01$. $n = 4$ for all samples.

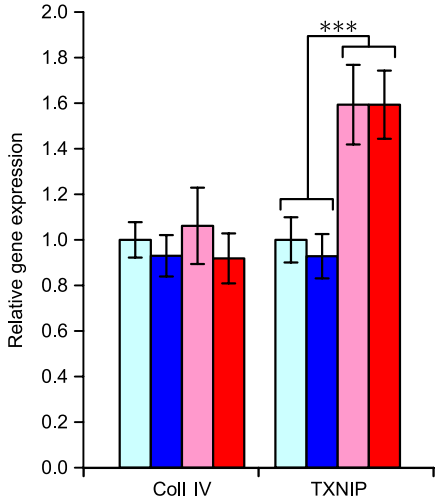

Figure 9.6: Hyperglycaemia-related gene expression in HK-2 cells *in vitro*. −G−T; −G+T; +G−T; +G+T. $*** = p < 0.001$. $n = 4$ for all samples.

9.1.3 Comparison of gene expression in HK-2 cells and human kidney cortex

Total RNA was extracted from frozen human kidney cortex which had been stored at −80°C to prevent degradation. Cortex RNA was compared to that from HK-2 cells grown in 5 mM glucose and 4 nM thiamine (−G−T) by qPCR. The abundance of mRNA relative to β-actin was determined for eight genes and the ratio of the abundance of mRNA in the kidney to the abundance of mRNA in the cells was derived. This yields data on the normalised relative abundance of each mRNA species in kidney and HK-2 cells (Figure 9.7).

As HK-2 cells are derived from a normal human kidney, the ratios are expected to be close to unity. This is the case for the majority of genes studied with ratios from 0.73 for GFAT-1 to 3.5 for Sp1. The ratio of abundance for THTR-2 is an exception; it is 120 times relatively more abundant in kidney extract than in HK-2 cells. This is further evidence for how far removed the HK-2 cell line has become from its source tissue and is discussed in more detail in Chapter 14.

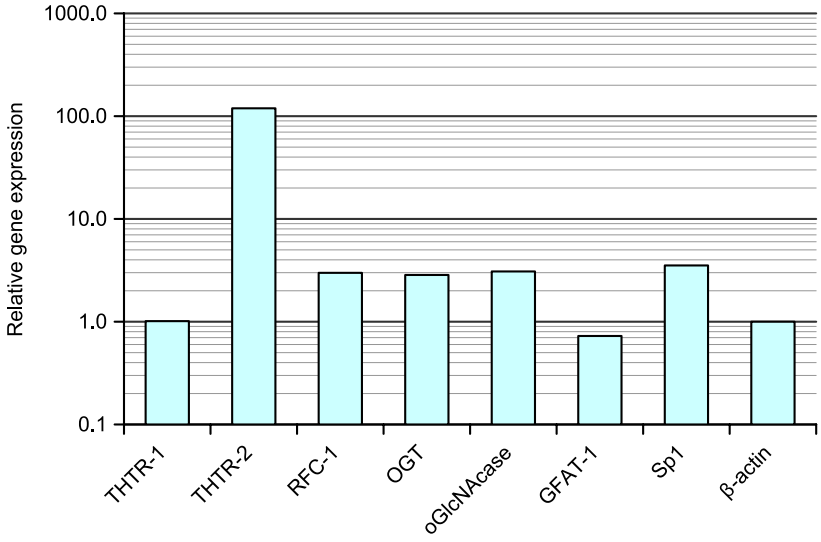

Figure 9.7: Gene expression in HK-2 cells *in vitro* compared to human kidney cortex. Note the logarithmic y-axis. $n = 1$, only one human kidney was tested.

9.2 Thiamine transporter protein abundance

The abundance of THTR-1 protein was assayed by western blot. Cell membrane extracts were prepared from both primary PTECs and HK-2 cells in order to relatively enrich membrane proteins above cytosolic proteins. The membranes were heat-denatured under reducing conditions before being separated using SDS-PAGE, transferred to a PVDF membrane and blotted using appropriate antibodies followed by ECL-based detection. In all cases, membranes were stripped, re-blocked and re-probed for β-actin as a loading control. Results are expressed as an arbitrary ratio of the two observed band densities.

9.2.1 Primary PTEC THTR-1 protein abundance *in vitro*

Primary PTECs were cultured in −G−T and +G−T for five days before harvesting and analysis. These conditions were chosen to see the effect of elevated glucose at physiological thiamine concentrations. THTR-1 abundance was decreased 77% in +G−T with respect to −G−T ($p < 0.05$; Figure 9.8). Primary PTECs were also cultured in −G+T and +G+T for five days. THTR-1 abundance was not significantly different between the two conditions ($p > 0.05$; Figure 9.9).

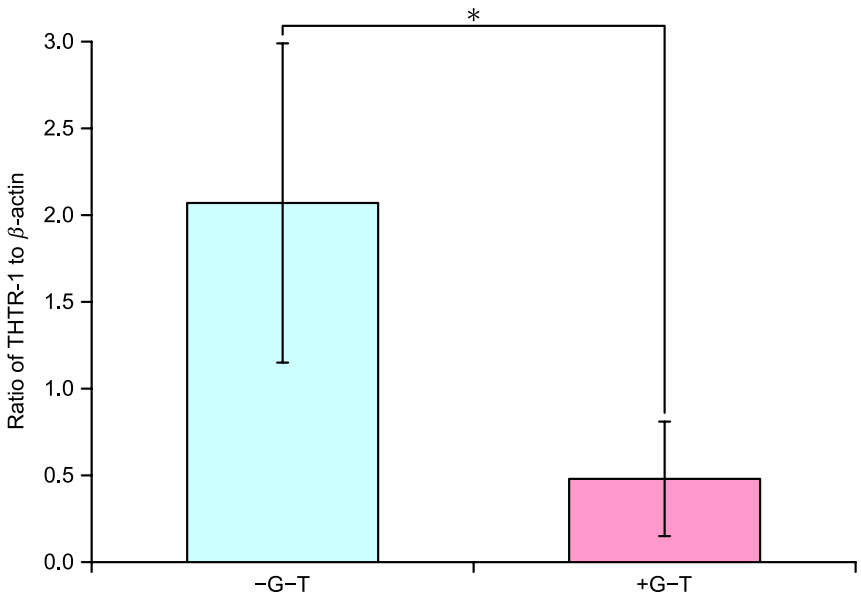

Figure 9.8: THTR-1 abundance in primary PTECs cultured in low thiamine conditions *in vitro* expressed as an arbitrary ratio of target intensity to β-actin intensity. □−G−T; □+G−T. $* = p < 0.05$. $n = 3$ for each condition.

9.2.2 HK-2 cell THTR-1 protein abundance *in vitro*

HK-2 cells were cultured in a similar manner to primary PTECs in both −G−T and +G−T conditions for five days before harvesting and analysis. THTR-1 abundance was decreased 52% in +G−T with respect to −G−T ($p < 0.05$; Figure 9.10).

HK-2 cells were also cultured in −G+T and +G+T for five days to determine if high thiamine effects a change in this response. THTR-1 abundance was decreased 53% in +G+T with respect to −G+T ($p < 0.05$; Figure 9.11). Example images of bands are given in Figure 9.12.

9.2.3 Discussion

The immunoblots obtained for the primary PTECs were not as easy to quantify as the HK-2 cell immunoblots. This is because there were multiple bands present at approximately 55 kDa, the molecular mass of THTR-1. The bands were difficult to resolve because they were not discrete (Figure 9.13).

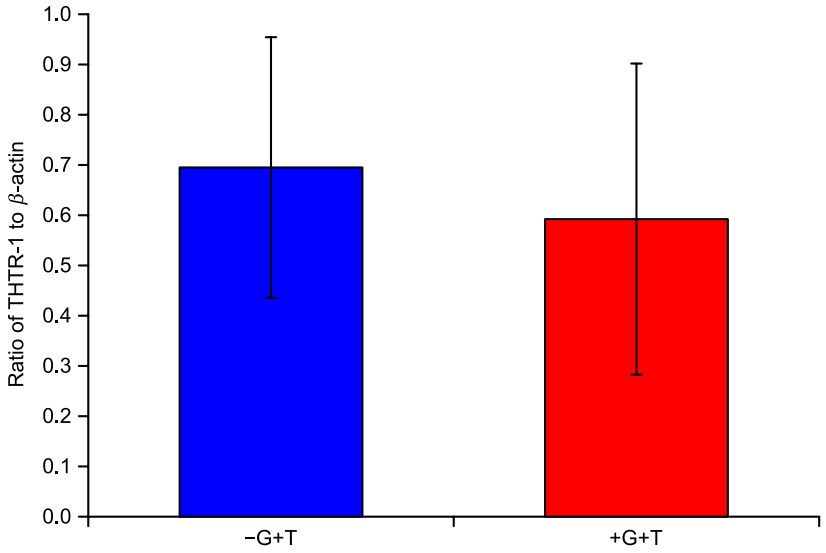

Figure 9.9: THTR-1 abundance in primary PTECs cultured in high thiamine conditions *in vitro* expressed as an arbitrary ratio of target intensity to β-actin intensity. ■ −G+T; ■ +G+T. $n = 3$ for each condition.

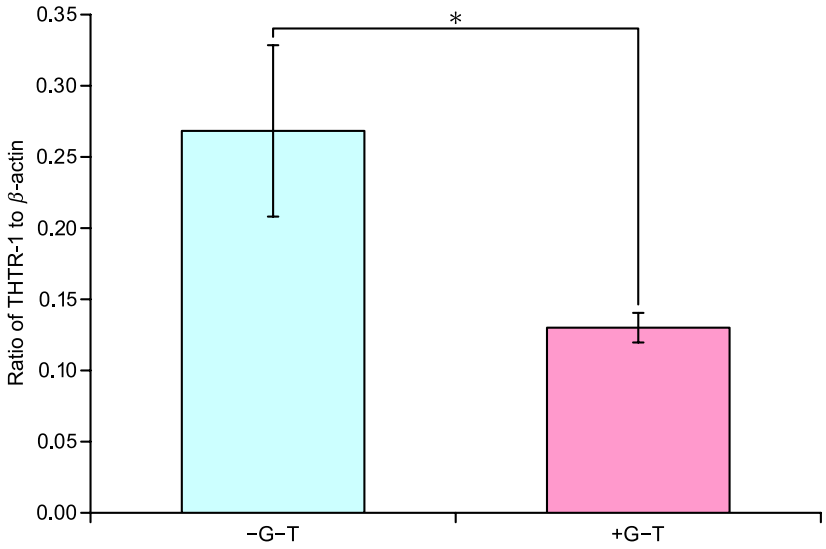

Figure 9.10: THTR-1 abundance in HK-2 cells cultured in low thiamine conditions *in vitro* expressed as an arbitrary ratio of target intensity to β-actin intensity. □ −G−T; ■ +G−T. $* = p < 0.05$. $n = 3$ for each condition.

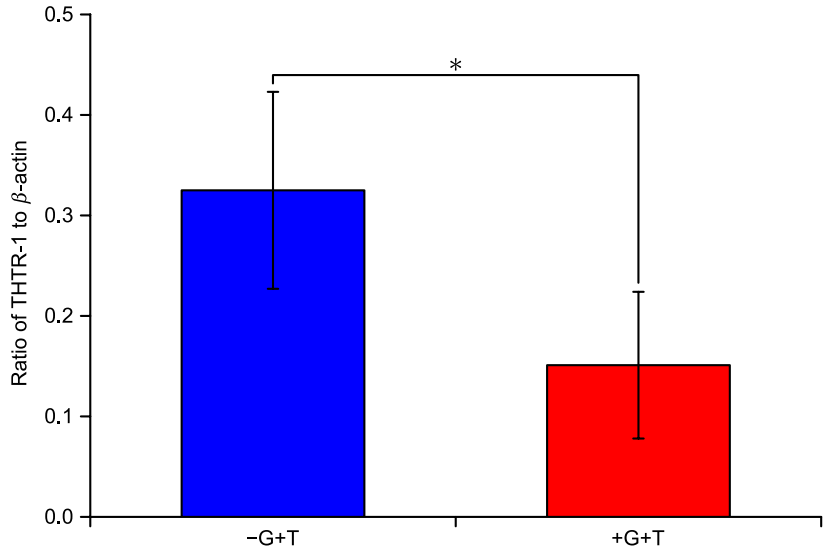

Figure 9.11: THTR-1 abundance in HK-2 cells cultured in high thiamine conditions *in vitro* expressed as an arbitrary ratio of target intensity to β-actin intensity. ■ −G+T; ■ +G+T. $* = p < 0.05$. $n = 4$ for each condition.

The following observations were made regarding these blots:

(i) Correct identification of the THTR-1 band This was problematic and was solved using a positive control prepared from the membranes of erythrocytes which are rich in THTR-1. The fact that erythrocyte membranes are rich in THTR-1 was demonstrated by fluorescent confocal microscopy imaging of kidney sections. When probed with an anti-THTR-1 antibody, the kidney epithelial cells have a relatively weak signal intensity but erythrocytes are clearly visible in the images (e.g. Figure 9.14). Figure 9.15 presents an example of a blot performed with HK-2 cell membrane extracts and an erythrocyte membrane extract. By comparing the apparent molecular mass of the true THTR-1 protein with the the primary PTEC extract blots, it can be seen that the middle band of the three in Figure 9.13 is at the correct molecular mass for THTR-1.

(ii) Antigen bands are not discrete An example densitometry analysis of lane 2 from Figure 9.13 is given in Figure 9.16 and illustrates the problem of non-discrete bands. The black line represents mean density of exposure of the film from the top to the bottom of the lane. The coloured lines represent several options as to how the peaks should be individually quantified with relevant background subtraction. The area bounded by the red drop lines and the grey baseline was quantified in line with common practice on HPLC systems. This analysis technique was used for all immunoblot densitometry analysis.

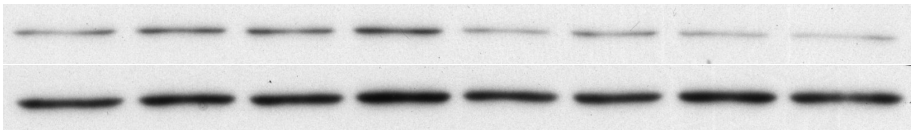

Figure 9.12: THTR-1 HK-2 cell immunoblot specimen bands. These two sets of bands represent THTR-1 (upper bands) and β-actin (lower bands) which were quantified and presented in Figure 9.11. In each blot, lanes 1–4 (the left-most bands) represent samples from −G−T and lanes 5–8 (the right-most bands) represent samples from +G−T.

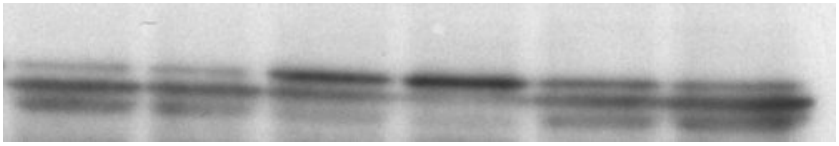

Figure 9.13: THTR-1 primary PTEC immunoblot specimen bands typical of those obtained for primary PTEC THTR-1 immunoblot analyses. In this particular sample image, lanes 1 and 2 are samples from −G+T, lanes 3 and 4 are samples from +G−T and lanes 5 and 6 are samples from −G−T.

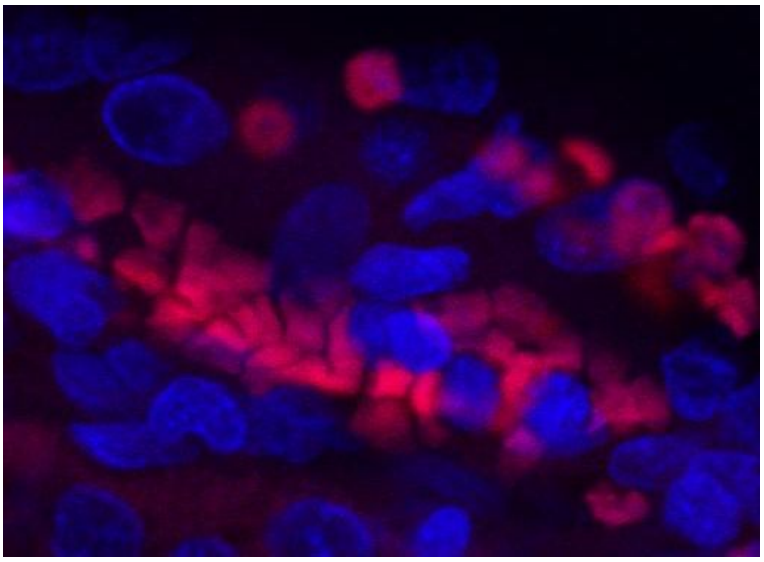

Figure 9.14: Confocal fluorescence microscopy of THTR-1 immunostaining in a kidney section. Cell nuclei are stained blue with DAPI. THTR-1 is stained red. Note the strong staining in the erythrocytes. These are more clearly differentiated at the top of this image.

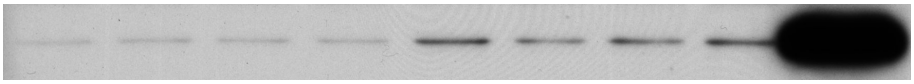

Figure 9.15: THTR-1 immunoblot positive control. Lanes 1–8 contain HK-2 cell membrane extracts (lanes 1–4 from +G−T and lanes 5–8 from −G−T) and lane 9 contains an equal amount of protein extracted from erythrocyte membranes.

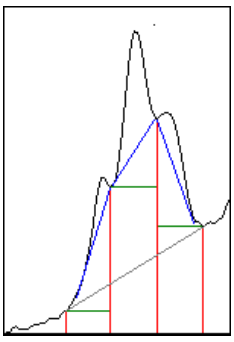

Figure 9.16: Densitometry analysis of lane 2 from the THTR-1 immunoblot shown in Figure 9.13.

(iii) Each of the three bands may represent isoforms of THTR-1 (splice variants or post-translationally modified forms) If this is the case, the interpretation offered here could be inaccurate as this thesis makes the assumption that the middle band alone represents THTR-1. This possibility could only be explored through sequencing or tryptic digest analysis of the bands—an avenue of research not further explored here.

These factors combined may contribute to the differences between THTR-1 abundance in HK-2 cell primary PTEC membrane extracts. In the HK-2 cells extracts, THTR-1 abundance was decreased in both hyperglycaemic conditions, irrespective of thiamine concentration. In high glucose primary PTEC extracts, THTR-1 abundance did not decrease in the high thiamine condition but did decrease in the low thiamine condition with respect to the 5 mM conditions. The immunoblot images for the primary PTECs exhibited a poor signal-to-noise ratio leading to higher uncertainties in the results. This may explain why a significant difference was not observed in +G+T with respect to −G+T in primary PTECs.

In addition to problems identifying and resolving bands, it is not possible to compare multiple western blots with each other. Western blot results from a single gel are expressed as an arbitrary ratio of one intensity to another. This approach is useful for intra-gel comparisons but not for inter-gel comparisons where slight differences between gels (e.g. efficiency of antibody binding, temperature or exposure duration) will vary the ratio obtained considerably. This is especially so for strongly binding antibodies—such as those used against β-actin—which yield high signal intensities. These antibodies need short exposures and slight variations in exposure duration give widely varying intensities and ratios. The inability to combine gel images means that large numbers of samples cannot be quantified in a relative manner. Two sizes of gel are commonly available for western blotting: mini-gels (up to 10 samples) and large gels (up to 20 samples). Mini-gel blots can only compare a maximum of 2 samples at $n = 4$ each. Large gels could be used for a maximum of 4 samples at $n = 4$ (allowing lanes for ladders) but larger gels give poorer immunoblot results with higher errors. This is because the larger surface area requires a more antibody solution which does not distribute as evenly over the membrane. High quality, strongly binding antibodies (e.g. those available against β-actin) counter this problem but for other proteins, such as THTR-1, antibodies were of insufficient quality to allow proper comparison.

Both the primary PTEC and the HK-2 cell THTR-1 abundance data, with the exception of the high error primary PTEC blots in high thiamine conditions, support the hypothesis that hyperglycaemia is decreasing the abundance of THTR-1. This is supported by mRNA evidence in primary PTECs but not in HK-2 cells.

Chapter 10

The hexosamine pathway, glycosylation and Sp1 in PTECs *in vitro*

10.1 Hexosamine pathway metabolite concentration

10.1.1 Primary PTEC hexosamine pathway metabolite concentration *in vitro*

Human PTECs grown in primary culture in the four conditions −G−T, −G+T, +G−T and +G+T for five days were prepared for assay of the hexosamine pathway products UDP-*N*-acetylglucosamine (UDP-GlcNAc) and UDP-glucose by HPLC. Results are expressed as nmol metabolite per mg protein (quantified by Bradford assay) and are presented in Figure 10.1. The amount of UDP-GlcNAc decreased slightly in +G−T with respect to the low glucose conditions (−G−T, −22%; −G+T −23%; both $p < 0.01$). The amount of UDP-GlcNAc increased 28% in +G+T with respect to +G−T ($p < 0.01$). The amount of UDP-glucose increased in +G+T with respect to both −G+T (+16%; $p < 0.05$) and +G−T (+26%; $p < 0.001$). No other changes were significant.

10.1.2 HK-2 cell hexosamine pathway metabolite concentration *in vitro*

There were no significant differences between any conditions in HK-2 cells (Figure 10.2). The amount of each analyte was higher in HK-2 cells with respect to primary PTECs (UDP-Glc, >2-fold higher; UDP-GlcNAc, ∼4-fold higher).

10.1.3 Hexosamine pathway metabolite assay controls

As a positive control for the assay, HK-2 cells were cultured with glucosamine hydrochloride to bypass the initial step in the hexosamine biosynthesis pathway. The GFAT-catalysed reaction forming glucosamine-6-phosphate from glutamine and fructose-6-phosphate has most control over flux through the pathway [Virkamäki et al., 1997]. A typical pharmacological dose for glucosamine is 1500 mg day^{-1} which if dissolved in a typical human's 4.7 L of blood gives a concentration of about 1.8 mM. Glucosamine (5 mM) was added for positive control and produced an increase in UDP-GlcNAC of >44-fold relative to control ($p < 0.001$; Figure 10.3).

The effect of glutamine was also investigated. Four cell incubation conditions were studied: low and high glucose concentration (5 and 26 mM, −/+G) and with or without

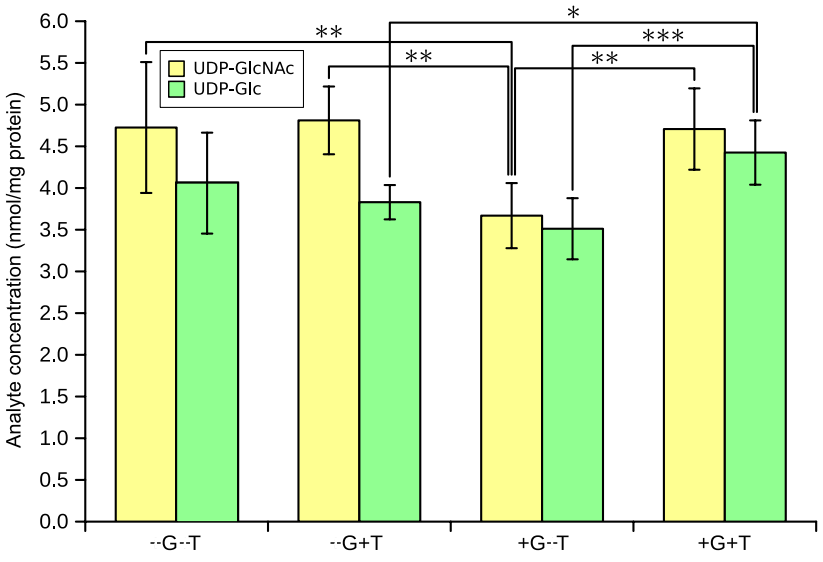

Figure 10.1: Hexosamine pathway metabolite abundance in primary PTECs *in vitro*. UDP-glucose; UDP-*N*-acetylglucosamine. $* = p < 0.05$; $** = p < 0.01$; $*** = p < 0.001$. $n = 8$ for each condition.

2 mM glutamine supplementation (+/−Q). Each condition contained 4 nM thiamine. The amounts of UDP-GlcNAc are given in Figure 10.4. The amount of UDP-GlcNAc was not altered by glutamine supplementation in HK-2 cells. The amount of UDP-GlcNAc was decreased by 12–16% in hyperglycaemic conditions with respect to normoglycaemic conditions ($p < 0.05$).

10.1.4 Discussion

The hexosamine biosynthesis pathway (HBP) has two starting metabolites: glucose and glutamine (Figure 1.8). The study with glutamine supplementation has shown that the cells are limited by neither glutamine nor glucose. The study bypassing GFAT activity using glucosamine has demonstrated that the remainder of the HBP is unregulated and that increased amounts of UDP-GlcNAc result if GFAT is bypassed. Therefore, the abundance of metabolites from the HBP is limited solely by the activity of the highly regulated GFAT.

The prevailing evidence in the literature suggests that there is an increased flux through the hexosamine pathway in hyperglycaemic conditions accompanied by an increase in production of UDP-GlcNAc (Section 3.4). This has not been translated in these experiments into increased absolute concentrations of UDP-GlcNAc in either the primary PTECs or the HK-2 cells. The positive controls for the assay show that the cells are not constrained

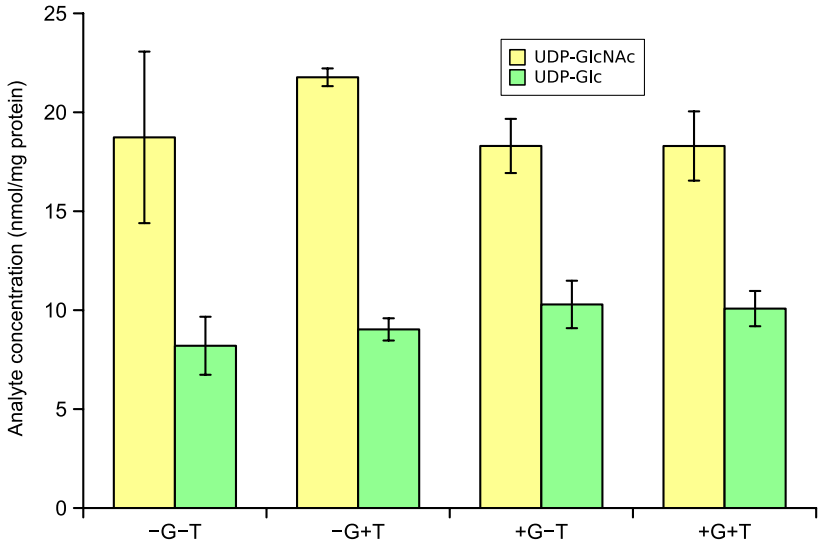

Figure 10.2: Hexosamine pathway metabolite abundance in HK-2 cells *in vitro*. ■UDP-glucose; ■UDP-*N*-acetylglucosamine. $n = 4$ for each condition.

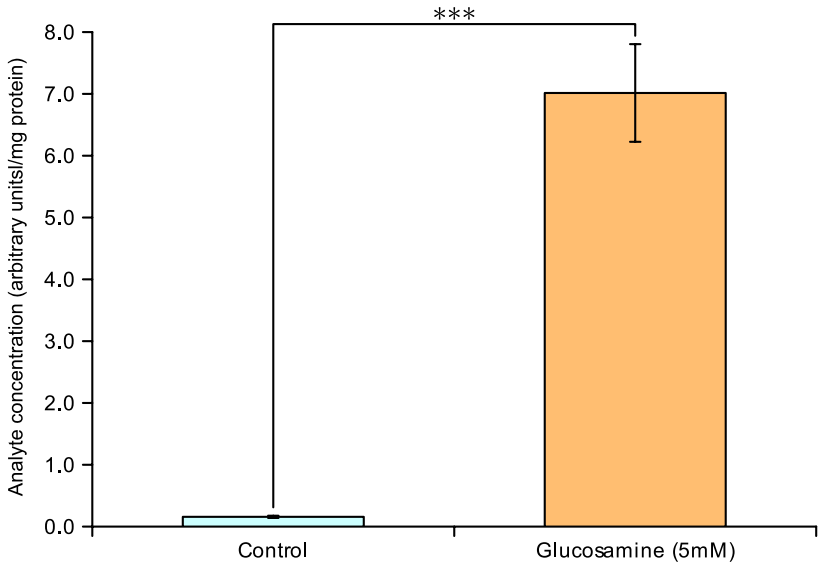

Figure 10.3: UDP-GlcNAc abundance in HK-2 cells supplemented with 5 mM glucosamine *in vitro*. $*** = p < 0.001$. $n = 4$ for each condition.

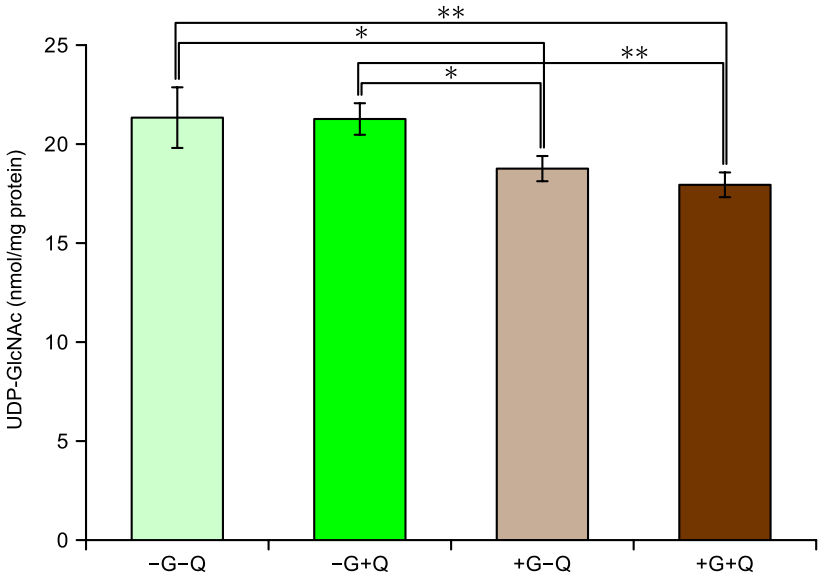

Figure 10.4: UDP-GlcNAc abundance in HK-2 cells supplemented with 2 mM glutamine in low and high glucose concentrations *in vitro*. −G−Q; −G+Q; +G−Q; +G+Q $* = p < 0.05$; $** = p < 0.01$. $n = 4$ for each condition.

by artificial limits such as lack of glutamine and that the assay is capable of detecting changes in analyte concentration if they were present. Thus if the theory regarding increased glycosylation is to stand to scrutiny then there must be increased activity of OGT, the enzyme performing *O*-GlcNAcylation of proteins using UDP-GlcNAc as a substrate. This could account for an unchanged or even decreased concentration of UDP-GlcNAc as seen in the primary PTECs. The mRNA evidence shows that OGT is down-regulated in hyperglycaemic conditions in the primary PTECs. OGT protein abundance and activity have not been investigated. It is possible that the gene has been down-regulated in response to the excess of glycosylation in the cell in a negative feedback mechanism. Another plausible scenario involves the corepressor mSin3A. mSin3A has been shown by Yao et al. [2007] to exhibit a two-fold increase in modification by methylglyoxal in hyperglycaemia in mouse kidney endothelial cells. The increase in glycation was shown to increase the binding of mSin3A to OGT, increasing the activity of OGT. A similar scheme could be conceived in our model system whereby the increased binding of glycated mSin3A to OGT could lead to an increase in the activity of OGT despite a down-regulation of its gene. It may be that binding of the corepressor to the OGT leads to an increased protein stability and decreased degradation.

The differences between the HK-2 cell model and the primary PTEC model are again highlighted by the differing relative amounts of each analyte. The amount of UDP-GlcNAc in the HK-2 cells is ∼4-fold higher than that found in the primary cells and the concentration of UDP-Glc is between 1.5–3-fold higher in the HK-2 cells. This is both unexpected and difficult to rationalise given the identical culture and analysis conditions. The result could be considered further evidence of the HK-2 cell line drifting genetically further from its source material.

10.2 Sp1 and glycosylation

10.2.1 HK-2 cell Sp1 abundance and glycosylation *in vitro*

The glycosylation status of Sp1 was investigated by western blotting. HK-2 cells were cultured in −G−T and +G−T media for five days prior to harvesting. On the day of harvesting, nuclear extracts were prepared to concentrate Sp1 relative to other proteins. The nuclear extracts were prepared for western blotting and blotted with a primary antibody against *O*-GlcNAc. The membranes were stripped and re-probed for Sp1. The ratio of density of *O*-GlcNAc to Sp1 is shown in Figure 10.5. The ratio of *O*-GlcNAc to Sp1 density

increased 63% in +G−T with respect to −G−T ($p < 0.01$).

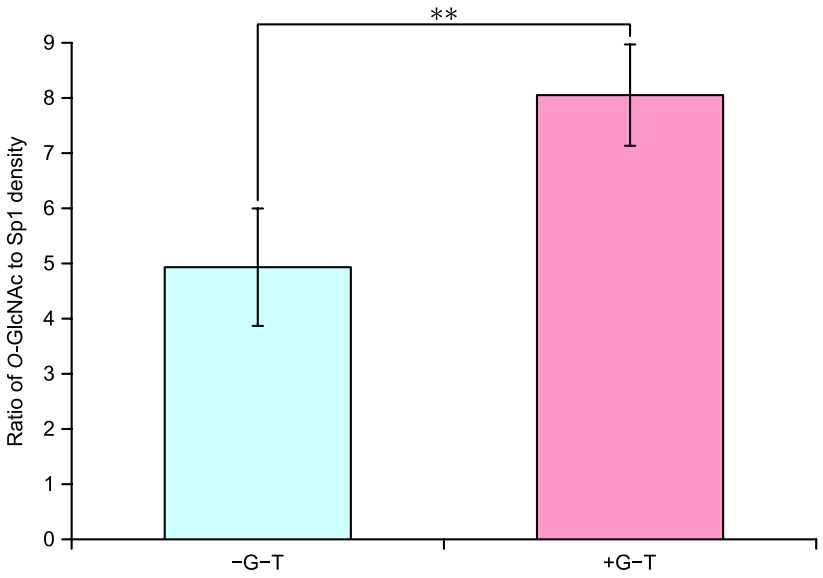

Figure 10.5: Glycosylation status of Sp1 in HK-2 cell nuclear extracts *in vitro* presented as the ratio of *O*-GlcNAc to Sp1 band density after five days of culture. □−G−T; □+G−T. ** = $p < 0.01$;. $n = 4$ for each condition.

To determine if absolute amounts of Sp1 were affected by hyperglycaemic culture, a second blot was performed with the same samples. This blot compared the ratio of Sp1 to lamin A, a nuclear loading control (Figure 10.6). Relative amounts of Sp1 did not change in HK-2 cells cultured in +G−T relative to −G−T ($p > 0.05$).

10.2.2 HK-2 cell *O*-GlcNAc transferase abundance *in vitro*

HK-2 cells cultured in −G−T and +G−T conditions for five days were lysed and a total protein extract prepared. Samples were analysed by western blotting to determine the amount of OGT relative to the loading control β-actin (Figure 10.7). OGT relative abundance in +G−T was 43% decreased with respect to −G−T ($p < 0.01$).

To test the effect of thiamine supplementation on the abundance of OGT in hyperglycaemic culture, HK-2 cell extracts were prepared after five days of culture in +G−T and +G+T. Samples were analysed by western blotting to determine the amount of OGT relative to the loading control β-actin (Figure 10.8). There was no difference between relative OGT abundance in either of the two hyperglycaemic conditions.

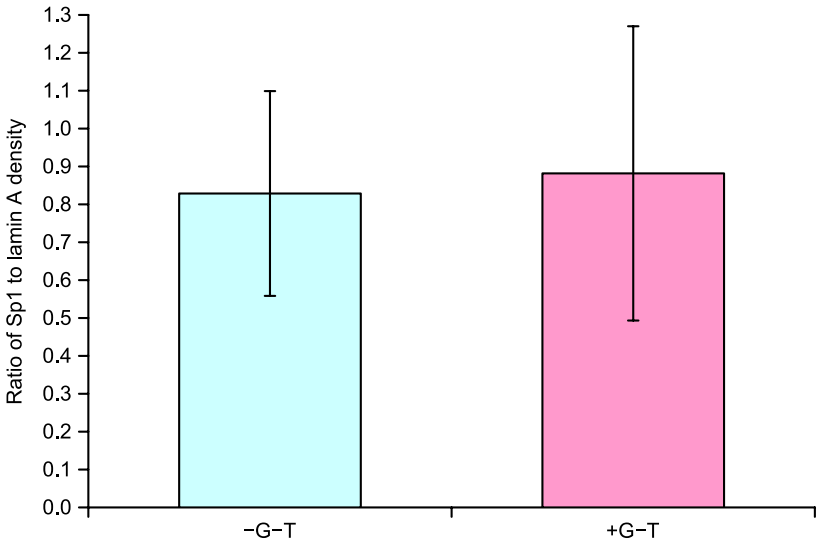

Figure 10.6: Abundance of Sp1 in HK-2 cell nuclear extracts *in vitro* presented as a ratio of Sp1 to lamin A band density after five days of culture. □−G−T; □+G−T. $n = 4$ for each condition.

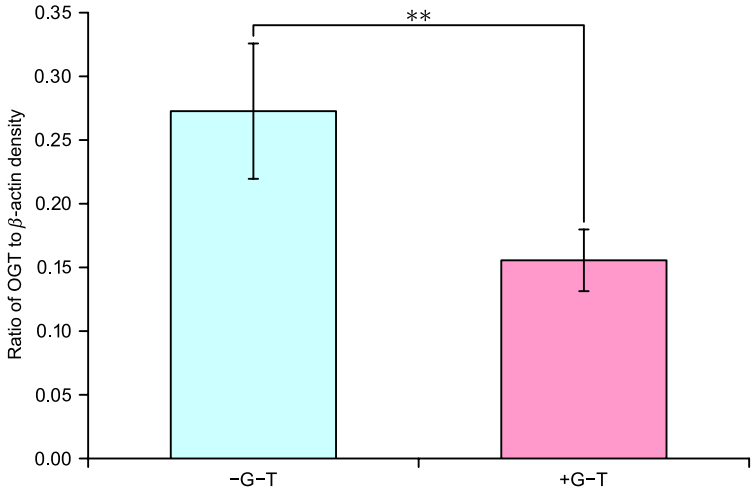

Figure 10.7: Abundance of OGT in HK-2 cell extracts from cells cultured in low thiamine concentration (4 nM) *in vitro* presented as the ratio of OGT to β-actin image density after five days of culture. □−G−T; □+G−T. $** = p < 0.01$;. $n = 4$ for each condition.

10.2.3 Discussion

These experiments were designed to test the theory that the hexosamine pathway is involved in the down-regulation of the thiamine transporters. The data corroborates the theory that *O*-GlcNAcylation of proteins is increased under hyperglycaemic conditions (Section 3.4). However, the increase in the glycosylation status of Sp1 is in spite of the fact that HK-2 cells under the same conditions did not demonstrate an increase in UDP-GlcNAc concentration. This may be accounted for by an increase in either the abundance of or activity of OGT, however these results demonstrate that the abundance of OGT is not increased in HK-2 cells in hyperglycaemia. The abundance data presented here corroborate the mRNA evidence in the primary PTECs but not the mRNA evidence in the HK-2 cells where there is a slight increase in OGT mRNA abundance in hyperglycaemic conditions. To elucidate the exact mechanisms involved here, studies on the turnover and activity of OGT would have to be performed. These would be able to demonstrate if the activity of OGT had been increased despite its lower abundance, thereby accounting for increased glycosylation of Sp1.

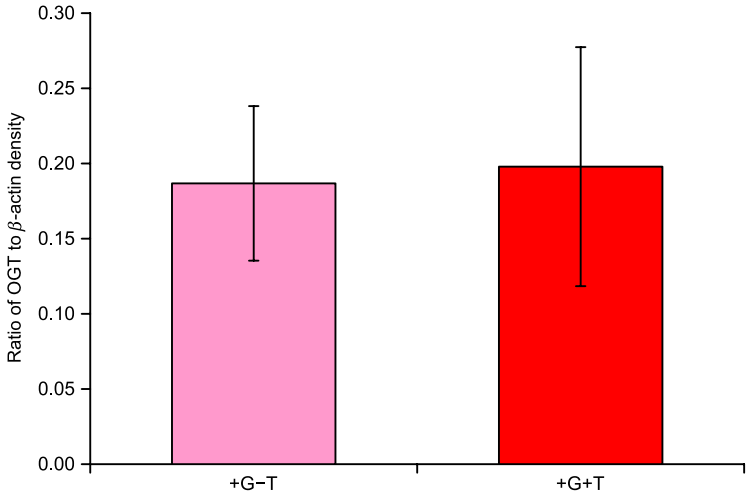

Figure 10.8: Abundance of OGT in HK-2 cell extracts from cells cultured in high glucose concentration (26 mM) *in vitro* presented as the ratio of OGT to β-actin image density after five days of culture. +G−T; +G+T. $n = 4$ for each condition.

Chapter 11

Intracellular thiamine metabolite concentration and transketolase activity in PTECs *in vitro*

11.1 Concentration of intracellular thiamine

Both primary PTECs and HK-2 cells were cultured for five days in the four conditions (−G−T, −G+T, +G−T and +G+T) and the amount of intracellular thiamine and thiamine phosphate esters assayed by HPLC. Protein concentrations were quantified by Bradford assay and the results expressed as pmol analyte per mg protein.

11.1.1 Primary PTEC intracellular thiamine metabolite concentration *in vitro*

The amount of thiamine in primary PTECs is given in Figure 11.1. Thiamine was not detectable in samples from either low thiamine condition (< 0.15 pmol per mg protein). The amounts of thiamine were high in both high thiamine conditions but were 20% decreased in +G+T with respect to −G+T ($p < 0.001$).

The amounts of TPP showed a similar trend to the amounts of cellular thiamine

with the exception that TPP was detectable in the low thiamine conditions (Figure 11.2). The amount of TPP was increased 210% in −G+T with respect to −G−T ($p < 0.001$) and the amount of TPP was increased 180% in +G+T with respect to +G−T ($p < 0.001$). The amount of cellular TPP was decreased 23% in +G+T with respect to −G+T ($p < 0.001$). No other differences were significant. There was no thiamine monophosphate detectable in any condition.

11.1.2 HK-2 cell intracellular thiamine metabolite concentration *in vitro*

The amount of intracellular thiamine in −G+T was increased 65-fold with respect to −G−T and 33-fold with respect to +G−T (both $p < 0.001$). The amount of intracellular thiamine in +G+T was increased 71-fold with respect to −G−T and 38-fold with respect to +G−T (both $p < 0.001$). No other changes were significant. The concentration of glucose had no effect on the amount of thiamine in the HK-2 cells, unlike the primary PTECs.

Thiamine monophosphate was detectable in HK-2 cells, unlike in the primary PTECs (Figure 11.4). The pattern is similar to that observed for intracellular thiamine. Both high thiamine conditions had increased amounts of TMP with respect to both low thiamine conditions (increased 160–240%; $p < 0.001$). No other changes were significant. The con-

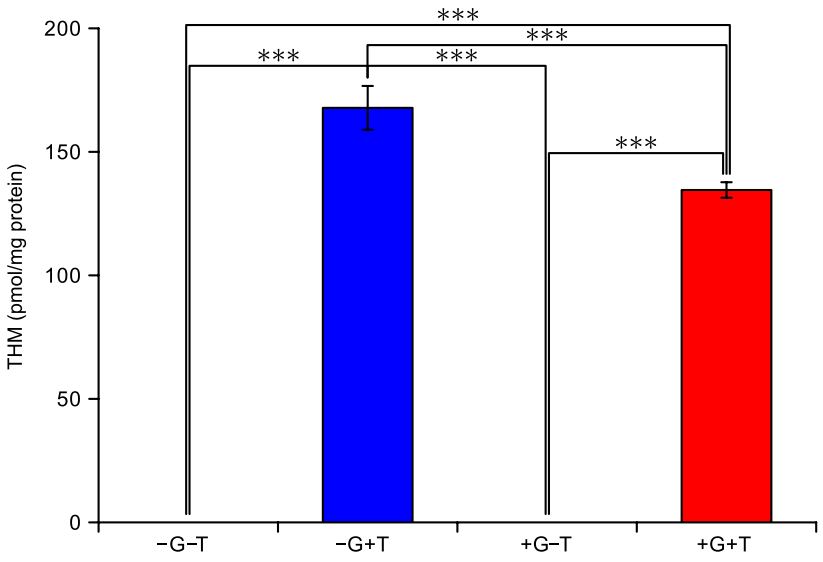

Figure 11.1: Intracellular thiamine content of primary PTECs *in vitro*. □−G−T; ■−G+T; □+G−T; ■+G+T. $* * * = p < 0.001$. $n = 8$ for each condition.

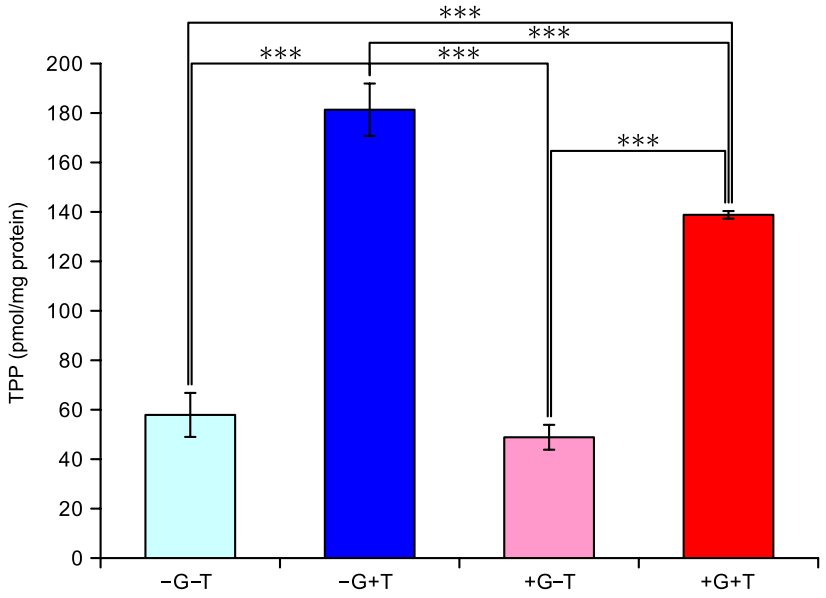

Figure 11.2: Intracellular thiamine pyrophosphate content of primary PTECs *in vitro*. □ −G−T; ■ −G+T; □ +G−T; ■ +G+T. $*** = p < 0.001$. $n = 8$ for each condition.

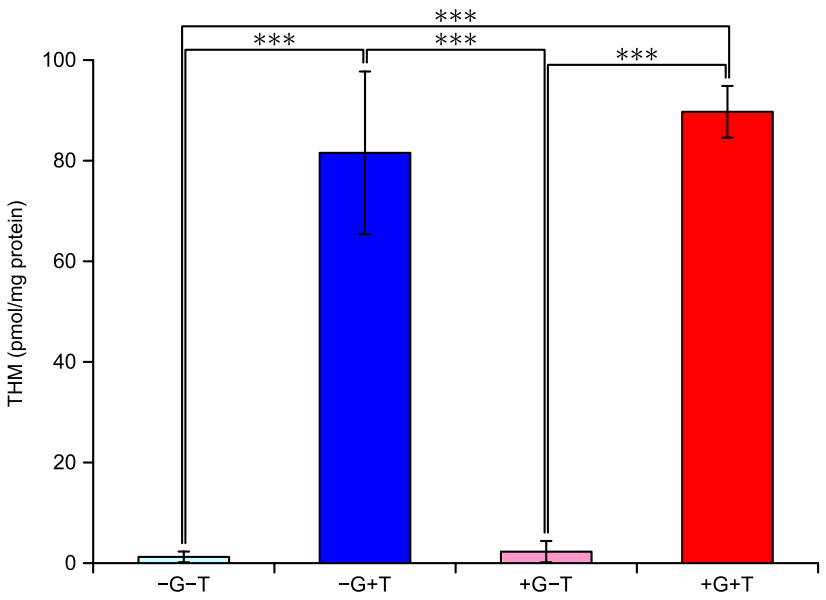

Figure 11.3: Intracellular thiamine content of HK-2 cells *in vitro*. □ −G−T; ■ −G+T; □ +G−T; ■ +G+T. $*** = p < 0.001$. $n = 4$ for each condition.

centration of glucose had no effect on the amount of thiamine monophosphate in the HK-2 cells.

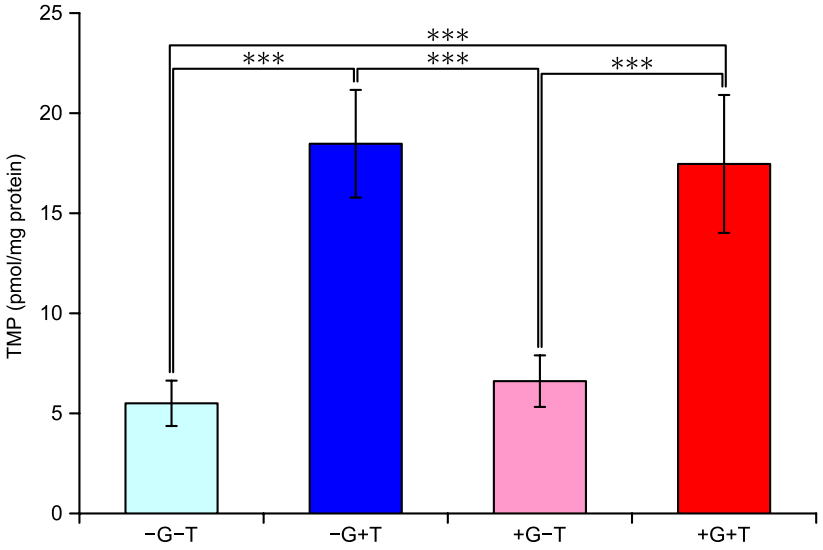

Figure 11.4: Intracellular thiamine monophosphate content of HK-2 cells *in vitro*. □−G−T; ■−G+T; □+G−T; ■+G+T. $***=p<0.001$. $n=4$ for each condition.

The amount of thiamine pyrophosphate present in the HK-2 cells *in vitro* is shown in Figure 11.5. There was no difference in the amount of TPP present in the cells in either of the low thiamine conditions. The amount of TPP in HK-2 cells in +G+T was increased 43% with respect to −G+T ($p<0.05$). The amount of TPP was increased 77% in −G+T with respect to −G−T ($p<0.01$) and the amount of TPP was increased 140% in +G+T with respect to +G−T ($p<0.001$). The pattern observed is similar to that seen for thiamine monophosphate except that there are increased amounts of thiamine pyrophosphate present in +G+T relative to −G+T.

11.1.3 Discussion

There are notable differences between the two model systems when comparing intracellular thiamine concentrations. Firstly there is the difference in overall thiamine analyte concentrations in each of the models. The intracellular thiamine metabolite concentration in −G−T was increased by 88% in the primary PTEC cultures with respect to the HK-2 cell cultures ($57.9\pm8.9\,\text{pmol mg protein}^{-1}$ versus $30.7\pm4.2\,\text{pmol mg protein}^{-1}$). Increases in the intracellular thiamine metabolite concentration were also observed in primary

PTEC cultures with respect to the HK-2 cell cultures in other conditions: −G+T: 144% increase (349±13 versus 142±18 pmol mg protein^{-1}); +G+T: 42% increase (48.9±5.0 versus 34.2±5.8 pmol mg protein^{-1}) and +G+T: 62% increase (273±3.5 versus 168±7.2 pmol mg protein^{-1}).

The proportion of the thiamine metabolite pool held in the form of TPP is also increased in the primary PTEC cultures with respect to the HK-2 cell cultures. The entire thiamine metabolite pool was held in the form of TPP in the low thiamine conditions in the primary PTEC cultures whereas the HK-2 cells held a substantial portion of their thiamine pool in the form of TMP and THM in the same conditions (TMP and THM comprised 22% and 25% of the thiamine metabolite pool in HK-2 cells cultured in −G−T and +G−T conditions respectively versus 0% in the primary PTEC cultures in the same conditions).

The increases in intracellular thiamine metabolite concentration in the primary PTEC cultures suggest two possible alternatives. The first is that primary PTEC cultures have a higher concentration of thiamine-dependent enzymes which necessitates a higher concentration of thiamine and a higher efficiency of conversion to TPP. This scenario may suggest that the transketolase activity in the primary PTEC cultures would be higher than that in the HK-2 cell cultures but this does not appear to be the case (Section 11.2). A

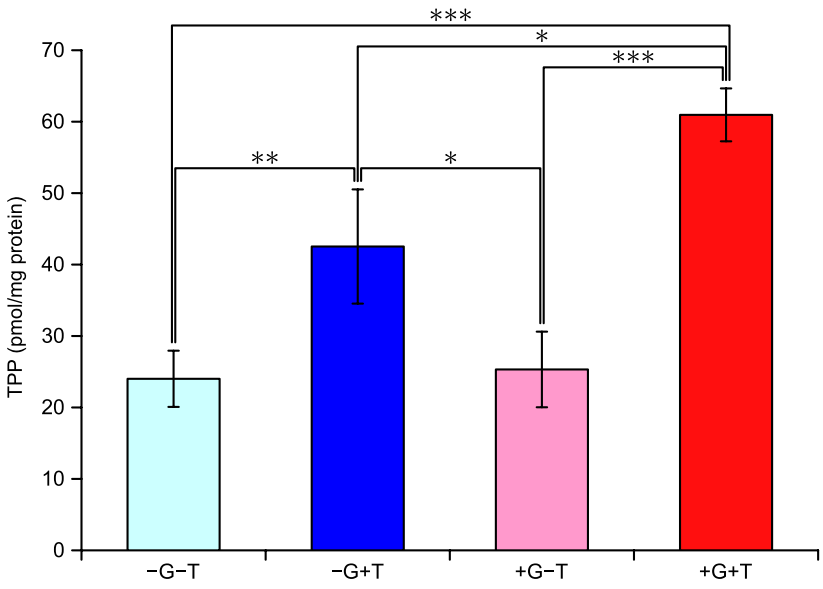

Figure 11.5: Intracellular thiamine pyrophosphate content of HK-2 cells *in vitro*. □−G−T; ■−G+T; □+G−T; ■+G+T. $* = p < 0.05$; $** = p < 0.01$; $*** = p < 0.001$. $n = 4$ for each condition.

second more likely explanation would be that the thiamine metabolism of the HK-2 cells has drifted away from the native *in vivo* metabolism expected of PTECs after extended periods in culture in high thiamine medium since isolation—normal tissue culture medium contains ∼6.5 µM thiamine. In an environment with such an abundance of thiamine, there is no selective pressure on the cells to maintain an efficient thiamine metabolism or transport system. Thus it is likely that the cells respond in an abnormal manner when placed in medium with a low thiamine concentration. The primary PTEC cultures have never been exposed to non-physiological thiamine concentrations (except during experimental procedures) and are thus more representative of *in vivo* metabolism.

In the primary PTEC cultures it can also be seen that high glucose causes a decrease in total intracellular thiamine metabolite concentration (both TPP and free thiamine), but only when cultured with a high thiamine concentration. Since TPP in synthesised from free thiamine, it is possible that the decrease in TPP concentration is simply a result of decreased thiamine availability as a substrate of thiamine diphosphokinase. To confirm or refute this would require investigating the activity of thiamine diphosphokinase, a topic not covered in this thesis. It is likely that the decrease in free thiamine in the high glucose cultures is due to the decreased abundance of the thiamine transporters.

All results regarding intracellular thiamine metabolite concentrations discussed here must also be considered with regard to the experimental conditions. The cells have been cultured in a medium that is of a constant thiamine concentration for five days. This is not analogous to the *in vivo* conditions where the cells would be exposed to a glomerular ultrafiltrate only transiently before it leaves the body as urine. In the kidney, if uptake were impaired it could potentially have a more marked effect than in this *in vitro* system where even if thiamine transport were impaired, it is possible that an optimal internal thiamine concentration could be achieved through extended exposure duration alone. One possible factor which would partially correct for this is that the cells *in vitro* were growing exponentially during the culture period, something that cells *in vivo* would not be doing. With cells growing exponentially, intracellular volume would also be increasing exponentially and, with no thiamine transport, intracellular concentration would decay exponentially. Thus it can be seen that any defects in the uptake system could manifest as a decrease in intracellular concentration, even in a "steady-state" culture system. This may be an explanation for the decreased thiamine concentration observed in the +G+T condition relative to the −G+T condition in the primary PTEC cultures. These deficiencies were partially addressed with trans-membrane monolayer studies (Section 12.1, page 187).

11.2 Transketolase activity

Assays for the activity of the TKT were performed on both primary PTECs and HK-2 cells. In both cases, cells were incubated for five days in one of the four glucose and thiamine concentration combinations (−G−T, −G+T, +G−T or +G+T). After culture, the cells were harvested and assayed for both TKT activity and percentage saturation of the enzyme with its TPP cofactor.

11.2.1 Primary PTEC transketolase activity *in vitro*

The TKT activities in human PTECs in primary culture are given in Figure 11.6. Only the 10% thiamine effect (i.e. unsaturation of TKT) in −G−T was significant ($p < 0.01$). TKT activity was increased 12.5% in +G+T with respect to −G−T ($p < 0.05$). No other changes in TKT activity were significant.

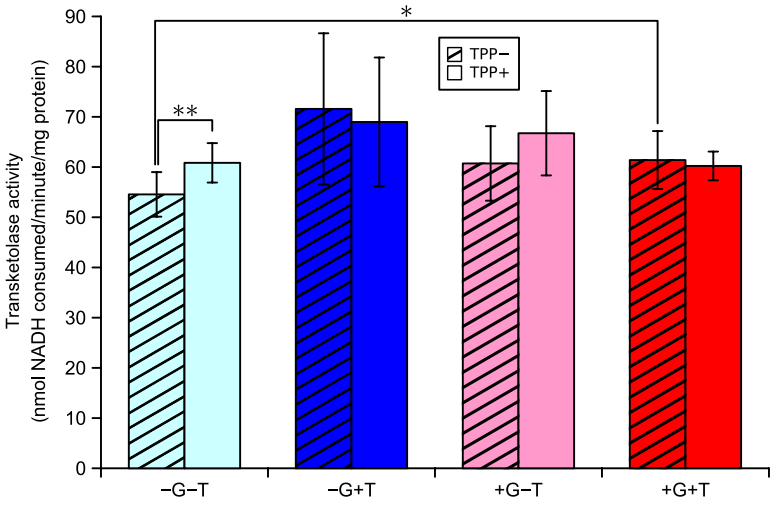

Figure 11.6: Transketolase activity in primary PTECs *in vitro*. TKT activity levels were measured with and without additional TPP in each condition to assay the "thiamine effect". □−G−T; ■−G+T; □+G−T; ■+G+T. $* = p < 0.05$; $** = p < 0.01$. $n = 8$ for each condition.

11.2.2 HK-2 cell transketolase activity *in vitro*

The TKT activities in HK-2 cells are given in Figure 11.7. TKT activity was decreased 35–39% in +G+T (with and without TPP) with respect to −G−T and −G+T (with and without TPP; $p < 0.001$). TKT activity in +G−T (without TPP) was 21% decreased with

respect to −G+T (without TPP; $p < 0.05$). There was no thiamine effect in any culture condition.

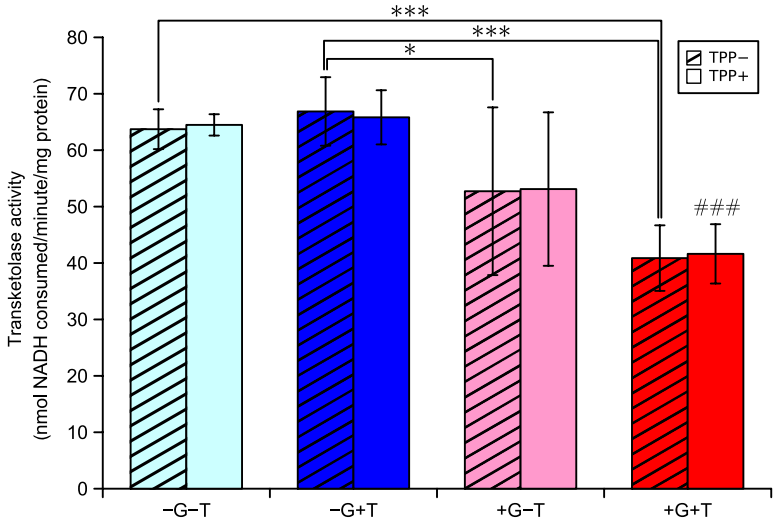

Figure 11.7: Transketolase activity in HK-2 cells *in vitro*. TKT activity levels were measured with and without additional TPP in each condition to assay the "thiamine effect". □ −G−T; ■ −G+T; □ +G−T; ■ +G+T. $* = p < 0.05$; $*** = p < 0.001$; $\#\#\# = p < 0.001$ relative to both low glucose TPP+ conditions. $n = 4$ for each condition.

11.2.3 Discussion

The 10% thiamine effect observed in the −G−T condition in the primary PTEC cultures was the only significant thiamine effect observed. A thiamine effect of 10% falls within the 0–15% range expected in erythrocytes in normal individuals. The fact that no conditions are markedly thiamine deficient is expected since the apo-TKT (without an attached TPP moiety) is markedly less stable than the holo-enzyme form and is rapidly degraded [Jeyasingham et al., 1986; Esakova et al., 2005]. In erythrocytes, where protein half life is the same as the erythrocyte half life (i.e. around 50 days), this unsaturation is detectable after extended periods. In cells with active protein synthesis and degradation systems, apo-TKT would be degraded leading to a lower overall activity, not a thiamine effect.

Considering the primary PTEC cultures, there are no statistically significant differences in TPP-saturated TKT activity. This suggests that no condition is thiamine deficient, an assertion corroborated by the intracellular concentrations of TPP which never drop below 24 pmol mg protein^{-1} under any condition. The stability of TKT activity across the four conditions is in contrast to the data on the abundance of TKT mRNA in the primary PTEC

cultures. The abundance of TKT mRNA in +G−T and +G+T was decreased 62% and 59% respectively with respect to −G−T. The fact that the decreases in abundance of mRNA do not translate into lower enzyme activities suggests that the stability of transketolase has been markedly increased in the high glucose cultures. Alternative explanations such as transketolase having a naturally long half life do not stand to scrutiny when considering the exponential growth of cells in culture. The stability of transketolase was not investigated in this thesis.

The results in the HK-2 cell cultures are again different to those obtained in the primary PTEC cultures. The decrease in TKT activity in the HK-2 cells in the +G+T condition relative to both the low glucose conditions is hard to rationalise. The cells in the +G+T condition do not have a lower intracellular concentration of TPP and they do not have a decreased abundance of TKT mRNA present. Other theories attempting to explain the result would be unfounded speculation, especially considering that the same result was not observed in the primary PTEC cultures. It is likely that the factor causing the decreased TKT activity is peculiar to the HK-2 cell line and is not relevant *in vivo*.

Chapter 12

Thiamine uptake and handling in PTECs *in vitro*

12.1 Primary PTEC monolayer transport studies *in vitro*

12.1.1 Primary PTEC monolayer integrity

Transport experiments simulating *in vivo* conditions with cells grown on semi-permeable supports, not solid surfaces, were conducted with primary PTECs. Primary PTEC monolayer integrity in Transwell inserts was assayed using Lucifer yellow prior to transport experiments. The mean P_{app} for primary cells cultured under four conditions (−G−T, −G+T, +G−T and +G+T) was found to be $8.3 \times 10^{-6} \pm 2.3 \times 10^{-6}\,\mathrm{cm\,s^{-1}}$ (mean ± SD). The P_{app} for an empty Transwell insert with no cells was determined to be $4.8 \times 10^{-4}\,\mathrm{cm\,s^{-1}}$ meaning that the monolayers had a P_{app} 1.7% that of the blank insert. There was no difference in P_{app} between the four culture conditions ($p > 0.05$) and no wells were discarded prior to analysis due to high P_{app}. These P_{app} values are similar to those expected as discussed in Section 6.11.4.

12.1.2 Monolayer [^{3}H]thiamine transport studies in primary PTECs *in vitro*

A transport experiment from the apical to the basal chamber was conducted with five Transwell membranes of primary PTEC in each of the four conditions. P_{app} was determined for the time 0–15 minutes after addition of the tritiated thiamine to the apical chamber.

The experiment was repeated with 6 thiamine concentrations in the range of 10–200 nM. All wells with a mass balance (i.e. total recovery of tritiated thiamine) outside the range 90–110% were discarded from analysis. The plot of P_{app} against thiamine concentration is given in Figure 12.1. There are no significant differences between any pairs of conditions. In addition, it is not possible to fit a curve describing Michaelis-Menten kinetics to these data because the thiamine concentrations used do not exceed, or even approach, the apparent K_{m}. All disintegration rates recorded fell within the range 500–6500 disintegrations per minute—within the linear range for the detector.

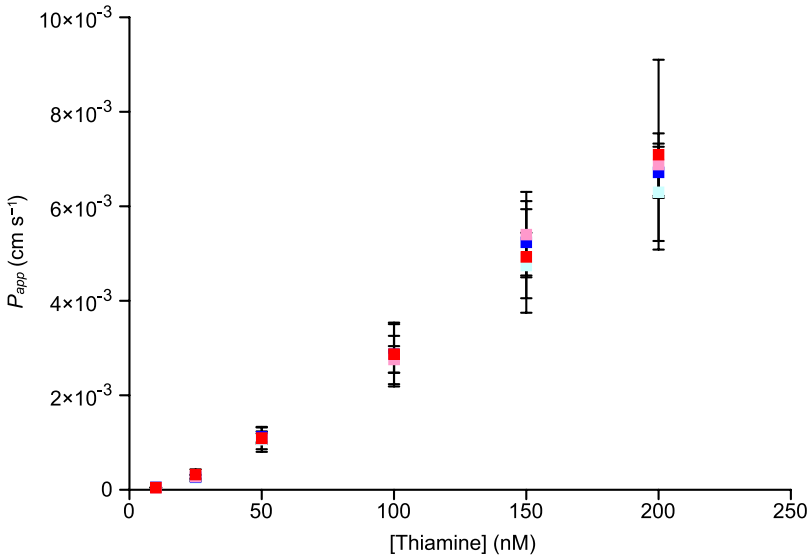

Figure 12.1: P_{app} for thiamine at different concentrations in primary PTECs *in vitro*. □ −G−T; ■ −G+T; □ +G−T; ■ +G+T. $n = 5$ for each condition.

A similar set of membranes were assayed to quantify forward and reverse transport under a single condition: 15 nM thiamine over 20 minutes. The mass balance for all wells lay within 90–110%. The P_{app} values for all wells were calculated for both apical to basal and basal to apical directions (Figure 12.2). There was no significant difference between any of the groups' apical to basal (forward) P_{app} values. The reverse (basal to apical) P_{app} was increased in −G+T, +G−T and +G+T with respect to −G−T (+52%; $p < 0.001$).

Ratios of forward P_{app} to reverse P_{app} indicate the strength of the polarity of transport (Figure 12.3). The ratios are strongly in favour of transport of thiamine from the apical side to the basal side of the monolayers. The ratio was less in favour of apical to basal transport in −G+T, +G−T and +G+T than in −G−T (ratios deceased 23–27%; $p < 0.001$).

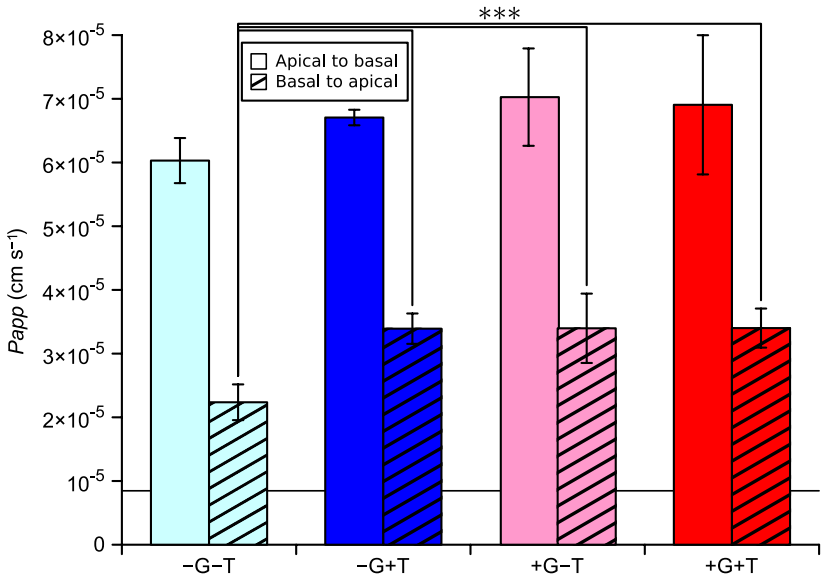

Figure 12.2: P_{app} values for forward and reverse [^{3}H]thiamine transport in primary PTEC monolayers *in vitro*. The black line shows the P_{app} value for Lucifer yellow determined before the transport experiments started for reference (8.3×10^{-6} cm s^{-1}). −G−T; −G+T; +G−T; +G+T. $*** = p < 0.001$. $n = 5$

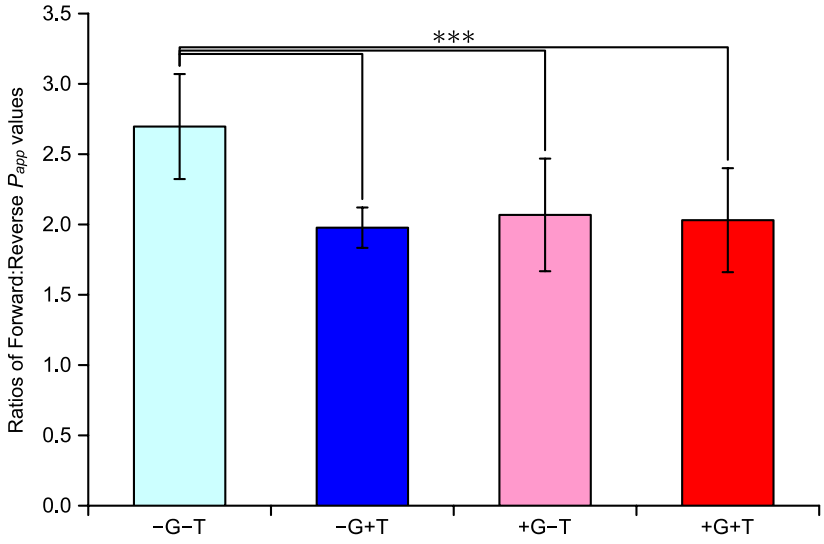

Figure 12.3: P_{app} ratios forward:reverse *in vitro*. −G−T; −G+T; +G−T; +G+T. $*** = p < 0.001$. $n = 5$

12.1.3 Discussion

The published literature indicates that two K_{m} values for thiamine uptake in PTECs should be found: one in the nanomolar range and one in the low micromolar range. The experiment was not designed to determine the K_{m} value in the micromolar range but should have been adequately powered to find a K_{m} value at or around 70 nM [Ashokkumar et al., 2006]. Instead of observing kinetics following the Michaelis-Menten equation, all four culture conditions showed first-order kinetics with rate of transport being directly proportional to substrate concentration over the measured range. Since published evidence demonstrates that thiamine transport is saturable, this leaves two options: (i) the model system analysed does not have a K_{m} value low enough to be near the highest 200 nM concentration used, an unlikely scenario or, (ii) the experiment was flawed in some manner. It is possible that the integrity of the membranes degraded during the lengthy procedure. Each monolayer was used repeatedly with increasing concentrations of thiamine with rest periods in between. Repeated changes of basal and apical fluid could have damaged the monolayers in a way that was not noted because monolayer integrity was not determined after the experiment was completed.

The separate monolayers used for single condition forward and reverse studies have shown that forward P_{app} of thiamine (i.e. apical to basal) appears not to change in a manner dependent on culture conditions whilst the reverse basal to apical P_{app} does. This leads to a significant increase in forward transport in the −G−T condition relative to the other three conditions. This lies in corroboration with other evidence, in HK-2 cells, showing a decreased rate of net uptake in the high glucose conditions (below).

12.2 Rate of uptake of thiamine by HK-2 cells *in vitro*

Experiments with tritiated thiamine ([^{3}H]thiamine) were performed to investigate if the decrease in THTR-1 abundance observed in the HK-2 cells led to a decreased rate of uptake of thiamine. HK-2 cells were cultured in 6-well plates for five days in four conditions (−G−T, −G+T, +G−T and +G+T). [^{3}H]thiamine uptake rate was assayed as described in Section 6.11.1. Nine wells in each condition were assayed for uptake rate and three further wells were used as a negative control with non-radioactive thiamine to allow blanking of the samples to background radiation levels. The uptake rates are given in Figure 12.4.

The uptake rates are identical in both 5 mM conditions ($p > 0.05$) but are decreased significantly in +G−T with respect to the low glucose conditions (−31%; $p < 0.001$). The

uptake rate in +G+T was decreased by 17% with respect to −G+T ($p < 0.05$) but the decreased uptake rate in +G+T with respect to −G−T was not significant ($p = 0.053$). The addition of thiamine to either the low or high glucose concentration conditions did not alter [^{3}H]thiamine uptake rate.

12.2.1 Discussion

The decreased rate of uptake of [^{3}H]thiamine in HK-2 cells in hyperglycaemic conditions corroborates evidence that there is a decreased abundance of THTR-1 in hyperglycaemic conditions. The 31% decrease in uptake rate in +G−T with respect to −G−T does not correspond exactly with the 53% decrease in abundance of THTR-1 seen in the same cells. The results must be interpreted taking into account the simplistic nature of the uptake model. PTECs *in vivo* use THTR-1 and THTR-2 to transfer thiamine from the apical membrane to the basal membrane. HK-2 cells do not have a normal THTR-2 expression, as indicated by qPCR and immunohistochemistry analysis. This leaves only THTR-1 taking thiamine up on the apical face (exposed to the [^{3}H]thiamine) and perhaps attempting to expel thiamine from the basal membrane, adhering to the polystyrene sub-stratum. These differences alone may explain the difference in magnitude between THTR-1 abundance and thiamine uptake rate.

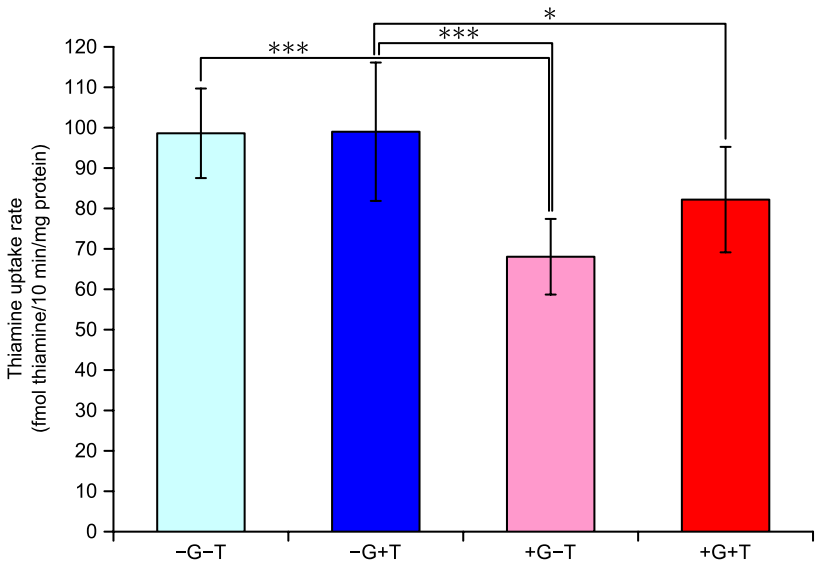

Figure 12.4: [^{3}H]thiamine uptake rate into HK-2 cells *in vitro*. □−G−T; ■−G+T; ■+G−T; ■+G+T. $* = p < 0.05$; $*** = p < 0.001$. $n = 9$ for each condition.

12.3 Rate of release of thiamine from HK-2 cells *in vitro*

The rate of release of thiamine from HK-2 cells cultured in the four conditions (−G−T, −G+T, +G−T and +G+T) was studied by pre-loading cells with [^{3}H]thiamine for 5 h and then subjecting cells to a 10 min release period into fresh Krebs-Ringer solution containing no thiamine. Full details of the method are given in Section 6.11.2 on page 124.

The results for release rates must be presented in the context of the total [^{3}H]thiamine taken up during the pre-loading period. This is because uptake rates during the pre-loading period are unique to the relevant condition. In addition, as intracellular [^{3}H]thiamine concentration rises during the pre-loading period, some will be pumped back out into the medium. The net result is that there are different intracellular [^{3}H]thiamine concentrations for each condition at the start of the release period. By measuring [^{3}H]thiamine released from the cells into the Krebs-Ringer solution (T_{released}) and final [^{3}H]thiamine content of the cells (T_{after}), the initial [^{3}H]thiamine content of the cells (T_{before}) could be deduced (Figure 12.5). −G−T cells contained the most [^{3}H]thiamine. With respect to −G−T, the amount of intracellular [^{3}H]thiamine is decreased in −G+T (−28%; $p < 0.01$), +G−T (−35%; $p < 0.001$) and +G+T (−50%; $p < 0.001$). Intracellular [^{3}H]thiamine in +G+T was decreased by 31% with respect to −G+T ($p < 0.01$) and was decreased by 24% with respect to +G−T ($p < 0.05$). There were no other significant differences. These data can be considered as results to an extended uptake rate experiment over 5 h and show that both glucose and thiamine affect the storage of thiamine during this uptake period. In both high and low glucose, prior incubation in a high thiamine culture medium leads to lower accumulation of thiamine (perhaps as a result of high intracellular thiamine concentrations). Also, high glucose causes a decrease in thiamine accumulation, irrespective of thiamine status. When compared to the dedicated 10 min uptake experiment performed, these results show a similar trend but an increased magnitude. This increased magnitude could be attributable to the longer uptake period.

The data in Table 12.1 indicates T_{before} as a percentage of the total [^{3}H]thiamine available in the system (1 mL × 15 nM; 15 pmol available [^{3}H]thiamine). This confirms that the [^{3}H]thiamine in the medium is still greatly in excess during the pre-loading period since in no condition do the cells contain more than 0.3% of available [^{3}H]thiamine. Also in Table 12.1 is data showing T_{released} as a percentage of T_{before}. This value, $T_{\%}$, is calculated from Equation 12.1 where T_{after} is the amount of intracellular [^{3}H]thiamine in the cells after

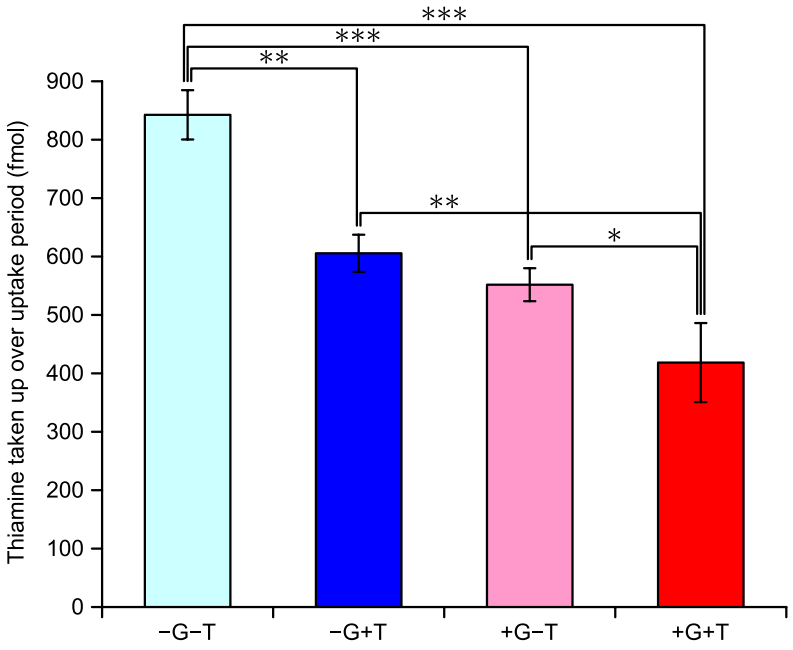

Figure 12.5: [^{3}H]thiamine content of HK-2 cells *in vitro* before release window after pre-loading with [^{3}H]thiamine. □−G−T; ■−G+T; □+G−T; ■+G+T. $* = p < 0.05$; $** = p < 0.01$; $*** = p < 0.001$. $n = 3$ for each condition.

the release period has elapsed. These values all exceed 90% which means that <10% of [^{3}H]thiamine is released from the cells during the release window and that the data are for intitial rate conditions.

$$T_{\%} = \frac{T_{\text{after}}}{(T_{\text{after}} + T_{\text{released}})} \times 100 \tag{12.1}$$

Condition	[^{3}H]thiamine taken up (% available)	[^{3}H]thiamine remaining in cells (% intracellular [^{3}H]thiamine at start of release window)
−G−T	0.28%	95.1%
−G+T	0.27%	94.0%
+G−T	0.21%	93.2%
+G+T	0.21%	92.3%

Table 12.1: [^{3}H]thiamine handling in HK-2 cells *in vitro*

The release rates from the pre-loaded HK-2 cells can be expressed as absolute release rates (in $\text{fmol}\,10\,\text{min}^{-1}\,\text{mg protein}^{-1}$; Figure 12.6) or as a release rate constant, K_r (in min^{-1}; Figure 12.7), derived from:

$$\text{Release rate} = T_{\text{before}} \times K_r$$

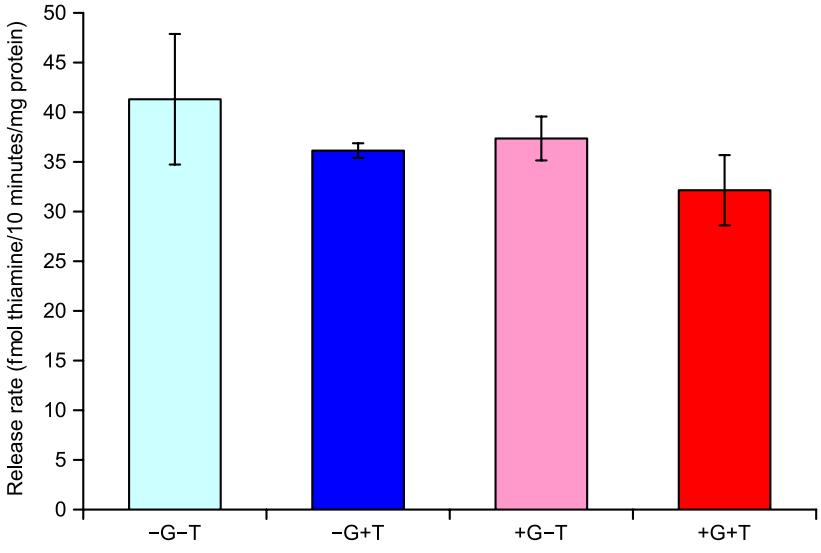

Figure 12.6: [^{3}H]thiamine absolute release rate from HK-2 cells *in vitro*. □ −G−T; ■ −G+T; □ +G−T; ■ +G+T. $n = 3$ for each condition.

These results show that the absolute release rate is independent of intracellular [^{3}H]thiamine concentration. This could be attributed to the polarised HK-2 cells not being able to release thiamine from their basal faces (due to occlusion by a solid sub-stratum) and releasing thiamine in a uniform, and perhaps uncontrolled, manner from their apical faces.

The release rate constant (Figure 12.7) is increased in +G+T with respect to −G−T (+57%; $p < 0.001$) and with respect to −G+T (+29%; $p < 0.01$). Also, the release rate constant is increased in +G−T with respect to −G−T (+38%; $p < 0.01$). The higher release rate constants are attributable to a similar absolute release rate combined with a lower intracellular [^{3}H]thiamine concentration prior to efflux (T_{before}).

It is important to remember that these data represent only the initial rate of efflux from the cells. This is likely to be the fastest rate because at the start, the cells have the highest intracellular concentration of [^{3}H]thiamine. If each efflux ratio were to be multiplied by 30 (5 h uptake ÷ 10 min release) then values would range from 1.5–2.5 representing an efflux rate faster than the accumulation rate. In reality, the efflux rate would drop as the intracellular concentration of the [^{3}H]thiamine was reduced.

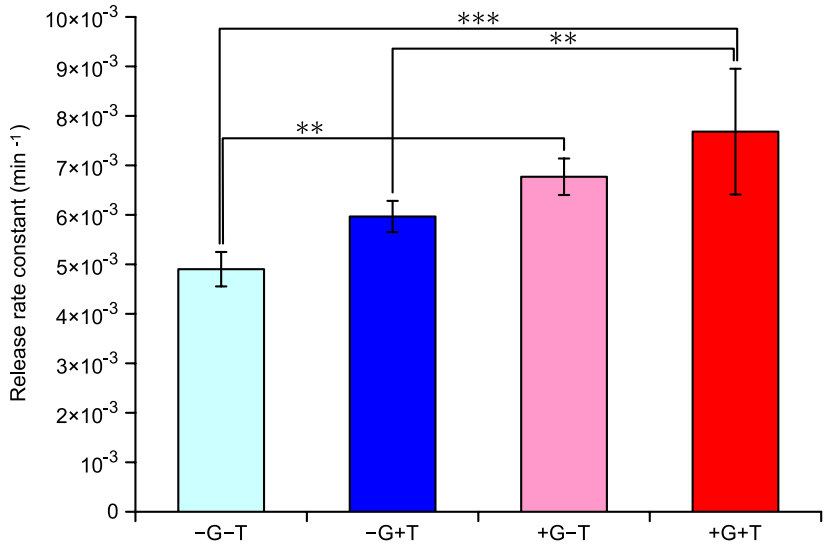

Figure 12.7: [^{3}H]thiamine release rate constant from HK-2 cells *in vitro*. K_r = (release rate/T_{before}). □ −G−T; ■ −G+T; ■ +G−T; ■ +G+T. ∗∗ = $p < 0.01$; ∗∗∗ = $p < 0.001$. n = 3 for each condition.

Chapter 13

Double blind placebo-controlled trial of thiamine supplementation in patients with type 2 diabetes and microalbuminuria

13.1 Patient characteristics

In the Pakistan thiamine intervention trial placebo group there were 11 male and 9 female patients (age 52.4±8.7 years and BMI 28.3±4.4 $\mathrm{kg\,m^{-2}}$). In the thiamine treatment group there were 10 male and 10 female patients (age 52.7±8.4 years and BMI 28.1±4.6 $\mathrm{kg\,m^{-2}}$). Throughout the duration of the study, nine patients in the thiamine treatment group and three in the placebo group were receiving insulin therapy ($p < 0.05$). There were no other significant differences between the groups with regard to therapeutic agents taken. One patient achieved glycaemic control through diet alone; all other patients received therapeutic hypoglycaemic agents (sulphonylureas, metformin and thiazolidinediones). Nine patients in the placebo group and eight in the thiamine treatment group received therapy with antihypertensive agents. Three patients in the thiamine treatment group and one in the

placebo group were receiving statins at baseline compared with seven and two respectively after three months and seven and three after the washout period from 3–5 months. One patient in the thiamine treatment group was receiving antihyperlipidaemic fibrate therapy. Whilst these patient therapies are not all in line with current recommendations for best clinical practice [American Diabetes Association, 2009] they are typical for treatments found on the Indian sub-continent; as a comparison, see the Chennai Urban Rural Epidemiology Study [Unnikrishnan et al., 2007]. The patient characteristics at baseline are presented in Table 13.1.

There was no significant difference between the groups for any clinical chemical variable at baseline. The median plasma thiamine concentration of diabetic patients was 7.5 nM, markedly lower than the normal range of healthy human volunteers we saw in our survey in Colchester (44.6–93.7 nM) [Thornalley et al., 2007]. The median urinary thiamine excretion was 1.38 µmol 24 hours^{-1}. This value is in excess of the 0.2 µmol 24 hours^{-1} value suggested by Finglas [1993] as a minimum for indicating adequate dietary sufficiency. On this basis, all patients in this study had adequate dietary thiamine intake. One patient had a plasma thiamine concentration above the normal range and a urinary thiamine output 30-fold greater than the normal mean [Thornalley et al., 2007], consistent with prior thiamine supplementation, and was excluded from the data analysis.

At baseline, there was a negative correlation of plasma thiamine concentration with thiamine clearance ($r = -0.52$; $p < 0.01$) and a positive correlation of urinary thiamine excretion and thiamine clearance ($r = 0.52$; $p < 0.01$). There was no significant difference in the plasma thiamine concentration, urinary thiamine excretion and renal clearance of thiamine for patients with and without antihypertensive therapy. There were negative correlations of plasma thiamine concentration and urinary thiamine excretion with plasma von Willebrand factor (vWF) ($r = -0.41$ and -0.42, respectively; $p < 0.05$). There was a significant negative linear regression of soluble vascular cell adhesion molecule-1 (sVCAM-1) on plasma thiamine [sVCAM-1 (ng mL^{-1}) = 687 − (5.5 × plasma thiamine (nmol L^{-1})); $p < 0.05$]. These results corroborate findings made previously by this group [Thornalley et al., 2007].

Multivariate analysis was not conducted on the data from this trial. A study such as this one would lend itself to multivariate analysis as there are multiple factors which have been measured and could have an influence on the final endpoint. A univariate analysis assumes that one factor (the increase in plasma thiamine concentration) is responsible for the change in urinary albumin excretion. A multivariate analysis would confirm or refute

Variable	Thiamine group			Placebo group		
	Baseline	Therapy	Washout	Baseline	Therapy	Washout
Plasma thiamine (nM)	10.6 (0.8–84.5)	98.2 (2.6–294.5)$^{***}_{\dagger\dagger\dagger}$	10.9 (3.6–22.7) §§§	7.1 (1.1–31.3)	7.1 (2.4–16.6)	9.1 (4.2–16.3)
Urinary thiamine (μmol day^{-1})	1.63 (0.45–7.66)	47.7 (0.40–182.8) $^{***}_{\dagger\dagger\dagger}$	1.42 (0.10–9.72) §§§	1.53 (0.67–4.46)	1.71 (0.15–9.73)	1.16 (0.00–5.44)
Thiamine clearance (mL min^{-1})	112 (8–819)	273 (3–789) †	92 (18–237) §§	189 (26–955)	149 (12–663)	102 (12–334) ††
UAE (mg 24 hours^{-1})	43.7 (33.0–120.9)	30.1 (12.0–38.2) $^{**}_{\dagger\dagger\dagger}$	20.9 (7.0–35.0) $^{\dagger\dagger\dagger}_{\S\S}$	50.9 (32.9–121.7)	35.5 (6.4–82.0)	30.0 (3.5–80.4) †††
Plasma glucose (mM)	10.1±3.2	10.1±3.9	8.0±3.5 †	9.5±3.1	8.8±2.4	8.0±3.1 †
HbA_{1c} (%)	9.2±1.3	9.0±1.8	7.8±1.6 $^{\dagger\dagger}_{\S\S}$	8.8±1.8	8.5±1.7	8.4±1.7
Total cholesterol (mM)	5.26±1.30	4.87 (2.59–9.69)	4.61 (3.29–7.20)	4.79±1.06	4.43±1.66	5.57±1.97 §§
LDL cholesterol (mM)	2.75±1.22	2.56±1.71	2.41±0.83 *	2.75±0.93	2.38±1.19	3.19±1.24 §
HDL cholesterol (mM)	1.29±0.35	1.08±0.37 †	1.15±0.24	1.24±0.27	0.97±0.23 †††	1.37±0.56 §§
Triacylglycerol (mM)	2.23 (0.60–8.31)	2.27 (0.92–6.97)	2.60 (0.89–8.27)	1.51 (0.82–4.24)	1.79 (0.63–4.02) †	1.97 (1.08–4.46) †
Systolic BP (mmHg)	126±14	133±20	135±14 †	131±10	130±17	130±13
Diastolic BP (mmHg)	87±8	85±9	87±7	84±6	84±8	83±7
GFR (mL min^{-1})	85±19	90±30	77±20	93±23	97±18	87±21
sVCAM1 (ng mL^{-1})	588±267	554±224	481±192 $^{\dagger}_{\S}$	648±255	608±178	600±232
VWF (IU mL^{-1})	0.60 (0.07–5.18)	0.48 (0.01–2.95)	0.51 (0.071–1.97)	0.48 (0.01–4.35)	0.48 (0.01–4.41)	0.59 (0.01–1.61)

Table 13.1: Pakistan trial patient characteristics. Data are means ± SD or medians (minimum–maximum). * = $p < 0.05$, ** = $p < 0.01$, *** = $p < 0.001$ compared with placebo. † = $p < 0.05$, †† = $p < 0.01$, ††† = $p < 0.001$ compared with baseline. §= $p < 0.05$, §§= $p < 0.01$, §§§= $p < 0.001$ compared with post-therapy.

this and provide evidence of contributions to the endpoint from other factors.

13.1.1 Clearance rate definition

For clarification, the thiamine clearance rate is a measure of how fast thiamine is being removed from the blood by the kidneys. It is measured in $\mathrm{mL\,min^{-1}}$ which represents a time-averaged clearance rate over the measurement time (e.g. 1 day). The clearance rate is calculated using the following formula:

$$\text{Clearance } (\mathrm{mL\,min^{-1}}) = \frac{\text{Concentration }_{\text{urine}} \text{ (mM)} \times \text{Urine flow } (\mathrm{mL\,min^{-1}})}{\text{Concentration }_{\text{plasma}} \text{ (mM)}}$$

The thiamine excretion rate is a measure of the amount removed from the body in a given time e.g. $\mu\mathrm{g\,day^{-1}}$. It is derived from the product of urinary concentration and urinary volume per unit time. The fractional excretion of thiamine is the ratio of thiamine excreted by the kidneys to the total amount of thiamine filtered by the kidneys. It is calculated in two parts with the amount of thiamine excreted forming the numerator and the denominator being the total amount of thiamine filtered by the kidneys (glomerular filtration rate × plasma thiamine concentration). When appropriately cancelled, the formula for determining fractional excretion is:

$$FE_{\text{thiamine}} = 100 \times \frac{[\text{Thiamine}]_{\text{urine}} \times [\text{Creatinine}]_{\text{plasma}}}{[\text{Thiamine}]_{\text{plasma}} \times [\text{Creatinine}]_{\text{urine}}}$$

13.2 Effect of therapy with high-dose thiamine on type 2 diabetes patients

Thiamine treatment for 3 months increased the median plasma concentration of thiamine by 10-fold and urinary excretion of thiamine by 29-fold (Table 13.1 and Figure 13.1). All liver function tests were within the normal range, indicating the expected absence of adverse effects of treatment with thiamine. This demonstrates that it is sufficient to use a simple and inexpensive oral dosing regime to counter plasma thiamine deficiency.

The primary endpoint of this study was the effect of thiamine supplementation on UAE. After the treatment period, patients receiving thiamine therapy had decreased median UAE, with respect to patients receiving the placebo (30.1 versus $35.5\,\mathrm{mg\,24\,h^{-1}}$; $p < 0.01$). UAE was decreased significantly with respect to baseline in the patients treated

for 3 months with thiamine ($-17.7\,\mathrm{mg\,24\,h^{-1}}$; $p < 0.001$) but not in patients treated with placebo. The decrease was maintained after the washout period when the decrease in urinary albumin in the patients treated with placebo also became significant (Table 13.1 and Figure 13.2). The time course of changes in UAE in patients treated with thiamine and placebo showed a progressive decrease in UAE with time throughout the treatment period. Linear regression of UAE in relation to treatment time indicated that the rate of decrease in UAE was increased about fourfold in patients treated with thiamine with respect to placebo (-5.62 versus $-1.52\,\mathrm{mg\,24\,h^{-1}\,month^{-1}}$; Figure 13.2). Since there was a large dispersion of baseline UAE data and it was the response to therapy rather than the absolute change in UAE that was of most interest in this study, plots of each patient's response to therapy relative to their own baseline were constructed (Figure 13.3). These plots show that all diabetic patients receiving therapy had decreases in their UAE whilst patients receiving a placebo varied in their response over the treatment period. These decreases in UAE were in addition to those attributable to renin-angiotensin-aldosterone system (RAAS) blockade by angiotensin-converting enzyme inhibitors (ACE-Is) and angiotensin receptor blockers (ARBs; Figure 13.4). Median UAE rates for patients receiving thiamine supplementation decreased from 44.8 to $29.8\,\mathrm{mg\,24\,h^{-1}}$ in the ACE-I/ARB therapy subset (-33%; $n = 6$;

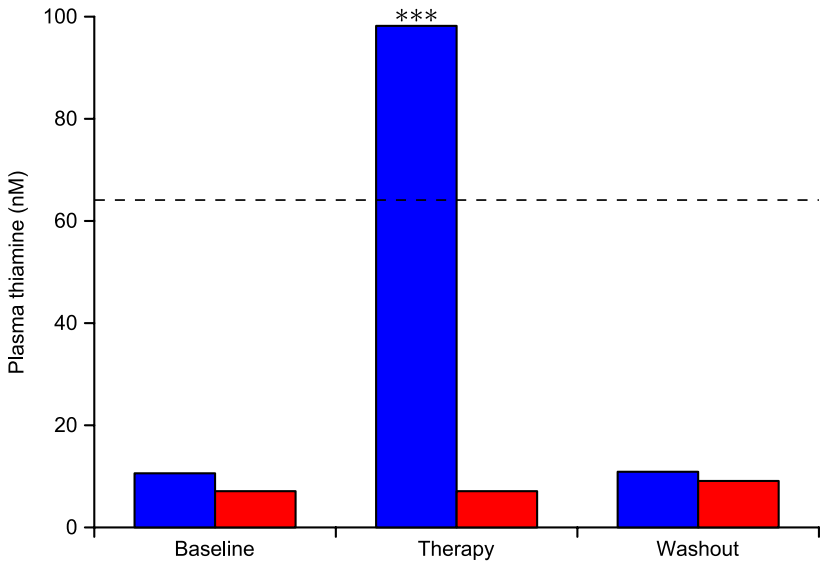

Figure 13.1: Effect of high-dose thiamine on plasma thiamine concentration in type 2 diabetes patients (median values). The normal median plasma thiamine concentration from Thornalley et al. [2007] is indicated by the black dashed line. ■ Therapy; ■ Placebo. $*** = p < 0.001$ with respect to both placebo group after therapy and therapy group at baseline.

$p < 0.05$) and from 43.7 to 30.1 mg 24 h^{-1} in the subset not receiving ACE-I/ARB therapy (-31%; $n = 13$; $p < 0.01$).

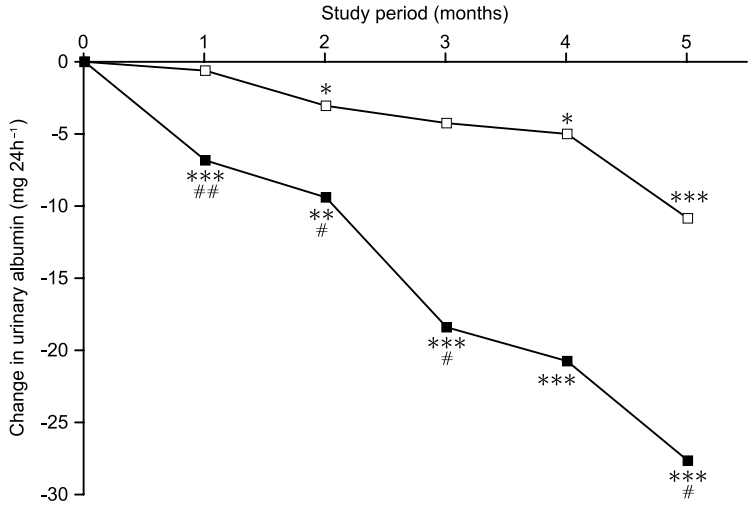

Figure 13.2: Effect of high-dose thiamine on UAE in type 2 diabetes patients. Data represent the change from baseline of UAE in type 2 diabetic patients receiving thiamine (black squares) or placebo (white squares). Data are median values. $* = p < 0.05$; $** = p < 0.01$; $*** = p < 0.001$ with respect to baseline. $\# = p < 0.05$; $\#\# = p < 0.01$ with respect to baseline change for the placebo.

There was no significant effect of thiamine supplementation on glycaemic control, dyslipidaemia, blood pressure, GFR or markers of vascular dysfunction during the treatment period. After the washout period, fasting plasma glucose was decreased with respect to baseline concentration in the thiamine treatment and placebo groups ($p < 0.05$) and HbA_{1c} was decreased with respect to baseline and 3 months after therapy in the thiamine treatment group ($p < 0.01$). At this time, total cholesterol and LDL-cholesterol increased in patients treated with placebo, and LDL-cholesterol decreased in patients who had received thiamine therapy. HDL-cholesterol decreased significantly from baseline after the 3 month treatment period in patients treated with both thiamine (-16%; $p < 0.05$) and placebo (-22%; $p < 0.01$). HDL-cholesterol returned to baseline values in both groups after the washout period. Patients receiving placebo showed significant increases in triacylglycerol from baseline after the 3 month treatment and washout periods ($+18\%$ and $+30\%$, respectively; $p < 0.05$). Patients receiving thiamine had a significant increase in systolic BP after the washout period ($+7.1\%$; $p < 0.05$). After the washout period, there was also a decrease from baseline and post-therapy concentrations of sVCAM-1 in patients receiving thiamine (-107 and -73 ng mL^{-1} respectively; $p < 0.05$) (Table 13.1).

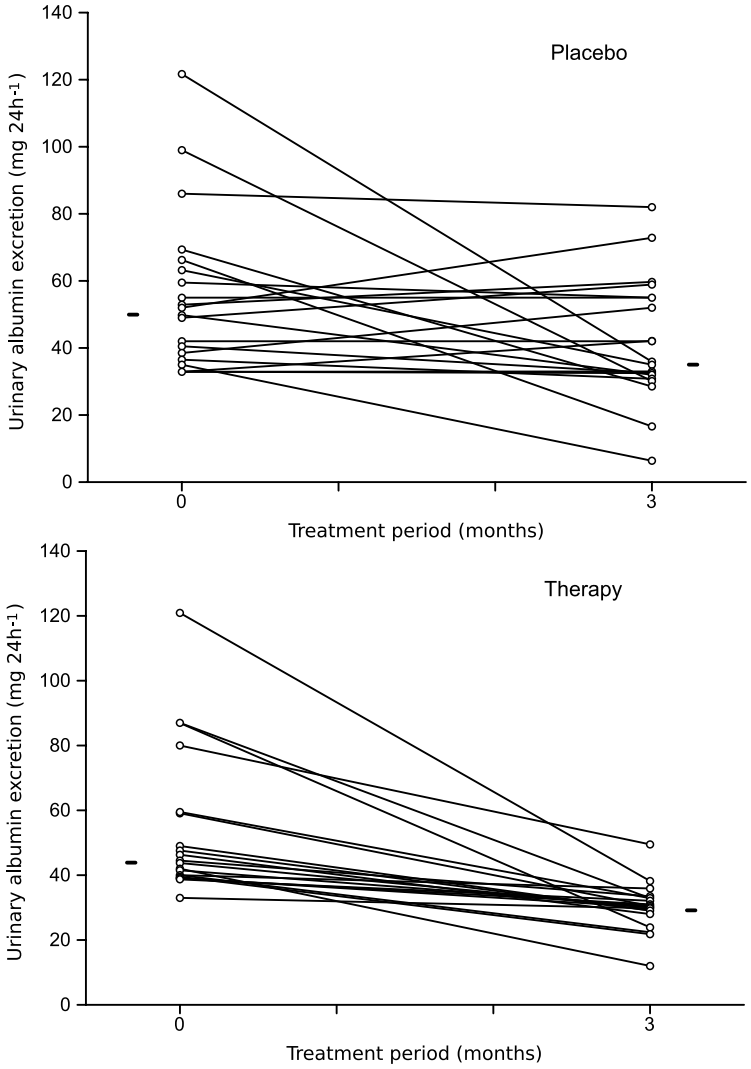

Figure 13.3: Individual changes in UAE of patients receiving placebo (top; $p > 0.05$) or thiamine therapy (bottom; $p < 0.001$). Median values are indicated by black horizontal bars.

In order to explain why the effects of the supplementation continue into the washout period, it is necessary to consider the biological half-life of thiamine. This is only two days in the plasma [Weber and Kewitz, 1985] but the overall biological half-life is much longer at 9–18 days [Ariaey-Nejad et al., 1970]. The plasma concentration and urinary excretion of thiamine in the thiamine treatment arm of the study return to baseline concentrations after the washout period but it is reasonable to assume that the tissue concentration of thiamine remained elevated for at least one half-life which may explain the extra benefit obtained by patients during the washout. This extension of the therapeutic affect may have contributed to the decrease in median plasma sVCAM-1 concentration which only achieved significance after the washout period.

The placebo effect observed, which is often present in such trials, may be potentially explained by two factors. The first is a possible increase in the quality of primary care afforded to patients whilst participating in the trial. The second is that patients on the trial may be more acutely aware of their health. As a result they may be making more of a concious or unconcious effort to follow good practice with regard to diet, exercise and so on whilst on the trial. Either of these factors could contribute to the effects seen.

This pilot study has demonstrated that high dose thiamine therapy at $3 \times 100\,\text{mg}$ daily decreased UAE in type 2 diabetes patients with microalbuminuria after 3 months of therapy. In 35% of cases after 3 months' therapy, a regression to a normal albumin excretion

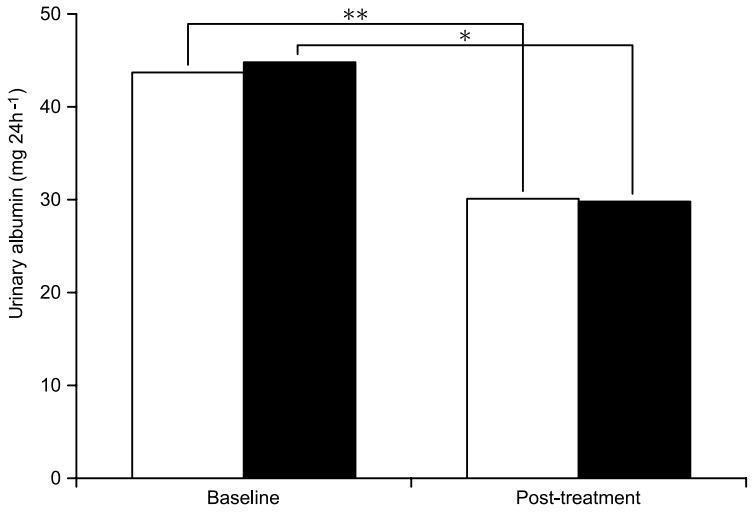

Figure 13.4: Effect of ACE-I/ARB therapy on UAE. Data represent the median UAE for patients receiving thiamine therapy with (black bars) and without (white bars) concomitant ACE-I/ARB therapy. $* = p < 0.05$; $** = p < 0.01$.

rate from microalbuminuria was observed. The study also confirmed previous reports that diabetic patients have a low plasma thiamine concentration and the correlation between plasma thiamine and sVCAM-1 concentrations [Thornalley et al., 2007]. Since this was a pilot-scale project, a larger study will be needed to confirm the therapeutic effects of thiamine in diabetic patients.

Chapter 14

General discussion

The aim of this project was to investigate the link between diabetes and thiamine status, specifically the role of the kidney in the state of plasma thiamine deficiency seen in diabetic patients [Thornalley et al., 2007]. This link was investigated using a multi-strategy approach. The location of the thiamine transporters THTR-1 and THTR-2 was investigated in normal kidneys by immunohistochemistry. Secondly, many aspects of thiamine metabolism in low and high glucose and low and high thiamine concentrations were investigated *in vitro* in PTECs, both HK-2 cell line cells and those freshly isolated from a human kidney. Finally, the effect of thiamine supplementation on nephropathy in patients with type 2 diabetes was investigated in a supplementation trial based in Pakistan.

14.1 Comparison of model systems

Three different models of diabetes have been used throughout this thesis. The most relevant of these is not semantically speaking a model for diabetes but rather a model for the entire diabetic population. These are the patients who volunteered for the Pakistan thiamine supplementation trial. Since there is no abstraction between the experimental volunteer and the target of the research, patient volunteers are the gold standard for experimentation. Many experiments though require more abstract models to avoid technical, financial or ethical constraints. This abstraction requires that the results of such experiments, and their implications and limitations, are interpreted accordingly.

The other two models used herein are the *in vitro* cell systems. Both the human PTEC primary cultures and the HK-2 cell line cultures are representative of the epithelium of the human proximal tubule. However, they have been treated very differently since

extraction from a kidney. These differences in treatment are important since they affect the cells and thus also the experimental results gained from them. One major difference is that the cells in the HK-2 cell line were immortalised shortly after removal from the kidney. The immortalisation used viral transduction with the HPV 16 E6 and E7 genes. E6 acts with the host E6 associated protein to ubiquitinate the tumour suppressor p53, thereby targeting it for degradation [Münger and Howley, 2002; Hawley-Nelson et al., 1989]. E7 competitively inhibits the binding of the transcription factor E2F-1 to retinoblastoma protein (pRb) which would normally act to suppress its activity. With no pRb bound, E2F-1 acts with its binding partner DP-1 to transactivate its targets which promote cell cycle progression by stimulating the G1/S transition and S-phase progression [Münger and Howley, 2002; Halbert et al., 1991]. E6 and E7 have also been implicated in the decreased expression of TGF-βR1 [Hypes et al., 2009]. This transduction process applied a selective pressure to the cells during the transduction period and removed certain selective pressures after transduction: with p53 effectively inactive, mutations due to genetic instability which would normally cause a cell to undergo apoptosis are allowed to persist. If such mutations confer even a slight selective advantage over the wild-type cells then the mutated cells will easily out-compete the wild-type within a few generations [Masters, 2002; Capes-Davis et al., 2010].

As well as the selective pressures of the immortalisation procedure, the HK-2 cells have been removed from the kidney for an extended period of time. Such cells would normally have been stored in a liquid nitrogen cryostore for large portions of that time. However, there remains the possibility of large periods of time when the cells were under culture. The HK-2 cell line was first established in 1993 [Ryan et al., 1994] yet it is not stated exactly which cells were deposited with the ATCC, only that the cells had been growing in their laboratory for periods of more than one year. It is thus possible that the original frozen cells deposited with the ATCC were one year old. The ATCC will have defrosted these to expand the stocks and then re-frozen again. Upon receipt from the ATCC, I defrosted, re-froze and defrosted the cells again. This is three freezings and three defrostings in a best-case scenario assuming optimal handling since extraction. Each of these freezings exposed the cells to cryoprotectants such as DMSO and it is clear from survival rates of only 70–90% upon defrosting that freezing applies a substantial selective pressure on the cells. The nature of this selective pressure can not be readily known.

The situation is further complicated by the composition of routine commercially available tissue culture medium. The concentrations of thiamine (6.5 µM) and glucose

(>15 mM) amongst others are chosen to aid growth in an *in vitro* environment. During cell culture with a physiological 5 mM glucose, the concentration of glucose in the medium dropped to between 3.5–4 mM after 24 hours depending on the confluence of the cells. Thus, medium was changed daily to prevent extreme hypoglycaemia. Daily medium changes would be an inconvenient expense for many experiments which is why routine culture medium is supplied with a higher glucose concentration. However, knowledge of why the concentrations are non-physiological does not alter the fact that both glucose and thiamine concentrations are above the normal physiological upper limit (thiamine concentrations should be in the low nanomolar range and glucose concentrations should ideally be lower than 6.1 mM [World Health Organization, 2006]). These high concentrations pose specific problems to research. At such concentrations of thiamine, a cell needs no active transport mechanism for the vitamin since sufficient acyclic, unionised thiamine could diffuse directly across the membrane. This means that all the aforementioned selective pressures have been applied in an environment where there is no need for the cells to maintain a normal thiamine metabolism. It is indeed advantageous, evolutionarily, for cells to stop manufacturing thiamine transport proteins since they are metabolically costly to synthesise and unnecessary. This is most evident observing the expression of THTR-2 in HK-2 cells. THTR-2 is an important part of normal cellular thiamine transport and yet appears to be completely absent in the HK-2 cells. Immunohistochemistry images do not show the presence of any THTR-2 and real time qPCR results comparing HK-2 cells to human kidney cortex stored at −80℃ show that the kidney has 120× the relative abundance of THTR-2 mRNA transcript compared to β-actin. It is likely that a mutation that stops cells expressing THTR-2 would provide a selective advantage in such a system because the protein is not necessary and by not expressing it the new population of cells would be able to grow quicker and out-compete the wild-type cells.

The PTECs extracted from the human kidney and grown in primary culture are very different from the HK-2 cells. They have never been exposed to non-physiological concentrations of *any* metabolite, growth factor, vitamin or similar compound. They were growing in primary culture within 48 hours of the death of the donor and were only exposed to high glucose and thiamine concentrations as part of an experimental procedure. However, these cells are not free of potential problems. The kidney they were isolated from was chilled on ice immediately after removal and remained on ice without a circulatory system for the duration of transport to the laboratory. They were digested from the kidney using type 2 collagenase, which despite being more highly purified than type 1 collagenase, still

contains residual clostripain activity. Clostripain, also known as endoproteinase Arg-C, is a sulphydryl proteinase that cleaves proteins on the carboxyl peptide bond of arginine residues. This means that proteins expressed on the cell surface other than the collagen in the ECM will have been partially hydrolysed. It is impossible to know what effect this will have had on the cells. Although it is likely that effects would have been short-lived and confined to the first few generations of cells grown *in vitro*, trypsin was subsequently routinely used to separate the cells from the substratum during passaging. This would have further damaged the cells in ways that were unknown in common with every *in vitro* cell experiment. Other selective pressures applied during the isolation of the kidney proximal tubule cells include their shaking in a water bath during the digestion period, their chilling to 4℃ and their separation in Percoll at $30\,000 \times g$. This centrifugal force is not as devastating as first imagined because the cells are buoyant meaning that the force is applied only across the narrow diameter of each cell. The effects of the shaking, chilling, spinning and re-warming are not known and can not be controlled for.

From this discussion it is clear that the two cell models are not equal. The human proximal tubule epithelium primary cell cultures represent only a relatively small abstraction from the *in vivo* diabetic kidney proximal tubule and so are likely to produce results more representative of *in vivo* conditions. The HK-2 cell line has been manipulated relatively extensively since its removal from a kidney and is thus even further removed from a diabetic kidney. This abstraction is often tolerated throughout *in vitro* research because cell line models offers an ease of use and availability far above that of primary cell cultures.

14.2 Experimental and analytical decisions

It is important to be able to justify experimental choices made throughout the period of study. These choices can be subdivided into those about which experiments were performed and those which guide experimental design. To begin, there were differences between experiments performed in the HK-2 cells and experiments performed in the primary cultures of PTECs. For example, there was no analysis of glycosylation performed in the primary PTEC cultures, nor was the abundance of Sp1 analysed. This can be explained by circumstance. The original research plan was to use solely the HK-2 cell model as this was commercially available. This meant that for the early part of the research, all experiments were conducted in HK-2 cells. The opportunity for using freshly isolated PTECs cells was welcomed but unplanned. The decision was made to attempt the same experiments in cells

in primary culture as those conducted in the HK-2 cell model. At all times the experimental choices were guided by the original hypothesis for the project. Thus, after PTEC characterisation, the abundance of THTR-1, the mRNA quantitation data, intracellular thiamine concentrations, intracellular hexosamine pathway product concentrations, transketolase activity and [^{3}H]thiamine handling were prioritised. The differences between HK-2 cells and the fresh PTECs were marked which has serendipitously revealed that the HK-2 cell model may not be suitable for many of the *in vitro* investigations.

14.2.1 Cell culture methods

It is equally important to discuss the choices made for individual experiments. One common element to all *in vitro* work conducted was the use of cell culture. In the case of both cell types, culture was carried out in an identical manner to ensure comparability between the results. Each harvest of cells was preceded by five days of culture in the relevant experimental culture condition. This five day period was chosen based on the doubling time of the cells (around 24–30 hours). Assuming pure exponential growth with a 24 hour doubling time, there are 32× the starting number of cells at the point of harvest than at the start of the incubation; a 30 hour doubling time yields 16× as many cells in the same period. This is important because it allows sufficient dilution of the original cell stock for factors such as protein turnover not to be critically important. By way of example, if cells were at near confluence and then exposed to an experimental condition which caused decreased expression of protein x, unless protein x was actively degraded, the decreased expression may not be represented by decreased abundance in the cells at harvest. The effective dilution of protein and metabolites (by exponential growth of both intracellular volume and membrane area under culture) means that even if protein x is not actively degraded, an effect on expression should translate to an observable change in protein abundance. In reality, many proteins have a relatively short half-life, but this was not investigated so could not be relied upon. The same principle of exponential decay applies to intracellular metabolite concentration.

In addition to the extended culture periods for each experiment, HK-2 cells were cultured in 5 mM glucose, 4 nM thiamine medium for a minimum of two weeks after removal from the cryostore. This extended period of culture was intended to ameliorate the effect of any "metabolic memory" that the cells may have had from previous culture in high glucose and high thiamine conditions [Ceriello et al., 2009]. There is no precedent for how long cells should be cultured to remove any possible memory effect and there is no known way to quantify any potential memory although there is evidence that memory may be

epigenetically mediated [Siebel et al., 2010; Tonna et al., 2010]. The two week period was an arbitrary decision based on the rate of growth of the cells. Assuming exponential growth with a relatively slow 30 hour doubling time, cells grown for two weeks will have grown to $2^{((14\times24)/30)}$ or around 2300× their original number over 11 generations. Given that it is not possible to assay effectiveness of this treatment, the only guarantee of using cells that have no metabolic memory of previous conditions is to use cells isolated from a human kidney which have never been exposed to non-physiological concentrations of either thiamine or glucose.

Another factor which should be considered with regard to cell culture is the potential for 26 mM glucose to cause an effect in cells by osmotic stress alone. If this were the case then any high concentration sugar would cause effects in a similar manner to D-glucose. This can be controlled for using D-mannose or L-glucose as an osmotic control to D-glucose. Such a control was performed but only with the HK-2 cells and only when quantifying mRNA abundance. The cells were grown in 5 mM glucose medium and the hexose concentration was raised to 26 mM by addition of D-glucose, L-glucose or D-mannose. A PBS blank was also performed. There was no difference between PBS, L-glucose or D-mannose treated cells in expression of 6 representative genes. To be rigorous, an osmotic control should have been used in all situations where cells were exposed to high glucose concentrations.

14.2.2 Discrepancies between the HK-2 cell and the primary cell cultures

The results presented throughout this thesis demonstrate several differences between the two cellular model systems and many have been discussed in individual sections. One set of results, the mRNA abundance data from the qPCR experiments, are of particular note. The gene TXNIP was included in the mRNA analysis because it is a useful positive control for exposure to hyperglycaemia. Qi et al. [2007] demonstrated an 11–12-fold increase in expression in TXNIP in HK-2 cells cultured for 11 days in 30 mM glucose relative to 5 mM glucose. The results for expression of TXNIP in HK-2 cells presented in Figure 9.6 only showed a 1.6–1.7-fold increase after culture in 26 mM glucose for 5 days. In contrast, the primary cell cultures showed a 48–65-fold increase in expression of TXNIP under the same conditions (Figure 9.3). In all other cases, the HK-2 cell results show similar signs of being decreased in magnitude relative to the primary cell result. In some cases, the HK-2 cell result is opposite to the primary culture result e.g. the GFAT-1 mRNA abundance in the primary cell cultures was ablated by 90% in the hyperglycaemic cultures—a strong response.

The same results in the HK-2 cell line shows a relatively mild 30% increase in abundance.

The fact that the HK-2 cells do not exhibit a marked change in gene expression in response to a 26 mM glucose assault in a manner similar to the primary cell cultures suggests that they have somehow become adapted to the higher glucose conditions. They do respond in some cases but only in a muted fashion. It is conceivable that have adapted to routine high glucose culture so much that even periods of extended culturing in 5 mM glucose can not promote a marked change in gene expression when cells are returned to 26 mM glucose culture.

The case for abnormal thiamine handling in HK-2 cells is strongest when data from immunohistochemical and qPCR are combined to corroborate the lack of the THTR-2 transporter, an important part of thiamine transport *in vivo*: the abundance of mRNA for THTR-2 in the HK-2 cells is less than $^1/_{100}$ of that found in normal kidney cortex and there is no evidence of immunostaining for THTR-2 in HK-2 cells. Further evidence from intracellular thiamine metabolite concentrations suggests that the interconversion of the thiamine metabolites is not the same as *in vivo*. When cultured in physiological concentrations of thiamine, the HK-2 cells maintain a substantial portion of their thiamine pool in the forms of TMP (22–25%) and THM (22–26%)—something not seen in the primary PTEC cultures where all thiamine is held in the form of TPP in the low thiamine conditions. Since the aim of this thesis was to investigate thiamine mis-handling in diabetes, it would be improper to rely upon results generated in a model system which clearly doesn't represent *in vivo* thiamine handling prior to experimental manipulation.

14.3 Effects of hyperglycaemia on PTECs *in vitro*

The effects of hyperglycaemia on the PTECs *in vitro* were not all concordant and in keeping with the proposed hypothesis of hexosamine pathway activation and down regulation of thiamine transporter expression in model hyperglycaemia. There is strong evidence supporting our hypothesis explaining why diabetic patients are thiamine deficient—decreased renal re-uptake of thiamine—but the evidence does not support the mechanistic hypothesis regarding why thiamine transport becomes deficient. Our hypothesis proposes that the plasma thiamine deficiency is caused by decreased renal re-uptake of thiamine elicited by a decrease in abundance and expression of thiamine transporters. Primary PTECs cultured in hyperglycaemic primary culture exhibit substantial decreases in abundance of mRNA for both the main thiamine transporters, THTR-1 and THTR-2, with a smaller decrease for

the TMP-transporting RFC-1. These decreases are mirrored by a decrease in abundance of THTR-1 as demonstrated by western blotting, and a shift in the (apical to basal):(basal to apical) P_{app} ratio away from apical to basal transport of thiamine across monolayers. These steady state observations alone could potentially explain the decreased plasma thiamine concentration in diabetic patients—the decrease in mRNA abundance of THTR-1 in the primary cultures is approximately equal to the decreases in abundance of THTR-1 protein in the same cells which in turn is approximately equal to the plasma thiamine deficiency seen in diabetic patients surveyed in Colchester [Thornalley et al., 2007]. It is unfortunate that the monolayer experiments designed to determine parameters of transport kinetics of thiamine across monolayers of PTECs were not successful. No experiment yielded a K_{m} or a $V_{\max}$ value for thiamine transport which leaves most kinetic questions unanswerable. The intracellular concentration of thiamine pyrophosphate is not altered in +G−T relative to −G−T in the primary PTEC cultures (discussed detail in Section 11.1). Also TKT activity is also unchanged in hyperglycaemic culture (discussed in Section 11.2) despite down-regulation of TKT mRNA in primary PTECs in high glucose conditions.

Whilst the data may support our hypothesis as to *why* diabetic patients are thiamine deficient, they do not support it regarding *how* this deficiency is brought about. The hexosamine-pathway based theory posited in Chapter 5 proposes that an increased flux through the hexosamine pathway causes increased *O*-GlcNAcylation of target proteins including Sp1 which in turn leads to decreases in expression of the thiamine transporters. The evidence against our hypothesis includes the unchanged or decreased intracellular UDP-GlcNAc concentrations, the profound down-regulation of GFAT (−90%; the enzyme with most control of flux through the HBP), the down-regulation of OGT (responsible for *O*-GlcNAcylation of proteins), and the down-regulation of Sp1 in primary PTECs exposed to hyperglycaemia. There is also a trend for increased expression of *O*-GlcNAcase, the enzyme responsible for removal of *O*-GlcNAc residues from proteins. Combined, these data suggest that the flux through the hexosamine pathway may be decreased in hyperglycaemia in the primary PTECs. Even though functional data on Sp1, OGT, *O*-GlcNAcase and GFAT are not available in primary PTECs, alternative hypotheses must be sought to attempt to tie these disparate observations together.

14.3.1 Alternative hypotheses

Down-regulation of Sp1 The transcription rate of the genes for THTR-1 and THTR-2 (*SLC19A2* and *SLC19A3*) is dependent on the transcription factor Sp1. Although Sp1

glycosylation has been shown to be important in the regulation of many genes, it has not been demonstrated for these two genes. Instead, what has been shown is that the transcription of *SLC19A2* is increased in a dose-dependent manner by the addition of Sp1 and that the transcription of *SLC19A3* is dependent on a GC box element bound by both Sp1 and Sp3 (Section 2.8.4). Perhaps then, it is the abundance of Sp1—and not the glycosylation status—which is important in determining transcription rate of the *SLC19A2* and *SLC19A3* genes. *Sp1* expression was decreased in the primary PTECs exposed to hyperglycaemia. It was not decreased in the HK-2 cells in the same conditions but neither was the abundance of Sp1 protein. My opinions regarding the use of the HK-2 cell model are discussed above.

Nicolás et al. [2003] studied the transcriptional regulation of the *Sp1* gene and identified binding sites for Sp1 and Sp3, nuclear factor Y (NF-Y), activator protein 2 (AP-2), CCAAT/enhancer-binding protein (C/EBP) and E2F transcription factors. Increased *Sp1* gene expression was observed upon overexpression of Sp1 (in a positive feedback mechanism), NF-Y and E2F. The activation of *Sp1* transcription by Sp1 overexpression was countered by simultaneous Sp3 overexpression. Nicolás et al. [2003] conclude that the expression of *Sp1* is dependent on the relative abundance of Sp1, Sp3, E2F and NY-F proteins in the cell with only Sp3 down-regulating *Sp1* expression.

The balance of evidence in the primary PTECs is in support of decreased *O*-GlcNAcylation in hyperglycaemia. This would potentially lead to the decreased glycosylation of Sp1. Hypoglycosylated Sp1 is unstable and rapidly targeted for degradation in the proteasome [Han and Kudlow, 1997] which would initiate a feedback loop whereby Sp1 is degraded, leading to decreased transcription of Sp1. The decreased abundance of Sp1 could then be responsible for the decreased abundance of the thiamine transporters.

Poor hexosamine pathway activity in hyperglycaemia There is strong evidence that the flux through the HBP is increased in hyperglycaemic conditions in a wide variety of cell types including bovine aortic endothelial cells [Du et al., 2000], pancreatic β-cells [Kaneto et al., 2001], cardiomyocytes [Clark et al., 2003], lymphocytes [Srinivasan et al., 2007] and mesangial cells [Kolm-Litty et al., 1998; Zheng et al., 2008]. However, little evidence has been published regarding podocytes or proximal tubules. Recent work in podocytes has indicated that GFAT-1 activity is low and that they may need to take up exogenous glucosamine to increase *O*-GlcNAcylation *in vivo* [Rogacka et al., 2010]. Work by Rocco et al. [1992] demonstrated that hyperglycaemia induces TGF-β expression in a mouse proximal tubule cell line but gave no indication of increased hexosamine pathway

flux. Glucosamine has also been shown to activate TGF-β expression in proximal tubule cell lines [Schleicher and Weigert, 2000] but addition of exogenous glucosamine is highly removed from *in vivo* conditions. It is certainly a possibility that hexosamine pathway flux is not increased in proximal tubule cells in hyperglycaemic conditions *in vivo*, indeed the intracellular UDP-GlcNAc concentrations and mRNA evidence presented herein suggests a decrease in flux through the HBP.

GFAT has a high degree of control over flux through the hexosamine pathway and is a finely regulated enzyme. The layers of GFAT regulation include its low affinity for both its substrates (3–10 mM), allosteric feedback inhibition by its ultimate product UDP-GlcNAc and cAMP-dependent phosphorylation which increases its activity [Schleicher and Weigert, 2000]. The promoter elements for the mouse GFAT-1 gene were investigated by Sayeski et al. [1997] who concluded that the promoter does not have a TATA box but does have several GC boxes within a rich GC domain. Sp1 binds to three elements in this promoter and plays a key role in the regulation of GFAT-1 transcription but the authors conclude that there are other proteins involved in regulation of transcription which remain unidentified. The evidence presented in Chapter 10 showing UDP-GlcNAc abundance in PTECs supplemented with glucosamine, glutamine and glucose has confirmed that GFAT activity is crucial in controlling the intracellular concentration of UDP-GlcNAc. The biological half life of GFAT in adipocytes was estimated to be less than 1 hour by Marshall et al. [1991] and there was a strong correlation between GFAT activity and expression found in lymphocytes [Srinivasan et al., 2007]. Even if the biological half-life of GFAT was 10$\times$ longer in PTECs than in adipocytes, then despite the lack of protein evidence, it is reasonable to assume that GFAT activity will be decreased in line the decrease in its expression after five days of culture in hyperglycaemic conditions. In the absence of data on total cellular glycosylation, it is highly unreasonable to assume that flux through the hexosamine pathway and cellular glycosylation are increased given the mRNA and UDP-GlcNAc concentration data.

If increased flux through the hexosamine pathway is not responsible for down-regulation of THTR-1 and THTR-2 then this may also explain why the expression of the thiamine transporters is not restored by addition of high dose thiamine. The hexosamine pathway-based theory proposes that transketolase activation by addition of thiamine diverts glucose away from the HBP, thereby lowering cellular *O*-GlcNAcylation. However, if cellular *O*-GlcNAcylation is not responsible for the down-regulation of THTR-1 and THTR-2 then there is no reason that high thiamine should restore their expression. This is something borne out by all results in this thesis: high dose thiamine does not correct hyperglycaemia-

induced dysfunction in PTECs. High dose thiamine may still be affecting flux through the HBP in other cell types (e.g. mesangial cells), something that may be behind the mechanism of thiamine therapy in type 2 diabetes patients with microalbuminuria.

PKC activation Another proposed mechanism of hyperglycaemia-mediated damage in diabetes is the activation of protein kinase C (Section 1.7.3). PKC activation has been linked to decreased activity and expression of the reduced folate carrier, RFC-1 [Halwachs et al., 2007]. The genes *SLC19A2* and *SLC19A3* for THTR-1 and THTR-2 are in the same family as the gene *SLC19A1* for RFC-1. It is therefore at least possible that the decreases in THTR-1 and THTR-2 expression are due to increased activity of protein kinase C in hyperglycaemia, something that would require further investigation to confirm or refute.

14.4 Effect of high thiamine supplementation

This thesis has demonstrated two incongruous results upon thiamine supplementation in diabetic model systems. The data from the Pakistan thiamine supplementation trial have demonstrated that thiamine has a beneficial effect on the rate of urinary albumin excretion, halting its increase or even lowering it. Conversely, *in vitro* work has shown that thiamine supplementation does *not* have a noticeable effect on hyperglycaemia-induced changes. For example, there is no restoration in abundance of thiamine transporter mRNA or protein when PTECs exposed to hyperglycaemia are supplemented with thiamine.

These observations are at odds with one another. It was proposed that hyperglycaemia was the cause of the diabetic thiamine deficiency in the manner shown in Figure 14.1. The hypothesis was that supplementation with thiamine would intervene with this spiral at the point of reduced transketolase activity: high thiamine supplementation should increase the activity of the enzyme transketolase. This in turn would allow a greater flux through the reductive pentose phosphate pathway, increasing the flux from glycolysis to relatively low reactivity metabolites such as ribose-5-phosphate. However, when measuring transketolase activity in the primary cell cultures, there is no decrease observed in hyperglycaemic conditions and no increase in activity in high thiamine conditions. There are at least three explanations for this conundrum.

Thiamine therapy affects glomerular and not tubular cells It is possible that thiamine supplementation is not affecting proximal tubules, either in diabetic patients or *in vitro*. The trial in Pakistan assessed urinary albumin excretion without assessing the

kidney tissue directly. It is generally accepted that the cells of the glomeruli play the major part in the excretion of albumin into the urine with the tubules playing a more minor role (discussed in Section 1.6.2.5). This opens the possibility that thiamine therapy is affecting the glomerular cells (or a subset thereof) and not the tubules. This would also explain why thiamine therapy does nothing to reverse the underlying cause of the deficiency—patients receiving thiamine therapy in the Pakistan trial saw no reduction in the clearance rate of thiamine at the end of the washout period relative to baseline. Thiamine clearance is solely determined by the rate of re-absorption by the proximal tubules since it is filtered completely in the glomerulus. Perhaps thiamine therapy only serves to replenish the vitamin faster than it can be lost through the kidneys. In this manner, a normal or even elevated plasma thiamine concentration (and by extension, glomerular cell concentration) can be maintained despite high losses in the urine. This is corroborated by the evidence in this thesis that thiamine thiamine supplementation does nothing to correct hyperglycaemia-induced thiamine mishandling in PTECs *in vitro*.

Artefacts of *in vitro* culture are obscuring the effect of thiamine The steady state conditions of the *in vitro* experiment may be confounding the results. It could be that *in vivo*, a decreased thiamine transporter expression markedly decreases the intracellular

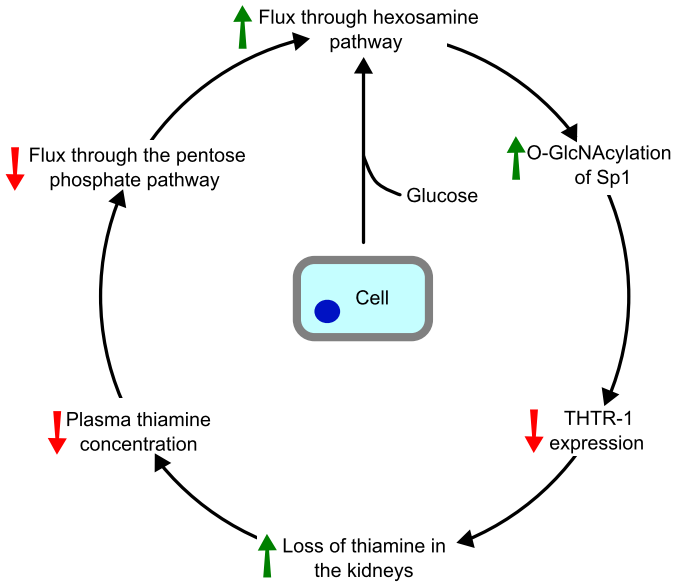

Figure 14.1: Thiamine deficiency spiral beginning with hyperglycaemic assault and ending trapped in a low thiamine state.

concentration of thiamine in the PTECs. *In vitro*, the decreased abundance of thiamine transporters does not present a functional problem to the cell because they are continually bathed in a constant thiamine concentration. Even with a low uptake rate, it may be possible for cells to acquire an optimal intracellular concentration of thiamine. Both of these possibilities could be investigated further using an *in vivo* model of diabetes and measuring thiamine status and transketolase activity in tubules and glomeruli (see Appendix C).

Thiamine therapy primarily affects TPP-dependent enzymes other than TKT Transketolase was chosen as a representative of TPP-dependent enzymes but it is also possible that another enzyme such as pyruvate dehydrogenase or α-ketoglutarate dehydrogenase is affected by a thiamine deficiency. Work by Tylicki et al. [2008] has demonstrated that thiamine supplementation can increase both PDH and α-KGDH activity in rat hearts following myocardial infarction. By extension, it is possible that thiamine supplementation is having a similar effect in the kidney but this has not been investigated. If this were the case then it may be possible that PDH or α-KGDH activity is diminished in the PTECs *in vitro* when exposed to hyperglycaemic conditions and that the high thiamine supplementation corrects this deficiency. However, since the published literature is so sparse, without study of the activities of TPP-dependent enzymes other than TK *in vitro*, and perhaps *in vivo*, this possibility remains only a speculation.

In summary, there is a discrepancy between the beneficial effect of thiamine *in vivo* and the absence of any effect of thiamine on PTECs *in vitro*. Three main possibilities present themselves as explanations of this conflict. The first is that the supplementation is not affecting tubules at all, but rather mesangial cells or other glomerular cells. The second is that there is a problem with the *in vitro* experimental design which is masking any effect that would be seen *in vivo* and the third is that the involvement of other TPP-dependent enzymes is masking the effects *in vitro* since only TK was investigated. Of course, a combination of these factors is also possible.

14.5 Benfotiamine intervention trials

Our thiamine intervention trial has shown a beneficial effect of thiamine supplementation on UAE in type 2 diabetic patients. Recently, Alkhalaf et al. [2010] published a trial investigating the effect of the thiamine monophosphate derivative Benfotiamine on UAE and the tubular damage marker kidney injury molecule 1 (KIM-1) in patients with type

2 diabetes and nephropathy. Patients recruited to the study had a UAE between 15–300 mg day^{-1} despite treatment with ACE inhibitors or angiotensin receptor blockers. 86 patients were randomized to treatment (3× 300 mg oral Benfotiamine daily) or placebo arms and the study was carried out over 12 weeks with measurements at baseline, 6 weeks and termination.

At baseline, there was no difference in whole blood or plasma thiamine concentration between the therapy arm and the placebo arm. The plasma thiamine concentrations were 31.8±7.7 nM in the therapy arm and 31.6±9.8 nM in the placebo arm. Whole blood thiamine concentrations were 126±23 nM in the therapy arm and 122±23 nM in the placebo arm. Supplementation with Benfotiamine increased the whole blood thiamine concentration relative to the placebo at both 6 weeks and 12 weeks; $p < 0.001$ (6 weeks: 290±21 nM versus 124±25 nM; 12 weeks: 300±0 nM versus 138±30 nM). The authors did not report plasma thiamine concentrations at 6 or 12 weeks. The Benfotiamine supplementation also increased erythrocyte transketolase activity (0.41±0.10 mU mgHb^{-1} at baseline and 0.53±0.15 mU mgHb^{-1} at 12 weeks in the therapy arm; 0.38±0.11 mU mgHb^{-1} at baseline and 0.41±0.10 mU mgHb^{-1} at 12 weeks in the placebo arm; $p < 0.001$).

These improvements in thiamine status did not translate to improvements in the primary endpoints of the study, however. There was no significant decrease in UAE in the therapy arm relative to the placebo arm ($p = 0.36$). The change in the UAE from baseline to 12 weeks was −18 mg day^{-1} in the therapy arm and −1 mg day^{-1} in the placebo arm. Likewise there was no difference in KIM-1 excretion between therapy and placebo ($p = 0.12$). These results are in contrast to the results we obtained in Pakistan (Chapter 13, [Rabbani et al., 2009]). There are several differences between the two studies which may explain this discrepancy. A key difference is that the two studies use different therapies: Benfotiamine and thiamine. Benfotiamine is a thiamine monophosphate derivative and markedly increases the plasma thiamine monophosphate concentration in a way that thiamine does not (demonstrated in rats by Babaei-Jadidi et al. [2004]). Thiamine monophosphate can be taken up into cells by the reduced folate carrier (RFC-1). Once in the cells, there is no direct mammalian enzymatic route to convert TMP to TPP, instead TMP is dephosphorylated to thiamine and then pyrophosphorylated to TPP by thiamine pyrophosphokinase (Figure 2.6, page 38). Thiamine pyrophosphokinase is non-competitively inhibited by TMP (K_i = 200 µM) and it is thus conceivable that the influx of TMP is preventing its enzymatic conversion to the active TPP. Of course, there are a large number of hydrolases which are capable of dephosphorylating TMP to THM so the effect of this inhibition may be miti-

gated. Studies in streptozotocin-induced diabetic rats investigating the effects of thiamine and Benfotiamine on dyslipidaemia also show that thiamine alone, and not Benfotiamine, is able to counter dyslipidaemia [Babaei-Jadidi et al., 2004].

The two trials differ also in the extent of albuminuria exhibited at baseline. The median UAE at baseline in our study was 44 mg day^{-1} (33–121 mg day^{-1}) in the thiamine therapy arm and 51 mg day^{-1} (33–122 mg day^{-1}) in the placebo arm. These values are only half the magnitude of the those reported by Alkhalaf et al. [2010] despite that 100% of their patients were receiving ACE-I and ARB therapy compared to fewer than 50% in our trial in Pakistan. It is thus possible that the effect of thiamine is only noticeable in patients with early nephropathy and that the benefit is of limited effect for patients with more advanced nephropathy. *In vivo* studies such as those conducted by Babaei-Jadidi et al. [2003] that show a beneficial effect of thiamine on the progression of DN began supplementation with thiamine soon after induction of diabetes, before nephropathy was present.

Another factor which could explain the difference between the results of the two trials is the different genetic background of the two groups of participants. The trial conducted by Alkhalaf et al. [2010] recruited people in the Netherlands of European descent and our trial recruited people of Pakistani descent. It is unknown what effect differences in genetics, diet, local health-care or baseline prevalence of thiamine deficiency could have on the trial outcomes. The patients recruited for the Dutch study had a mean plasma thiamine concentration at baseline of 31.8±7.7 nM for the Benfotiamine arm and the 31.6±9.8 nM in the placebo arm, higher than we reported in Pakistan but still lower than our estimate of a normal plasma thiamine concentration of 64.1±12 nM [Thornalley et al., 2007].

Two further pilot-scale trials investigating Benfotiamine intervention in patients with microalbuminuria and either type 1 (Oslo study; clinical trials identifier NCT00117026) or type 2 diabetes (Melbourne study) are due to report soon.

Chapter 15

Conclusions

This project was divided into two main parts: the investigations on why diabetic patients are thiamine deficient and the study of thiamine therapy in diabetic patients with microalbuminuria. The *in vitro* investigations were conducted with immortalised HK-2 PTECs and primary PTECs from a healthy human kidney and were based around the hypothesis that the decreased plasma thiamine concentration seen in diabetic patients was caused by an increase in flux through the hexosamine biosynthesis pathway leading to increased *O*-GlcNAcylation of the transcription factor Sp1 which in turn led to a down-regulation of the thiamine transporters THTR-1 and THTR-2.

One of the most important results from these studies was the marked difference between the two cellular models of diabetes. The extended periods of time that the HK-2 cells have spent removed from a human kidney has allowed them to drift genetically from their original genotype. The nature of routine tissue culture conditions—with high thiamine and glucose concentrations—has modified the selective pressures experienced by the HK-2 cells and yielded a cell model no longer suitable for the study of thiamine handling in hyperglycaemia. The HK-2 cells are completely deficient in THTR-2 and have markedly different thiamine handling characteristics, as exemplified by the ratios of thiamine metabolites held intracellularly. In addition, the HK-2 cells hold higher intracellular concentrations of hexosamine pathway products and have a different ratio of UDP-GlcNAc to UDP-glucose. These results present the quality of the HK-2 cell data as being of very poor quality and thus untrustworthy for further interpretation.

The results from the primary PTECs provide evidence as to why diabetic patients are thiamine deficient. There was a marked 48–80% decline in thiamine transporter expression

in primary PTECs when exposed to hyperglycaemia, irrespective of thiamine concentration. This decline in expression was accompanied by a 77% decline in THTR-1 abundance in high glucose conditions. Also, the ratio of forward to reverse P_{app} values for monolayers of primary PTECs cultured in hyperglycaemia shifted in favour of less apical-to-basal transport in hyperglycaemia. Combined, these data provide strong evidence that there is a diminished rate of uptake of thiamine in proximal tubule epithelial cells in hyperglycaemic conditions.

This project has also yielded interesting data with regard to the hexosamine pathway-based theory of reduction of expression of thiamine transporters. Rather than an increase in flux through the hexosamine pathway, the evidence presented herein supports a decreased flux. There was a 90% decrease in mRNA abundance of GFAT, the enzyme with most control over flux through the HBP, accompanied by decreases in mRNA abundance for OGT and Sp1 in hyperglycaemic conditions. There was a trend for increased abundance of *O*-GlcNAcase mRNA in hyperglycaemia. In addition, the intracellular concentrations of UDP-GlcNAc were decreased in +G−T relative to −G−T. Even without protein abundance or activity data, these suggest a down-regulation in the flux through the hexosamine pathway which does not corroborate the original hypothesis.

Alternative explanations for the decreased abundance of THTR-1 and THTR-2 include the possibility that it is Sp1 abundance, not glycosylation status that is the important factor. If flux through the hexosamine pathway is decreased, then Sp1 is likely to become hypoglycosylated and prone to proteolytic degradation. This decrease in Sp1 would be self-reinforcing because Sp1 protein is able to promote transcription of the *Sp1* gene.

One factor that should not be forgotten is that the primary PTECs were extracted from only one human kidney and there remains a possibility (however remote) that the donor did not have a normal thiamine metabolism. This could only be investigated by comparison with multiple kidneys.

The placebo-controlled thiamine supplementation trial in type 2 diabetic patients with microalbuminuria has shown that 3× 100 mg oral thiamine daily for three months restores plasma thiamine to a normal concentration, despite the increased renal clearance of the vitamin found in diabetic patients. This restoration of plasma thiamine concentration was accompanied by a decrease in urinary albumin excretion after 1–3 months of therapy. After three months, 35% of patients receiving thiamine had regressed from microalbuminuria to normoalbuminuria.

15.1 Further work

Many questions regarding the role of hyperglycaemia in diabetic thiamine deficiency remain unanswered after these investigations and there look to be several promising research topics for the future. Type 2 diabetic patients with early-stage nephropathy have been shown to benefit from thiamine therapy in the placebo-controlled supplementation trial in Pakistan. This trial yielded promising data but was still only of pilot scale with 20 patients recruited to each arm of the study. The findings must be repeated with a larger sample population to confirm the benefit of thiamine to diabetic patients. Further studies would benefit from including patients from a wide variety of ethnic backgrounds with nephropathy covering a wider range of urinary albumin excretion values. The inclusion of type 1 diabetic patients would be a valuable addition to any future study.

In addition to work furthering investigation of thiamine as a therapeutic agent, much work still remains on elucidating the mechanism behind the thiamine deficiency. This thesis has demonstrated a decreased abundance of *SLC19A2* and *SLC19A3* genes accompanied by a decrease in THTR-1 protein in primary PTECs in hyperglycaemia. Quantitation of the abundance of THTR-2 in the same system is of high importance to corroborate the mRNA evidence. To thoroughly investigate the hexosamine pathway-based theory, the abundance and activity of GFAT protein as well as abundance of Sp1 should be established in primary PTECs. Also, direct assessment of total cellular *O*-GlcNAcylation by means of western blot would confirm or refute the evidence that there is a decreased flux through the hexosamine pathway in hyperglycaemia in PTECs. Likewise to test if *O*-GlcNAcylation itself causes down-regulation of THTR-1 and THTR-2, primary PTECs could be incubated with glucosamine to boost the HBP or an inhibitor of GFAT such as azaserine to inhibit the HBP and the abundance of THTR-1 and THTR-2 assayed. Another interesting research topic would be to examine the timecourse that these changes happen over. How long an incubation in high glucose is sufficient to lead to a decrease in expression and abundance of thiamine transporters? Perhaps simulation of elevated post-prandial glucose could be examined to see if that has an effect on the thiamine transporters.

Moving beyond *in vitro* studies, studies in animal models of diabetes would be invaluable in understanding the mechanisms involved on a whole-body scale. Work conducted with cells growing in a flask provides valuable information but cannot hope to recreate the complexities and intricacies of a diabetic animal. There are currently two active projects within the research group which are studying streptozotocin-induced diabetic rats in the hope of answering some of the outstanding questions. The first project is investigating

the effects of thiamine supplementation or tight glycaemic control on the expression and abundance of thiamine transport systems in the glomeruli, tubules, retina, sciatic nerve and other tissues. The second *in vivo* project is investigating whole body thiamine handling by injecting stable isotopically labelled [^{13}C]thiamine and monitoring transport of thiamine into key organs or excretion from the body in diabetic and control animals. Between them, these two studies should reveal crucial information on the handling of thiamine in both healthy animals and diabetic animals (see Appendix C for further details of ongoing work).

Appendix A

Supplementary statistical data

The table in this appendix includes exact p-values and differences for all comparisons made within this thesis. All important statistical data is discussed in the main text. Each row has a figure and page reference followed by a base condition and a target condition. The effect % is the change from the base condition to the target condition. Effect percentages and p-values are given to two significant figures.

Table A.1: Supplementary statistical information

Figure	**Page**	**Base condition**	**Comparison**	**Effect (%)**	p **value**
9.1	158	THTR-1 −G−T	THTR-1 −G+T	−19%	0.0046
9.1	158	THTR-1 −G−T	THTR-1 +G−T	−76%	1.5×10^{-10}
9.1	158	THTR-1 −G−T	THTR-1 +G+T	−80%	6.5×10^{-11}
9.1	158	THTR-1 −G+T	THTR-1 +G−T	−70%	1.1×10^{-8}
9.1	158	THTR-1 −G+T	THTR-1 +G+T	−76%	3.7×10^{-9}
9.1	158	THTR-1 +G−T	THTR-1 +G+T	−18%	0.79
9.1	158	THTR-2 −G−T	THTR-2 −G+T	−8.7%	0.16
9.1	158	THTR-2 −G−T	THTR-2 +G−T	−53%	1.9×10^{-9}
9.1	158	THTR-2 −G−T	THTR-2 +G+T	−54%	1.5×10^{-9}
9.1	158	THTR-2 −G+T	THTR-2 +G−T	−48%	2.7×10^{-8}
9.1	158	THTR-2 −G+T	THTR-2 +G+T	−49%	2.0×10^{-8}
9.1	158	THTR-2 +G−T	THTR-2 +G+T	−2.1%	0.99
9.1	158	RFC-1 −G−T	RFC-1 −G+T	−24%	2.2×10^{-5}
9.1	158	RFC-1 −G−T	RFC-1 +G−T	−39%	5.0×10^{-8}
9.1	158	RFC-1 −G−T	RFC-1 +G+T	−32%	5.9×10^{-7}
9.1	158	RFC-1 −G+T	RFC-1 +G−T	−19%	0.0051
9.1	158	RFC-1 −G+T	RFC-1 +G+T	−11%	0.15
9.1	158	RFC-1 +G−T	RFC-1 +G+T	+10%	0.32
9.2	159	OGT −G−T	OGT −G+T	−19%	0.013
9.2	159	OGT −G−T	OGT +G−T	−63%	2.1×10^{-8}
9.2	159	OGT −G−T	OGT +G+T	−64%	1.5×10^{-8}
9.2	159	OGT −G+T	OGT +G−T	−54%	3.1×10^{-6}
9.2	159	OGT −G+T	OGT +G+T	−56%	2.0×10^{-6}
9.2	159	OGT +G−T	OGT +G+T	−3.9%	0.99

Continued on the next page

Table A.1—continued from the previous page

Figure	Page	Base condition	Comparison	Effect (%)	p value
9.2	159	oGlcNAcase −G−T	oGlcNAcase −G+T	+9.2%	0.93
9.2	159	oGlcNAcase −G−T	oGlcNAcase +G−T	+39%	0.078
9.2	159	oGlcNAcase −G−T	oGlcNAcase +G+T	+52%	0.015
9.2	159	oGlcNAcase −G+T	oGlcNAcase +G−T	+27%	0.23
9.2	159	oGlcNAcase −G+T	oGlcNAcase +G+T	+39%	0.050
9.2	159	oGlcNAcase +G−T	oGlcNAcase +G+T	+9.1%	0.83
9.2	159	GFAT-1 −G−T	GFAT-1 −G+T	−24%	0.019
9.2	159	GFAT-1 −G−T	GFAT-1 +G−T	−93%	3.0×10^{-9}
9.2	159	GFAT-1 −G−T	GFAT-1 +G+T	−93%	3.2×10^{-9}
9.2	159	GFAT-1 −G+T	GFAT-1 +G−T	−91%	2.1×10^{-7}
9.2	159	GFAT-1 −G+T	GFAT-1 +G+T	−90%	2.2×10^{-7}
9.2	159	GFAT-1 +G−T	GFAT-1 +G+T	+4.9%	1.0
9.2	159	Sp1 −G−T	Sp1 −G+T	−17%	0.24
9.2	159	Sp1 −G−T	Sp1 +G−T	−77%	5.6×10^{-7}
9.2	159	Sp1 −G−T	Sp1 +G+T	−76%	6.6×10^{-7}
9.2	159	Sp1 −G+T	Sp1 +G−T	−72%	1.3×10^{-5}
9.2	159	Sp1 −G+T	Sp1 +G+T	−71%	1.6×10^{-5}
9.2	159	Sp1 +G−T	Sp1 +G+T	+4.3%	1.0
9.2	159	TKT −G−T	TKT −G+T	−38%	3.5×10^{-7}
9.2	159	TKT −G−T	TKT +G−T	−62%	2.6×10^{-10}
9.2	159	TKT −G−T	TKT +G+T	−59%	6.1×10^{-10}
9.2	159	TKT −G+T	TKT +G−T	−39%	8.6×10^{-5}
9.2	159	TKT −G+T	TKT +G+T	−34%	4.3×10^{-4}
9.2	159	TKT +G−T	TKT +G+T	+8.8%	0.83
9.3	160	Coll IV −G−T	Coll IV −G+T	−16%	0.21
9.3	160	Coll IV −G−T	Coll IV +G−T	+7.6%	0.78
9.3	160	Coll IV −G−T	Coll IV +G+T	+12%	0.46
9.3	160	Coll IV −G+T	Coll IV +G−T	+28%	0.038
9.3	160	Coll IV −G+T	Coll IV +G+T	+33%	0.013
9.3	160	Coll IV +G−T	Coll IV +G+T	+4.0%	0.95
9.3	160	TXNIP −G−T	TXNIP −G+T	−10%	1.0
9.3	160	TXNIP −G−T	TXNIP +G−T	+4800%	1.2×10^{-10}
9.3	160	TXNIP −G−T	TXNIP +G+T	+5800%	6.9×10^{-12}
9.3	160	TXNIP −G+T	TXNIP +G−T	+5300%	1.1×10^{-10}
9.3	160	TXNIP −G+T	TXNIP +G+T	+6500%	6.7×10^{-12}
9.3	160	TXNIP +G−T	TXNIP +G+T	+21%	0.014
9.4	161	THTR-1 −G−T	THTR-1 −G+T	−5.3%	0.72
9.4	161	THTR-1 −G−T	THTR-1 +G−T	+22%	0.0046
9.4	161	THTR-1 −G−T	THTR-1 +G+T	+19%	0.011
9.4	161	THTR-1 −G+T	THTR-1 +G−T	+29%	8.0×10^{-4}
9.4	161	THTR-1 −G+T	THTR-1 +G+T	+26%	0.0018
9.4	161	THTR-1 +G−T	THTR-1 +G+T	−2.1%	0.96
9.4	161	THTR-2 −G−T	THTR-2 −G+T	−0.036%	1.0
9.4	161	THTR-2 −G−T	THTR-2 +G−T	+3.9%	0.88
9.4	161	THTR-2 −G−T	THTR-2 +G+T	+9.8%	0.29
9.4	161	THTR-2 −G+T	THTR-2 +G−T	+3.9%	0.87
9.4	161	THTR-2 −G+T	THTR-2 +G+T	+9.8%	0.28
9.4	161	THTR-2 +G−T	THTR-2 +G+T	+5.7%	0.67
9.4	161	RFC-1 −G−T	RFC-1 −G+T	−5.3%	0.42
9.4	161	RFC-1 −G−T	RFC-1 +G−T	+9.3%	0.064
9.4	161	RFC-1 −G−T	RFC-1 +G+T	+2.9%	0.81

Continued on the next page

Table A.1—continued from the previous page

Figure	Page	Base condition	Comparison	Effect (%)	p value
9.4	161	RFC-1 −G+T	RFC-1 +G−T	+15%	0.0040
9.4	161	RFC-1 −G+T	RFC-1 +G+T	+8.6%	0.11
9.4	161	RFC-1 +G−T	RFC-1 +G+T	−5.9%	0.26
9.5	162	OGT −G−T	OGT −G+T	+3.3%	0.93
9.5	162	OGT −G−T	OGT +G−T	+28%	0.0010
9.5	162	OGT −G−T	OGT +G+T	+26%	0.0020
9.5	162	OGT −G+T	OGT +G−T	+24%	0.0028
9.5	162	OGT −G+T	OGT +G+T	+22%	0.0055
9.5	162	OGT +G−T	OGT +G+T	−1.6%	0.98
9.5	162	oGlcNAcase −G−T	oGlcNAcase −G+T	−1.6%	0.98
9.5	162	oGlcNAcase −G−T	oGlcNAcase +G−T	+9.4%	0.21
9.5	162	oGlcNAcase −G−T	oGlcNAcase +G+T	+15%	0.031
9.5	162	oGlcNAcase −G+T	oGlcNAcase +G−T	+11%	0.12
9.5	162	oGlcNAcase −G+T	oGlcNAcase +G+T	+16%	0.016
9.5	162	oGlcNAcase +G−T	oGlcNAcase +G+T	+4.8%	0.66
9.5	162	GFAT-1 −G−T	GFAT-1 −G+T	−2.7%	0.99
9.5	162	GFAT-1 −G−T	GFAT-1 +G−T	+33%	0.0086
9.5	162	GFAT-1 −G−T	GFAT-1 +G+T	+31%	0.012
9.5	162	GFAT-1 −G+T	GFAT-1 +G−T	+36%	0.0049
9.5	162	GFAT-1 −G+T	GFAT-1 +G+T	+35%	0.0068
9.5	162	GFAT-1 +G−T	GFAT-1 +G+T	−1.2%	1.0
9.5	162	Sp1 −G−T	Sp1 −G+T	+15%	0.83
9.5	162	Sp1 −G−T	Sp1 +G−T	+40%	0.16
9.5	162	Sp1 −G−T	Sp1 +G+T	−8.0%	0.97
9.5	162	Sp1 −G+T	Sp1 +G−T	+22%	0.50
9.5	162	Sp1 −G+T	Sp1 +G+T	−20%	0.58
9.5	162	Sp1 +G−T	Sp1 +G+T	−34%	0.073
9.5	162	TKT −G−T	TKT −G+T	+14%	0.083
9.5	162	TKT −G−T	TKT +G−T	+0.13%	1.0
9.5	162	TKT −G−T	TKT +G+T	+15%	0.070
9.5	162	TKT −G+T	TKT +G−T	−12%	0.087
9.5	162	TKT −G+T	TKT +G+T	+0.52%	1.0
9.5	162	TKT +G−T	TKT +G+T	+15%	0.073
9.6	162	Coll IV −G−T	Coll IV −G+T	−7.0%	0.78
9.6	162	Coll IV −G−T	Coll IV +G−T	+6.2%	0.83
9.6	162	Coll IV −G−T	Coll IV +G+T	−8.1%	0.69
9.6	162	Coll IV −G+T	Coll IV +G−T	+14%	0.32
9.6	162	Coll IV −G+T	Coll IV +G+T	−1.2%	1.0
9.6	162	Coll IV +G−T	Coll IV +G+T	−13%	0.26
9.6	162	TXNIP −G−T	TXNIP −G+T	−7.2%	0.73
9.6	162	TXNIP −G−T	TXNIP +G−T	+59%	9.2×10^{-6}
9.6	162	TXNIP −G−T	TXNIP +G+T	+59%	9.2×10^{-6}
9.6	162	TXNIP −G+T	TXNIP +G−T	+72%	2.8×10^{-6}
9.6	162	TXNIP −G+T	TXNIP +G+T	+72%	2.8×10^{-6}
9.6	162	TXNIP +G−T	TXNIP +G+T	−0.011%	1.0
9.8	164	Primary −G−T	Primary +G−T	−77%	0.048
9.9	165	Primary −G+T	Primary +G+T	−15%	0.68
9.10	166	HK-2 −G−T	HK-2 +G−T	−52%	0.017
9.11	166	HK-2 −G+T	HK-2 +G+T	−53%	0.029
10.1	171	UDP-Glc −G−T	UDP-Glc −G+T	−5.6%	0.70
10.1	171	UDP-Glc −G−T	UDP-Glc +G−T	−13%	0.062

Continued on the next page

Table A.1—continued from the previous page

Figure	Page	Base condition	Comparison	Effect (%)	p value
10.1	171	UDP-Glc −G−T	UDP-Glc +G+T	+9.0%	0.32
10.1	171	UDP-Glc −G+T	UDP-Glc +G−T	−8.3%	0.43
10.1	171	UDP-Glc −G+T	UDP-Glc +G+T	+16%	0.038
10.1	171	UDP-Glc +G−T	UDP-Glc +G+T	+26%	8.1×10^{-4}
10.1	171	UDP-GlcNAc −G−T	UDP-GlcNAc −G+T	+1.8%	0.99
10.1	171	UDP-GlcNAc −G−T	UDP-GlcNAc +G−T	−22%	0.0030
10.1	171	UDP-GlcNAc −G−T	UDP-GlcNAc +G+T	−0.39%	1.0
10.1	171	UDP-GlcNAc −G+T	UDP-GlcNAc +G−T	−24%	0.0013
10.1	171	UDP-GlcNAc −G+T	UDP-GlcNAc +G+T	−2.2%	0.98
10.1	171	UDP-GlcNAc +G−T	UDP-GlcNAc +G+T	+28%	0.0035
10.2	172	UDP-Glc −G−T	UDP-Glc −G+T	+10%	0.70
10.2	172	UDP-Glc −G−T	UDP-Glc +G−T	+25%	0.075
10.2	172	UDP-Glc −G−T	UDP-Glc +G+T	+23%	0.12
10.2	172	UDP-Glc −G+T	UDP-Glc +G−T	+14%	0.39
10.2	172	UDP-Glc −G+T	UDP-Glc +G+T	+12%	0.54
10.2	172	UDP-Glc +G−T	UDP-Glc +G+T	−2.0%	0.99
10.2	172	UDP-GlcNAc −G−T	UDP-GlcNAc −G+T	+16%	0.34
10.2	172	UDP-GlcNAc −G−T	UDP-GlcNAc +G−T	−2.3%	0.99
10.2	172	UDP-GlcNAc −G−T	UDP-GlcNAc +G+T	−2.3%	0.99
10.2	172	UDP-GlcNAc −G+T	UDP-GlcNAc +G−T	−16%	0.24
10.2	172	UDP-GlcNAc −G+T	UDP-GlcNAc +G+T	−16%	0.24
10.2	172	UDP-GlcNAc +G−T	UDP-GlcNAc +G+T	−0.0088%	1.0
10.3	173	Control	Glucosamine	+4400%	2.4×10^{-6}
10.4	173	UDP-GlcNAc −G−Q	UDP-GlcNAc −G+Q	−0.33%	1.0
10.4	173	UDP-GlcNAc −G−Q	UDP-GlcNAc +G−Q	−12%	0.013
10.4	173	UDP-GlcNAc −G−Q	UDP-GlcNAc +G+Q	−16%	0.0017
10.4	173	UDP-GlcNAc −G+Q	UDP-GlcNAc +G−Q	−12%	0.015
10.4	173	UDP-GlcNAc −G+Q	UDP-GlcNAc +G+Q	−16%	0.0020
10.4	173	UDP-GlcNAc +G−Q	UDP-GlcNAc +G+Q	−4.4%	0.64
10.5	175	HK-2 −G−T	HK-2 +G−T	+63%	0.0098
10.6	176	HK-2 −G−T	HK-2 +G−T	+6.4%	0.83
10.7	176	HK-2 −G−T	HK-2 +G−T	−43%	0.0070
10.8	177	HK-2 +G−T	HK-2 +G+T	+6.0%	0.82
11.1	179	THM −G−T	THM −G+T	Incalculable	1.6×10^{-12}
11.1	179	THM −G−T	THM +G−T	Incalculable	1.0
11.1	179	THM −G−T	THM +G+T	Incalculable	4.7×10^{-12}
11.1	179	THM −G+T	THM +G−T	−100%	1.6×10^{-12}
11.1	179	THM −G+T	THM +G+T	−20%	1.0×10^{-5}
11.1	179	THM +G−T	THM +G+T	Incalculable	5.3×10^{-12}
11.2	180	TPP −G−T	TPP −G+T	+210%	7.4×10^{-10}
11.2	180	TPP −G−T	TPP +G−T	−16%	0.39
11.2	180	TPP −G−T	TPP +G+T	+140%	1.5×10^{-7}
11.2	180	TPP −G+T	TPP +G−T	−73%	3.5×10^{-10}
11.2	180	TPP −G+T	TPP +G+T	−23%	8.7×10^{-5}
11.2	180	TPP +G−T	TPP +G+T	+180%	4.9×10^{-8}
11.3	180	THM −G−T	THM −G+T	+6500%	1.0×10^{-6}
11.3	180	THM −G−T	THM +G−T	+84%	1.0
11.3	180	THM −G−T	THM +G+T	+7100%	2.7×10^{-6}
11.3	180	THM −G+T	THM +G−T	−97%	1.1×10^{-6}
11.3	180	THM −G+T	THM +G+T	+10%	0.73
11.3	180	THM +G−T	THM +G+T	+3800%	3.1×10^{-6}

Continued on the next page

Table A.1—continued from the previous page

Figure	Page	Base condition	Comparison	Effect (%)	p value
11.4	181	TMP −G−T	TMP −G+T	+240%	2.3×10^{-5}
11.4	181	TMP −G−T	TMP +G−T	+20%	0.87
11.4	181	TMP −G−T	TMP +G+T	+220%	2.6×10^{-4}
11.4	181	TMP −G+T	TMP +G−T	−64%	5.0×10^{-5}
11.4	181	TMP −G+T	TMP +G+T	−5.5%	0.94
11.4	181	TMP +G−T	TMP +G+T	+160%	5.7×10^{-4}
11.5	182	TPP −G−T	TPP −G+T	+77%	0.0075
11.5	182	TPP −G−T	TPP +G−T	+5.4%	0.99
11.5	182	TPP −G−T	TPP +G+T	+150%	1.3×10^{-4}
11.5	182	TPP −G+T	TPP +G−T	−40%	0.012
11.5	182	TPP −G+T	TPP +G+T	+43%	0.022
11.5	182	TPP +G−T	TPP +G+T	+140%	1.8×10^{-4}
11.6	184	−TPP −G−T	−TPP −G+T	+31%	0.81
11.6	184	−TPP −G−T	−TPP +G−T	+11%	0.50
11.6	184	−TPP −G−T	−TPP +G+T	+13%	0.018
11.6	184	−TPP −G+T	−TPP +G−T	−15%	0.95
11.6	184	−TPP −G+T	−TPP +G+T	−14%	0.13
11.6	184	−TPP +G−T	−TPP +G+T	+1.1%	0.31
11.6	184	+TPP −G−T	+TPP −G+T	+13%	0.99
11.6	184	+TPP −G−T	+TPP +G−T	+9.7%	1.0
11.6	184	+TPP −G−T	+TPP +G+T	−1.0%	0.88
11.6	184	+TPP −G+T	+TPP +G−T	−3.2%	0.98
11.6	184	+TPP −G+T	+TPP +G+T	−13%	0.97
11.6	184	+TPP +G−T	+TPP +G+T	−9.8%	0.85
11.6	184	−TPP −G−T	+TPP −G−T	+10%	0.0096
11.6	184	−TPP −G+T	+TPP −G+T	−3.8%	0.72
11.6	184	−TPP +G−T	+TPP +G−T	+9.0%	0.16
11.6	184	−TPP +G+T	+TPP +G+T	−1.9%	0.62
11.7	185	−TPP −G−T	−TPP −G+T	+4.9%	0.92
11.7	185	−TPP −G−T	−TPP +G−T	−17%	0.14
11.7	185	−TPP −G−T	−TPP +G+T	−36%	4.1×10^{-4}
11.7	185	−TPP −G+T	−TPP +G−T	−21%	0.036
11.7	185	−TPP −G+T	−TPP +G+T	−39%	7.3×10^{-5}
11.7	185	−TPP +G−T	−TPP +G+T	−22%	0.099
11.7	185	+TPP −G−T	+TPP −G+T	+2.1%	0.99
11.7	185	+TPP −G−T	+TPP +G−T	−18%	0.11
11.7	185	+TPP −G−T	+TPP +G+T	−35%	3.0×10^{-4}
11.7	185	+TPP −G+T	+TPP +G−T	−19%	0.060
11.7	185	+TPP −G+T	+TPP +G+T	−37%	1.4×10^{-4}
11.7	185	+TPP +G−T	+TPP +G+T	−22%	0.10
11.7	185	−TPP −G−T	+TPP −G−T	+1.2%	0.86
11.7	185	−TPP −G+T	+TPP −G+T	−1.6%	0.78
11.7	185	−TPP +G−T	+TPP +G−T	+0.72%	0.95
11.7	185	−TPP +G+T	+TPP +G+T	+1.8%	0.87
12.4	191	HK-2 −G−T	HK-2 −G+T	+0.39%	1.0
12.4	191	HK-2 −G−T	HK-2 +G−T	−31%	1.1×10^{-4}
12.4	191	HK-2 −G−T	HK-2 +G+T	−17%	0.053
12.4	191	HK-2 −G+T	HK-2 +G−T	−31%	9.6×10^{-5}
12.4	191	HK-2 −G+T	HK-2 +G+T	−17%	0.046
12.4	191	HK-2 +G−T	HK-2 +G+T	+21%	0.12
12.4	191	HK-2 −G−T	HK-2 −G+T	+0.39%	1.0

Continued on the next page

Table A.1 – concluded from the previous page

Figure	Page	Base condition	Comparison	Effect (%)	p value
12.4	191	HK-2 −G−T	HK-2 +G−T	−31%	1.1×10^{-4}
12.4	191	HK-2 −G−T	HK-2 +G+T	−17%	0.053
12.4	191	HK-2 −G+T	HK-2 +G−T	−31%	9.6×10^{-5}
12.4	191	HK-2 −G+T	HK-2 +G+T	−17%	0.046
12.4	191	HK-2 +G−T	HK-2 +G+T	+21%	0.12
12.5	193	HK-2 −G−T	HK-2 −G+T	−28%	0.0014
12.5	193	HK-2 −G−T	HK-2 +G−T	−35%	3.4×10^{-4}
12.5	193	HK-2 −G−T	HK-2 +G+T	−50%	2.2×10^{-5}
12.5	193	HK-2 −G+T	HK-2 +G−T	−8.9%	0.55
12.5	193	HK-2 −G+T	HK-2 +G+T	−31%	0.0060
12.5	193	HK-2 +G−T	HK-2 +G+T	−24%	0.037
12.6	194	HK-2 −G−T	HK-2 −G+T	−13%	0.42
12.6	194	HK-2 −G−T	HK-2 +G−T	−9.6%	0.62
12.6	194	HK-2 −G−T	HK-2 +G+T	−22%	0.080
12.6	194	HK-2 −G+T	HK-2 +G−T	+3.4%	0.98
12.6	194	HK-2 −G+T	HK-2 +G+T	−11%	0.62
12.6	194	HK-2 +G−T	HK-2 +G+T	−14%	0.41
12.7	195	HK-2 −G−T	HK-2 −G+T	+22%	0.055
12.7	195	HK-2 −G−T	HK-2 +G−T	+38%	0.0027
12.7	195	HK-2 −G−T	HK-2 +G+T	+57%	1.6×10^{-4}
12.7	195	HK-2 −G+T	HK-2 +G−T	+13%	0.18
12.7	195	HK-2 −G+T	HK-2 +G+T	+29%	0.0041
12.7	195	HK-2 +G−T	HK-2 +G+T	+13%	0.089
12.2	189	A to B −G−T	A to B −G+T	+11%	0.50
12.2	189	A to B −G−T	A to B +G−T	+17%	0.20
12.2	189	A to B −G−T	A to B +G+T	+15%	0.30
12.2	189	A to B −G+T	A to B +G−T	+4.8%	0.89
12.2	189	A to B −G+T	A to B +G+T	+3.0%	0.97
12.2	189	A to B +G−T	A to B +G+T	−1.7%	0.93
12.2	189	B to A −G−T	B to A −G+T	+52%	6.5×10^{-4}
12.2	189	B to A −G−T	B to A +G−T	+52%	6.2×10^{-4}
12.2	189	B to A −G−T	B to A +G+T	+52%	6.1×10^{-4}
12.2	189	B to A −G+T	B to A +G−T	+0.18%	1.0
12.2	189	B to A −G+T	B to A +G+T	+0.27%	1.0
12.2	189	B to A +G−T	B to A +G+T	+0.095%	1.0
12.3	189	Ratio −G−T	Ratio −G+T	−27%	1.4×10^{-4}
12.3	189	Ratio −G−T	Ratio +G−T	−23%	7.9×10^{-4}
12.3	189	Ratio −G−T	Ratio +G+T	−25%	2.7×10^{-4}
12.3	189	Ratio −G+T	Ratio +G−T	+4.6%	0.76
12.3	189	Ratio −G+T	Ratio +G+T	+2.7%	0.98
12.3	189	Ratio +G−T	Ratio +G+T	−1.8%	0.93

Appendix B

Primer sequences

Table B.1: Primer sequences

Gene	Direction	Sequence
THTR-1	Forward	ACCCCAGCTTCTAACCACCT
THTR-1	Reverse	GGCGAGAGGAGTAGCACATC
THTR-2	Forward	CTGGCTCTGGTGGTCTTCTC
THTR-2	Reverse	AGGCATAGCGTTCCACATTC
RFC-1	Forward	CCATGGTCCTGTCTGTCCTT
RFC-1	Reverse	TAGCGCTCCTTAGACCCTGA
OGT	Forward	GCAACCTAGCCAATGCTCTC
OGT	Reverse	GCAGCAAACTCTGGGAAGAC
oGlcNAcase	Forward	GTCTTAGGGGACATGGCAGA
oGlcNAcase	Reverse	ACAACATGCCTGAACCAACA
GFAT-1	Forward	GATTCTGCTGGTGTGGGATT
GFAT-1	Reverse	AGGACTGGGTTCTCCATGTG
Sp1	Forward	TGCAGCAGAATTGAGTCACC
Sp1	Reverse	CACAACATACTGCCCACCAG
TKT	Forward	CATCTCCGAGAGCAACATCA
TKT	Reverse	TTGTATTGGCGGCTAGTTCC
Collagen IV	Forward	TGGTCCAAGAGGATTTCCAG
Collagen IV	Reverse	TCATTGCCTTGCACGTAGAG
TXNIP	Forward	CTGGCGTAAGCTTTTCAAGG
TXNIP	Reverse	AGTGCACAAAGGGGAAACAC
β-actin	Forward	GGACTTCGAGCAAGAGATGG
β-actin	Reverse	AGCACTGTGTTGGCGTACAG

Appendix C

Other experiments undertaken

Other than the experiments described in this thesis, others have been carried out but not included in the main text body. These experiments have not been included because they represent part of larger projects with multiple researchers involved and sample analysis has not progressed to a sufficient level to enable meaningful conclusions to be drawn. Continuing work by colleagues in the Protein Damage and Systems Biology research group will bring these projects to fruition. They are included here to allow the interested reader to see the future experimental framework.

C.1 *In vivo* thiamine metabolism

Two projects using streptozotocin-induced diabetic rats have reached practical completion but samples remain to be analysed. The first project was designed to investigate the effects of three treatments on thiamine metabolism in diabetic rats. The three treatments were oral thiamine therapy for a 6 week period, intensive glycaemic control (achieved via subcutaneous implantation of slow-release insulin implants), and restoration of normoglycaemia by administration of phloridzin, an inhibitor of renal glucose re-uptake. Each of these groups were compared to normal control rats and diabetic control rats. Samples harvested were renal glomeruli, total renal cortex, retinas, lenses, sciatic nerve, liver, heart, small intestine, brain, skeletal muscle, urine, plasma and erythrocytes. Abundance of thiamine, activity of thiamine-dependent enzymes, abundance of thiamine transporters, mRNA abundance for

genes related to thiamine metabolism and routine biochemical measurements will be made for each of the samples where relevant.

The second project was designed to investigate thiamine handling and partitioning in normal and diabetic animals with the aim of constructing a mathematical model of thiamine metabolism. Control and diabetic animals were kept for six weeks after induction of diabetes. After this period, each animal had [^{13}C]thiamine injected intraperioneally at $0.1\,\mathrm{mg\,kg^{-1}}$. Animals were sacrificed in satellite groups at 0.75, 1.5, 3, 6, 12, 24 and 48 h. Tissues were harvested as for the first project and stored immediately at −80°C. These will be analysed by HPLC to determine total thiamine content and by LC-MS/MS to determine the ratio of [^{12}C]thiamine to [^{13}C]thiamine. This data will be used to construct the mathematical model of thiamine metabolism.

C.2 Residual binding domain computation

Bioinformatic approach to studying the proteome offer a vast often untapped potential. Gallet et al. [2000] published a method to use a plot of amino acid hydrophobicity (H) versus mean hydrophobic moment (μH) for any protein sequence in the absence of structural information, and identify in general terms which amino acids are likely to lie in particular domains. For example, amino acids with a high hydrophobicity and a low mean hydrophobic moment are likely to lie in a membranous region whereas residues with a high hydrophobicity and mean hydrophobic moment are likely to lie on the surface of proteins. Also, residues lying in an area to the left of centre are said to lie in the receptor binding domain (RBD) and are likely to be involved in protein-protein interactions. In particular, arginine residues within the RBD have been implicated in being both chemically active within the enzyme and prone to modification by methylglyoxal and thus of high importance for investigation. I have been working with a bioinformatician developing a system to automate interrogation of the entire Swiss-Prot database for amino acid residues that are in the RBD and highly probable to be targets for glycation whilst combining factors such as predicted secondary structure.

References

N. Abdel Wahab and R. M. Mason. Modulation of neutral protease expression in human mesangial cells by hyperglycaemic culture. *Biochem. J.*, 320(3):777–83, 1996. ISSN 0264-6021 (Print).

ACCORD Study Group, W. C. Cushman, G. W. Evans, R. P. Byington, D. C. Goff, R. H. Grimm, J. A. Cutler, D. G. Simons-Morton, J. N. Basile, M. A. Corson, J. L. Probstfield, L. Katz, K. A. Peterson, W. T. Friedewald, J. B. Buse, J. T. Bigger, H. C. Gerstein, and F. Ismail-Beigi. Effects of intensive blood-pressure control in type 2 diabetes mellitus. *N. Engl. J. Med.*, 362(17):1575–1585, Apr 2010. doi: 10.1056/NEJMoa1001286.

Action to Control Cardiovascular Risk in Diabetes Study Group, H. C. Gerstein, M. E. Miller, R. P. Byington, D. C. Goff, J. T. Bigger, J. B. Buse, W. C. Cushman, S. Genuth, F. Ismail-Beigi, R. H. Grimm, J. L. Probstfield, D. G. Simons-Morton, and W. T. Friedewald. Effects of intensive glucose lowering in type 2 diabetes. *N. Engl. J. Med.*, 358(24): 2545–2559, Jun 2008. doi: 10.1056/NEJMoa0802743.

A. I. Adler, R. J. Stevens, S. E. Manley, R. W. Bilous, C. A. Cull, R. R. Holman, and UKPDS group. Development and progression of nephropathy in type 2 diabetes: the United Kingdom Prospective Diabetes Study (UKPDS 64). *Kidney Int.*, 63(1):225–232, Jan 2003. doi: 10.1046/j.1523-1755.2003.00712.x.

L. P. Aiello, R. L. Avery, P. G. Arrigg, B. A. Keyt, H. D. Jampel, S. T. Shah, L. R. Pasquale, H. Thieme, M. A. Iwamoto, and J. E. Park. Vascular endothelial growth factor in ocular fluid of patients with diabetic retinopathy and other retinal disorders. *N. Engl. J. Med.*, 331(22):1480–1487, Dec 1994.

H. Al Ali. 2nd Year Report, University of Essex. Unpublished internal report., 2006.

A. Alkhalaf, A. Klooster, W. van Oeveren, U. Achenbach, N. Kleefstra, R. J. Slingerland, G. S. Mijnhout, H. J. G. Bilo, R. O. B. Gans, G. J. Navis, and S. J. L. Bakker. A Double-Blind, Randomized, Placebo-Controlled Clinical Trial on Benfotiamine Treatment in Patients with Diabetic Nephropathy. *Diabetes Care*, 33:1598–1601, Apr 2010. doi: 10.2337/dc09-2241.

F. Allen and C. C. Tisher. Morphology of the ascending thick limb of Henle. *Kidney Int.*, 9(1):8–22, 1976. doi: 10.1038/ki.1976.2.

A. S. Alzahrani, E. Baitei, M. Zou, and Y. Shi. Thiamine transporter mutation: an example of monogenic diabetes mellitus. *Eur. J. Endocrinol.*, 155(6):787–792, Dec 2006. doi: 10.1530/eje.1.02305.

American Diabetes Association. Nephropathy in Diabetes (Position Statement). *Diabetes Care*, 27(Supplement 1):S79–S83, 2004.

American Diabetes Association. Standards of medical care in diabetes—2009. *Diabetes Care*, 32 Suppl 1:S13–S61, Jan 2009. doi: 10.2337/dc09-S013.

American Diabetes Association. Diagnosis and classification of diabetes mellitus. *Diabetes Care*, 33 Suppl 1:S62–S69, Jan 2010a. doi: 10.2337/dc10-S062.

American Diabetes Association. Summary of revisions for the 2010 Clinical Practice Recommendations. *Diabetes Care*, 33 Suppl 1:S3, Jan 2010b. doi: 10.2337/dc10-S003.

M. R. Ariaey-Nejad, M. Balaghi, E. M. Baker, and H. E. Sauberlich. Thiamin metabolism in man. *Am. J. Clin. Nutr.*, 23(6):764–778, Jun 1970.

E. Ascher, P. V. Gade, A. Hingorani, S. Puthukkeril, S. Kallakuri, M. Scheinman, and T. Jacob. Thiamine reverses hyperglycemia-induced dysfunction in cultured endothelial cells. *Surgery*, 130(5):851–858, Nov 2001. doi: 10.1067/msy.2001.117194.

B. Ashokkumar, N. D. Vaziri, and H. M. Said. Thiamin uptake by the human-derived renal epithelial (HEK-293) cells: cellular and molecular mechanisms. *Am. J. Physiol. Renal Physiol.*, 291(4):F796–F805, Oct 2006. doi: 10.1152/ajprenal.00078.2006.

R. C. Atkins and P. Zimmet. Diabetic kidney disease: act now or pay later. *Saudi J. Kidney Dis. Transpl.*, 21(2):217–221, Mar 2010.

E. Aughey and E. P. Daniel. Effect of Cooking Upon the Thiamin Content of Foods. *J. Nutr.*, 19(3):285–296, 1940.

S. H. Ayo, R. A. Radnik, J. A. Garoni, W. F. Glass, and J. I. Kreisberg. High glucose causes an increase in extracellular matrix proteins in cultured mesangial cells. *Am. J. Pathol.*, 136(6):1339–1348, Jun 1990.

A. Azzi, D. Boscoboinik, S. Clément, D. Marilley, N. K. Ozer, R. Ricciarelli, and A. Tasinato. α-tocopherol as a modulator of smooth muscle cell proliferation. *Prostaglandins Leukot. Essent. Fatty Acids*, 57(4–5):507–514, Oct 1997. doi: 10.1016/S0952-3278(97)90436-1.

E. Azzini, P. Vitaglione, F. Intorre, A. Napolitano, A. Durazzo, M. S. Foddai, A. Fumagalli, G. Catasta, L. Rossi, E. Venneria, A. Raguzzini, L. Palomba, V. Fogliano, and G. Maiani. Bioavailability of strawberry antioxidants in human subjects. *Br. J. Nutr.*, Epub ahead of print:1–9, May 2010. doi: 10.1017/S000711451000187X.

R. Babaei-Jadidi, N. Karachalias, N. Ahmed, S. Battah, and P. J. Thornalley. Prevention of incipient diabetic nephropathy by high-dose thiamine and benfotiamine. *Diabetes*, 52 (8):2110–2120, Aug 2003.

R. Babaei-Jadidi, N. Karachalias, C. Kupich, N. Ahmed, and P. J. Thornalley. High-dose thiamine therapy counters dyslipidaemia in streptozotocin-induced diabetic rats. *Diabetologia*, 47(12):2235–2246, Dec 2004. doi: 10.1007/s00125-004-1582-5.

J. F. Bach. Insulin-dependent diabetes mellitus as an autoimmune disease. *Endocr. Rev.*, 15(4):516–542, Aug 1994.

P. C. Baer, W. A. Nockher, W. Haase, and J. E. Scherberich. Isolation of proximal and distal tubule cells from human kidney by immunomagnetic separation. Technical note. *Kidney Int.*, 52(5):1321–1331, Nov 1997.

D. S. Bahia, N. Sartania, R. J. Ward, A. Cavalli, T. L. Z. Jones, K. M. Druey, and G. Milligan. Concerted stimulation and deactivation of pertussis toxin-sensitive G proteins by chimeric G protein-coupled receptor-regulator of G protein signaling 4 fusion proteins: analysis of the contribution of palmitoylated cysteine residues to the GAP activity of RGS4. *J. Neurochem.*, 85(5):1289–1298, Jun 2003. doi: 10.1046/j.1471-4159.2003.01769.x.

S. J. Bakker, E. K. Hoogeveen, G. Nijpels, P. J. Kostense, J. M. Dekker, R. O. Gans, and R. J. Heine. The association of dietary fibres with glucose tolerance is partly explained by concomitant intake of thiamine: the Hoorn Study. *Diabetologia*, 41(10):1168–1175, Oct 1998. doi: 10.1007/s001250051047.

K. Balamurugan and H. M. Said. Functional role of specific amino acid residues in human thiamine transporter *SLC19A2*: mutational analysis. *Am. J. Physiol. Gastrointest. Liver Physiol.*, 283(1):G37–G43, Jul 2002. doi: 10.1152/ajpgi.00547.2001.

F. G. Banting, C. H. Best, J. B. Collip, W. R. Campbell, and A. A. Fletcher. Pancreatic extracts in the treatment of diabetes mellitus: preliminary report. 1922. *Can. Med. Assoc. J.*, 145(10):1281–1286, Nov 1991.

T. P. Begley, A. Chatterjee, J. W. Hanes, A. Hazra, and S. E. Ealick. Cofactor biosynthesis–still yielding fascinating new biological chemistry. *Curr. Opin. Chem. Biol.*, 12(2):118–125, Apr 2008. doi: 10.1016/j.cbpa.2008.02.006.

E. Beltramo, E. Berrone, S. Buttiglieri, and M. Porta. Thiamine and benfotiamine prevent increased apoptosis in endothelial cells and pericytes cultured in high glucose. *Diabetes Metab. Res. Rev.*, 20(4):330–336, 2004. doi: 10.1002/dmrr.470.

E. Beltramo, K. Nizheradze, E. Berrone, S. Tarallo, and M. Porta. Thiamine and benfotiamine prevent apoptosis induced by high glucose-conditioned extracellular matrix in human retinal pericytes. *Diabetes Metab. Res. Rev.*, 25(7):647–656, Oct 2009. doi: 10.1002/dmrr.1008.

A. K. Bergmann, I. Sahai, J. F. Falcone, J. Fleming, A. Bagg, C. Borgna-Pignati, R. Casey, L. Fabris, E. Hexner, L. Mathews, M. L. Ribeiro, K. J. Wierenga, and E. J. Neufeld. Thiamine-responsive megaloblastic anemia: identification of novel compound heterozygotes and mutation update. *J. Pediatr.*, 155(6):888–892.e1, Dec 2009. doi: 10.1016/j.jpeds.2009.06.017.

E. Berrone, E. Beltramo, C. Solimine, A. U. Ape, and M. Porta. Regulation of intracellular glucose and polyol pathway by thiamine and benfotiamine in vascular cells cultured in high glucose. *J. Biol. Chem.*, 281(14):9307–9313, Apr 2006. doi: 10.1074/jbc.M600418200.

L. Bettendorff, B. Hennuy, A. D. Clerck, and P. Wins. Chloride permeability of rat brain membrane vesicles correlates with thiamine triphosphate content. *Brain Res.*, 652(1): 157–160, Jul 1994a. doi: 10.1016/0006-8993(94)90331-X.

L. Bettendorff, P. Wins, and M. Lesourd. Subcellular localization and compartmentation of thiamine derivatives in rat brain. *Biochim. Biophys. Acta*, 1222(1):1–6, May 1994b. doi: 10.1016/0167-4889(94)90018-3.

D. J. Betteridge. Effects of pioglitazone on lipid and lipoprotein metabolism. *Diabetes Obes. Metab.*, 9(5):640–647, Sep 2007. doi: 10.1111/j.1463-1326.2007.00715.x.

G. P. Biewenga, G. R. Haenen, and A. Bast. The pharmacology of the antioxidant lipoic acid. *Gen. Pharmacol.-Vasc. S.*, 29(3):315–331, Sep 1997. doi: 10.1016/S0306-3623(96)00474-0.

G. L. Blatch and M. Lässle. The tetratricopeptide repeat: a structural motif mediating protein-protein interactions. *Bioessays*, 21(11):932–939, Nov 1999. doi: 10.1002/(SICI)1521-1878(199911)21:11<932::AID-BIES5>3.0.CO;2-N.

L. Blonde. Current antihyperglycemic treatment strategies for patients with type 2 diabetes mellitus. *Cleve. Clin. J. Med.*, 76 Supplement 5:S4–S11, December 2009. doi: 10.3949/ccjm.76.s5.02.

W. A. Border and N. A. Noble. Transforming growth factor β in tissue fibrosis. *N. Engl. J. Med.*, 331(19):1286–1292, Nov 1994. doi: 10.1056/NEJM199411103311907.

L. G. Boros, J. L. Brandes, W. N. Lee, M. Cascante, J. Puigjaner, E. Revesz, T. M. Bray, W. J. Schirmer, and W. S. Melvin. Thiamine supplementation to cancer patients: a double edged sword. *Anticancer Res.*, 18(1B):595–602, 1998.

A. J. M. Boulton. Management of Diabetic Peripheral Neuropathy. *Clin. Diabetes*, 23(1): 9–15, 2005. doi: 10.2337/diaclin.23.1.9.

A. J. M. Boulton. The diabetic foot—an update. *Foot Ankle Surg.*, 14(3):120–124, 2008. doi: 10.1016/j.fas.2008.05.004.

M. J. Boulware, V. S. Subramanian, H. M. Said, and J. S. Marchant. Polarized expression of members of the solute carrier *SLC19A* gene family of water-soluble multivitamin transporters: implications for physiological function. *Biochem. J.*, 376(1):43–48, Nov 2003. doi: 10.1042/BJ20031220.

M. M. Bradford. A rapid and sensitive method for the quantitation of microgram quantities of protein utilizing the principle of protein-dye binding. *Anal. Biochem.*, 72:248–254, May 1976.

J. A. Brady, C. L. Rock, and M. R. Horneffer. Thiamin status, diuretic medications, and the management of congestive heart failure. *J. Am. Diet. Assoc.*, 95(5):541–544, May 1995. doi: 10.1016/S0002-8223(95)00148-4.

M. D. Brand. The sites and topology of mitochondrial superoxide production. *Exp. Gerontol.*, 45(7–8):466–472, Jan 2010. doi: 10.1016/j.exger.2010.01.003.

H. Brem and M. Tomic-Canic. Cellular and molecular basis of wound healing in diabetes. *J. Clin. Invest.*, 117(5):1219–1222, May 2007. doi: 10.1172/JCI32169.

R. Brigelius-Flohé and M. G. Traber. Vitamin E: function and metabolism. *FASEB J.*, 13 (10):1145–1155, Jul 1999.

R. Brightwell and A. L. Tappel. Lysosomal acid pyrophosphatase and acid phosphatase. *Arch. Biochem. Biophys.*, 124(1):333–343, Mar 1968.

F. C. Brosius. New insights into the mechanisms of fibrosis and sclerosis in diabetic nephropathy. *Rev. Endocr. Metab. Disord.*, 9(4):245–254, Dec 2008. doi: 10.1007/s11154-008-9100-6.

M. J. Brown, S. J. Bird, S. Watling, H. Kaleta, L. Hayes, S. Eckert, H. L. Foyt, and Z. study. Natural progression of diabetic peripheral neuropathy in the Zenarestat study population. *Diabetes Care*, 27(5):1153–1159, May 2004. doi: 10.2337/diacare.27.5.1153.

M. Brownlee. Biochemistry and molecular cell biology of diabetic complications. *Nature*, 414(6865):813–820, Dec 2001. doi: 10.1038/414813a.

M. Brownlee, H. Vlassara, A. Kooney, P. Ulrich, and A. Cerami. Aminoguanidine prevents diabetes-induced arterial wall protein cross-linking. *Science*, 232(4758):1629–1632, Jun 1986. doi: 10.1126/science.3487117.

P. Bruneval, J. M. Foidart, D. Nochy, J. P. Camilleri, and J. Bariety. Glomerular matrix proteins in nodular glomerulosclerosis in association with light chain deposition disease and diabetes mellitus. *Hum. Pathol.*, 16(5):477–484, May 1985.

R. F. Butterworth. Thiamin deficiency and brain disorders. *Nutr. Res. Rev.*, 16(2):277–284, Dec 2003. doi: 10.1079/NRR200367.

H. Cabezas, R. R. Raposo, and E. Meléndez-Hevia. Activity and metabolic roles of the pentose phosphate cycle in several rat tissues. *Mol. Cell. Biochem.*, 201(1–2):57–63, Nov 1999.

G. W. Camiener and G. M. Brown. The biosynthesis of thiamine. 1. Enzymatic formation of thiamine and phosphate esters of the pyrimidine moiety of thiamine. *J. Biol. Chem.*, 235:2404–2410, Aug 1960a.

G. W. Camiener and G. M. Brown. The biosynthesis of thiamine. 2. Fractionation of enzyme system and identification of thiazole monophosphate and thiamine monophosphate as intermediates. *J. Biol. Chem.*, 235:2411–2417, Aug 1960b.

A. Capes-Davis, G. Theodosopoulos, I. Atkin, H. G. Drexler, A. Kohara, R. A. F. MacLeod, J. R. Masters, Y. Nakamura, Y. A. Reid, R. R. Reddel, and R. I. Freshney. Check your cultures! A list of cross-contaminated or misidentified cell lines. *Int. J. Cancer*, 127(1): 1–8, Jul 2010. doi: 10.1002/ijc.25242.

K. J. Carpenter. *Beriberi, White Rice, and Vitamin B: A Disease, a Cause, and a Cure*. University of California Press, illustrated edition, 2000.

K. J. Carpenter. Casimir Funk. *ELS*, page 1, 2001. doi: 10.1038/npg.els.0002799.

A. Cerami. Aging of proteins and nucleic acids: what is the role of glucose? *Trends Biochem. Sci.*, 11(8):311–314, Aug 1986. doi: 10.1016/0968-0004(86)90281-1.

A. Ceriello, M. A. Ihnat, and J. E. Thorpe. The "metabolic memory": is more than just tight glucose control necessary to prevent diabetic complications? *J. Clin. Endocrinol. Metab.*, 94(2):410–415, Feb 2009. doi: 10.1210/jc.2008-1824.

A. F. Ceylan-Isik, S. Wu, Q. Li, S.-Y. Li, and J. Rench. High-dose benfotiamine rescues cardiomyocyte contractile dysfunction in streptozotocin-induced diabetes mellitus. *J. Appl. Physiol.*, 100(1):150–156, Jan 2006. doi: 10.1152/japplphysiol.00988.2005.

Y.-M. Chae, K.-K. Park, J. Magae, I.-S. Lee, C.-H. Kim, H.-C. Kim, S. Hong, J.-G. Lee, I.-J. Choi, H.-S. Kim, K.-S. Min, I.-K. Lee, and Y.-C. Chang. Sp1-decoy oligodeoxynucleotide inhibits high glucose-induced mesangial cell proliferation. *Biochem. Biophys. Res. Commun.*, 319(2):550–555, Jun 2004. doi: 10.1016/j.bbrc.2004.05.025.

B. R. Chamberlain, J. E. Buttery, and P. R. Pannall. A stable reagent mixture for the whole blood transketolase assay. *Ann. Clin. Biochem.*, 33(4):352–354, Jul 1996.

I. P. Chatziralli, T. N. Sergentanis, P. Keryttopoulos, N. Vatkalis, A. Agorastos, and L. Papazisis. Risk factors associated with diabetic retinopathy in patients with diabetes mellitus type 2. *BMC Res. Notes*, 3(1):153, Jun 2010. doi: 10.1186/1756-0500-3-153.

J. M. Chirgwin, A. E. Przybyla, R. J. MacDonald, and W. J. Rutter. Isolation of biologically active ribonucleic acid from sources enriched in ribonuclease. *Biochemistry (Mosc.)*, 18 (24):5294–5299, Nov 1979.

J.-Y. Chuang, Y.-T. Wang, S.-H. Yeh, Y.-W. Liu, W.-C. Chang, and J.-J. Hung. Phosphorylation by c-Jun NH_2-terminal kinase 1 regulates the stability of transcription factor Sp1 during mitosis. *Mol. Biol. Cell*, 19(3):1139–1151, Mar 2008. doi: 10.1091/mbc.E07-09-0881.

A. C. K. Chung, H. Zhang, Y.-Z. Kong, J.-J. Tan, X. R. Huang, J. B. Kopp, and H. Y. Lan. Advanced glycation end-products induce tubular CTGF via TGF-β-independent Smad3 signaling. *J. Am. Soc. Nephrol.*, 21(2):249–260, Feb 2010. doi: 10.1681/ASN.2009010018.

E. M. Ciszak, L. G. Korotchkina, P. M. Dominiak, S. Sidhu, and M. S. Patel. Structural basis for flip-flop action of thiamin pyrophosphate-dependent enzymes revealed by human pyruvate dehydrogenase. *J. Biol. Chem.*, 278(23):21240–21246, Jun 2003. doi: 10.1074/jbc.M300339200.

R. J. Clark, P. M. McDonough, E. Swanson, S. U. Trost, M. Suzuki, M. Fukuda, and W. H. Dillmann. Diabetes and the accompanying hyperglycemia impairs cardiomyocyte calcium cycling through increased nuclear O-GlcNAcylation. *J. Biol. Chem.*, 278(45): 44230–44237, Nov 2003. doi: 10.1074/jbc.M303810200.

M. P. Cohen, V. Y. Wu, and J. A. Cohen. Glycated albumin stimulates fibronectin and collagen IV production by glomerular endothelial cells under normoglycemic conditions. *Biochem. Biophys. Res. Commun.*, 239(1):91–94, Oct 1997. doi: 10.1006/bbrc.1997.7420.

R. N. Cole and G. W. Hart. Glycosylation sites flank phosphorylation sites on synapsin I: O-linked *N*-acetylglucosamine residues are localized within domains mediating synapsin I interactions. *J. Neurochem.*, 73(1):418–428, Jul 1999. doi: 10.1046/j.1471-4159.1999.0730418.x.

F. I. Comer and G. W. Hart. *O*-Glycosylation of nuclear and cytosolic proteins. Dynamic interplay between *O*-GlcNAc and *O*-phosphate. *J. Biol. Chem.*, 275(38):29179–29182, Sep 2000. doi: 10.1074/jbc.R000010200.

W. D. Comper and L. M. Russo. Where does albuminuria come from in diabetic kidney disease? *Curr. Diab. Rep.*, 8(6):477–485, Dec 2008.

N. Comtesse, E. Maldener, and E. Meese. Identification of a nuclear variant of *MGEA5*, a cytoplasmic hyaluronidase and a β-N-acetylglucosaminidase. *Biochem. Biophys. Res. Commun.*, 283(3):634–640, May 2001. doi: 10.1006/bbrc.2001.4815.

W. F. Cook and G. W. Pickering. A rapid method for separating glomeruli from rabbit kidney. *Nature*, 182(4642):1103–1104, Oct 1958.

L. J. Coppey, J. S. Gellett, E. P. Davidson, J. A. Dunlap, D. D. Lund, and M. A. Yorek. Effect of antioxidant treatment of streptozotocin-induced diabetic rats on endoneurial blood flow, motor nerve conduction velocity, and vascular reactivity of epineurial arterioles of the sciatic nerve. *Diabetes*, 50(8):1927–1937, Aug 2001. doi: 10.2337/diabetes.50.8.1927.

A. J. Courey and R. Tjian. Analysis of Sp1 *in vivo* reveals multiple transcriptional domains, including a novel glutamine-rich activation motif. *Cell*, 55(5):887–898, Dec 1988.

R. J. M. Coward, G. I. Welsh, J. Yang, C. Tasman, R. Lennon, A. Koziell, S. Satchell, G. D. Holman, D. Kerjaschki, J. M. Tavaré, P. W. Mathieson, and M. A. Saleem. The human glomerular podocyte is a novel target for insulin action. *Diabetes*, 54(11):3095–3102, Nov 2005. doi: 10.2337/diabetes.54.11.3095.

E. T. Cunningham, A. P. Adamis, M. Altaweel, L. P. Aiello, N. M. Bressler, D. J. D'Amico, M. Goldbaum, D. R. Guyer, B. Katz, M. Patel, S. D. Schwartz, and M. D. R. S. Group. A phase II randomized double-masked trial of pegaptanib, an anti-vascular endothelial growth factor aptamer, for diabetic macular edema. *Ophthalmology*, 112(10):1747–1757, Oct 2005.

P. A. Dalby, J. P. Aucamp, R. George, and R. J. Martinez-Torres. Structural stability of an enzyme biocatalyst. *Biochem. Soc. Trans.*, 35(6):1606–1609, Dec 2007. doi: 10.1042/BST0351606.

A. G. Datta and E. Racker. Mechanism of action of transketolase. I. Properties of the crystalline yeast enzyme. *J. Biol. Chem.*, 236:617–623, Mar 1961.

S. M. Dauphinee, M. Ma, and C. K. L. Too. Role of *O*-linked β-*N*-acetylglucosamine modification in the subcellular distribution of α4 phosphoprotein and Sp1 in rat lymphoma cells. *J. Cell. Biochem.*, 96(3):579–588, Oct 2005. doi: 10.1002/jcb.20508.

R. M. C. Dawson, D. C. Elliott, W. H. Elliott, and K. M. Jones. *Data for biochemical research*. Oxford Science Publications, third edition, 1986.

T. de Beer, J. F. Vliegenthart, A. Löffler, and J. Hofsteenge. The hexopyranosyl residue that is *C*-glycosidically linked to the side chain of tryptophan-7 in human RNase U_s is α-mannopyranose. *Biochemistry (Mosc.)*, 34(37):11785–11789, Sep 1995.

M. C. I. de la Cruz, F. N. Ziyadeh, M. Isono, M. Kouahou, D. C. Han, R. Kalluri, P. Mundel, and S. Chen. Effects of high glucose and TGF-β1 on the expression of collagen IV and vascular endothelial growth factor in mouse podocytes. *Kidney Int.*, 62(3):901–913, Sep 2002. doi: 10.1046/j.1523-1755.2002.00528.x.

T. Deckert, J. E. Poulsen, and M. Larsen. Prognosis of diabetics with diabetes onset before the age of thirty-one. I. Survival, causes of death, and complications. *Diabetologia*, 14(6): 363–370, Jun 1978.

W. M. Deen. What determines glomerular capillary permeability? *J Clin Invest*, 114(10): 1412–1414, Nov 2004. doi: 10.1172/JCI23577.

P. Degrell, J. Cseh, M. Mohás, G. A. Molnár, L. Pajor, J. C. Chatham, N. Fülöp, and I. Wittmann. Evidence of *O*-linked *N*-acetylglucosamine in diabetic nephropathy. *Life Sci.*, 84(13–14):389–393, Mar 2009. doi: 10.1016/j.lfs.2009.01.007.

Department of Health. Dietary Reference Values for Food Energy and Nutrients for the United Kingdom. Report of the Panel on Dietary Reference Values of the Committee on Medical Aspects of Food Policy. Report on Health and Social Subjects 41. Technical report, Her Majestey's Stationery Office, 1991.

C. Dessapt, M. O. Baradez, A. Hayward, A. D. Cas, S. M. Thomas, G. Viberti, and L. Gnudi. Mechanical forces and TGFβ1 reduce podocyte adhesion through $\alpha3\beta1$ integrin downregulation. *Nephrol. Dial. Transplant.*, 24(9):2645–2655, Sep 2009. doi: 10.1093/ndt/gfp204.

Diabetes Control and Complications Trial writing team. Effect of intensive therapy on the microvascular complications of type 1 diabetes mellitus. *JAMA*, 287(19):2563–2569, May 2002.

Diabetes UK. Diabetes in the UK 2010: Key statistics on diabetes. Online publication, March 2010.

W. B. Dias and G. W. Hart. *O*-GlcNAc modification in diabetes and Alzheimer's disease. *Mol. Biosyst.*, 3(11):766–772, Nov 2007. doi: 10.1039/b704905f.

G. A. Diaz, M. Banikazemi, K. Oishi, R. J. Desnick, and B. D. Gelb. Mutations in a new gene encoding a thiamine transporter cause thiamine-responsive megaloblastic anaemia syndrome. *Nat. Genet.*, 22(3):309–312, Jul 1999. doi: 10.1038/10385.

V. Dilis and A. Trichopoulou. Antioxidant Intakes and Food Sources in Greek Adults. *J. Nutr.*, Epub ahead of print, May 2010. doi: 10.3945/jn.110.121848.

J. B. Dixon. The effect of obesity on health outcomes. *Mol. Cell. Endocrinol.*, 316(2): 104–108, Mar 2010. doi: 10.1016/j.mce.2009.07.008.

D. Dobler, N. Ahmed, L. Song, K. E. Eboigbodin, and P. J. Thornalley. Increased dicarbonyl metabolism in endothelial cells in hyperglycemia induces anoikis and impairs angiogenesis by RGD and GFOGER motif modification. *Diabetes*, 55(7):1961–1969, Jul 2006. doi: 10.2337/db05-1634.

V. Dolce, G. Fiermonte, M. J. Runswick, F. Palmieri, and J. E. Walker. The human mitochondrial deoxynucleotide carrier and its role in the toxicity of nucleoside antivirals. *Proc. Natl. Acad. Sci. U. S. A.*, 98(5):2284–2288, Feb 2001. doi: 10.1073/pnas.031430998.

D. L. Dong and G. W. Hart. Purification and characterization of an *O*-GlcNAc selective *N*-acetyl-β-D-glucosaminidase from rat spleen cytosol. *J. Biol. Chem.*, 269(30):19321–19330, Jul 1994.

G. D. Doyle and E. Campbell. The periodic Schiff-methenamine (PASM) staining of renal biopsies–a light electron microscopic study. *Ir. J. Med. Sci.*, 145(4):127–134, Apr 1976. doi: 10.1007/BF02938932.

A. J. Drake, A. Smith, P. R. Betts, E. C. Crowne, and J. P. H. Shield. Type 2 diabetes in obese white children. *Arch. Dis. Child.*, 86(3):207–208, Mar 2002. doi: 10.1136/adc.86.3.207.

D. J. Drucker. The biology of incretin hormones. *Cell Metab.*, 3(3):153–165, Mar 2006. doi: 10.1016/j.cmet.2006.01.004.

X. Du, T. Matsumura, D. Edelstein, L. Rossetti, Z. Zsengellér, C. Szabó, and M. Brownlee. Inhibition of GAPDH activity by poly(ADP-ribose) polymerase activates three major pathways of hyperglycemic damage in endothelial cells. *J. Clin. Invest.*, 112(7):1049–1057, Oct 2003. doi: 10.1172/JCI18127.

X. L. Du, D. Edelstein, L. Rossetti, I. G. Fantus, H. Goldberg, F. Ziyadeh, J. Wu, and M. Brownlee. Hyperglycemia-induced mitochondrial superoxide overproduction activates the hexosamine pathway and induces plasminogen activator inhibitor-1 expression by increasing Sp1 glycosylation. *Proc. Natl. Acad. Sci. U. S. A.*, 97(22):12222–12226, Oct 2000. doi: 10.1073/pnas.97.22.12222.

J. M. Duclos and P. Haake. Ring opening of thiamine analogs. The role of ring opening in physiological function. *Biochemistry (Mosc.)*, 13(26):5358–5362, Dec 1974. doi: 10.1021/bi00723a016.

P. K. Dudeja, S. Tyagi, R. Gill, and H. M. Said. Evidence for a carrier-mediated mechanism for thiamine transport to human jejunal basolateral membrane vesicles. *Dig. Dis. Sci.*, 48(1):109–115, Jan 2003.

L. A. Dunbar, P. Aronson, and M. J. Caplan. A transmembrane segment determines the steady-state localization of an ion-transporting adenosine triphosphatase. *J. Cell Biol.*, 148(4):769–778, Feb 2000. doi: 10.1083/jcb.148.4.769.

B. Duran-Jimenez, D. Dobler, S. Moffatt, N. Rabbani, C. H. Streuli, P. J. Thornalley, D. R. Tomlinson, and N. J. Gardiner. Advanced glycation end products in extracellular matrix proteins contribute to the failure of sensory nerve regeneration in diabetes. *Diabetes*, 58 (12):2893–2903, Dec 2009. doi: 10.2337/db09-0320.

B. Dutta, W. Huang, M. Molero, R. Kekuda, F. H. Leibach, L. D. Devoe, V. Ganapathy, and P. D. Prasad. Cloning of the human thiamine transporter, a member of the folate transporter family. *J. Biol. Chem.*, 274(45):31925–31929, Nov 1999.

E. Dvornik, N. Simard-Duquesne, M. Krami, K. Sestanj, K. H. Gabbay, J. H. Kinoshita, S. D. Varma, and L. O. Merola. Polyol accumulation in galactosemic and diabetic rats: control by an aldose reductase inhibitor. *Science*, 182(117):1146–1148, Dec 1973.

B. K. Dwivedi and R. G. Arnold. Chemistry of thiamine degradation in food products and model systems: a review. *J. Agric. Food Chem.*, 21(1):54–60, 1973. doi: 10.1021/jf60185a003.

W. S. Dynan and R. Tjian. Isolation of transcription factors that discriminate between different promoters recognized by RNA polymerase II. *Cell*, 32(3):669–680, Mar 1983.

S. Ehtisham, T. G. Barrett, and N. J. Shaw. Type 2 diabetes mellitus in UK children–an emerging problem. *Diabet. Med.*, 17(12):867–871, Dec 2000. doi: 10.1111/j.1464-5491.2000.00409.x.

S. Ehtisham, A. T. Hattersley, D. B. Dunger, T. G. Barrett, B. S. for Paediatric Endocrinology, and D. C. T. Group. First UK survey of paediatric type 2 diabetes and MODY. *Arch. Dis. Child.*, 89(6):526–529, Jun 2004. doi: 10.1136/adc.2003.027821.

K. A. Elliget and B. F. Trump. Primary cultures of normal rat kidney proximal tubule epithelial cells for studies of renal cell injury. *In Vitro Cell. Dev. Biol.*, 27A(9):739–748, Sep 1991. doi: 10.1007/BF02633220.

M. M. Engelgau, L. S. Geiss, J. B. Saaddine, J. P. Boyle, S. M. Benjamin, E. W. Gregg, E. F. Tierney, N. Rios-Burrows, A. H. Mokdad, E. S. Ford, G. Imperatore, and K. M. V. Narayan. The evolving diabetes burden in the United States. *Ann. Intern. Med.*, 140(11): 945–950, Jun 2004.

EPA. 40 CFR (Code of Federal Regulation) § 136. Title 40: Protection of Environment; Part 136: Guidelines establishing test procedures for the analysis of pollutants. Appendix B, August 2010.

E. Erdmann, B. Charbonnel, and R. Wilcox. Thiazolidinediones and cardiovascular risk—a question of balance. *Curr. Cardiol. Rev.*, 5(3):155–165, Aug 2009. doi: 10.2174/157340309788970333.

O. A. Esakova, L. E. Meshalkina, and G. A. Kochetov. Effects of transketolase cofactors on its conformation and stability. *Life Sci.*, 78(1):8–13, Nov 2005. doi: 10.1016/j.lfs.2004.12.055.

J. D. Eudy, O. Spiegelstein, R. C. Barber, B. J. Wlodarczyk, J. Talbot, and R. H. Finnell. Identification and characterization of the human and mouse *SLC19A3* gene: a novel member of the reduced folate family of micronutrient transporter genes. *Mol. Genet. Metab.*, 71(4):581–590, Dec 2000. doi: 10.1006/mgme.2000.3112.

D. J. Ewing and B. F. Clarke. Diagnosis and management of diabetic autonomic neuropathy. *Br. Med. J. (Clin. Res. Ed.)*, 285(6346):916–918, Oct 1982. doi: 10.1136/bmj.285.6346.916.

Expert Group On Vitamins and Minerals. Review of Thiamin. EVM/00/14/P. Technical report, UK Food Standards Agency, 2000.

Expert Group On Vitamins and Minerals. Thiamine risk assessment. Technical report, UK Food Standards Agency, 2003.

F. Fang, Z. Kang, and C. Wong. Vitamin E tocotrienols improve insulin sensitivity through activating peroxisome proliferator-activated receptors. *Mol. Nutr. Food Res.*, 54(3):345–352, Mar 2010. doi: 10.1002/mnfr.200900119.

V. Fayol. High-performance liquid chromatography determination of total thiamin in biological and food products. *Methods Enzymol.*, 279:57–66, 1997. doi: 10.1016/S0076-6879(97)79009-8. Published in same journal and same issue as Gerrits - Also several other thiamine papers that issue.

P. M. Finglas. Thiamin. *Int. J. Vitam. Nutr. Res.*, 63(4):270–274, 1993.

J. C. Fleming, E. Tartaglini, M. P. Steinkamp, D. F. Schorderet, N. Cohen, and E. J. Neufeld. The gene mutated in thiamine-responsive anaemia with diabetes and deafness (TRMA) encodes a functional thiamine transporter. *Nat. Genet.*, 22(3):305–308, Jul 1999. doi: 10.1038/10379.

V. Foulon, V. D. Antonenkov, K. Croes, E. Waelkens, G. P. Mannaerts, P. P. V. Veldhoven, and M. Casteels. Purification, molecular cloning, and expression of 2-hydroxyphytanoyl-CoA lyase, a peroxisomal thiamine pyrophosphate-dependent enzyme that catalyzes the carbon-carbon bond cleavage during α-oxidation of 3-methyl-branched fatty acids. *Proc. Natl. Acad. Sci. U. S. A.*, 96(18):10039–10044, Aug 1999.

D. Fraser, L. Wakefield, and A. Phillips. Independent regulation of transforming growth factor-β1 transcription and translation by glucose and platelet-derived growth factor. *Am. J. Pathol.*, 161(3):1039–1049, Sep 2002.

B. I. Freedman, J.-P. Wuerth, K. Cartwright, R. P. Bain, S. Dippe, K. Hershon, A. D. Mooradian, B. S. Spinowitz, and for the ACTION II Study Investigators. Design and Baseline Characteristics for the Aminoguanidine Clinical Trial in Overt Type 2 Diabetic Nephropathy (ACTION II). *Control. Clin. Trials*, 20(5):493–510, October 1999. doi: 10.1016/S0197-2456(99)00024-0.

C. A. Frye and C. W. Patrick. Isolation and culture of rat microvascular endothelial cells. *In Vitro Cell. Dev. Biol. Anim.*, 38(4):208–212, Apr 2002. doi: 10.1290/1071-2690(2002)038<0208:IACORM>2.0.CO;2.

A. Fujita. Thiaminase. *Adv. Enzymol. Relat. Subj. Biochem.*, 15:389–421, 1954.

A. Fujita, Y. Nose, and Kuratanik. The second type of bacterial thiaminase. *J. Vitaminol. (Kyoto)*, 1(1):1–7, Jul 1954.

M. Fujiwara, H. Nanjo, T. Arai, and S. Ziro. "Allithiamine" A newly found derivative of vitamin B_1. II Effect of allithiamine on living organism. *J. Biochem. (Tokyo)*, 41(2): 273–285, 1954a.

M. Fujiwara, H. Watanabe, and K. Majsui. "Allithiamine" A newly found derivative of vitamin B_1. I Discovery of Allithiamine. *J. Biochem. (Tokyo)*, 41(1):29–39, 1954b.

N. Fülöp, M. M. Mason, K. Dutta, P. Wang, A. J. Davidoff, R. B. Marchase, and J. C. Chatham. Impact of Type 2 diabetes and aging on cardiomyocyte function and *O*-linked *N*-acetylglucosamine levels in the heart. *Am. J. Physiol. Cell. Physiol.*, 292(4):C1370–C1378, Apr 2007. doi: 10.1152/ajpcell.00422.2006.

C. Funk. On the chemical nature of the substance which cures polyneuritis in birds, induced by a diet of polished rice. *J. Physiol. (Lond.)*, 43:395–400, 1912a.

C. Funk. The Vitamines. *Dublin HE (transl.). Baltimore: Williams & Wilkins*, 1912b.

X. Gallet, B. Charloteaux, A. Thomas, and R. Brasseur. A fast method to predict protein interaction sites from sequences. *J. Mol. Biol.*, 302(4):917–926, Sep 2000. doi: 10.1006/jmbi.2000.4092.

V. Ganapathy, S. B. Smith, and P. D. Prasad. *SLC19*: the folate/thiamine transporter family. *Pflugers Arch.*, 447(5):641–646, Feb 2004. doi: 10.1007/s00424-003-1068-1.

V. Gandhi, S. Wagh, and K. Menon. Lipoic acid and Diabetes II: Mode of action of Lipoic acid. *J. Biosci.*, 9:117–127, 1985.

W. Gepts. Islet morphology in type I diabetes. *Behring Inst. Mitt.*, 75:39–41, Jul 1984.

W. Gepts and P. M. Lecompte. The pancreatic islets in diabetes. *Am. J. Med.*, 70(1): 105–115, Jan 1981.

P. Geraldes and G. L. King. Activation of protein kinase C isoforms and its impact on diabetic complications. *Circ. Res.*, 106(8):1319–1331, Apr 2010. doi: 10.1161/CIRCRESAHA.110.217117.

J. Gerrits, H. Eidhof, J. W. Brunnekreeft, and J. Hessels. Determination of thiamin and thiamin phosphates in whole blood by reversed-phase liquid chromatography with precolumn derivatization. *Methods Enzymol.*, 279:74–82, 1997. doi: 10.1016/S0076-6879(97)79011-6. Published in same journal and same issue as Fayol - Also several other thiamine papers that issue.

G. Gill, E. Pascal, Z. H. Tseng, and R. Tjian. A glutamine-rich hydrophobic patch in transcription factor Sp1 contacts the $dTAF_{II}110$ component of the *Drosophila* TFIID complex and mediates transcriptional activation. *Proc. Natl. Acad. Sci. USA*, 91(1):192–196, Jan 1994.

A. Godbout and J.-L. Chiasson. Who Should Benefit from the Use of α-Glucosidase Inhibitors? *Curr. Diab. Rep.*, 7:33–339, 2007.

C.-X. Gong, F. Liu, I. Grundke-Iqbal, and K. Iqbal. Impaired brain glucose metabolism leads to Alzheimer neurofibrillary degeneration through a decrease in tau *O*-GlcNAcylation. *J. Alzheimers Dis.*, 9(1):1–12, Mar 2006.

M. González-Ortiz, E. Martínez-Abundis, J. A. Robles-Cervantes, V. Ramírez-Ramírez, and M. G. Ramos-Zavala. Effect of thiamine administration on metabolic profile, cytokines and inflammatory markers in drug-naïve patients with type 2 diabetes. *Eur. J. Nutr.*, Epub ahead of print, Jul 2010. doi: 10.1007/s00394-010-0123-x.

M. B. Graeber, K. G. Kupke, and U. Müller. Delineation of the dystonia-parkinsonism syndrome locus in Xq13. *Proc. Natl. Acad. Sci. U. S. A.*, 89(17):8245–8248, Sep 1992.

D. A. Greene, J. C. Arezzo, and M. B. Brown. Effect of aldose reductase inhibition on nerve conduction and morphometry in diabetic neuropathy. Zenarestat Study Group. *Neurology*, 53(3):580–91, 1999. ISSN 0028-3878 (Print).

J. Gregory and S. Lowe. National Diet and Nutrition Survey: young people aged 4 to 18 years. Volume 1. Technical report, Her Majestey's Stationery Office, 2000.

L. S. Griffith and B. Schmitz. O-linked N-acetylglucosamine levels in cerebellar neurons respond reciprocally to pertubations of phosphorylation. *Eur. J. Biochem.*, 262(3):824–831, Jun 1999. doi: 10.1046/j.1432-1327.1999.00439.x.

J. L. Gross, M. J. de Azevedo, S. P. Silveiro, L. H. Canani, M. L. Caramori, and T. Zelmanovitz. Diabetic nephropathy: diagnosis, prevention, and treatment. *Diabetes Care*, 28(1):164–176, Jan 2005.

G. R. Grotendorst. Connective tissue growth factor: a mediator of TGF-β action on fibroblasts. *Cytokine Growth Factor Rev.*, 8(3):171–179, Sep 1997.

C. Guinez, A.-M. Mir, V. Dehennaut, R. Cacan, A. Harduin-Lepers, J.-C. Michalski, and T. Lefebvre. Protein ubiquitination is modulated by *O*-GlcNAc glycosylation. *FASEB J.*, 22(8):2901–2911, Aug 2008. doi: 10.1096/fj.07-102509.

P. Haake, L. P. Bausher, and J. P. McNeal. Fundamental studies on models for thiamine. Generation of ylides of oxazolium, imidazolium, and thiazolium ions by decarboxylation. Applications to the structure of the thiamine ylide. *J. Am. Chem. Soc.*, 93(25):7045–7049, Dec 1971.

R. H. Haas. Thiamin and the brain. *Annu. Rev. Nutr.*, 8:483–515, 1988. doi: 10.1146/annurev.nu.08.070188.002411.

C. L. Halbert, G. W. Demers, and D. A. Galloway. The E7 gene of human papillomavirus type 16 is sufficient for immortalization of human epithelial cells. *J. Virol.*, 65(1):473–478, Jan 1991.

R. S. Haltiwanger, M. A. Blomberg, and G. W. Hart. Glycosylation of nuclear and cytoplasmic proteins. Purification and characterization of a uridine diphospho-*N*-acetylglucosamine:polypeptide β-*N*-acetylglucosaminyltransferase. *J. Biol. Chem.*, 267 (13):9005–9013, May 1992.

S. Halwachs, C. Kneuer, and W. Honscha. Downregulation of the reduced folate carrier transport activity by phenobarbital-type cytochrome P450 inducers and protein kinase C activators. *Biochim. Biophys. Acta*, 1768(6):1671–1679, Jun 2007. doi: 10.1016/j.bbamem.2007.03.023.

H.-P. Hammes, X. Du, D. Edelstein, T. Taguchi, T. Matsumura, Q. Ju, J. Lin, A. Bierhaus, P. Nawroth, D. Hannak, M. Neumaier, R. Bergfeld, I. Giardino, and M. Brownlee. Benfotiamine blocks three major pathways of hyperglycemic damage and prevents experimental diabetic retinopathy. *Nat. Med.*, 9(3):294–299, Mar 2003. doi: 10.1038/nm834.

I. Han and J. E. Kudlow. Reduced O glycosylation of Sp1 is associated with increased proteasome susceptibility. *Mol. Cell. Biol.*, 17(5):2550–2558, May 1997.

G. W. Hart, M. P. Housley, and C. Slawson. Cycling of *O*-linked *β*-*N*-acetylglucosamine on nucleocytoplasmic proteins. *Nature*, 446(7139):1017–1022, Apr 2007. doi: 10.1038/nature05815.

Y. Hashitani and J. R. Cooper. The partial purification of thiamine triphosphatase from rat brain. *J. Biol. Chem.*, 247(7):2117–2119, Apr 1972.

H. N. Haugen. The blood concentration of thiamine in diabetes. *Scand. J. Clin. Lab. Invest.*, 16:260–266, 1964.

E. Havivi, H. B. On, A. Reshef, P. Stein, and I. Raz. Vitamins and trace metals status in non insulin dependent diabetes mellitus. *Int. J. Vitam. Nutr. Res.*, 61(4):328–333, 1991.

M. Hawkins, N. Barzilai, R. Liu, M. Hu, W. Chen, and L. Rossetti. Role of the glucosamine pathway in fat-induced insulin resistance. *J. Clin. Invest.*, 99(9):2173–2182, May 1997. doi: 10.1172/JCI119390.

P. Hawley-Nelson, K. H. Vousden, N. L. Hubbert, D. R. Lowy, and J. T. Schiller. HPV16 E6 and E7 proteins cooperate to immortalize human foreskin keratinocytes. *EMBO J.*, 8 (12):3905–3910, Dec 1989.

P. A. Haynes. Phosphoglycosylation: a new structural class of glycosylation? *Glycobiology*, 8(1):1–5, Jan 1998.

M. Hazel, R. C. Cooksey, D. Jones, G. Parker, J. L. Neidigh, B. Witherbee, E. A. Gulve, and D. A. McClain. Activation of the hexosamine signaling pathway in adipose tissue results in decreased serum adiponectin and skeletal muscle insulin resistance. *Endocrinology*, 145 (5):2118–2128, May 2004. doi: 10.1210/en.2003-0812.

L. F. Hebert, M. C. Daniels, J. Zhou, E. D. Crook, R. L. Turner, S. T. Simmons, J. L. Neidigh, J. S. Zhu, A. D. Baron, and D. A. McClain. Overexpression of glutamine:fructose-6-phosphate amidotransferase in transgenic mice leads to insulin resistance. *J. Clin. Invest.*, 98(4):930–936, Aug 1996. doi: 10.1172/JCI118876.

C. W. Heilig, L. A. Concepcion, B. L. Riser, S. O. Freytag, M. Zhu, and P. Cortes. Overexpression of glucose transporters in rat mesangial cells cultured in a normal glucose milieu mimics the diabetic phenotype. *J. Clin. Invest.*, 96(4):1802–1814, Oct 1995. doi: 10.1172/JCI118226.

C. W. Heilig, J. I. Kreisberg, S. Freytag, T. Murakami, Y. Ebina, L. Guo, K. Heilig, R. Loberg, X. Qu, Y. Jin, D. Henry, and F. C. Brosius. Antisense GLUT-1 protects mesangial cells from glucose induction of GLUT-1 and fibronectin expression. *Am. J. Physiol. Renal Physiol.*, 280(4):F657–F666, Apr 2001.

P. C. Heinrich, H. Steffen, P. Janser, and O. Wiss. Studies on the reconstitution of apotransketolase with thiamine pyrophosphate and analogs of the coenzyme. *Eur. J. Biochem.*, 30(3):533–541, Nov 1972.

H. G. Hers. The mechanism of the transformation of glucose in fructose in the seminal vesicles. *Biochim. Biophys. Acta*, 22(1):202–203, Oct 1956.

H. P. Himsworth. Diabetes mellitus: Its differentiation into insulin-sensitive and insulin-insensitive types. *Lancet*, 227:127–130, January 1936. doi: 10.1016/S0140-6736(01)36134-2.

P. Hovind, P. Rossing, L. Tarnow, U. M. Smidt, and H. H. Parving. Progression of diabetic nephropathy. *Kidney Int.*, 59(2):702–709, Feb 2001. doi: 10.1046/j.1523-1755.2001.059002702.x.

I. Hubatsch, E. G. E. Ragnarsson, and P. Artursson. Determination of drug permeability and prediction of drug absorption in Caco-2 monolayers. *Nat. Protoc.*, 2(9):2111–2119, 2007. doi: 10.1038/nprot.2007.303.

G. M. Huber and H. P. V. Rupasinghe. Phenolic profiles and antioxidant properties of apple skin extracts. *J. Food Sci.*, 74(9):C693–C700, 2009. doi: 10.1111/j.1750-3841.2009.01356.x.

T. C. Huynh, B. Aungst, and I. Hidalgo. *Ex Vivo* Human Intestinal Permeability. *AAPS*, Abstracts volume:1293, 2002.

M. K. Hypes, L. Pirisi, and K. E. Creek. Mechanisms of decreased expression of transforming growth factor-beta receptor type I at late stages of HPV16-mediated transformation. *Cancer Lett.*, 282(2):177–186, Sep 2009. doi: 10.1016/j.canlet.2009.03.014.

International Diabetes Federation. Diabetes atlas, fourth edition, 2009. Note: These figures are based on self-reported data from countries so differing screening strategies will affect the data.

Y. Itokawa and J. R. Cooper. The enzymatic synthesis of triphosphothiamin. *Biochim. Biophys. Acta*, 158(1):180–182, Apr 1968.

A. Iwashima, H. Nishino, and Y. Nose. Conversion of thiamine to thiamine monophosphate by cell-free extracts of *Escherichia coli*. *Biochim. Biophys. Acta*, 258(1):333–336, Jan 1972.

S. P. Jackson and R. Tjian. *O*-glycosylation of eukaryotic transcription factors: implications for mechanisms of transcriptional regulation. *Cell*, 55(1):125–133, Oct 1988.

S. P. Jackson and R. Tjian. Purification and analysis of RNA polymerase II transcription factors by using wheat germ agglutinin affinity chromatography. *Proc. Natl. Acad. Sci. U. S. A.*, 86(6):1781–1785, Mar 1989.

L. R. James, D. Tang, A. Ingram, H. Ly, K. Thai, L. Cai, and J. W. Scholey. Flux through the hexosamine pathway is a determinant of nuclear factor κB-dependent promoter activation. *Diabetes*, 51(4):1146–1156, Apr 2002. doi: 10.2337/diabetes.51.4.1146.

R. G. Janes and J. Brady. Thiamine deficiency in normal rats and in rats made diabetic with alloxan. *Am. J. Physiol.*, 153(3):417–424, Jun 1948.

B. C. P. Jansen. *Rec. Trav. Chim. Pays-Bas*, 55:1046, 1936.

J. A. Jedziniak, L. T. Chylack, H. M. Cheng, M. K. Gillis, A. A. Kalustian, and W. H. Tung. The sorbitol pathway in the human lens: aldose reductase and polyol dehydrogenase. *Invest. Ophthalmol. Vis. Sci.*, 20(3):314–326, Mar 1981.

G. Jermendy. Evaluating thiamine deficiency in patients with diabetes. *Diab. Vasc. Dis. Res.*, 3(2):120–121, Sep 2006. doi: 10.3132/dvdr.2006.014.

M. D. Jeyasingham, O. E. Pratt, A. D. Thomson, and G. K. Shaw. Reduced stability of rat brain transketolase after conversion to the apo form. *J. Neurochem.*, 47(1):278–281, Jul 1986. doi: 10.1111/j.1471-4159.1986.tb02859.x.

P. G. Johansen, R. D. Marshall, and A. Neuberger. Carbohydrates in protein. 3 The preparation and some of the properties of a glycopeptide from hen's-egg albumin. *Biochem. J.*, 78:518–527, Mar 1961.

J. T. Kadonaga, K. R. Carner, F. R. Masiarz, and R. Tjian. Isolation of cDNA encoding transcription factor Sp1 and functional analysis of the DNA binding domain. *Cell*, 51(6): 1079–1090, Dec 1987.

J. T. Kadonaga, A. J. Courey, J. Ladika, and R. Tjian. Distinct regions of Sp1 modulate DNA binding and transcriptional activation. *Science*, 242(4885):1566–1570, Dec 1988.

M. Kanehisa and S. Goto. KEGG: Kyoto encyclopedia of genes and genomes. *Nucleic Acids Res.*, 28(1):27–30, Jan 2000.

H. Kaneto, Y. Kajimoto, J. Miyagawa, T. Matsuoka, Y. Fujitani, Y. Umayahara, T. Hanafusa, Y. Matsuzawa, Y. Yamasaki, and M. Hori. Beneficial effects of antioxidants in diabetes: possible protection of pancreatic β-cells against glucose toxicity. *Diabetes*, 48 (12):2398–2406, Dec 1999.

H. Kaneto, G. Xu, K. H. Song, K. Suzuma, S. Bonner-Weir, A. Sharma, and G. C. Weir. Activation of the hexosamine pathway leads to deterioration of pancreatic β-cell function through the induction of oxidative stress. *J. Biol. Chem.*, 276(33):31099–31104, Aug 2001. doi: 10.1074/jbc.M104115200.

H. T. Kang, J. W. Ju, J. W. Cho, and E. S. Hwang. Down-regulation of Sp1 activity through modulation of *O*-glycosylation by treatment with a low glucose mimetic, 2-deoxyglucose. *J. Biol. Chem.*, 278(51):51223–51231, Dec 2003. doi: 10.1074/jbc.M307332200.

J. Kang and D. C. Samuels. The evidence that the DNC (*SLC25A19*) is not the mitochondrial deoxyribonucleotide carrier. *Mitochondrion*, 8(2):103–108, Mar 2008. doi: 10.1016/j.mito.2008.01.001.

J. Kaprio, J. Tuomilehto, M. Koskenvuo, K. Romanov, A. Reunanen, J. Eriksson, J. Stengård, and Y. A. Kesäniemi. Concordance for type 1 (insulin-dependent) and type 2 (non-insulin-dependent) diabetes mellitus in a population-based cohort of twins in Finland. *Diabetologia*, 35(11):1060–1067, Nov 1992.

N. Karachalias, R. Babaei-Jadidi, N. Ahmed, and P. J. Thornalley. Accumulation of fructosyl-lysine and advanced glycation end products in the kidney, retina and peripheral nerve of streptozotocin-induced diabetic rats. *Biochem. Soc. Trans.*, 31(6):1423–1425, Dec 2003.

N. Karachalias, R. Babaei-Jadidi, N. Rabbani, and P. J. Thornalley. Increased protein damage in renal glomeruli, retina, nerve, plasma and urine and its prevention by thiamine and benfotiamine therapy in a rat model of diabetes. *Diabetologia*, 53(7):1506–1516, Jul 2010a. doi: 10.1007/s00125-010-1722-z.

N. Karachalias, R. Babaei-Jadidi, N. Rabbani, and P. J. Thornalley. Prevention of decline in glycaemic control in streptozotocin-induced diabetic rats by thiamine but not by Benfotiamine. *Diabet. Med.*, 27:Suppl 1 Abstract, 2010b.

C. N. Keembiyehetty, R. P. Candelaria, G. Majumdar, R. Raghow, A. Martinez-Hernandez, and S. S. Solomon. Paradoxical regulation of Sp1 transcription factor by glucagon. *Endocrinology*, 143(4):1512–1520, Apr 2002.

N. Khidekel, S. Arndt, N. Lamarre-Vincent, A. Lippert, K. G. Poulin-Kerstien, B. Ramakrishnan, P. K. Qasba, and L. C. Hsieh-Wilson. A chemoenzymatic approach toward the rapid and sensitive detection of *O*-GlcNAc posttranslational modifications. *J. Am. Chem. Soc.*, 125(52):16162–16163, Dec 2003. doi: 10.1021/ja038545r.

N. Khidekel, S. B. Ficarro, E. C. Peters, and L. C. Hsieh-Wilson. Exploring the *O*-GlcNAc proteome: direct identification of *O*-GlcNAc-modified proteins from the brain. *Proc. Natl. Acad. Sci. U. S. A.*, 101(36):13132–13137, Sep 2004. doi: 10.1073/pnas.0403471101.

K. Kida. Genetics of type 1 diabetes in childhood. *Diabetes Nutr. Metab.*, 12(2):58–67, Apr 1999.

C. Kingsley and A. Winoto. Cloning of GT box-binding proteins: a novel Sp1 multigene family regulating T-cell receptor gene expression. *Mol. Cell. Biol.*, 12(10):4251–4261, Oct 1992.

J. H. Kinoshita, D. Dvornik, M. Kraml, and K. H. Gabbay. The effect of an aldose reductase inhibitor on the galactose-exposed rabbit lens. *Biochim. Biophys. Acta*, 158(3):472–475, Jun 1968.

M. Kirchhof, N. Popat, and J. Malowany. A Historical Perspective of the Diagnosis of Diabetes. *UWOMJ*, 78(1):7–11, 2008.

D. Kirpichnikov, S. I. McFarlane, and J. R. Sowers. Metformin: an update. *Ann. Intern. Med.*, 137(1):25–33, Jul 2002.

G. A. Kochetov and A. E. Izotova. [Reconstruction of holotransketolase from the apoenzyme and coenzyme]. *Biokhimiia*, 38(3):552–560, 1973.

Y. Kohda, H. Shirakawa, K. Yamane, K. Otsuka, T. Kono, F. Terasaki, and T. Tanaka. Prevention of incipient diabetic cardiomyopathy by high-dose thiamine. *J. Toxicol. Sci.*, 33(4):459–472, Oct 2008.

V. Kolm-Litty, U. Sauer, A. Nerlich, R. Lehmann, and E. D. Schleicher. High glucose-induced transforming growth factor β1 production is mediated by the hexosamine pathway in porcine glomerular mesangial cells. *J. Clin. Invest.*, 101(1):160–169, Jan 1998. doi: 10.1172/JCI119875.

D. Kong, Y. Zhu, H. Wu, X. Cheng, H. Liang, and H.-Q. Ling. *AtTHIC*, a gene involved in thiamine biosynthesis in *Arabidopsis thaliana*. *Cell Res.*, 18(5):566–576, May 2008. doi: 10.1038/cr.2008.35.

S. Kono, H. Miyajima, K. Yoshida, A. Togawa, K. Shirakawa, and H. Suzuki. Mutations in a thiamine-transporter gene and Wernicke's-like encephalopathy. *N. Engl. J. Med.*, 360 (17):1792–1794, Apr 2009. doi: 10.1056/NEJMc0809100.

R. Konsoula and F. A. Barile. Correlation of *in vitro* cytotoxicity with paracellular permeability in Caco-2 cells. *Toxicol. in Vitro*, 19(5):675–684, Aug 2005. doi: 10.1016/j.tiv.2005.03.006.

S. S. Korshunov, V. P. Skulachev, and A. A. Starkov. High protonic potential actuates a mechanism of production of reactive oxygen species in mitochondria. *FEBS Lett.*, 416(1): 15–18, Oct 1997.

D. Koya and G. L. King. Protein kinase C activation and the development of diabetic complications. *Diabetes*, 47(6):859–866, Jun 1998.

G. R. Kracke, G. G. Preston, and T. H. Stanley. Identification of a sorbitol permease in human erythrocytes. *Am. J. Physiol.*, 266(2 Pt 1):C343–C350, Feb 1994.

L. K. Kreppel, M. A. Blomberg, and G. W. Hart. Dynamic glycosylation of nuclear and cytosolic proteins. Cloning and characterization of a unique *O*-GlcNAc transferase with multiple tetratricopeptide repeats. *J. Biol. Chem.*, 272(14):9308–9315, Apr 1997.

N. J. Kruger and A. von Schaewen. The oxidative pentose phosphate pathway: structure and organisation. *Curr. Opin. Plant Biol.*, 6(3):236–246, Jun 2003. doi: 10.1016/S1369-5266(03)00039-6.

A. Kundu, R. T. Avalos, C. M. Sanderson, and D. P. Nayak. Transmembrane domain of influenza virus neuraminidase, a type II protein, possesses an apical sorting signal in polarized MDCK cells. *J. Virol.*, 70(9):6508–6515, Sep 1996.

K. O. Kyvik, A. Green, and H. Beck-Nielsen. Concordance rates of insulin dependent diabetes mellitus: a population based study of young Danish twins. *BMJ*, 311(7010): 913–917, Oct 1995.

V. Labay, T. Raz, D. Baron, H. Mandel, H. Williams, T. Barrett, R. Szargel, L. McDonald, A. Shalata, K. Nosaka, S. Gregory, and N. Cohen. Mutations in *SLC19A2* cause thiamine-responsive megaloblastic anaemia associated with diabetes mellitus and deafness. *Nat. Genet.*, 22(3):300–304, Jul 1999. doi: 10.1038/10372.

F. M.-M. Lai, C.-C. Szeto, P. C. L. Choi, K. K. L. Ho, N. L. S. Tang, K.-M. Chow, P. K. T. Li, and K.-F. To. Isolate diffuse thickening of glomerular capillary basement membrane: a renal lesion in prediabetes? *Mod. Pathol.*, 17(12):1506–1512, Dec 2004. doi: 10.1038/modpathol.3800219.

W. Lam, C. Chen, S. Ruan, C.-H. Leung, and Y.-C. Cheng. Expression of deoxynucleotide carrier is not associated with the mitochondrial DNA depletion caused by anti-HIV dideoxynucleoside analogs and mitochondrial dNTP uptake. *Mol. Pharmacol.*, 67(2): 408–416, Feb 2005. doi: 10.1124/mol.104.007120.

A. Y. Lee and S. S. Chung. Contributions of polyol pathway to oxidative stress in diabetic cataract. *FASEB J.*, 13(1):23–30, Jan 1999.

R. Lehmann, M. Huber, A. Beck, T. Schindera, T. Rinkler, B. Houdali, C. Weigert, H. U. Häring, W. Voelter, and E. D. Schleicher. Simultaneous, quantitative analysis of UDP-*N*-acetylglucosamine, UDP-*N*-acetylgalactosamine, UDP-glucose and UDP-galactose in human peripheral blood cells, muscle biopsies and cultured mesangial cells by capillary zone electrophoresis. *Electrophoresis*, 21(14):3010–3015, Aug 2000. doi: 10.1002/1522-2683(20000801)21:14<3010::AID-ELPS3010>3.0.CO;2-C.

R. Leonardi and P. L. Roach. Thiamine biosynthesis in *Escherichia coli*: in vitro reconstitution of the thiazole synthase activity. *J. Biol. Chem.*, 279(17):17054–17062, Apr 2004. doi: 10.1074/jbc.M312714200.

J. Letovsky and W. S. Dynan. Measurement of the binding of transcription factor Sp1 to a single GC box recognition sequence. *Nucleic Acids Res.*, 17(7):2639–53, 1989. ISSN 0305-1048 (Print).

F. Leuthardt and H. Nielsen. Phosphorylation biologique de la thiamine. *Helv. Chim. Acta*, 35:1196–1209, 1952.

B. Lewko and J. Stepinski. Hyperglycemia and mechanical stress: targeting the renal podocyte. *J. Cell. Physiol.*, 221(2):288–295, Nov 2009. doi: 10.1002/jcp.21856.

L. Li, S. He, J.-M. Sun, and J. R. Davie. Gene regulation by Sp1 and Sp3. *Biochem. Cell Biol.*, 82(4):460–471, Aug 2004. doi: 10.1139/o04-045.

S. Lin, H. Y. Naim, A. C. Rodriguez, and M. G. Roth. Mutations in the middle of the transmembrane domain reverse the polarity of transport of the influenza virus hemagglutinin in MDCK epithelial cells. *J. Cell Biol.*, 142(1):51–57, Jul 1998. doi: 10.1083/jcb.142.1.51.

K. Lindhardt and E. Bechgaard. Sodium glycocholate transport across Caco-2 cell monolayers, and the enhancement of mannitol transport relative to transepithelial electrical resistance. *Int. J. Pharm.*, 252(1-2):181–186, Feb 2003.

M. J. Lindhurst, G. Fiermonte, S. Song, E. Struys, F. D. Leonardis, P. L. Schwartzberg, A. Chen, A. Castegna, N. Verhoeven, C. K. Mathews, F. Palmieri, and L. G. Biesecker. Knockout of *Slc25a19* causes mitochondrial thiamine pyrophosphate depletion, embryonic lethality, CNS malformations, and anemia. *Proc. Natl. Acad. Sci. U. S. A.*, 103(43): 15927–15932, Oct 2006. doi: 10.1073/pnas.0607661103.

Y. Lindqvist, G. Schneider, U. Ermler, and M. Sundström. Three-dimensional structure of transketolase, a thiamine diphosphate dependent enzyme, at 2.5 Angstrom resolution. *EMBO J.*, 11(7):2373–2379, Jul 1992.

S. S. Lo, R. Y. Tun, M. Hawa, and R. D. Leslie. Studies of diabetic twins. *Diabetes. Metab. Rev.*, 7(4):223–238, Dec 1991.

K. Lohmann. A study of the enzymatic transformation of synthetic methylglyoxal to lactic acid. *Biochem. Z.*, 254:332–354, 1932.

D. Lonsdale. A review of the biochemistry, metabolism and clinical benefits of thiamin(e) and its derivatives. *Evid. Based Compl. Alt. Med.*, 3(1):49–59, Mar 2006. doi: 10.1093/ecam/nek009.

O. H. Lowry, N. J. Rosebrough, A. L. Farr, and R. J. Randall. Protein measurement with the Folin phenol reagent. *J. Biol. Chem.*, 193(1):265–275, Nov 1951.

A. Luhe, H. Hildebrand, U. Bach, T. Dingermann, and H.-J. Ahr. A new approach to studying ochratoxin A (OTA)-induced nephrotoxicity: expression profiling *in vivo* and *in vitro* employing cDNA microarrays. *Toxicol. Sci.*, 73(2):315–328, Jun 2003. doi: 10.1093/toxsci/kfg073.

T. Lüthi, R. S. Haltiwanger, P. Greengard, and M. Bähler. Synapsins contain *O*-linked *N*-acetylglucosamine. *J. Neurochem.*, 56(5):1493–1498, May 1991.

J. Mabley, M. Brownlee, H. Hammes, and C. Szabo. The B_1 vitamin analog benfotiamine inhibits poly(ADP-ribose) polymerase. *FASEB J.*, 18:A1189–1190, 2004.

M. A. Mahajan and M. Acara. Uptake and phosphorylation of thiamine in rat kidney cortical slices. I. Effect of ethanol. *J. Pharmacol. Exp. Ther.*, 268(3):1311–1315, Mar 1994.

G. Majumdar, J. Wright, P. Markowitz, A. Martinez-Hernandez, R. Raghow, and S. S. Solomon. Insulin stimulates and diabetes inhibits *O*-linked *N*-acetylglucosamine transferase and *O*-glycosylation of Sp1. *Diabetes*, 53(12):3184–3192, Dec 2004. doi: 10.2337/diabetes.53.12.3184.

G. Majumdar, A. Harrington, J. Hungerford, A. Martinez-Hernandez, I. C. Gerling, R. Raghow, and S. Solomon. Insulin dynamically regulates calmodulin gene expression by sequential *O*-glycosylation and phosphorylation of Sp1 and its subcellular compartmentalization in liver cells. *J. Biol. Chem.*, 281(6):3642–3650, Feb 2006. doi: 10.1074/jbc.M511223200.

A. F. Makarchikov, B. Lakaye, I. E. Gulyai, J. Czerniecki, B. Coumans, P. Wins, T. Grisar, and L. Bettendorff. Thiamine triphosphate and thiamine triphosphatase activities: from bacteria to mammals. *Cell. Mol. Life Sci.*, 60(7):1477–1488, Jul 2003. doi: 10.1007/s00018-003-3098-4.

M. Marin, A. Karis, P. Visser, F. Grosveld, and S. Philipsen. Transcription factor Sp1 is essential for early embryonic development but dispensable for cell growth and differentiation. *Cell*, 89(4):619–628, May 1997. doi: 10.1016/S0092-8674(00)80243-3.

Marine Biotechnology Research Centre. Absorption Assay Drug Absorption / Permeability Caco-2 Assay, 2009.

E. Marmstål and B. Mannervik. Evaluation of the two-substrate pathway of glyoxalase from yeast by use of carbonic anhydrase and rapid kinetic studies. *FEBS Lett.*, 131:301–304, 1981.

S. Marshall, V. Bacote, and R. R. Traxinger. Complete inhibition of glucose-induced desensitization of the glucose transport system by inhibitors of mRNA synthesis. Evidence for rapid turnover of glutamine:fructose-6-phosphate amidotransferase. *J. Biol. Chem.*, 266 (16):10155–10161, Jun 1991.

R. M. Mason and N. A. Wahab. Extracellular matrix metabolism in diabetic nephropathy. *J. Am. Soc. Nephrol.*, 14(5):1358–1373, May 2003. doi: 10.1097/01.ASN.0000065640.77499.D7.

J. R. Masters. False cell lines: The problem and a solution. *Cytotechnology*, 39(2):69–74, Jul 2002. doi: 10.1023/A:1022908930937.

I. A. Mastrangelo, A. J. Courey, J. S. Wall, S. P. Jackson, and P. V. Hough. DNA looping and Sp1 multimer links: a mechanism for transcriptional synergism and enhancement. *Proc. Natl. Acad. Sci. U. S. A.*, 88(13):5670–5674, Jul 1991.

P. W. Mathieson. Update on the podocyte. *Curr. Opin. Nephrol. Hypertens.*, 18(3):206–211, May 2009. doi: 10.1097/MNH.0b013e328326f3ca.

D. A. McClain, W. A. Lubas, R. C. Cooksey, M. Hazel, G. J. Parker, D. C. Love, and J. A. Hanover. Altered glycan-dependent signaling induces insulin resistance and hyperleptinemia. *Proc. Natl. Acad. Sci. U. S. A.*, 99(16):10695–10699, Aug 2002. doi: 10.1073/pnas.152346899.

C. H. S. McIntosh, H.-U. Demuth, J. A. Pospisilik, and R. Pederson. Dipeptidyl peptidase IV inhibitors: how do they work as new antidiabetic agents? *Regul. Pept.*, 128(2):159–165, Jun 2005. doi: 10.1016/j.regpep.2004.06.001.

L. Mee, S. M. Nabokina, V. T. Sekar, V. S. Subramanian, K. Maedler, and H. M. Said. Pancreatic β cells and islets take up thiamin by a regulated carrier-mediated process: studies using mice and human pancreatic preparations. *Am. J. Physiol. Gastrointest. Liver Physiol.*, 297(1):G197–G206, Jul 2009. doi: 10.1152/ajpgi.00092.2009.

T. W. Meyer, P. H. Bennett, and R. G. Nelson. Podocyte number predicts long-term urinary albumin excretion in Pima Indians with Type II diabetes and microalbuminuria. *Diabetologia*, 42(11):1341–1344, Nov 1999. doi: 10.1007/s001250051447.

R. K. Mitra, J. M. Woodley, and M. D. Lilly. *Escherichia coli* transketolase-catalyzed carbon-carbon bond formation: biotransformation characterization for reactor evaluation and selection. *Enzyme Microb. Technol.*, 22(1):64–70, Jan 1998. doi: 10.1016/S0141-0229(97)00106-3.

A. P. Mizisin, L. Li, and N. A. Calcutt. Sorbitol accumulation and transmembrane efflux in osmotically stressed JS1 schwannoma cells. *Neurosci. Lett.*, 229(1):53–56, Jun 1997. doi: 10.1016/S0304-3940(97)00416-3.

K. Münger and P. M. Howley. Human papillomavirus immortalization and transformation functions. *Virus Res.*, 89(2):213–228, Nov 2002. doi: 10.1016/S0168-1702(02)00190-9.

M. Murphy, C. Godson, S. Cannon, S. Kato, H. S. Mackenzie, F. Martin, and H. R. Brady. Suppression subtractive hybridization identifies high glucose levels as a stimulus for expression of connective tissue growth factor and other genes in human mesangial cells. *J. Biol. Chem.*, 274(9):5830–5834, Feb 1999.

S. M. Nabokina and H. M. Said. Characterization of the 5'-regulatory region of the human thiamin transporter *SLC19A3*: *in vitro* and *in vivo* studies. *Am. J. Physiol. Gastrointest. Liver Physiol.*, 287(4):G822–G829, Oct 2004. doi: 10.1152/ajpgi.00234.2004.

B. Najafian and M. Mauer. Progression of diabetic nephropathy in type 1 diabetic patients. *Diabetes Res. Clin. Pract.*, 83(1):1–8, Jan 2009. doi: 10.1016/j.diabres.2008.08.024.

H. Nakagami, Y. Kaneda, T. Ogihara, and R. Morishita. Endothelial dysfunction in hyperglycemia as a trigger of atherosclerosis. *Curr. Diabetes Rev.*, 1(1):59–63, Feb 2005.

T. Nakamura, C. Ushiyama, S. Suzuki, M. Hara, N. Shimada, I. Ebihara, and H. Koide. Urinary excretion of podocytes in patients with diabetic nephropathy. *Nephrol. Dial. Transplant.*, 15(9):1379–1383, Sep 2000.

K. Nakashima, X. Zhou, G. Kunkel, Z. Zhang, J. M. Deng, R. R. Behringer, and B. de Crombrugghe. The novel zinc finger-containing transcription factor osterix is required for osteoblast differentiation and bone formation. *Cell*, 108(1):17–29, Jan 2002.

National Diet & Nutrition Survey. The National Diet & Nutrition Survey: adults aged 19 to 64 years. Technical Report Volume 2, Office for National Statistics, 2002.

National Institute of Diabetes and Digestive and Kidney Diseases. National Diabetes Statistics, 2007 fact sheet. Bethesda, MD, 2008. U.S. Department of Health and Human Services, National Institutes of Health,.

National Research Council. Water-soluble vitamins. In: Recommended dietary allowances, 10th Edition pp 115–173. Technical report, National Research Council Subcommittee on the Tenth Edition of the RDAs, Food and Nutrition Board, Commission on Life Sciences, National Academy Press, Washington DC., 1989.

E. J. Neufeld, H. Mandel, T. Raz, R. Szargel, C. N. Yandava, A. Stagg, S. Fauré, T. Barrett, N. Buist, and N. Cohen. Localization of the gene for thiamine-responsive megaloblastic anemia syndrome, on the long arm of chromosome 1, by homozygosity mapping. *Am. J. Hum. Genet.*, 61(6):1335–1341, Dec 1997. doi: 10.1086/301642.

H. O. Nghiêm, L. Bettendorff, and J. P. Changeux. Specific phosphorylation of *Torpedo* 43K rapsyn by endogenous kinase(s) with thiamine triphosphate as the phosphate donor. *FASEB J.*, 14(3):543–554, Mar 2000.

Q. D. Nguyen, S. Tatlipinar, S. M. Shah, J. A. Haller, E. Quinlan, J. Sung, I. Zimmer-Galler, D. V. Do, and P. A. Campochiaro. Vascular endothelial growth factor is a critical stimulus for diabetic macular edema. *Am. J. Ophthalmol.*, 142(6):961–969, Dec 2006. doi: 10.1016/j.ajo.2006.06.068.

K. Nicholls and T. E. Mandel. Advanced glycosylation end-products in experimental murine diabetic nephropathy: effect of islet isografting and of aminoguanidine. *Lab. Invest.*, 60 (4):486–491, Apr 1989.

M. Nicolás, V. Noé, and C. J. Ciudad. Transcriptional regulation of the human *Sp1* gene promoter by the specificity protein (Sp) family members nuclear factor Y (NF-Y) and E2F. *Biochem. J.*, 371(2):265–275, Apr 2003. doi: 10.1042/BJ20021166.

M. Nikkola, Y. Lindqvist, and G. Schneider. Refined structure of transketolase from *Saccharomyces cerevisiae* at 2.0 Angstrom resolution. *J. Mol. Biol.*, 238(3):387–404, May 1994. doi: 10.1006/jmbi.1994.1299.

H. Nishino. Biogenesis of cocarboxylase in *Escherichia coli*. Partial purification and some properties of thiamine monophosphate kinase. *J. Biochem. (Tokyo)*, 72(5):1093–1100, Nov 1972.

S. E. Nissen and K. Wolski. Effect of rosiglitazone on the risk of myocardial infarction and death from cardiovascular causes. *N. Engl. J. Med.*, 356(24):2457–2471, Jun 2007. doi: 10.1056/NEJMoa072761.

C. F. Niven and K. L. Smiley. A microbiological assay method for thiamine. *J. Biol. Chem.*, 150:1–9, 1943.

NoAb BioDiscoveries. Discovery services. Permeability assays. Website 2009, 2009.

D. K. Obatomi and P. H. Bach. Inhibition of mitochondrial respiration and oxygen uptake in isolated rat renal tubular fragments by atractyloside. *Toxicol. Lett.*, 89(2):155–161, Dec 1996. doi: 10.1016/S0378-4274(96)03799-X.

K. Oishi and G. A. Diaz. Thiamine-Responsive Megaloblastic Anemia Syndrome (Last revision November 19, 2007). Technical report, GeneReviews at GeneTests: Medical Genetics Information Resource (database online), 2007.

M. A. C. Onuigbo and J. Skalski. Newly symptomatic central diabetes insipidus in ESRD with adult polycystic kidney disease following intracranial hemorrhage: the first reported case. *Med. Sci. Monit.*, 16(3):CS29–CS32, Feb 2010.

P. S. Oturai, R. Rasch, E. Hasselager, P. B. Johansen, H. Yokoyama, M. K. Thomsen, B. Myrup, A. Kofoed-Enevoldsen, and T. Deckert. Effects of heparin and aminoguanidine on glomerular basement membrane thickening in diabetic rats. *APMIS*, 104(4):259–264, Apr 1996.

S. Özcan, S. S. Andrali, and J. E. L. Cantrell. Modulation of transcription factor function by *O*-GlcNAc modification. *Biochim. Biophys. Acta*, 1799(5–6):353–364, 2010. doi: 10.1016/j.bbagrm.2010.02.005.

G. Öztürk, M. R. Şekeroğlu, E. Erdoğan, and M. Öztürk. The effect of non-enzymatic glycation of extracellular matrix proteins on axonal regeneration *in vitro*. *Acta Neuropathol. (Berl.)*, 112(5):627–632, Nov 2006. doi: 10.1007/s00401-006-0124-2.

D. Pachapurkar and L. N. Bell. Kinetics of Thiamin Degradation in Solutions under Ambient Storage Conditions. *J. Food Sci.*, 70(7):C423–C426, 2005. doi: 10.1111/j.1365-2621.2005.tb11463.x.

M. E. Pagtalunan, P. L. Miller, S. Jumping-Eagle, R. G. Nelson, B. D. Myers, H. G. Rennke, N. S. Coplon, L. Sun, and T. W. Meyer. Podocyte loss and progressive glomerular injury in type II diabetes. *J. Clin. Invest.*, 99(2):342–348, Jan 1997. doi: 10.1172/JCI119163.

X. Pan, S. S. Solomon, D. M. Borromeo, A. Martinez-Hernandez, and R. Raghow. Insulin deprivation leads to deficiency of Sp1 transcription factor in H-411E hepatoma cells and in streptozotocin-induced diabetic ketoacidosis in the rat. *Endocrinology*, 142(4):1635–1642, Apr 2001.

Y. Pang, P. Bounelis, J. C. Chatham, and R. B. Marchase. Hexosamine pathway is responsible for inhibition by diabetes of phenylephrine-induced inotropy. *Diabetes*, 53(4): 1074–1081, Apr 2004. doi: 10.2337/diabetes.53.4.1074.

P. Pannunzio, A. S. Hazell, M. Pannunzio, K. V. R. Rao, and R. Butterworth. Thiamine Deficiency Results in Metabolic Acidosis and Energy Failure in Cerebellar Granule Cells: An *In Vitro* Model for the Study of Cell Death Mechanisms in Wernicke's Encephalopathy. *J. Neurosci. Res.*, 62:286–292, 2000.

M. Pantaleon, H. Y. Tan, G. R. Kafer, and P. L. Kaye. Toxic effects of hyperglycemia are mediated by the hexosamine signaling pathway and *O*-linked glycosylation in early mouse embryos. *Biol. Reprod.*, 82(4):751–758, Apr 2010. doi: 10.1095/biolreprod.109.076661.

S. K. Park, J. Kim, Y. Seomun, J. Choi, D. H. Kim, I. O. Han, E. H. Lee, S. K. Chung, and C. K. Joo. Hydrogen peroxide is a novel inducer of connective tissue growth factor. *Biochem. Biophys. Res. Commun.*, 284(4):966–971, Jun 2001. doi: 10.1006/bbrc.2001.5058.

M. C. D. Pascale, A. M. Bassi, V. Patrone, L. Villacorta, A. Azzi, and J.-M. Zingg. Increased expression of transglutaminase-1 and PPARγ after vitamin E treatment in human keratinocytes. *Arch. Biochem. Biophys.*, 447(2):97–106, Mar 2006. doi: 10.1016/j.abb.2006.02.002.

R. Pazdro and J. R. Burgess. The role of vitamin E and oxidative stress in diabetes complications. *Mech. Ageing Dev.*, 131(4):276–286, Apr 2010. doi: 10.1016/j.mad.2010.03.005.

V. K. Pedchenko, S. V. Chetyrkin, P. Chuang, A.-J. L. Ham, M. A. Saleem, P. W. Mathieson, B. G. Hudson, and P. A. Voziyan. Mechanism of perturbation of integrin-mediated cell-matrix interactions by reactive carbonyl compounds and its implication for pathogenesis of diabetic nephropathy. *Diabetes*, 54(10):2952–2960, Oct 2005. doi: 10.2337/diabetes.54.10.2952.

C. Peñaranda, A. García-Ocaña, J. L. Sarasa, and P. Esbrit. Hypertrophy of rabbit proximal tubule cells is associated with overexpression of TGF β. *Life Sci.*, 59(21):1773–1782, 1996. doi: 10.1016/0024-3205(96)00520-6.

M. W. Pfaffl. A new mathematical model for relative quantification in real-time RT-PCR. *Nucleic Acids Res.*, 29(9):e45, May 2001.

S. Philipsen and G. Suske. A tale of three fingers: the family of mammalian Sp/XKLF transcription factors. *Nucleic Acids Res.*, 27(15):2991–3000, Aug 1999.

A. O. Phillips. The role of renal proximal tubular cells in diabetic nephropathy. *Curr. Diab. Rep.*, 3(6):491–496, Dec 2003. doi: 10.1007/s11892-003-0013-1.

A. O. Phillips, N. Topley, R. Steadman, K. Morrisey, and J. D. Williams. Induction of TGF-β 1 synthesis in D-glucose primed human proximal tubular cells by IL-1 β and TNF α. *Kidney Int.*, 50(5):1546–1554, Nov 1996.

A. O. Phillips, N. Topley, K. Morrisey, J. D. Williams, and R. Steadman. Basic fibroblast growth factor stimulates the release of preformed transforming growth factor β 1 from human proximal tubular cells in the absence of *de novo* gene transcription or mRNA translation. *Lab. Invest.*, 76(4):591–600, Apr 1997.

F. Pietruck, M. K. Kuhlmann, B. Lange, T. Feldkamp, S. Herget-Rosenthal, U. Rauen, G. Burkhardt, H. Kohler, T. Philipp, and A. Kribben. Effect of quercetin on hypoxic injury in freshly isolated rat proximal tubules. *J. Lab. Clin. Med.*, 142(2):106–112, Aug 2003. doi: 10.1016/S0022-2143(03)00065-9.

F. Pietruck, M. Horbelt, T. Feldkamp, K. Engeln, S. Herget-Rosenthal, T. Philipp, and A. Kribben. Digital fluorescence imaging of organic cation transport in freshly isolated rat proximal tubules. *Drug Metab. Dispos.*, 34(3):339–342, Mar 2006. doi: 10.1124/dmd.105.006403.

D. Pohlers, J. Brenmoehl, I. Löffler, C. K. Müller, C. Leipner, S. Schultze-Mosgau, A. Stallmach, R. W. Kinne, and G. Wolf. TGF-β and fibrosis in different organs - molecular pathway imprints. *Biochim. Biophys. Acta*, 1792(8):746–756, Aug 2009. doi: 10.1016/j.bbadis.2009.06.004.

D. R. Potter, J. Jiang, and E. R. Damiano. The recovery time course of the endothelial cell glycocalyx *in vivo* and its implications *in vitro*. *Circ. Res.*, 104(11):1318–1325, Jun 2009. doi: 10.1161/CIRCRESAHA.108.191585.

Prescrire Group. Preventing blindness due to diabetic retinopathy. Control glycaemia and blood pressure, and monitor the eyes. *Prescrire Int.*, 19(105):35–38, Feb 2010.

J. Q. Purnell and C. Weyer. Weight effect of current and experimental drugs for diabetes mellitus: from promotion to alleviation of obesity. *Treat. Endocrinol.*, 2(1):33–47, 2003.

W. Qi, X. Chen, R. E. Gilbert, Y. Zhang, M. Waltham, M. Schache, D. J. Kelly, and C. A. Pollock. High glucose-induced thioredoxin-interacting protein in renal proximal tubule cells is independent of transforming growth factor-β1. *Am. J. Pathol.*, 171(3):744–754, Sep 2007. doi: 10.2353/ajpath.2007.060813.

P. Qu, R. C. Ji, and S. Kato. Histochemical analysis of lymphatic endothelial cells in the pancreas of non-obese diabetic mice. *J. Anat.*, 203(5):523–530, Nov 2003. doi: 10.1046/j.1469-7580.2003.00234.x.

N. Rabbani, S. S. Alam, S. Riaz, J. R. Larkin, M. W. Akhtar, T. Shafi, and P. J. Thornalley. High-dose thiamine therapy for patients with type 2 diabetes and microalbuminuria: a randomised, double-blind placebo-controlled pilot study. *Diabetologia*, 52(2):208–212, Feb 2009. doi: 10.1007/s00125-008-1224-4.

G. Raddatz and H. Bisswanger. Receptor site and stereospecifity of dihydrolipoamide dehydrogenase for *R*- and *S*-lipoamide: a molecular modeling study. *J. Biotechnol.*, 58(2): 89–100, Oct 1997. doi: 10.1016/S0168-1656(97)00135-1.

U. Rajamani and M. F. Essop. Hyperglycemia-mediated activation of the hexosamine biosynthetic pathway results in myocardial apoptosis. *Am. J. Physiol. Cell. Physiol.*, 299(1):C139–C147, Jul 2010. doi: 10.1152/ajpcell.00020.2010.

A. Rajgopal, A. Edmondnson, I. D. Goldman, and R. Zhao. *SLC19A3* encodes a second thiamine transporter ThTr2. *Biochim. Biophys. Acta*, 1537(3):175–178, Nov 2001. doi: 10.1016/S0925-4439(01)00073-4.

M. A. Ramirez and N. L. Borja. Epalrestat: an aldose reductase inhibitor for the treatment of diabetic neuropathy. *Pharmacotherapy*, 28(5):646–655, May 2008. doi: 10.1592/phco.28.5.646.

I. Raška, P. J. Shaw, and D. Cmarko. New insights into nucleolar architecture and activity. *Int. Rev. Cytol.*, 255:177–235, 2006. doi: 10.1016/S0074-7696(06)55004-1.

J. C. Reidling and H. M. Said. *In vitro* and *in vivo* characterization of the minimal promoter region of the human thiamin transporter *SLC19A2*. *Am. J. Physiol. Cell. Physiol.*, 285 (3):C633–C641, Sep 2003. doi: 10.1152/ajpcell.00076.2003.

J. C. Reidling, V. S. Subramanian, P. K. Dudeja, and H. M. Said. Expression and promoter analysis of *SLC19A2* in the human intestine. *Biochim. Biophys. Acta*, 1561(2):180–187, Apr 2002. doi: 10.1016/S0005-2736(02)00341-3.

J. C. Reidling, N. Lambrecht, M. Kassir, and H. M. Said. Impaired intestinal vitamin B_1 (thiamin) uptake in thiamin transporter-2-deficient mice. *Gastroenterology*, 138(5): 1802–1809, May 2010. doi: 10.1053/j.gastro.2009.10.042.

M. Reljanovic, G. Reichel, K. Rett, M. Lobisch, K. Schuette, W. Möller, H. J. Tritschler, and H. Mehnert. Treatment of diabetic polyneuropathy with the antioxidant thioctic acid (α-lipoic acid): a two year multicenter randomized double-blind placebo-controlled trial (ALADIN II). Alpha Lipoic Acid in Diabetic Neuropathy. *Free Radic. Res.*, 31(3): 171–179, Sep 1999. doi: 10.1080/10715769900300721.

B. L. Riser, M. Denichilo, P. Cortes, C. Baker, J. M. Grondin, J. Yee, and R. G. Narins. Regulation of connective tissue growth factor activity in cultured rat mesangial cells and its expression in experimental diabetic glomerulosclerosis. *J. Am. Soc. Nephrol.*, 11(1): 25–38, Jan 2000.

K. A. Robinson, M. L. Weinstein, G. E. Lindenmayer, and M. G. Buse. Effects of diabetes and hyperglycemia on the hexosamine synthesis pathway in rat muscle and liver. *Diabetes*, 44(12):1438–1446, Dec 1995.

M. V. Rocco, Y. Chen, S. Goldfarb, and F. N. Ziyadeh. Elevated glucose stimulates TGF-β gene expression and bioactivity in proximal tubule. *Kidney Int.*, 41(1):107–114, Jan 1992.

D. Rogacka, A. Piwkowska, M. Jankowski, K. Kocbuch, M. H. Dominiczak, J. K. Stepiński, and S. Angielski. Expression of GFAT1 and OGT in podocytes: transport of glucosamine and the implications for glucose uptake into these cells. *J. Cell. Physiol.*, Epub ahead of print., May 2010. doi: 10.1002/jcp.22242.

L. E. Rogers, F. S. Porter, and J. B. Sidbury. Thiamine-responsive megaloblastic anemia. *J. Pediatr.*, 74(4):494–504, Apr 1969.

M. D. Roos, K. Su, J. R. Baker, and J. E. Kudlow. O glycosylation of an Sp1-derived peptide blocks known Sp1 protein interactions. *Mol. Cell. Biol.*, 17(11):6472–6480, Nov 1997.

H. R. Rosenberg and R. Culik. Effect of α-lipoic acid on vitamin C and vitamin E deficiencies. *Arch. Biochem. Biophys.*, 80(1):86–93, January 1959. doi: 10.1016/0003-9861(59)90345-5.

L. Rossetti, M. Hawkins, W. Chen, J. Gindi, and N. Barzilai. *In vivo* glucosamine infusion induces insulin resistance in normoglycemic but not in hyperglycemic conscious rats. *J. Clin. Invest.*, 96(1):132–140, Jul 1995. doi: 10.1172/JCI118013.

S. Rozen and H. Skaletsky. Primer3 on the WWW for general users and for biologist programmers. *Methods Mol. Biol.*, 132:365–386, 2000.

L. H. L. Rudolfs K. Zalups. *Methods in renal toxicology.* CRC Press, 1996. ISBN: 0849333415, 9780849333415.

A. C. Ruifrok and D. A. Johnston. Quantification of histochemical staining by color deconvolution. *Anal. Quant. Cytol. Histol.*, 23(4):291–299, Aug 2001.

M. J. Ryan, G. Johnson, J. Kirk, S. M. Fuerstenberg, R. A. Zager, and B. Torok-Storb. HK-2: an immortalized proximal tubule epithelial cell line from normal adult human kidney. *Kidney Int.*, 45(1):48–57, Jan 1994.

H. M. Said, J. C. Reidling, and A. Ortiz. Cellular and molecular aspects of thiamin uptake by human liver cells: studies with cultured HepG2 cells. *Biochim. Biophys. Acta*, 1567 (1–2):106–112, Dec 2002.

H. M. Said, K. Balamurugan, V. S. Subramanian, and J. S. Marchant. Expression and functional contribution of hTHTR-2 in thiamin absorption in human intestine. *Am. J. Physiol. Gastrointest. Liver Physiol.*, 286(3):G491–G498, Mar 2004. doi: 10.1152/ajpgi.00361.2003.

N. Saito, M. Kimura, A. Kuchiba, and Y. Itokawa. Blood thiamine levels in outpatients with diabetes mellitus. *J. Nutr. Sci. Vitaminol. (Tokyo)*, 33(6):421–430, Dec 1987.

S. Saitou, T. Ozawa, and I. Tomita. The purification and some properties of brewer's yeast apotransketolase. *FEBS Lett.*, 40(1):114–118, Mar 1974. doi: 10.1016/0014-5793(74)80906-3.

S. Sander, A. Hahn, J. Stein, and G. Rehner. Comparative studies on the high-performance liquid chromatographic determination of thiamine and its phosphate esters with chloroethylthiamine as an internal standard using pre- and post-column derivatization procedures. *J. Chromatogr. A*, 558:115–124, 1991. doi: 10.1016/0021-9673(91)80116-X.

S. C. Satchell and J. E. Tooke. What is the mechanism of microalbuminuria in diabetes: a role for the glomerular endothelium? *Diabetologia*, 51(5):714–725, May 2008. doi: 10.1007/s00125-008-0961-8.

P. P. Sayeski and J. E. Kudlow. Glucose metabolism to glucosamine is necessary for glucose stimulation of transforming growth factor-α gene transcription. *J. Biol. Chem.*, 271(25): 15237–15243, Jun 1996. doi: 10.1074/jbc.271.25.15237.

P. P. Sayeski, D. Wang, K. Su, I. O. Han, and J. E. Kudlow. Cloning and partial characterization of the mouse glutamine:fructose-6-phosphate amidotransferase (GFAT) gene promoter. *Nucleic Acids Res.*, 25(7):1458–1466, Apr 1997.

J. I. Scheinman, A. J. Fish, A. J. Matas, and A. F. Michael. The immunohistopathology of glomerular antigens. II. The glomerular basement membrane, actomyosin, and fibroblast surface antigens in normal, diseased, and transplanted human kidneys. *Am. J. Pathol.*, 90(1):71–88, Jan 1978.

F. P. Schena and L. Gesualdo. Pathogenetic mechanisms of diabetic nephropathy. *J. Am. Soc. Nephrol.*, 16 Suppl 1:S30–S33, Mar 2005. doi: 10.1681/ASN.2004110970.

G. Schenk, R. G. Duggleby, and P. F. Nixon. Properties and functions of the thiamin diphosphate dependent enzyme transketolase. *Int. J. Biochem. Cell Biol.*, 30(12):1297–1318, Dec 1998.

E. D. Schleicher and C. Weigert. Role of the hexosamine biosynthetic pathway in diabetic nephropathy. *Kidney Int. Suppl.*, 77:S13–S18, Sep 2000. doi: 10.1046/j.1523-1755.2000.07703.x.

R. W. Schrier, R. O. Estacio, A. Esler, and P. Mehler. Effects of aggressive blood pressure control in normotensive type 2 diabetic patients on albuminuria, retinopathy and strokes. *Kidney Int.*, 61(3):1086–1097, Mar 2002. doi: 10.1046/j.1523-1755.2002.00213.x.

J. B. Schüttert, G. M. Fiedler, C. Grupp, S. Blaschke, and R. W. Grunewald. Sorbitol transport in rat renal inner medullary interstitial cells. *Kidney Int.*, 61(4):1407–1415, Apr 2002. doi: 10.1046/j.1523-1755.2002.00285.x.

I. U. Scott, A. R. Edwards, R. W. Beck, N. M. Bressler, C. K. Chan, M. J. Elman, S. M. Friedman, C. M. Greven, R. K. Maturi, D. J. Pieramici, M. Shami, L. J. Singerman, C. R. Stockdale, and Diabetic Retinopathy Clinical Research Network. A phase II randomized clinical trial of intravitreal bevacizumab for diabetic macular edema. *Ophthalmology*, 114 (10):1860–1867, Oct 2007. doi: 10.1016/j.ophtha.2007.05.062.

M. L. Selva, E. Beltramo, F. Pagnozzi, E. Bena, P. A. Molinatti, G. M. Molinatti, and M. Porta. Thiamine corrects delayed replication and decreases production of lactate and advanced glycation end-products in bovine retinal and human umbilical vein endothelial cells cultured under high glucose conditions. *Diabetologia*, 39(11):1263–1268, Nov 1996. doi: 10.1007/s001250050568.

R. Shafi, S. P. Iyer, L. G. Ellies, N. O'Donnell, K. W. Marek, D. Chui, G. W. Hart, and J. D. Marth. The O-GlcNAc transferase gene resides on the X chromosome and is essential for embryonic stem cell viability and mouse ontogeny. *Proc. Natl. Acad. Sci. U. S. A.*, 97 (11):5735–5739, May 2000. doi: 10.1073/pnas.100471497.

A. L. Siebel, A. Z. Fernandez, and A. El-Osta. Glycemic memory associated epigenetic changes. *Biochem. Pharmacol.*, Epub ahead of print, Jun 2010. doi: 10.1016/j.bcp.2010.06.005.

K. L. Sikri, C. L. Foster, N. MacHugh, and R. D. Marshall. Localization of Tamm-Horsfall glycoprotein in the human kidney using immuno-fluorescence and immuno-electron microscopical techniques. *J. Anat.*, 132(4):597–605, Jun 1981.

R. K. Simmons, K. G. M. M. Alberti, E. A. M. Gale, S. Colagiuri, J. Tuomilehto, Q. Qiao, A. Ramachandran, N. Tajima, I. B. Mirchov, A. Ben-Nakhi, G. Reaven, B. H. Sambo,

S. Mendis, and G. Roglic. The metabolic syndrome: useful concept or clinical tool? Report of a WHO Expert Consultation. *Diabetologia*, 53(4):600–605, Apr 2010. doi: 10.1007/s00125-009-1620-4.

R. Simó, A. Lecube, R. M. Segura, J. G. Arumí, and C. Hernńdez. Free insulin growth factor-I and vascular endothelial growth factor in the vitreous fluid of patients with proliferative diabetic retinopathy. *Am. J. Ophthalmol.*, 134(3):376–382, Sep 2002.

E. H. Smeets, H. Muller, and J. de Wael. A NADH-dependent transketolase assay in erythrocyte hemolysates. *Clin. Chim. Acta*, 33(2):379–386, Jul 1971. doi: 10.1016/0009-8981(71)90496-7.

S. S. Solomon, G. Majumdar, A. Martinez-Hernandez, and R. Raghow. A critical role of Sp1 transcription factor in regulating gene expression in response to insulin and other hormones. *Life Sci.*, 83(9–10):305–312, Aug 2008. doi: 10.1016/j.lfs.2008.06.024.

P. N. Span, M. J. Pouwels, A. J. Olthaar, R. R. Bosch, A. R. Hermus, and C. G. Sweep. Assay for hexosamine pathway intermediates (uridine diphosphate-*N*-acetyl amino sugars) in small samples of human muscle tissue. *Clin. Chem.*, 47(5):944–946, May 2001.

M. L. Spengler, L.-W. Guo, and M. G. Brattain. Phosphorylation mediates Sp1 coupled activities of proteolytic processing, desumoylation and degradation. *Cell Cycle*, 7(5): 623–630, Mar 2008.

R. G. Spiro. Glycoproteins. *Adv. Protein Chem.*, 27:349–467, 1973.

R. G. Spiro. Protein glycosylation: nature, distribution, enzymatic formation, and disease implications of glycopeptide bonds. *Glycobiology*, 12(4):43R–56R, Apr 2002.

V. Srinivasan, N. Sandhya, R. Sampathkumar, S. Farooq, V. Mohan, and M. Balasubramanyam. Glutamine fructose-6-phosphate amidotransferase (GFAT) gene expression and activity in patients with type 2 diabetes: inter-relationships with hyperglycaemia and oxidative stress. *Clin. Biochem.*, 40(13–14):952–957, Sep 2007. doi: 10.1016/j.clinbiochem.2007.05.002.

S. K. Srivastava, K. V. Ramana, and A. Bhatnagar. Role of aldose reductase and oxidative damage in diabetes and the consequent potential for therapeutic options. *Endocr. Rev.*, 26(3):380–392, May 2005. doi: 10.1210/er.2004-0028.

P. C. Stafylas, P. A. Sarafidis, and A. N. Lasaridis. The controversial effects of thiazolidinediones on cardiovascular morbidity and mortality. *Int. J. Cardiol.*, 131(3):298–304, Jan 2009. doi: 10.1016/j.ijcard.2008.06.005.

Standing Committee on the Scientific Evaluation of Dietary Reference Intakes. Thiamin, In Dietary Reference Intakes for Thiamin, Riboflavin, Niacin, Vitamin B_6, Folate, Vitamin B_{12}, Pantothenic Acid, Biotin, and Choline. Technical Report 58–86, Food and Nutrition Board, Institute of Medicine, National Academy Press, Washington, DC, 1999.

M. W. Steffes, D. Schmidt, R. McCrery, J. M. Basgen, and I. D. N. S. Group. Glomerular cell number in normal subjects and in type 1 diabetic patients. *Kidney Int.*, 59(6):2104–2113, Jun 2001. doi: 10.1046/j.1523-1755.2001.00725.x.

E. Stitt-Cavanagh, L. MacLeod, and C. Kennedy. The podocyte in diabetic kidney disease. *ScientificWorldJournal*, 9:1127–1139, 2009. doi: 10.1100/tsw.2009.133.

M. Stolar. Glycemic control and complications in type 2 diabetes mellitus. *Am. J. Med.*, 123(3 Suppl):S3–11, Mar 2010. doi: 10.1016/j.amjmed.2009.12.004.

A. Stonehouse, T. Okerson, D. Kendall, and D. Maggs. Emerging incretin based therapies for type 2 diabetes: incretin mimetics and DPP-4 inhibitors. *Curr. Diabetes Rev.*, 4(2): 101–109, May 2008.

H. Stracke, A. Lindemann, and K. Federlin. A benfotiamine-vitamin B combination in treatment of diabetic polyneuropathy. *Exp. Clin. Endocrinol. Diabetes*, 104(4):311–316, 1996. doi: 10.1055/s-0029-1211460.

H. Stracke, H. P. Hammes, D. Werkmann, K. Mavrakis, I. Bitsch, M. Netzel, J. Geyer, W. Köpcke, C. Sauerland, R. G. Bretzel, and K. F. Federlin. Efficacy of benfotiamine versus thiamine on function and glycation products of peripheral nerves in diabetic rats. *Exp. Clin. Endocrinol. Diabetes*, 109(6):330–336, 2001. doi: 10.1055/s-2001-17399.

I. M. Stratton, A. I. Adler, H. A. Neil, D. R. Matthews, S. E. Manley, C. A. Cull, D. Hadden, R. C. Turner, and R. R. Holman. Association of glycaemia with macrovascular and microvascular complications of type 2 diabetes (UKPDS 35): prospective observational study. *BMJ*, 321(7258):405–412, Aug 2000.

W. Su, S. Jackson, R. Tjian, and H. Echols. DNA looping between sites for transcriptional activation: self-association of DNA-bound Sp1. *Genes Dev.*, 5(5):820–826, May 1991.

V. S. Subramanian, J. S. Marchant, I. Parker, and H. M. Said. Cell biology of the human thiamine transporter-1 (hTHTR1). Intracellular trafficking and membrane targeting mechanisms. *J. Biol. Chem.*, 278(6):3976–3984, Feb 2003. doi: 10.1074/jbc.M210717200.

V. S. Subramanian, J. S. Marchant, and H. M. Said. Targeting and trafficking of the human thiamine transporter-2 in epithelial cells. *J. Biol. Chem.*, 281(8):5233–5245, Feb 2006. doi: 10.1074/jbc.M512765200.

J. C. Sullivan and J. S. Pollock. Coupled and uncoupled NOS: separate but equal? Uncoupled NOS in endothelial cells is a critical pathway for intracellular signaling. *Circ. Res.*, 98(6):717–719, Mar 2006. doi: 10.1161/01.RES.0000217594.97174.c2.

F. Taheri and H. E. P. Bazan. Platelet-activating factor overturns the transcriptional repressor disposition of Sp1 in the expression of MMP-9 in human corneal epithelial cells. *Invest. Ophthalmol. Vis. Sci.*, 48(5):1931–1941, May 2007. doi: 10.1167/iovs.06-1008.

M. K. Tallent, N. Varghis, Y. Skorobogatko, L. Hernandez-Cuebas, K. Whelan, D. J. Vocadlo, and K. Vosseller. In vivo modulation of *O*-GlcNAc levels regulates hippocampal synaptic plasticity through interplay with phosphorylation. *J. Biol. Chem.*, 284(1):174–181, Jan 2009. doi: 10.1074/jbc.M807431200.

M. Tanaka, S. Endo, T. Okuda, A. N. Economides, D. M. Valenzuela, A. J. Murphy, E. Robertson, T. Sakurai, A. Fukatsu, G. D. Yancopoulos, T. Kita, and M. Yanagita. Expression of BMP-7 and USAG-1 (a BMP antagonist) in kidney development and injury. *Kidney Int.*, 73(2):181–191, Jan 2008. doi: 10.1038/sj.ki.5002626.

G. A. Tanner. Glomerular sieving coefficient of serum albumin in the rat: a two-photon microscopy study. *Am J Physiol Renal Physiol*, 296(6):F1258–F1265, Jun 2009. doi: 10.1152/ajprenal.90638.2008.

V. Tanphaichitr, S. L. Vimokesant, S. Dhanamitta, and A. Valyasevi. Clinical and biochemical studies of adult beriberi. *Am. J. Clin. Nutr.*, 23(8):1017–1026, Aug 1970.

S. Tarallo, E. Beltramo, E. Berrone, P. Dentelli, and M. Porta. Effects of high glucose and thiamine on the balance between matrix metalloproteinases and their tissue inhibitors in vascular cells. *Acta Diabetol.*, 47(2):105–111, Apr 2010. doi: 10.1007/s00592-009-0124-5.

J. R. Tate and P. F. Nixon. Measurement of Michaelis constant for human erythrocyte transketolase and thiamin diphosphate. *Anal. Biochem.*, 160(1):78–87, Jan 1987. doi: 10.1016/0003-2697(87)90616-6.

C. F. Teo, E. E. Wollaston-Hayden, and L. Wells. Hexosamine flux, the *O*-GlcNAc modification, and the development of insulin resistance in adipocytes. *Mol. Cell. Endocrinol.*, 318(1–2):44–53, Apr 2010. doi: 10.1016/j.mce.2009.09.022.

S. Terryn, F. cois Jouret, F. Vandenabeele, I. Smolders, M. Moreels, O. Devuyst, P. Steels, and E. V. Kerkhove. A primary culture of mouse proximal tubular cells, established on collagen-coated membranes. *Am. J. Physiol. Renal Physiol.*, 293(2):F476–F485, Aug 2007. doi: 10.1152/ajprenal.00363.2006.

The Diabetes Control and Complications Trial Research Group. The effect of intensive treatment of diabetes on the development and progression of long-term complications in insulin-dependent diabetes mellitus. *N. Engl. J. Med.*, 329(14):977–986, Sep 1993.

M. C. Thomas, M. K. Walker, J. R. Emberson, A. G. Thomson, D. A. Lawlor, S. Ebrahim, and P. H. Whincup. Prevalence of undiagnosed Type 2 diabetes and impaired fasting glucose in older British men and women. *Diabet. Med.*, 22(6):789–793, Jun 2005. doi: 10.1111/j.1464-5491.2005.01516.x.

P. J. Thornalley. Glyoxalase I—structure, function and a critical role in the enzymatic defence against glycation. *Biochem. Soc. Trans.*, 31(6):1343–1348, Dec 2003a. doi: 10.1042/.

P. J. Thornalley. Use of aminoguanidine (Pimagedine) to prevent the formation of advanced glycation endproducts. *Arch. Biochem. Biophys.*, 419(1):31–40, Nov 2003b. doi: 10.1016/j.abb.2003.08.013.

P. J. Thornalley. The potential role of thiamine (vitamin B_1) in diabetic complications. *Curr. Diabetes Rev.*, 1(3):287–298, Aug 2005.

P. J. Thornalley, A. Langborg, and H. S. Minhas. Formation of glyoxal, methylglyoxal and 3-deoxyglucosone in the glycation of proteins by glucose. *Biochem. J.*, 344(1):109–116, Nov 1999.

P. J. Thornalley, I. Jahan, and R. Ng. Suppression of the accumulation of triosephosphates and increased formation of methylglyoxal in human red blood cells during hyperglycaemia by thiamine *in vitro*. *J. Biochem. (Tokyo)*, 129(4):543–549, Apr 2001.

P. J. Thornalley, R. Babaei-Jadidi, H. A. Ali, N. Rabbani, A. Antonysunil, J. Larkin, A. Ahmed, G. Rayman, and C. W. Bodmer. High prevalence of low plasma thiamine concentration in diabetes linked to a marker of vascular disease. *Diabetologia*, 50(10): 2164–2170, Oct 2007. doi: 10.1007/s00125-007-0771-4.

B. Tolner, A. Singh, T. Esaki, K. Roy, and F. M. Sirotnak. Transcription of the mouse RFC-1 gene encoding a folate transporter. Multiplicity and properties of promoters with minimum requirements for their basal activity. *Gene*, 231(1–2):163–172, Apr 1999.

S. Tonna, A. El-Osta, M. E. Cooper, and C. Tikellis. Metabolic memory and diabetic nephropathy: potential role for epigenetic mechanisms. *Nat. Rev. Nephrol.*, 6(6):332–341, Jun 2010. doi: 10.1038/nrneph.2010.55.

C. R. Torres and G. W. Hart. Topography and polypeptide distribution of terminal *N*-acetylglucosamine residues on the surfaces of intact lymphocytes. Evidence for *O*-linked GlcNAc. *J. Biol. Chem.*, 259(5):3308–3317, Mar 1984.

L. Tretter and V. Adam-Vizi. Alpha-ketoglutarate dehydrogenase: a target and generator of oxidative stress. *Philos. Trans. R. Soc. Lond. B. Biol. Sci.*, 360(1464):2335–2345, Dec 2005. doi: 10.1098/rstb.2005.1764.

D. Tsinalis and G. T. Thiel. An easy to calculate equation to estimate GFR based on inulin clearance. *Nephrol. Dial. Transplant.*, 24(10):3055–3061, Oct 2009. doi: 10.1093/ndt/gfp193.

P. K. Tubbs. The metabolism of D-α-hydroxy acids in animal tissues. *Ann. N. Y. Acad. Sci.*, 119(3):920–926, Jul 1965.

R. Turner, C. Cull, and R. Holman. United Kingdom Prospective Diabetes Study 17: a 9-year update of a randomized, controlled trial on the effect of improved metabolic control on complications in non-insulin-dependent diabetes mellitus. *Ann. Intern. Med.*, 124(1 Pt 2):136–145, Jan 1996.

S. M. Twigg, Z. Cao, S. V. McLennan, W. C. Burns, G. Brammar, J. M. Forbes, and M. E. Cooper. Renal connective tissue growth factor induction in experimental diabetes is prevented by aminoguanidine. *Endocrinology*, 143(12):4907–4915, Dec 2002.

A. Tylicki, J. Czerniecki, A. Godlewska, M. Kieliszek, T. Zebrowski, T. Bielawski, and B. Wojcik. Changes in ECG and enzyme activity in rat heart after myocardial infarction: effect of TPP and $MnCl_2$. *J. Physiol. Biochem.*, 64(2):93–101, Jun 2008.

UK Prospective Diabetes Study Group. Tight blood pressure control and risk of macrovascular and microvascular complications in type 2 diabetes: UKPDS 38. UK Prospective Diabetes Study Group. *BMJ*, 317(7160):703–713, Sep 1998.

UK Prospective Diabetes Study (UKPDS) Group. Intensive blood-glucose control with sulphonylureas or insulin compared with conventional treatment and risk of complications in patients with type 2 diabetes (UKPDS 33). *Lancet*, 352(9131):837–853, Sep 1998. doi: 10.1016/S0140-6736(98)07019-6.

R. I. Unnikrishnan, M. Rema, R. Pradeepa, M. Deepa, C. S. Shanthirani, R. Deepa, and V. Mohan. Prevalence and risk factors of diabetic nephropathy in an urban South Indian population: the Chennai Urban Rural Epidemiology Study (CURES 45). *Diabetes Care*, 30(8):2019–2024, Aug 2007. doi: 10.2337/dc06-2554.

US Renal Data System. USRDS 2009 Annual Data Report: Atlas of End-Stage Renal Disease in the United States. Technical report, National Institutes of Health, 2009.

J. v. Mering and O. Minkowski. Diabetes mellitus nach Pankreasexstirpation. *Naunyn. Schmiedebergs Arch. Pharmacol.*, 26(5–6):371–387, 1890. doi: 10.1007/BF01831214.

G. Valerio, A. Franzese, V. Poggi, and A. Tenore. Long-term follow-up of diabetes in two patients with thiamine-responsive megaloblastic anemia syndrome. *Diabetes Care*, 21(1): 38–41, Jan 1998. doi: 10.2337/diacare.21.1.38.

G. Valerio, A. Franzese, V. Poggi, C. Patrini, U. Laforenza, and A. Tenore. Lipophilic thiamine treatment in long-standing insulin-dependent diabetes mellitus. *Acta Diabetol.*, 36(1–2):73–76, Jun 1999. doi: 10.1007/s005920050148.

J. R. van Beijnum, M. Rousch, K. Castermans, E. van der Linden, and A. W. Griffioen. Isolation of endothelial cells from fresh tissues. *Nat. Protoc.*, 3(6):1085–1091, 2008. doi: 10.1038/nprot.2008.71.

H. van de Waterbeemd and B. Testa. *Drug bioavailability: estimation of solubility, permeability, absorption and bioavailability.* Wiley-VCH, 2nd edition, 2008.

C. M. van der Loos. Multiple immunoenzyme staining: methods and visualizations for the observation with spectral imaging. *J. Histochem. Cytochem.*, 56(4):313–328, Apr 2008. doi: 10.1369/jhc.2007.950170.

N. F. van Det, N. A. Verhagen, J. T. Tamsma, J. H. Berden, J. A. Bruijn, M. R. Daha, and F. J. van der Woude. Regulation of glomerular epithelial cell production of fibronectin and transforming growth factor-beta by high glucose, not by angiotensin II. *Diabetes*, 46 (5):834–840, May 1997. doi: 10.2337/diabetes.46.5.834.

R. van Heyningen. Formation of Polyols by the Lens of the Rat with 'Sugar' Cataract. *Nature*, 184:194–195, July 1959. doi: 10.1038/184194b0.

A. Varki, R. Cummings, J. Esko, H. Freeze, G. Hart, and J. Marth, editors. *Essentials of Glycobiology.* Cold Spring Harb or Laboratory Press, 2nd edition edition, 1999.

A. Vicart, T. Lefebvre, J. Imbert, A. Fernandez, and B. Kahn-Perlés. Increased chromatin association of Sp1 in interphase cells by PP2A-mediated dephosphorylations. *J. Mol. Biol.*, 364(5):897–908, Dec 2006. doi: 10.1016/j.jmb.2006.09.036.

S. A. Vindedzis, K. G. Stanton, J. L. Sherriff, and S. S. Dhaliwal. Thiamine deficiency in diabetes—is diet relevant? *Diab. Vasc. Dis. Res.*, 5(3):215, Sep 2008. doi: 10.3132/dvdr.2008.035.

A. Virkamäki, M. C. Daniels, S. Hämäläinen, T. Utriainen, D. McClain, and H. Yki-Järvinen. Activation of the hexosamine pathway by glucosamine *in vivo* induces insulin resistance in multiple insulin sensitive tissues. *Endocrinology*, 138(6):2501–2507, Jun 1997.

D. J. Vocadlo, H. C. Hang, E.-J. Kim, J. A. Hanover, and C. R. Bertozzi. A chemical approach for identifying *O*-GlcNAc-modified proteins in cells. *Proc. Natl. Acad. Sci. U. S. A.*, 100(16):9116–9121, Aug 2003. doi: 10.1073/pnas.1632821100.

J. S. Waby, C. D. Bingle, and B. M. Corfe. Post-translational control of Sp-family transcription factors. *Curr. Genomics*, 9(5):301–311, 2008. doi: 10.2174/138920208785133244.

N. A. Wahab, N. Yevdokimova, B. S. Weston, T. Roberts, X. J. Li, H. Brinkman, and R. M. Mason. Role of connective tissue growth factor in the pathogenesis of diabetic nephropathy. *Biochem. J.*, 359(1):77–87, Oct 2001.

J. L. E. Walgren, T. S. Vincent, K. L. Schey, and M. G. Buse. High glucose and insulin promote *O*-GlcNAc modification of proteins, including α-tubulin. *Am. J. Physiol. Endocrinol. Metab.*, 284(2):E424–E434, Feb 2003. doi: 10.1152/ajpendo.00382.2002.

Y. Wang, K. Heilig, T. Saunders, A. Minto, D. K. Deb, A. Chang, F. Brosius, C. Monteiro, and C. W. Heilig. Transgenic overexpression of GLUT1 in mouse glomeruli produces renal disease resembling diabetic glomerulosclerosis. *Am. J. Physiol. Renal Physiol.*, 299 (1):F99–F111, Jul 2010. doi: 10.1152/ajprenal.00466.2009.

M. W. Washabaugh and W. P. Jencks. Thiazolium C(2)-Proton Exchange: General-Base Catalysis, Direct Proton Transfer, and Acid Inhibition. *J. Am. Chem. Soc.*, 111:674–683, 1989. doi: 10.1021/ja00184a042.

M. W. Washabaugh, C. C. Yang, A. D. Hollenbach, and P. Chen. Hydrolysis of Thiamin: Evidence for Rate-Limiting Breakdown of the Tricyclic Dihydrothiachromine Intermediate in Neutral Aqueous Solution. *Bioorg. Chem.*, 21(2):170–191, 1993. doi: 10.1006/bioo.1993.1016.

M. E. Webb, A. Marquet, R. R. Mendel, F. Rébeillé, and A. G. Smith. Elucidating biosynthetic pathways for vitamins and cofactors. *Nat. Prod. Rep.*, 24(5):988–1008, Oct 2007. doi: 10.1039/b703105j.

W. Weber and H. Kewitz. Determination of thiamine in human plasma and its pharmacokinetics. *Eur. J. Clin. Pharmacol.*, 28(2):213–219, 1985.

C. Weiland, H. J. Ahr, H. W. Vohr, and H. Ellinger-Ziegelbauer. Characterization of primary rat proximal tubular cells by gene expression analysis. *Toxicol. in Vitro*, 21(3):466–491, Apr 2007. doi: 10.1016/j.tiv.2006.10.008.

J. M. Weinberg, J. A. Davis, M. Abarzua, and T. Rajan. Cytoprotective effects of glycine and glutathione against hypoxic injury to renal tubules. *J. Clin. Invest.*, 80(5):1446–1454, Nov 1987. doi: 10.1172/JCI113224.

L. Wells, K. Vosseller, and G. W. Hart. Glycosylation of nucleocytoplasmic proteins: signal transduction and *O*-GlcNAc. *Science*, 291(5512):2376–2378, Mar 2001. doi: 10.1126/science.1058714.

B. L. Wharram, M. Goyal, J. E. Wiggins, S. K. Sanden, S. Hussain, W. E. Filipiak, T. L. Saunders, R. C. Dysko, K. Kohno, L. B. Holzman, and R. C. Wiggins. Podocyte depletion causes glomerulosclerosis: diphtheria toxin-induced podocyte depletion in rats expressing human diphtheria toxin receptor transgene. *J. Am. Soc. Nephrol.*, 16(10):2941–2952, Oct 2005. doi: 10.1681/ASN.2005010055.

B. Wice, G. Trugman, M. Pinto, M. Rousset, G. Chevalier, E. Dussaulx, B. Lacroix, and A. Zweibaum. The intracellular accumulation of UDP-*N*-acetylhexosamines is concomitant with the inability of human colon cancer cells to differentiate. *J. Biol. Chem.*, 260: 139–146, 1985.

J. P. Wielders and C. J. Mink. Quantitative analysis of total thiamine in human blood, milk and cerebrospinal fluid by reversed-phase ion-pair high-performance liquid chromatography. *J. Chromatogr.*, 277:145–156, Oct 1983.

M. E. Williams. Diabetic CKD/ESRD 2010: a progress report? *Semin. Dial.*, 23(2): 129–133, Mar 2010. doi: 10.1111/j.1525-139X.2009.00698.x.

J. R. Williamson, K. Chang, M. Frangos, K. S. Hasan, Y. Ido, T. Kawamura, J. R. Nyengaard, M. van den Enden, C. Kilo, and R. G. Tilton. Hyperglycemic pseudohypoxia and diabetic complications. *Diabetes*, 42(6):801–813, Jun 1993.

World Health Organization. Diabetes Mellitus: Report of a WHO Study Group, 1985. Geneva.

World Health Organization. Definition, Diagnosis and Classification of Diabetes Mellitus and its Complications, 1999. Department of Noncommunicable Disease Surveillance.

World Health Organization. Definition and diagnosis of diabetes mellitus and intermediate hyperglycemia. Technical report, World Health Organization, 2006.

World Health Organization's Department of Nutrition for Health and Development. Thiamine deficiency and its prevention and control in major emergencies. Technical Report WHO/NHD/99.13, WHO, 1999.

K. D. Wrenn and C. M. Slovis. Is intravenous thiamine safe? *Am. J. Emerg. Med.*, 10(2): 165, Mar 1992.

K. D. Wrenn, F. Murphy, and C. M. Slovis. A toxicity study of parenteral thiamine hydrochloride. *Ann. Emerg. Med.*, 18(8):867–870, Aug 1989.

H. M. Wuest. The history of thiamine. *Ann. N. Y. Acad. Sci.*, 98:385–400, Apr 1962. doi: 10.1111/j.1749-6632.1962.tb30561.x.

X. Yang, F. Zhang, and J. E. Kudlow. Recruitment of *O*-GlcNAc transferase to promoters by corepressor mSin3A: coupling protein *O*-GlcNAcylation to transcriptional repression. *Cell*, 110(1):69–80, Jul 2002. doi: 10.1016/S0092-8674(02)00810-3.

D. Yao, T. Taguchi, T. Matsumura, R. Pestell, D. Edelstein, I. Giardino, G. Suske, N. Rabbani, P. J. Thornalley, V. P. Sarthy, H.-P. Hammes, and M. Brownlee. High glucose increases angiopoietin-2 transcription in microvascular endothelial cells through methylglyoxal modification of mSin3A. *J. Biol. Chem.*, 282(42):31038–31045, Oct 2007. doi: 10.1074/jbc.M704703200.

S. A. Yuzwa, M. S. Macauley, J. E. Heinonen, X. Shan, R. J. Dennis, Y. He, G. E. Whitworth, K. A. Stubbs, E. J. McEachern, G. J. Davies, and D. J. Vocadlo. A potent mechanism-inspired *O*-GlcNAcase inhibitor that blocks phosphorylation of tau *in vivo*. *Nat. Chem. Biol.*, 4(8):483–490, Aug 2008. doi: 10.1038/nchembio.96.

N. E. Zachara and G. W. Hart. *O*-GlcNAc a sensor of cellular state: the role of nucleocytoplasmic glycosylation in modulating cellular function in response to nutrition and stress. *Biochim. Biophys. Acta*, 1673(1-2):13–28, Jul 2004. doi: 10.1016/j.bbagen.2004.03.016.

R. A. Zager and C. A. Foerder. Effects of inorganic iron and myoglobin on *in vitro* proximal tubular lipid peroxidation and cytotoxicity. *J. Clin. Invest.*, 89(3):989–995, Mar 1992. doi: 10.1172/JCI115682.

R. A. Zager, B. A. Schimpf, and D. J. Gmur. Physiological pH. Effects on posthypoxic proximal tubular injury. *Circ. Res.*, 72(4):837–846, Apr 1993.

A. Zaid, Z. Hodny, R. Li, and B. D. Nelson. Sp1 acts as a repressor of the human adenine nucleotide translocase-2 (ANT2) promoter. *Eur. J. Biochem.*, 268(21):5497–5503, Nov 2001. doi: 10.1046/j.1432-1033.2001.02453.x.

W.-Q. Zeng, E. Al-Yamani, J. S. Acierno, S. Slaugenhaupt, T. Gillis, M. E. MacDonald, P. T. Ozand, and J. F. Gusella. Biotin-responsive basal ganglia disease maps to 2q36.3 and is due to mutations in *SLC19A3*. *Am. J. Hum. Genet.*, 77(1):16–26, Jul 2005. doi: 10.1086/431216.

F. Zhang, Y. Hu, P. Huang, C. A. Toleman, A. J. Paterson, and J. E. Kudlow. Proteasome function is regulated by cyclic AMP-dependent protein kinase through phosphorylation of Rpt6. *J. Biol. Chem.*, 282(31):22460–22471, Aug 2007. doi: 10.1074/jbc.M702439200.

W. Y. Zhang and A. L. W. Po. The effectiveness of topically applied capsaicin. A meta-analysis. *Eur. J. Clin. Pharmacol.*, 46(6):517–522, 1994. doi: 10.1007/BF00196108.

J. Zheng, J. Zhu, L. Li, and Z. Liu. Rhein reverses the diabetic phenotype of mesangial cells over-expressing the glucose transporter (GLUT1) by inhibiting the hexosamine pathway. *Br. J. Pharmacol.*, 153(7):1456–1464, April 2008. doi: 10.1038/bjp.2008.26.

P. Zimmet, K. G. Alberti, and J. Shaw. Global and societal implications of the diabetes epidemic. *Nature*, 414(6865):782–7, 2001. doi: 10.1038/414782a.

F. N. Ziyadeh. Different roles for TGF-β and VEGF in the pathogenesis of the cardinal features of diabetic nephropathy. *Diabetes Res. Clin. Pract.*, 82 Suppl 1:S38–S41, Nov 2008. doi: 10.1016/j.diabres.2008.09.016.